

# Data-Driven Flight Procedure Simulation and Noise Analysis in a Large-Scale Air Transportation System

by

Luke L. Jensen

B. S., University of Washington (2011)  
S.M., Massachusetts Institute of Technology (2014)

Submitted to the Department of Aeronautics & Astronautics in  
Partial Fulfillment of the Requirements for the Degree of

Doctor of Philosophy in Aeronautics & Astronautics

at the

Massachusetts Institute of Technology

June 2018

© Massachusetts Institute of Technology 2018. All rights reserved.

Author:

Signature redacted

Department of Aeronautics & Astronautics  
May 24, 2018

Certified by:

Signature redacted

Prof. R. John Hansman  
Professor of Aeronautics & Astronautics, MIT  
Thesis Supervisor

Certified by:

Signature redacted

Prof. Warren Hoburg  
Visiting Professor of Aeronautics & Astronautics, MIT

Certified by:

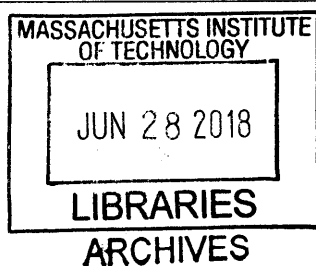
Signature redacted

Dr. Brian Yutko  
Vice President of Research & Development, Aurora Flight Sciences

Accepted by:

Signature redacted

Prof. Hamsa Balakrishnan  
Associate Professor of Aeronautics & Astronautics, MIT  
Chair, Graduate Program Committee





# **Data-Driven Flight Procedure Simulation and Noise Analysis in a Large-Scale Air Transportation System**

by  
Luke L. Jensen

Submitted to the Department of Aeronautics & Astronautics  
on May 25, 2018 in partial fulfillment of the requirements for the degree of  
Doctor of Philosophy in Aeronautics & Astronautics

## **Abstract**

Aircraft noise is a growing source of community concern around airports. Despite the introduction of quieter aircraft, increased precision of onboard guidance systems has resulted in new noise impacts driven by overflight frequency effects. Noise issues present a potential barrier to the continued rollout of advanced operational procedures in the US. This thesis presents a data-driven approach to simulating and communicating noise effects in the flight procedure development and modernization process, with input from multiple stakeholders with varying objectives that are technical, operational, and political in nature.

First, a system-level framework is introduced for developing novel noise-reducing arrival and departure flight procedures, clarifying the role of the analyst given diverse stakeholder objectives. The framework includes relationships between baseline impact assessment, community negotiation, iterative flight procedure development, and formal implementation processes. Variability in stakeholder objectives suggests a need to incorporate noise issues in conjunction with other key operational objectives as part of larger-scale US air transportation system modernization.

As part of this framework development, an airport-level noise modeling method is developed to enable rapid exposure and impact analysis for system-level evaluation of advanced operational procedures. The modeling method and framework are demonstrated by evaluating potential benefits of specific advanced procedures at 35 major airports in the US National Airspace System, including Performance Based Navigation guidance and a speed-managed departure concept.

Thesis Supervisor: R. John Hansman  
Title: Professor of Aeronautics and Astronautics, MIT



# Table of Contents

<b>Chapter 1. Motivation and Objectives .....</b>	<b>17</b>
1.1 Problem Introduction.....	17
1.2 PBN Track Concentration.....	19
1.3 Sociotechnical System Framework for Procedure Development.....	22
1.4 System Noise Benefits of Specific Operational Procedures.....	24
1.5 Thesis Outline.....	25
<b>Chapter 2. Literature Review and Background on Aircraft Noise.....</b>	<b>27</b>
2.1 Physics of Aircraft Noise.....	27
2.2 Effects of Aircraft Noise.....	31
2.3 Noise Reduction Literature Review .....	38
2.4 Modeling Aircraft Noise .....	40
2.5 Noise Metrics .....	45
2.6 Noise Management Objectives.....	50
2.7 Environmental Regulations.....	53
2.8 Capturing Annoyance from Overflight Frequency .....	55
2.9 Multi-Stakeholder System Modeling Literature Review .....	59
2.10 Change Propagation in Air Transportation Systems.....	61
<b>Chapter 3. Noise Analysis Methods.....</b>	<b>63</b>
3.1 Fleet Development.....	64
3.2 Procedure Development.....	66
3.3 Aircraft Performance Models.....	68
3.4 Detailed Trajectory Generation.....	70
3.5 Noise Modeling .....	71
3.6 Flight-Level Schedule Development.....	77
3.7 Calculating Integrated Impacts .....	80
3.8 Population Impact Modeling .....	80
3.9 Noise Impact Reporting and Visualization.....	84
<b>Chapter 4. Characteristics and Constraints for RNAV and RNP Approaches.....</b>	<b>87</b>
4.1 RNAV Approach Design Parameters and Criteria.....	88
4.2 RNP Approach Design Parameters and Criteria.....	98
4.3 Implications of RNAV and RNP Approach Design Parameters .....	101
4.4 RNAV and RNP Characteristics for Existing Procedures.....	103
4.5 RNAV Visual Flight Procedures .....	108
4.6 Nonstandard Instrument Flight Procedures and Waivers.....	110
<b>Chapter 5. System Noise Reduction Potential of RNAV and RNP Approaches .....</b>	<b>111</b>
5.1 Track Generation Method .....	111
5.2 Noise Contour Generation.....	114

5.3	Population Exposure Calculation .....	116
5.4	Average Hourly and Daily Schedule Generation .....	118
5.5	RNAV Procedures with Vertical Guidance.....	119
5.6	RNAV Procedures without Vertical Guidance.....	129
5.7	RNP Procedures.....	134
5.8	Comparison of PBN Approach Guidance Methods for Noise Reduction.....	140
5.9	Evaluating System-Level Population Exposure Rollup.....	146
5.10	Approach to Tradeoff Evaluation in Procedure Selection.....	149
<b>Chapter 6.</b>	<b>System Noise Reduction Potential for Reduced Speed Departures.....</b>	<b>159</b>
6.1	Technical Basis for Reduced Speed Departures .....	159
6.2	Speed Limitations for Existing Departure Procedures .....	162
6.3	Noise Modeling Approach for Reduced Speed Departures.....	164
6.4	System Noise Reduction Analysis for Reduced Speed Departures.....	168
<b>Chapter 7.</b>	<b>Framework for Noise-Reduction Procedure Development.....</b>	<b>173</b>
7.1	System Dynamic Model for Noise-Motivated Procedure Development.....	174
7.2	Baseline Conditions.....	176
7.3	Procedure Change Process .....	178
7.4	Implementation Process .....	184
7.5	Case Study at Boston Logan Airport.....	188
<b>Chapter 8.</b>	<b>Conclusion.....</b>	<b>205</b>
8.1	Thesis Framework and Analysis Results Summary.....	205
8.2	Key Outcomes .....	207
8.3	Research Recommendations and Future Work.....	208
<b>Appendix A</b>	<b>OEP-35 Airports.....</b>	<b>213</b>
<b>Appendix B</b>	<b>Full RNAV and RNP Approaches: Population Exposure Results.....</b>	<b>215</b>
<b>Appendix C</b>	<b>Reduced Speed Departures: Population Exposure Results .....</b>	<b>221</b>
<b>References</b>	<b>.....</b>	<b>227</b>

# Table of Figures

Figure 1. Aircraft flight tracks for operations at BOS before (2010) and after (2015) RNAV implementation (Source: Massport Noise and Operations Management System)	20
Figure 2. 65 dB DNL contour vs. noise complaint locations (red circles)	21
Figure 3. Sociotechnical system framework for flight procedure development	24
Figure 4. Sound pressure level time history at a single observer location illustrating $L_{MAX}$ and SEL metrics	32
Figure 5. Noise stage levels and certification values for common turbojet aircraft types as a function of certification year (Source: FAA [26])	33
Figure 6. Schultz Curve relating A-weighted DNL to community annoyance [19]	34
Figure 7. A-weighting filter function for determining equivalent instantaneous loudness within the frequency range of human hearing	47
Figure 8. BOS 33L departures complainant coverage for all scenarios by DNL contour level Source: Brenner 2017	57
Figure 9. BOS 33L departures complainant coverage for peak day by $N_{ABOVE}$ thresholds Source: Brenner 2017	57
Figure 10. Complaints captured by peak-day $N_{ABOVE}$ contours at BOS (60dB day, 50dB night)	58
Figure 11. Multi-stakeholder system transformation model developed by O'Neill [108]	60
Figure 12. System dynamic transition model developed by Mozdzanowska [116]	61
Figure 13. Noise analysis flowchart for single-event and cumulative impact evaluation of new procedures	63
Figure 14. Top 40 aircraft types by movement count at the OEP-35 airports in 2017	65
Figure 15. CIFP translation to trajectory centerline for noise analysis	68
Figure 16. Force-balance approach used to calculate thrust and drag for profile definitions [124]	70
Figure 17. 60dB $L_{MAX}$ contour for a Boeing 737-800 on a straight-in final approach segment with resulting contour half-width function shown in black.	73
Figure 18. Contour generated by applying the half-width functions orthogonal to an RNAV procedure centerline	74
Figure 19. Contours generated directly by AEDT for a Boeing 737-800 on a standard arrival profile with a turn of 0°, 30°, or 60° on the final approach segment	75
Figure 20. Contour half-width functions at the turn location based on contours from AEDT for a Boeing 737-800 on a standard arrival profile with a turn of 0°, 30°, or 60° on the final approach segment	75
Figure 21. Full contour comparison between AEDT output and rapid contour generation method for a 737-800 approach procedure to Runway 4R at BOS containing a 60° turn	76
Figure 22. Representative census blocks and population counts with calculated areas	81
Figure 23. 2010 US Census block-level absolute population counts converted to geospatial population density	81
Figure 24. Demonstration of area-based census data redistribution method for gridded population calculation	82
Figure 25. Re-Gridded 2010 Block-Level US Census Population Data	83
Figure 26. Re-gridded population data for six examples from the OEP-35 airports	84

Figure 27. Conceptual difference between conventional navigation, RNAV, and RNP.....	87
Figure 28. Flyby vs. flyover waypoints .....	88
Figure 29. Profile view for RNP Runway 19 approach at DCA with variable minimums depending on RNP level on the final approach segment.....	89
Figure 30. Illustration of minimum segment length between two fly-by RNAV waypoints...	93
Figure 31. 2-segment RNAV approach segment with 45° total heading change distributed between final turn and intermediate turn .....	94
Figure 32. Required Obstacle Clearance for initial and intermediate straight RNAV approach segments connecting fly-by waypoints.....	95
Figure 33. Obstacle clearance surface for vertically-guided RNAV final approach segments	96
Figure 34. Schematic of final approach segment geometry for RNAV procedures.....	98
Figure 35. Intermediate and final approach geometry for RNAV and RNP procedures .....	104
Figure 36. Example published RNAV (left) and RNP (right) instrument approach procedures with waypoint geometry near criteria limits.....	107
Figure 37. Example of a charted visual procedure and RNAV Visual serving the same runway	109
Figure 38. Assumed as-flown turn anticipation geometry for FB waypoints.....	113
Figure 39. Example lateral tracks for RNAV (a) and RNP (b) arrival procedures.....	114
Figure 40. Radar-based median arrival profile for a B737-800 (a) and resulting thrust profile calculated using BADA-4 (b) .....	115
Figure 41. Approach $L_{MAX}$ contour widths for 7 fleet types following radar median approach profiles.....	116
Figure 42. Illustration of population grid rotation at LGA airport showing the baseline north-oriented airport layout, a generic noise contour, and runway-aligned population grids .....	117
Figure 43. Noise-minimal RNAV approach with vertical guidance for LAX runway 25L (B737-800 60dB $L_{MAX}$ ).....	120
Figure 44. Noise-minimal RNAV approach with vertical guidance for BOS runway 33L (B737-800 60dB $L_{MAX}$ ).....	120
Figure 45. Noise-minimal RNAV approach with vertical guidance for ORD runway 10L (B737-800 50dB $L_{MAX}$ ).....	121
Figure 46. Threshold Sensitivity of Noise-Minimal RNAV Approach with Vertical Guidance for KBWI Runway 33R (B737-800 50dB vs. 60dB $L_{MAX}$ ).....	123
Figure 47. Threshold Sensitivity of Noise-Minimal RNAV Approach with Vertical Guidance for KBWI Runway 10 (B737-800 50dB vs. 60dB $L_{MAX}$ ).....	123
Figure 48. 2017 Daytime 60dB $L_{MAX}$ noise reduction potential from RNAV procedures with vertical guidance for all OEP-35 runways.....	125
Figure 49. 2017 Nighttime 50dB $L_{MAX}$ noise reduction potential from RNAV procedures with vertical guidance for all OEP-35 runways.....	127
Figure 50. Comparison between noise-minimal RNAV approach with and without vertical guidance at LGA runway 4.....	130
Figure 51. 2017 Daytime 60dB $L_{MAX}$ noise reduction potential from RNAV procedures without vertical guidance for all OEP-35 runways.....	131
Figure 52. 2017 Nighttime 50dB $L_{MAX}$ noise reduction potential from RNAV procedures without vertical guidance for all OEP-35 runways.....	131



Figure 53. ORD Runway 28C noise-minimal RNP procedure relative to a straight-in baseline (Boeing 737-800, 60dB L<sub>MAX</sub>)..... 135

Figure 54. DCA runway 19 noise-minimal RNP procedure relative to a straight-in baseline (Boeing 737-800, 60dB L<sub>MAX</sub>) compared with published RNAV (RNP) to the same runway..... 135

Figure 55. 2017 Daytime 60dB L<sub>MAX</sub> noise reduction potential from RNP procedures for all OEP-35 runways..... 137

Figure 56. 2017 Nighttime 50dB L<sub>MAX</sub> noise reduction potential from RNP procedures for all OEP-35 runways..... 137

Figure 57. Population exposure reduction (B737-800, 60dB L<sub>MAX</sub>) for PBN procedures at the highest-benefit 75 runways in the OEP-35..... 142

Figure 58. JFK runway 13R noise-minimal procedure centerlines for RNAV with and without vertical guidance and RNP relative to a straight-in baseline (Boeing 737-800, 60dB L<sub>MAX</sub>) ..... 143

Figure 59. JFK runway 13L noise-minimal procedure centerlines for RNAV with and without vertical guidance and RNP relative to a straight-in baseline (Boeing 737-800, 60dB L<sub>MAX</sub>) ..... 143

Figure 60. MSP runway 35 noise-minimal procedure centerlines for RNAV with and without vertical guidance and RNP relative to a straight-in baseline (Boeing 737-800, 60dB L<sub>MAX</sub>) ..... 144

Figure 61. SEA runway 34L noise-minimal procedure centerlines for RNAV with and without vertical guidance and RNP relative to a straight-in baseline (Boeing 737-800, 60dB L<sub>MAX</sub>) ..... 144

Figure 62. TPA runway 19L noise-minimal procedure centerlines for RNAV with and without vertical guidance and RNP relative to a straight-in baseline (Boeing 737-800, 60dB L<sub>MAX</sub>) ..... 145

Figure 63. LGA runway 4 noise-minimal procedure centerlines for RNAV with and without vertical guidance and RNP relative to a straight-in baseline (Boeing 737-800, 60dB L<sub>MAX</sub>) ..... 145

Figure 64. System-level change in Person-Event Impact from implementing noise-preferred PBN procedures for every jet arrival at the OEP-35 airports in 2017 ..... 147

Figure 65. Airport-level change in PEI from implementing noise-preferred PBN procedures for every jet arrival at the OEP-35 airports in 2017..... 148

Figure 66. Impact of maximizing net population reduction vs. benefit leverage ratio using RNAV procedures with vertical guidance for MSP runway 30R..... 150

Figure 67. Pareto set for the objectives of net population reduction and benefit leverage ratio for RNAV approaches with vertical guidance for MSP Runway 30R..... 151

Figure 68. Map view of set for the objectives of net population reduction and benefit leverage ratio for RNAV approaches with vertical guidance for MSP runway 30R..... 152

Figure 69. Pareto set for the objectives of net population reduction and benefit leverage ratio for RNAV approaches with vertical guidance for IAD runway 1L..... 153

Figure 70. Map view of population and benefit leverage-preferred RNAV procedure at IAD runway 1L..... 153

Figure 71. Subset of RNAV procedure designs showing notional track length implications for lateral track redesign relative to a straight-in baseline ..... 155

Figure 72. Pareto set trading net population reduction (60dB L <sub>MAX</sub> ) and track length reduction for RNAV approaches with vertical guidance for MSP Runway 30R (west arrivals)	156
Figure 73. Pareto set tracks for RNAV approaches with vertical guidance for MSP Runway 30R trading net population reduction (60dB L <sub>MAX</sub> ) and track length reduction (west arrivals)	156
Figure 74. Pareto set trading net population reduction (60dB L <sub>MAX</sub> ) and track length reduction for RNAV approaches with vertical guidance for MSP Runway 30R (east arrivals)	157
Figure 75. Pareto set tracks for RNAV approaches with vertical guidance for MSP Runway 30R trading net population reduction (60dB L <sub>MAX</sub> ) and track length reduction (east arrivals)	158
Figure 76. Standard jet departure profile	160
Figure 77. L <sub>MAX</sub> noise contours for a 737-800 departure with target climb speeds varying from 160 knots to 250 knots	161
Figure 78. Speed constraint notations on Las Vegas STAAV Eight RNAV SID	164
Figure 79. Reduced speed departure profile for the Embraer 170 with speed target of 220 Knots Indicated Airspeed	165
Figure 80. Reduced speed departure profile for the Boeing 737-800 with speed target of 220 Knots Indicated Airspeed	166
Figure 81. Reduced speed departure profile for the Boeing 777-300 with speed target of 240 Knots Indicated Airspeed	166
Figure 82. 60dB L <sub>MAX</sub> contour half-widths for reduced speed departures	167
Figure 83. 70dB L <sub>MAX</sub> contour half-widths for reduced speed departures	168
Figure 84. GLDMN Five RNAV SID from Runway 13 at LGA	169
Figure 85. B737-800 noise benefits from a reduced-speed departure on the GLDMN Five RNAV SID from LGA runway 13 (60dB L <sub>MAX</sub> )	169
Figure 86. B737-800 noise benefits from a reduced-speed departure on the PORTT4 RNAV SID from EWR runway 22R, ELIOT Transition (60dB L <sub>MAX</sub> )	171
Figure 87. B737-800 noise benefits from a reduced-speed departure on the PATSS5 RNAV SID from BOS runway 33L (60dB L <sub>MAX</sub> )	171
Figure 88. B737-800 60dB L <sub>MAX</sub> noise reduction potential from reduced speed departures as a function of average 2017 daytime jet departure frequency from the associated runway	172
Figure 89. System dynamic model for noise-motivated procedure development	175
Figure 90. NEPA environmental review process	185
Figure 91. Summary of FAA JO 7100.41A: PBN Implementation Process	187
Figure 92. Comparison between flight track density from BOS Runway 33L jet arrivals between 2010 and 2015 (Source: HMMH via [141])	191
Figure 93. jetBlue RNAV Visual approach procedure to Runway 33L (blue) compared with an example RNAV draft nonprecision instrument approach procedure	193
Figure 94. Noise exposure reduction for the Boeing 737-800 arriving Runway 33L descending via procedure recommendation 1-A1a on 3° descent profile	195
Figure 95. Comparison between flight track density from BOS Runway 33L jet departures between 2010 and 2015 (Source: HMMH via [141])	197

Figure 96. Comparison between flight track density from BOS Runway 27 jet departures between 2010 and 2015 (Source: HMMH via [141]) .....	198
Figure 97. Noise exposure reduction for the Boeing 737-800 departing runway 33L via the BLZZR4 departure on a standard climb profile compared to a 220-knot reduced speed departure. Noise Model: NASA ANOPP .....	200
Figure 98. Noise exposure reduction for the Boeing 777-300 departing runway 33L via the BLZZR4 departure on a standard climb profile compared to a 240-knot reduced speed departure. Noise Model: NASA ANOPP .....	201
Figure 99. Noise exposure reduction for the Embraer E-170 departing runway 33L via the BLZZR4 departure on a standard climb profile compared to a 220-knot reduced speed departure. Noise Model: NASA ANOPP .....	201
Figure 100. Noise exposure reduction for the Boeing 737-800 departing runway 27 via the BLZZR4 departure on a standard climb profile compared to a 220-knot reduced speed departure. Noise Model: NASA ANOPP .....	202
Figure 101. Unconstrained best-case cumulative person-event impact benefit for PBN guidance technologies at the OEP-35 airports with a notional comparison to RNAV Visual procedures.....	206
Figure 102. Map Depiction of OEP-35 Airports.....	214



# List of Acronyms and Abbreviations

Term	Definition
AAO	Adverse Assumption Obstacle
AEDT	Aviation Environmental Design Tool
AEP	Airport Environment Program
AGL	Above Ground Level
ANOPP	Aircraft Noise Prediction Program
ASDE-X	Airport Surface Detection Equipment Model X
ASPM	Aviation System Performance Metrics
ATC	Air Traffic Control
BADA	Base of Aircraft Data
Baro-VNAV	Barometric Vertical Navigation
BOS	Boston Logan Airport
BWI	Baltimore Washington International Airport
CATEX	Categorical Exclusion
CEQ	Council on Environmental Quality
CIFP	Coded Instrument Flight Procedures
dba	A-weighted Decibels
DCA	Washington National Airport
DLR	German Aerospace Center
DNL	Day-Night Average Level
DTA	Distance of Turn Anticipation
EA	Environmental Assessment
EIS	Environmental Impact Statement
Ej	Environmental Justice
FAA	Federal Aviation Administration
FAA/AFS	FAA Flight Standards Service Branch
FMS	Flight Management System
FONSI	Finding of No Significant Impact
FROP	Final Roll-Out Point
GBAS	Ground Based Augmentation System
GLS	GBAS Landing System
GPA	Glide Path Angle
GPS	Global Positioning System
IAF	Initial Approach Fix
IAP	Instrument Approach Procedure
ICAO	International Civil Aviation Organization
IF	Intermediate Fix
ILS	Instrument Landing System
INM	Integrated Noise Model
JFK	New York JFK Airport
KIAS	Knots Indicated Airspeed
KTAS	Knots True Airspeed

<b>Term</b>	<b>Definition</b>
LAX	Los Angeles International Airport
LGA	New York La Guardia Airport
LMAX	Maximum Sound Pressure Level
LNAV	Lateral Navigation
LOA	Letter of Agreement
LPV	Localizer Performance with Vertical Guidance
MAGENTA	Model for Assessing Global Exposure to the Noise of Transport Aircraft
MAP	Missed Approach Point
Massport	Massachusetts Port Authority
MCA	Multiple Criteria Analysis
MSP	Minneapolis - St. Paul Airport
NABOVE	Number of Overflights Above Noise Threshold
NADP	Noise Abatement Departure Procedure
NAS	National Airspace System
NASA	National Aeronautics and Space Administration
NCP	Noise Compatibility Program
NDI	Noise Depreciation Index
NEPA	National Environmental Policy Act
NextGen	FAA Next Generation Air Transportation System
NIRS	Noise Integrated Routing System
NPD	Noise-Power-Distance
OCS	Obstacle Clearance Surface
ODP	Obstacle Departure Procedure
OEP-35	Operational Evolution Partnership 35 airports
ORD	Chicago O'Hare Airport
PANAM	Parametric Aircraft Noise Analysis Module
PBN	Performance-Based Navigation
PEI	Person-Event Impact
PFAF	Precision Final Approach Fix
PNL	Perceived Noise Level
RF	Radius-to-Fix Leg Type
RNAV	Area Navigation
RNP	Required Navigation Performance
RNP-AR	RNP with Authorization Required
ROC	Required Obstacle Clearance
ROD	Record of Decision
RVFP	RNAV Visual Flight Procedure
SEA	Seattle-Tacoma International Airport
SEL	Sound Exposure Level
SID	Standard Instrument Departure
SOP	Standard Operating Procedure
SPL	Sound Pressure Level
STAR	Standard Terminal Arrival Route
TASOPT	Transport Aircraft System Optimization
TERPS	US Standard for Terminal Information Procedures

<b>Term</b>	<b>Definition</b>
TF	Track-to-Fix Leg Type
TPA	Tampa International Airport
VDA	Visual Descent Angle
VEB	Vertical Error Budget
VNAV	Vertical Navigation
VOR	VHF Omnidirectional Range
VREF	Approach Reference Speed
WAAS	Wide-Area Augmentation System
XTT	Cross-Track Tolerance





# Chapter 1. Motivation and Objectives

## 1.1 Problem Introduction

This thesis describes a system-level framework for developing new arrival and departure flight procedures, evaluating noise, and communicating impacts to communities and other stakeholders. Noise impacts are one of several key sociotechnical factors driving change in the modern air transportation system. A diverse set of stakeholder objectives and feedback mechanisms guide the system dynamic process of procedure inception, development, and implementation. The continued rollout of advanced satellite-based navigation and guidance technologies requires systematic integration of feedback from communities as well as operational stakeholders, considering the full diversity of objectives and stakeholder inputs. The methodological and analytical framework introduced in this thesis is applied to an example system-level best-case benefits analysis of modern satellite-based navigation procedures and reduced speed departure procedures.

Aircraft noise is an increasingly common source of community concern with respect to air transportation activity. The role of noise assessment in traditional procedure design incorporates community feedback in a manner that misses key elements driving complaints, often resulting in strained relations between airports and surrounding populations. While it is well understood that noise generation and propagation to the surface is an unavoidable consequence of aviation activity, operational and technological modifications can be used to reduce impact. Despite a reduction in single-event aircraft noise over time[1], changes in flight volume, procedure design, flight patterns, and community expectations have resulted in an increase in complaints.

Arrival and departure procedure modification for community noise reduction is complicated due to variable stakeholder priorities and complex technical constraints. Flexibility in aircraft flight tracks is limited by aircraft performance, navigation technology, traffic separation requirements, airspace capacity, and regulatory considerations. Furthermore, the success criteria for a procedure modification may be different for various communities surrounding an airport. A beneficial change

for one neighborhood may correspond to a detrimental noise increase for another. Stakeholder incentives are variable both across broad groups (airline incentive structures differ from surrounding communities and airports) as well as within groups (individual communities may favor solutions not in the best interest of other populations).

Operating under the assumption that airports provide valuable connectivity that drives economic activity on a regional and global level, it is important to preserve passenger and cargo throughput as part of any noise solution. All flights must take off and land from a limited set of runways at an airport, placing a constraint on where flights may be distributed in the immediate vicinity of the airport. Community expectations with respect to quality of life may not include personal evaluation of benefits from air transport. For example, an individual may rely on an early-morning flight to reach an important meeting one morning, only to be awakened by the same flight departing overhead the following morning. Despite the personal benefit arising from airport activity, being awakened by aircraft noise may generate a strong sense of annoyance nonetheless. While not all people impacted by noise utilize air transportation directly, most benefit from economic activity induced by thriving air transportation. It is important to explore opportunities to reduce annoyance from aircraft noise while simultaneously acknowledging the economic importance of airport activity.

In typical procedure redesign processes, community stakeholders have high-level noise reduction objectives and procedure modification concepts that do not account for complex technical constraints and opportunities. Analysts and regulators in the procedure development process may not be positioned to communicate these constraints and opportunities in a timely and effective manner, resulting in a disconnect between community desires and the realistic opportunity space for system modification. With a better understanding of the interactions and processes connecting these technical and political components, there is an opportunity to improve the system evolution process to more efficiently account for community desires while meeting technical and operational objectives.

The framework introduced in this thesis is demonstrated in the context of representative case studies evaluating specific advanced operational procedures with potential noise reduction implications. These procedures are introduced in a generic sense, evaluated at specific airports, and

applied to a simplified system-level analysis to determine potential noise implications. The benefits mechanisms and potential operational implications expected from each procedure are explored in the context of the noise evaluation framework developed in this thesis. These case studies suggest several best practices for noise-motivated arrival and departure procedure development.

## **1.2 PBN Track Concentration**

The drivers of aircraft noise complaints have shifted over the past decade. While noise has been a focal point of airport environmental planning and policy for decades, recent developments in navigation and surveillance technology have enabled new high-precision approach and departure operational procedures using GPS and Performance-Based Navigation (PBN) standards. These procedures have proven effective for reducing fuel consumption and streamlining some aspects of air traffic control. In addition, the procedures have resulted in increased access and improved safety at airports with challenging terrain or airspace constraints. However, flight tracks that were previously dispersed over wide areas due to less precise navigation or air traffic control (ATC) vectoring are more concentrated on specific published tracks with effects on underlying communities. Figure 1 shows flight track concentration for arrivals and departures at Boston Logan International Airport (BOS) before and after implementation of arrival and departure procedures using Area Navigation (RNAV), a type of PBN procedure. The change in flight path concentration that results from RNAV arrival and departure routes is qualitatively evident from the figure.

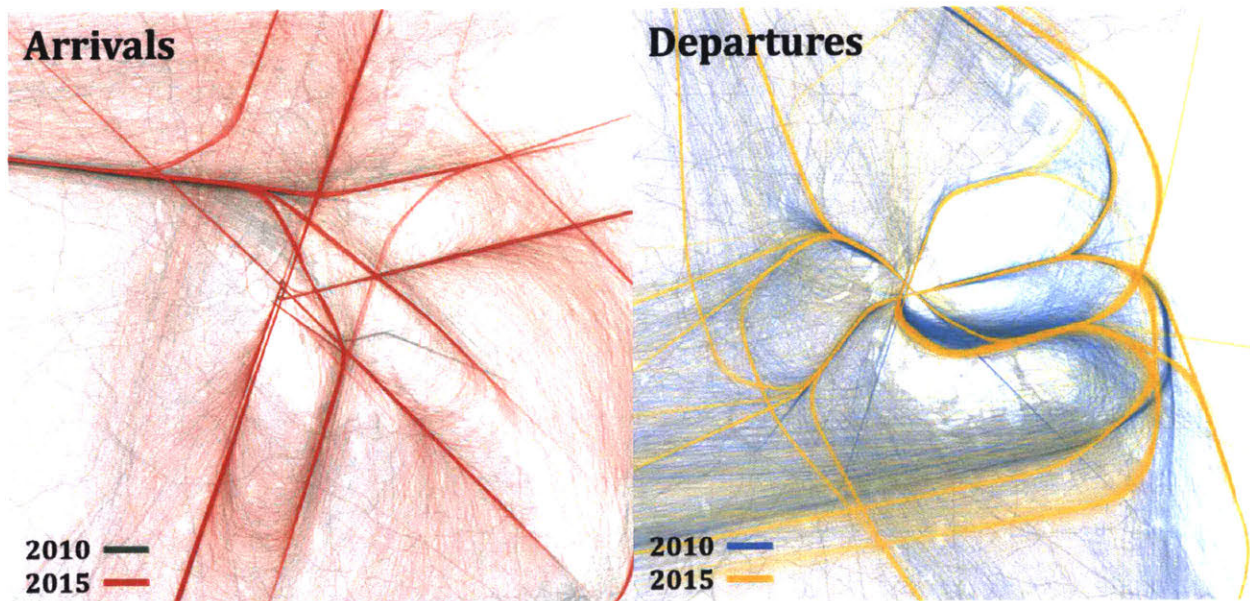


**Figure 1. Aircraft flight tracks for operations at BOS before (2010) and after (2015) RNAV implementation (Source: Massport Noise and Operations Management System)**

PBN procedure implementation is a central component of air traffic control modernization under the Federal Aviation Administration’s (FAA) Next Generation Air Transportation System (NextGen). The original objective of the procedures was to increase safety, fuel efficiency, and airport throughput while reducing pilot and ATC workload. In terms of noise, the new procedures were required to maintain or improve population exposure levels relative to existing procedures in accordance with federal environmental guidelines. This “no net harm” objective was defined relative to the existing regulatory noise metric (Day-Night Average Level, or DNL) and threshold (65 dB DNL) for significant exposure. In order to avoid triggering the need for costly and time-consuming Environmental Impact Statement based on NextGen procedure modifications, new RNAV and Required Navigation Performance (RNP) procedures were required to maintain or reduce the number of people exposed to these regulatory significant noise levels. In an effort to accelerate the development and implementation of RNAV procedures, Congress approved a special “categorical exclusion” from typical environmental assessment requirements under the National Environmental Policy Act (NEPA) for RNAV procedures. This approach to noise analysis and evaluation, combined with a development procedure that did not incorporate community stakeholder feedback early in the process, meant that the negative community reaction to PBN procedures was largely unanticipated.

Community concerns related to aircraft noise followed implementation of RNAV arrival and departure procedures are occurring at airports throughout the National Airspace System (NAS). It became evident that regulatory “noise significance” metrics and levels did not adequately capture annoyance and complaints arising from flight concentration. As an example of this phenomenon, Figure 2 shows the geographic location of noise complaints after RNAV deployment at BOS relative to the 65dB DNL contour. It is seen that most complaints occur well outside the 65dB contour. Vocal opposition and requests for reconsideration of RNAV procedures based on noise annoyance were directed to airports, the FAA, and political representatives. Noise became a fundamental political constraint to continued RNAV deployment throughout the NAS, increasing scrutiny on environmental review policies and NextGen priorities.

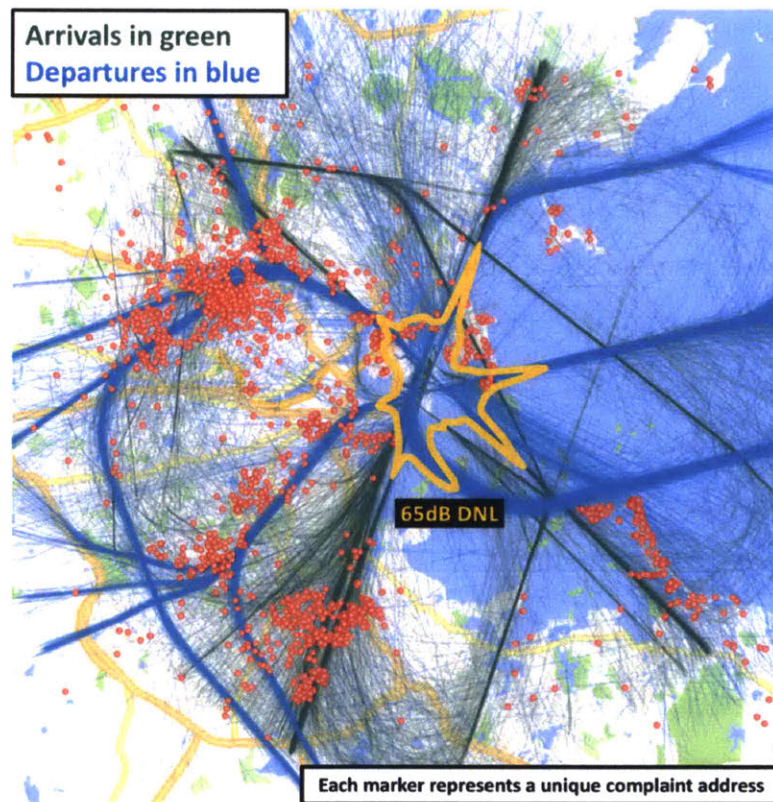


**Figure 2. 65 dB DNL contour vs. noise complaint locations (red circles)**

Communities around the US have expressed frustration with flight track concentration and noise arising from PBN implementation, resulting in increased political and legal action at airports throughout the country [2]. At the same time, operational and safety benefits of PBN and the worldwide implementation of new procedures make it difficult to revert to non-PBN procedures.

Ideally, PBN technology and procedures could be used to reduce overflight noise while retaining operational benefits [3]. The challenges associated with flight track concentration may be addressable through a clearer system-level view of noise evaluation processes, methods, and metrics. This thesis introduces a noise analysis framework that acknowledges the diversity of stakeholder priorities and interplay between complex sociotechnical factors in the noise management process. The presentation of this framework involves several key elements:

- Development of a noise analysis method and corresponding visualizations to enable feedback and negotiation between stakeholders from different technical and operational contexts, particularly with respect to available advanced operational procedures for noise reduction
- Discussion of several promising operational techniques available for noise reduction, including expected noise benefits at the 35 US Operational Evolution Partnership (OEP-35) airports and potential barriers to entry for each concept
- Introduction to a real-world case study involving procedure development incorporating stakeholder feedback within the sociotechnical framework developed above, utilizing noise analysis tools and visualizations to enable productive design iteration and refinement while respecting operational and safety requirements
- Discussion of emergent characteristics of particular operational procedures on a system level, including potential benefits and opportunities for advanced PBN procedure implementation

### **1.3 Sociotechnical System Framework for Procedure Development**

Arrival and departure procedure redesign programs may be initiated in response to operational, environmental, or technological drivers. Operationally-motivated procedures are normally intended to increased throughput, efficiency, and safety for runways and airspace. Procedures intended to reduce environmental impact may be initiated in response to community feedback and complaints or broad-based policy objectives with respect to noise, air quality, and emissions. In some cases, new technological capabilities in terms of navigation capability or aircraft performance standards may

allow for the design of new arrival and departure procedures to supplement or replace existing procedures that made use of older technology. Such redesign efforts enabled by technology infusion into the NAS may enable both operational and environmental benefits.

As discussed above, PBN navigation technology has enabled new and precise arrival and departure procedures. The design and implementation process of new RNAV and RNP procedures around the NAS has focused primarily on operational drivers (lowering minima for runways in the vicinity of terrain, increasing efficiency, and improving safety) while treating noise as a constraint on a “do no harm” basis according to existing metrics, thresholds, and NEPA review requirements. Regardless of the motivation and objectives for a new procedure development program, compliance with environment review and reporting regulations is mandatory. When developmental drivers are primarily operational, environmental evaluation and public feedback may not be considered during the preliminary development process.

It is clear that implementation of NextGen procedures in the NAS could be more successful if community feedback on noise impact was included in the procedure iteration process. While noise cannot be the sole concern in procedure development, consideration at a stage prior to NEPA review in the pre-implementation process has the potential to address community objections more effectively and increase buy-in for the eventual solution. This thesis introduces a framework for noise evaluation that incorporates environmental and operational objectives. This framework (shown in Figure 3) begins with the baseline procedure and noise environment (shown in the upper left) driving community responses and complaints (upper right). Communities react and request changes through a technical analysis process, which also accounts for operational system constraints and stakeholder values (shown in the lower right). Formal procedure requests from this process are ultimately forwarded to a formal pre-implementation process (shown on the left), including regulatory (NEPA) environmental review and operational implementation processes. Successful implementation pre-implementation processes result in new or modified procedures being integrated into the baseline noise environment. For this thesis, the framework and its implications for the procedure design process are discussed in the context of a specific PBN arrival and departure redesign effort at Boston Logan Airport.

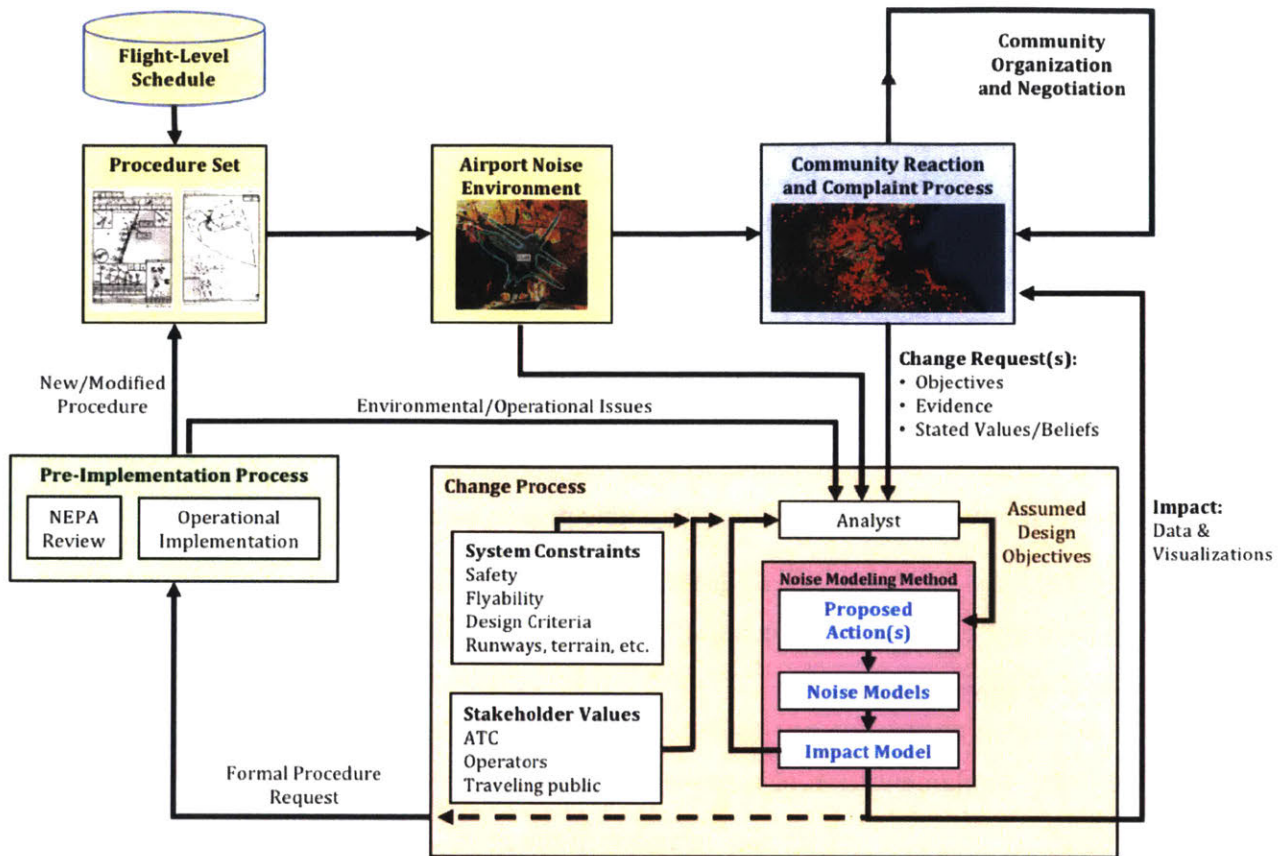


Figure 3. Sociotechnical system framework for flight procedure development

## 1.4 System Noise Benefits of Specific Operational Procedures

Advanced arrival and departure procedures have the potential to reduce noise through two pathways:

- Increased use of modern guidance and navigation technology
- Modifications to how airplanes are flown on existing procedures, including management of aircraft speed, thrust, altitude, and/or configuration

Such procedure modifications could also increase the options available to procedure designers and communities when discussing redesign efforts, providing opportunities for community engagement and successful outcomes consistent with air traffic control modernization efforts. This thesis discusses the potential system noise reduction potential examples from both advanced operational procedure pathways (advanced navigation and profile management), providing specific



examples of the opportunity space for procedure modification under the flight procedure development framework.

## **1.5 Thesis Outline**

Chapter 2 provides a background on the aircraft noise problem. This includes an introduction to the physics of noise generation and propagation, human response and impact, noise modeling techniques and tradeoffs, and regulatory frameworks constraining procedure design with respect to operational and environmental objectives.

Chapter 3 introduces an analysis framework used in this project for evaluating noise and population impacts from modifications to arrival and departure procedures. Noise metric selection and communication of impacts to communities are discussed.

Chapter 4 provides a summary of current design standards and other considerations for PBN approach procedure design. The key design constraints for RNAV and RNP procedures are discussed along with a discussion of current characteristics for published approaches around the NAS.

Chapter 5 provides an analysis of noise-reduction potential from PBN arrival procedures at every runway end for 35 major airports in the US OEP-35 airports. The potential benefits from RNAV and RNP procedures are discussed through an analysis at all 282 runways in the OEP-35.

Chapter 6 provides an analysis of noise-reduction potential from reduced-speed departure constraints applied to RNAV departure procedures at the major airports in the US.

Chapter 7 introduces the multi-stakeholder sociotechnical system framework for evaluating flight procedures. Implications for procedure design and implementation are discussed. An example procedure development process at Boston Logan Airport is introduced to illustrate practical opportunities and challenges using such a framework.

Chapter 8 draws conclusions about implementing an arrival and departure procedure design process that incorporates both operational and environmental objectives. The primary contributions of the thesis are summarized. Considerations for arrival and departure procedure design efforts are

discussed to maximize the positive environmental potential of NextGen technologies in conjunction with operational and safety objectives.

# Chapter 2. Literature Review and Background on Aircraft Noise

## 2.1 Physics of Aircraft Noise

Aircraft noise is a physical phenomenon defined as undesirable sound arising from an aircraft source. Noise generation arises from a combination of engine sources, aircraft aerodynamics (such as the turbulent flows around landing gear and high-lift devices), propulsive mixing and pressure fields in the aircraft wake, and mechanical interactions within the engine and aircraft systems.

### 2.1.1 Noise Sources on an Aircraft

Broadly speaking, aircraft noise emanates from both aerodynamic and engine sources. Engine noise from a turbojet arises from several independent sources. Each of these sources is associated with a directivity pattern as well as frequency and tonal characteristics that impact the far-field noise experienced by an observer on the ground. *Fan noise* occurs due to shock formation at the tips of engine intake fan blades at high thrust settings and due to wake interactions between fan blades. Additional *core noise* components occur due to mechanical/aerodynamic interactions and vibrations in the compressor, bypass duct, combustor, and turbine sections of the engine. Each of these noise sources can be mitigated with tailored component aerodynamics, engine material tuning, and acoustic liners in the engine nacelle [4]. *Jet noise* is generated at the shear layer between the high-velocity exhaust stream exiting the rear of the engine and the surrounding ambient airflow and/or bypass stream. The velocity differential in the shear layer is dissipated through vorticity and turbulence that is ultimately experienced as noise. The physics of this dissipation is fundamentally difficult to model due to the chaotic nature of turbulence, making theoretical jet noise prediction an area of fertile continued research and experimentation [5].

Engine noise was traditionally louder than airframe noise such that modeling efforts could focus on engine sources with only low-fidelity treatment of airframe sources without a major loss in overall

sound level prediction. With the reduction in engine noise corresponding to increasing bypass ratios and modern engine materials, airframe sources have become a larger contributor to the total perceptible noise signature from an aircraft. Airframe noise is generated due to bluff-body turbulence (large-scale irregular vortex shedding from large components including the fuselage, high-lift devices, and wings) and small-scale turbulence from parasitic components such as landing gear, high-lift device tracks and fairings, and flap/slat edge interactions [6].

The larger-scale bluff body noise sources, often referred to as clean-airframe noise, results from the shear mixing between turbulent boundary layers and the free-stream velocity. The theoretical far-field noise contribution from this effect is proportional to the fifth power of aircraft velocity, meaning that clean-airframe noise is significantly higher for fast-moving aircraft [7]. Airframe noise generated by landing gear and other parasitic sources is much more complicated from a detailed flow modeling perspective, involving both direct vortex shedding by components as well as aerodynamic interactions with downstream physical components and flow fields [6]. This effect is highly dependent on aircraft-specific configuration details. For example, the Airbus A320 family has a well-known airframe noise component arising due to fuel vent openings in the wings generating an audible whistle tone. While this tone specifically is addressable through the addition of vortex generators upstream of the vent openings [8], the original tonal noise problem would have been very difficult to predict with conventional modeling capability.

### **2.1.2 Propagation and Perception**

The perceptible loudness associated with a sound is proportional to the sound pressure level (SPL) of an acoustic wave striking the eardrum. Noise is typically quantified in decibels, a logarithmic unit that compares the magnitude of SPL in a sound wave to a reference level representative of the minimum sound perceptible to average human listeners. A ten-decibel increase in SPL corresponds to an approximate doubling in perceived loudness [9]. While the absolute SPL provides important information about the annoyance associated with a particular noise event, additional characteristics also play key roles in perceptibility and noise quality. In general, annoyance from noise is a function of sound intensity, spectral composition, tonality, exposure frequency, time of day, and personal preference among other factors.

To the first order, a transient broadband noise is not perceptible to a human observer when background environmental noise exceeds the SPL of the noise event and has similar spectral characteristics. However, much as a distinctive voice or laugh can be discerned in a crowded room, a noise below surrounding environmental SPL levels may be both perceptible and displeasing due to spectral and tonal variation from the background [10]. Aircraft noise signatures are often highly tonal due to steady-state mechanical movements inside the engine (e.g., rotational movement of engine components) and speed-based aerodynamic effects (including whistle tones excited at specific frequencies).

The magnitude and character of aircraft noise experienced on the surface is also impacted by the slant distance between the source and observer, atmospheric attenuation and refraction, surface composition, sound reflection and interference, terrain, and structural insulation. In the absence of other factors, simple spherical wavefront spreading results in a reduction in SPL of 6dB for a doubling of observer slant range distance. For realistic aircraft noise sources, sound energy is concentrated by directivity, resulting in reduction in expected attenuation from wavefront spreading.

Additional attenuation in the atmosphere occurs through conversion of sound energy to heat due to molecular excitation and interaction. The magnitude of atmospheric attenuation is highly dependent on temperature and humidity. Attenuation increases for higher-frequency noise sources, meaning that low-frequency spectral and tonal components are audible farther from the noise source than high-frequency components at the same source pressure level [11]. Meteorological conditions also play an important role, with non-linear influence from both temperature and humidity. In general, total attenuation is greatest in low-humidity conditions due to increased overall air density. There is also strong temperature dependence, although the functional relationship is non-monotonic and dependent on humidity and sound frequency [12]. Taken cumulatively, the variability of atmospheric attenuation based on temperature and humidity complicate modeling efforts for noise propagation to the surface, leading to potential modeling discrepancies when standard atmospheric conditions are assumed for all operations.

Temperature profiles with altitude, wind direction, and small-scale turbulence in the atmosphere also contribute to variations in noise absorption and propagation pathways from an

aircraft source to the surface. To the first order, sound waves refract (or bend) away from the surface in standard temperature profiles (warmer at lower altitudes) and toward the surface in temperature inversion conditions (increase in temperature with altitude). Wind profiles also contribute to sound wave refraction due to any wind velocity gradient with altitude. Increasing wind speed with altitude results in refraction toward the surface in the downwind direction and away from the surface in the upwind direction [11].

Surface composition has a strong effect on noise experienced on the surface. Surfaces are broadly categorized into acoustically “hard” and “soft” surfaces, indicating the degree to which sound pressure waves are reflected or absorbed. Acoustically hard surfaces are characterized by strong reflection, reducing attenuation on the ground and causing noise propagation distances to increase. This is commonly experienced over open water, for example. Acoustically soft surfaces reflect sound waves to a lesser degree and absorb more energy directly. Vegetation and soil reduce sound wave reflection. Acoustically hard surfaces also result in stronger ground effects including multi-path interactions between direct and reflected sound waves. Depending on the geometry of the noise source, reflecting surface, and observer, this can increase or decrease the absolute noise level experienced at an observer location through constructive or destructive interference between sound waves.

Sound propagation to an observer is also affected by barriers between the source and observer, whether natural or artificial. In the outdoor environment, topographic features or manmade structures impact wavefront propagation, normally providing a noise shielding effect. In addition, sound insulation of inhabited structures and dwellings reduces the noise experienced inside those structures. The quality and construction of windows, doors, walls, and ventilation systems have a strong impact on attenuation of noise from the outdoor environment to the indoor environment.

The physical characteristics of aircraft noise generation, propagation, and perception are sufficiently complicated to pose challenges for rapid and efficient computational modeling. Source noise fidelity and spectral characteristics, atmospheric assumptions, surface modeling, and underlying population data all impact the accuracy of noise models relative to empirical

measurement data. Section 2.4 introduces the typical approaches used for aircraft noise modeling and propagation.

## **2.2 Effects of Aircraft Noise**

This thesis focuses on the impact from aircraft noise on underlying population in terms of annoyance as expressed in broad community sentiment and complaints. A growing body of research aims to quantify human health and sociological impacts attributable to aircraft noise to a degree of confidence sufficient for policymaking. Broadly speaking, negative consequences arise from sleep interruption, learning disruption for children, and increased risk to cardiovascular health due to stress and other intermediary effects [13]. This section presents a brief introduction to the impacts of aircraft noise on human populations, motivating the importance of noise reduction research and mitigation efforts.

### **2.2.1 Annoyance from Noise**

The ultimate objective of any noise study is to quantify the psychological impact of noise on people in surrounding communities. If a given combination of sound characteristics does not produce annoyance, there should be no concern with that sound source. However, the meaning of ‘annoyance’ and the resulting analysis techniques are widely debated amongst experts and impacted communities [14].

Noise is a key component impacting the total environmental footprint from aviation, along with emissions (climate impacts and air quality) [15]. Despite subjectivity in the definition and evaluation of noise, many in the literature have attempted to quantify annoyance as a function of sound exposure. An SPL time history from a typical aircraft overflight event is shown in Figure 4. While absolute pressure level does not translate directly to human annoyance from noise, the characteristics of overflight events are used to calculate acoustic metrics such as Sound Exposure Level (SEL) and Maximum Sound Level ( $L_{MAX}$ ), both of which are used in population impact analysis. These metrics and other integrated derivatives are presented in more detail in Section 2.5.

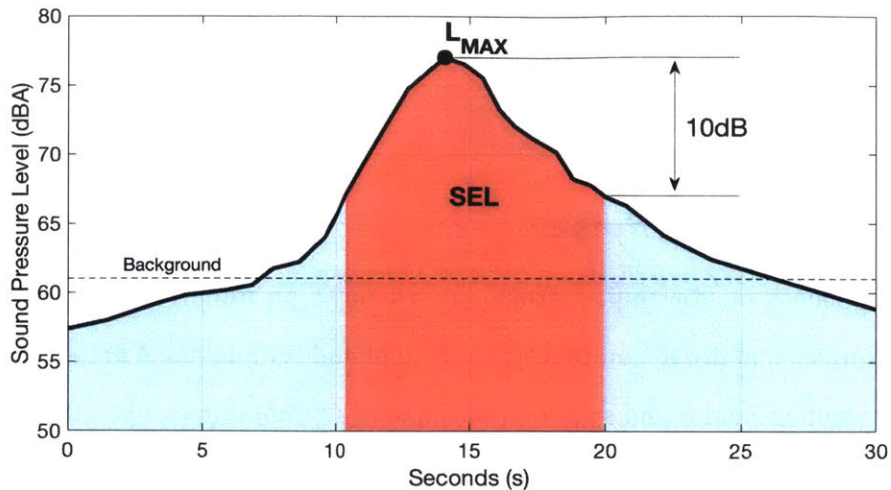


**Figure 4. Sound pressure level time history at a single observer location illustrating  $L_{MAX}$  and SEL metrics**

Annoyance measures generally account for the absolute magnitude of sound pressure level, tonal characteristics, frequency exposure, and other environmental variables. Early research in the field of aircraft acoustics attempted to identify which characteristics were primary drivers for perceived annoyance [16]. Kryter extended this research into early sound metric development that weighted particular frequency bands more heavily than others and accounted for tonality in an attempt to capture human annoyance response [17]. Perceived Noise Level (PNL) has been supplemented by a wide array of alternative metrics since Kryter's early work, notably DNL [18]. Different metrics are suitable for different types of analysis, leading to further complications in terms of translating quantitative noise metrics to community annoyance values.

Schultz established the first formal functional relationship between DNL and perceived annoyance using a survey approach [19]. This "Schultz Curve" was the basis for selecting 65 dB DNL as the significant noise threshold for the purpose of legal interpretation in the US. Others have extended this survey-based approach using larger data sets, also examining annoyance from other transportation methods [20]. In the intervening years, Fidell and others have evaluated the underlying assumptions driving the dose-response methods and metrics pioneered by Schultz and attempted to identify refinement opportunities (i.e. [21]). Finegold et al revisited the concept of annoyance to better emphasize disruptive noise exposure (i.e. sleep awakenings) compared to other types of annoyance [22]. Guski integrated social science surveys and international expert opinions to



establish differences in annoyance characteristics by country, indicating a strong cultural component to how noise is perceived [14].

Recent studies indicate that community sensitivity to aircraft noise has increased over time [23], [24]. This is despite the fact that aircraft have become quieter in terms of single-event noise levels. The FAA has implemented regulatory noise limitations based on the certification noise levels for turbojet aircraft. The total effective perceived noise from three measurement locations must fall underneath a threshold of increasing stringency over time. These thresholds are referred to as noise “stages” [25]. Figure 5 shows the increasing noise stringency from Stage 2 (the earliest and least stringent standard applicable to early jets) to Stage 5 (the latest standard applicable to new certifications). The figure also shows actual certification noise levels for common turbojet aircraft types, illustrating that aircraft noise levels are reducing over time at a rate that exceeds regulatory requirements.

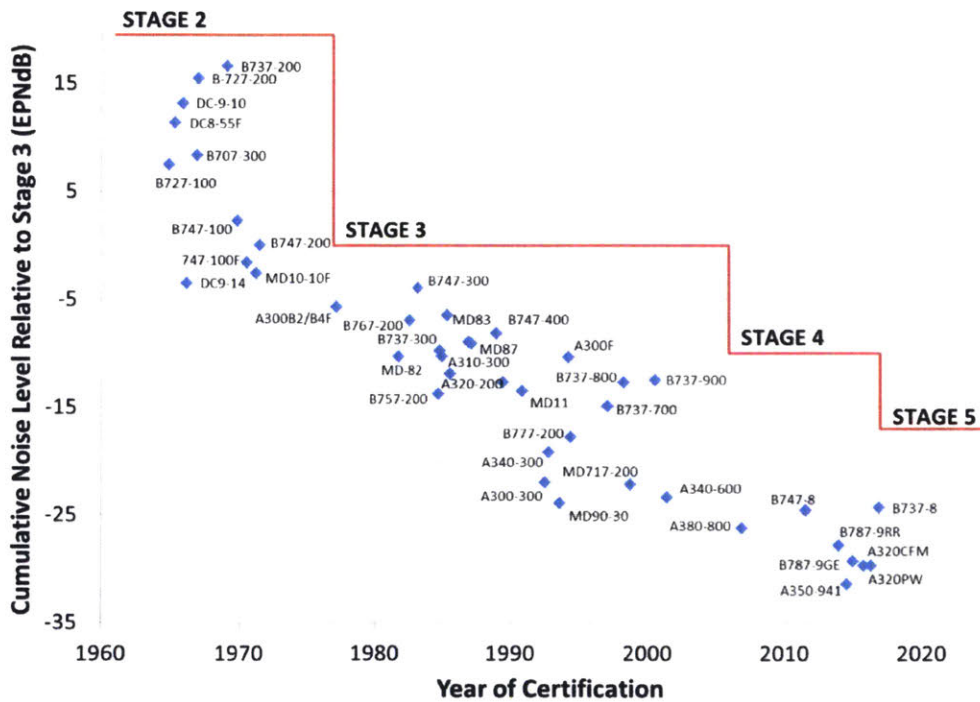


**Figure 5. Noise stage levels and certification values for common turbojet aircraft types as a function of certification year (Source: FAA [26])**

Technology improvements are expected to continue to reduce noise contour area [27], although this is not guaranteed to reduce community annoyance. Research by Brink indicates that changing

aircraft noise exposure (i.e. increased flight frequency or redesigned flight procedures) leads to stronger annoyance responses than steady-state noise [28]. In addition, research has consistently shown the importance of non-acoustic variables in determining community response to noise. Research by Job indicated that sound exposure accounted for less than 20% of variation in reported annoyance from community members, with the remainder associated with non-acoustic variables [29]. Non-acoustic variables that may have a stronger impact on annoyance than absolute sound levels were identified by Guski, such as general attitude toward aviation as well as sensitivity to noise regardless of level [30].

The general approach to quantifying annoyance is to correlate the measurable noise metrics introduced above with levels of subjective annoyance reported by sample subjects. These survey methods result in statistical distributions which are converted to annoyance functions using simple regression methods. Using these annoyance functions, appropriate regulatory thresholds for noise metrics can be established. For example, early synthesis done by Schultz led to the establishment of 65 dB Day-Night Average Level as a key regulatory cutoff for community noise mitigation programs, as shown in Figure 6. The analysis performed by Schultz compiled experimental data from 18 social surveys on noise annoyance correlated to annual average Day-Night Level arising from a combination of aviation, rail, and road noise [19].

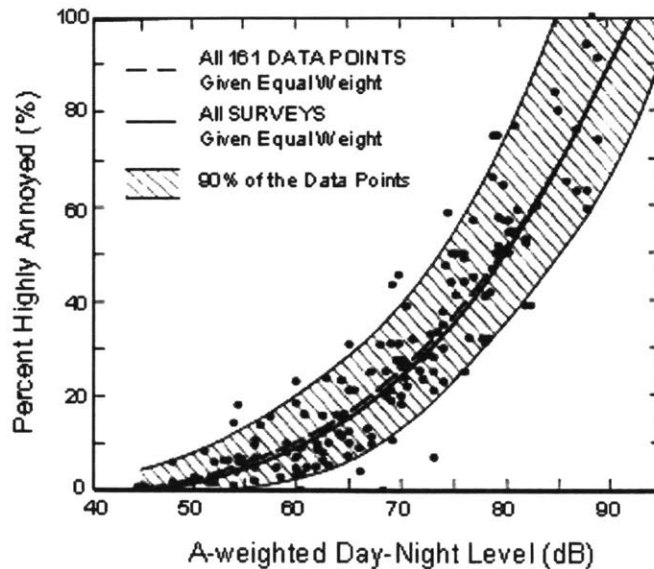


**Figure 6. Schultz Curve relating A-weighted DNL to community annoyance [19]**

The original work establishing the correlation between annual average DNL and community annoyance did not evaluate finer-resolution time impacts, such as frequency-driven annoyance occurring during peak utilization periods of transportation infrastructure. While the annual-average method is convenient for policy and regulatory purposes, its practical application is complicated by the large variation in community expectations between people and over time. Significant research effort has been devoted to quantifying annoyance levels. These studies attempt to refine methodology for collecting annoyance attitude data as well as the mathematical regression models used to fit these results. While refined models are available as a result of this work, most have not been implemented by regulators or analysts on account of longstanding legal precedent and policy use of existing metrics and tools [18]. Correlating measurable sound characteristics with community annoyance is central to the fundamental premise of noise regulation, which is to mitigate impacts of aircraft noise on quality of life for surrounding communities. Therefore, this correlation remains one of the great research and implementation challenges for aviation environmental specialists.

### **2.2.2 Sleep and Learning Effects from Noise**

Noise-induced delay of sleep onset and/or sleep disruption is associated with negative health and lifestyle outcomes including elements of general fatigue, immune system degradation, cardiovascular and endocrine system function, and psychiatric symptoms [31]. Measurable physiological responses to noise may be observed at sound pressure levels as low as 33 dB [32], although thresholds that cause awakenings are generally higher and are not consistent across samples. Local variables such as background noise levels, habituation patterns of residents, and sociopolitical norms result in highly contextual noise thresholds for sleep disturbance [33]. Nonetheless, sleep disturbance is one of the most acutely disruptive and noticeable byproducts of aircraft noise.

In terms of learning effects, several epidemiological studies appear to show that chronic noise exposure may impair reading and memory as well as standardized test scores ([34], [35]). The mechanism for this effect appears to be through communication disruption and distraction during school hours, as well as high correlation with heightened noise exposure outside of school hours and

at night due to proximity of schools to student homes. The World Health Organization recommends that classrooms be insulated to an equivalent sound pressure level of 35dB and that healthy outdoor playground environments be limited to equivalent sound pressure levels of 55dB to reduce learning impairment at schools due to noise [36].

### **2.2.3 Health Effects from Noise**

Research is ongoing with regard to direct health impacts from aircraft noise. Early work indicates possible links between noise and cardiovascular disease [37], [38]), hypertension [39], and psychological health [40], although the early-stage maturity of results has not led to noise policy changes pending further validation. Negative health effects of aircraft noise are generally determined through epidemiological studies that attempt to control for other risk factors leading to the outcome in question. While efforts are made to isolate noise impacts from other confounding variables, other demographic factors may be associated with housing locations in high-noise areas, suggesting a need for continued study in this area.

### **2.2.4 Social Effects from Noise**

Noise is a negative externality of air transportation imposed on communities. While this externality must be balanced with the positive economic benefits arising from air transportation, there are many potential methods for determining an appropriate level of noise (or other environmental impact) for a given economic benefit [41]. This is particularly difficult in the case of noise, where those experiencing the externality are often different from those experiencing the economic benefit. Social welfare is an integral component of noise regulation and policy, requiring simultaneous consideration with airline and airport efficiency objectives [42].

Social welfare is of particular concern to policymakers with respect to demographic variables including race and socioeconomic status. In the realm of environmental policymaking and system implementation, social welfare concerns are referred to as Environmental Justice (EJ). These concerns began entering the legal framework for policy evaluation in the 1990s, as fairness and equity became increasingly important in the evaluation of undesirable externalities from a wide variety of factors [43]. EJ considerations are a component of modern environmental assessments

performed for major transportation projects of all modes [44]. This concern is now considered a key component of noise assessment around airports [45]. Despite this growing consideration of EJ in the noise analysis process, there are no clear definitions or benchmarks of equity, meaning that analysis tools must be flexible to alternative policies and dynamic objectives moving forward.

Noise distribution around airports also has a strong impact on property values (quantified through the Noise Depreciation Index (NDI) [46]) and residential land development in metropolitan areas [47]. This leads to strong economic incentives for communities impacted by airport noise to request procedural modifications regardless of equity considerations [48]. Hedonic pricing models (which account for both internal and external price impact factors) and other methods have been applied in the economics literature to attempt to quantify the economic impact of noise on housing values, with potential implications for economic distribution of environmental externalities (e.g. [49]-[51]). Significant challenges remain with balancing economic and equity arguments in noise policy [52], further supporting the development of impact analysis tools capable of evaluating various stakeholder preferences and viewpoints.

### **2.2.5 Visual Effects on Perceived Noise**

Consistency of flight tracks on PBN arrival and departure procedures makes it easier for surface observers to visually acquire overflying aircraft. On clear-weather days, successive flights using the same procedure appear in nearly the same location in the visible line of sight from a structure or outdoor location. This results in heightened perceptibility of overflights regardless of acoustic factors. Aircraft size, speed, and lighting can also influence perceived altitude and noise levels.

Visual effects of air transportation activity are acknowledged as a source of environmental impact by FAA regulatory documentation [53]. State and local regulations, policies, and zoning ordinances that apply to visual effects on a case-by-case basis. However, there is no level of significance associated with “visual effects” from a federal standpoint. Furthermore, guidance states that “the visual sight of aircraft and commercial space launch vehicles, aircraft and commercial space launch vehicle contrails, or aircraft lights at night, particularly at a distance that is not intrusive,

should not be assumed to constitute an adverse effect<sup>1</sup>.” Therefore, while visual effects are an acknowledged non-acoustic factor associated with aircraft noise, visual concentration and/or dispersion of aircraft overflight locations is not generally considered in noise analysis.

## **2.3 Noise Reduction Literature Review**

Noise annoyance mitigation strategies can be classified in several broad categories. The International Civil Aviation Organization (ICAO) advocates a balanced approach between four strategies for noise reduction [54]:

- Noise Abatement Arrival and Departure Procedures
- Source Noise Reduction
- Operational Restrictions
- Land Use Restrictions

Girvin outlined the high-level potential for each area [55], [56]. Environmental planners hope to combine all of these techniques to maintain or reduce air transportation environmental impact despite forecasts for sustained growth [57].

In some cases, operational modifications are coupled with technological changes due to performance impacts, while in other cases the two effects can be treated independently. The most significant reductions in community noise impact have arisen from noise reduction at the source [58], most clearly as a result of engine technology improvement. Advanced research in acoustic signatures from aerodynamic sources continues, including an extensive body of research on flap and landing gear derived noise and physical modeling (i.e. [59], [60]). In 2008 Dobrzynski, et al presented a survey of current research for characterizing airframe noise with improved accuracy relative to legacy methods [61].

---

<sup>1</sup> FAA Order 1050.1F Desk Reference: Section 13.3.3

Air traffic management and operational strategies optimized for noise became an area of particular interest within the past 20 years. Clarke explored the implications of advanced air traffic management technology and operational procedures, with primary focus on arrival procedures including continuous descent approaches [62]–[64]. Kim, et al examined opportunities for procedure optimization including noise effects as well as sometimes-competing environmental objectives of fuel burn and emissions [65].

Much of the literature on procedure optimization for noise minimization has focused on single-procedure optimization given a population exposure reduction objective function. Betts provided a survey of numerical methods typically used in lateral flight route optimization [66]. Visser characterized the location-specific nature of the trajectory optimization problem with respect to noise [67]. Many researchers have examined specific lateral optimization algorithms. For example, Capozzi, et al examined lateral trajectory optimization schemes based on dynamically shifting population sensitivities [68]. Pratt, et al examined lateral optimization for departures given multiple discrete noise-sensitive surface locations and weightings [69]. However, it is widely agreed upon that future noise abatement arrival and departure procedures are likely to rely on altitude and speed dimensions in addition to lateral procedure design [70].

Aircraft performance modeling is a key component of noise modeling for advanced operational procedures that do not rely solely on lateral modification. All noise models require estimation of thrust throughout the various stages of a procedure, while more advanced models also make use of aircraft configuration to calculate airframe noise. Filippone reviewed current methods generally used for jet aircraft performance analysis for environmental studies [71]. Visser et al examined custom vertical profile generation and resulting noise analysis in Amsterdam in successive studies [72], [73].

Noise implications from specific procedures have been the subject of several recent studies. For example, Thomas et al developed a method to integrate performance models and advanced noise models to evaluate noise impacts of advanced operational procedures [74]. An example evaluation of a delayed deceleration approach procedure was analyzed using this framework to demonstrate its utility on an individual procedure basis with strong speed effects on airframe noise [75].

## **2.4 Modeling Aircraft Noise**

### **2.4.1 Noise Modeling Background and Literature Review**

Aircraft noise modeling has made significant strides in the past several decades. Initial noise models were driven primarily by engine noise as a function of thrust, derived broadly from empirical measurements. For example, the Aviation Environmental Design Tool (AEDT) uses a noise-power-distance (NPD) based approach that calculates noise based on thrust level and distance from the observer [76]. The primary drawback of this approach is a lack of aerodynamic noise modeling for various flap and slat configurations, landing gear settings, and general flow interactions causing noise on the airframe. Nonetheless, AEDT is the legal standard for noise analysis in current U.S. environmental reviews [77].

Over the past 40 years, increased audibility of airframe noise driven by quieter turbofan engine technology has driven improvements in modeling aerodynamic noise generation [6]. An example model with improved airframe noise treatment include NASA's Aircraft Noise Prediction Program (ANOPP) [78]. Several studies have attempted to validate the various models against empirical measurements (e.g. [79], [80]). No industry-standard noise analysis tool currently exists that capture all noise sources, with many competing alternatives. Full physics-based modeling of airframe noise may be feasible with advanced computation power in future tools, although the current set of alternatives rely on hybrid computational and heuristic methods [81].

### **2.4.2 Noise Model Fidelity**

Human perception of aircraft noise is driven by several components: source noise, propagation and atmospheric attenuation, ground reflection effects and absorption, background noise levels and characteristics at the observer location, and psychological factors affecting the observer. As modeling fidelity increases, computational burden can also increase significantly. All noise models include some accounting for variation in source noise, whether this is a simple correlation-based approach or a more involved physics-based method that accounts for various noise sources, accounting for speed and configuration among other factors. Due to the variety of complex aerodynamic and mechanical sources generating noise on an aircraft, a high-fidelity acoustic modeling approach can be too cumbersome for practical applications. Propagation, absorption, and shielding effects can be



accounted for with simplifying assumptions (such as standard atmospheric temperature, pressure, and humidity) or with higher-fidelity ray tracing methods [79]. Ground effects are dependent on surface composition, vegetation, and other factors such as snow cover. While accurate modeling of the surface may be incorporated in high-fidelity propagation models, the ground composition is normally classified as acoustically “hard” or “soft” to broadly characterize reflection and absorption properties without sacrificing computation time.

Environmental factors such as background noise are required for accurate determination of audibility metrics. However, background noise in a particular location is highly dependent on surrounding terrain and structures, time of day, observer location inside or outside of structures, and prevailing wind conditions. Background level mapping is typically unavailable at a sufficient resolution to enable audibility metrics on a case-by-case basis, resulting in standard threshold levels being applied in most cases.

Variation in psychoacoustic response factors between individuals also prevents effective incorporation of individual preferences in noise models. Therefore, noise models typically output acoustic variables directly. These acoustic variables can be further processed depending on a desired annoyance-response function or other impact evaluation strategy.

### **2.4.3 NPD Approach (AEDT)**

The standard analysis technique in the US for evaluating new flight procedures, paths, and schedules is the NPD approach. Noise levels are determined on a segment-by-segment basis using a lookup table or interpolation function based on slant-range distance between an observer and the aircraft location as well as aircraft thrust level. The NPD approach is implemented in the FAA’s AEDT and other third-party noise evaluation software packages based on Standard SAE-AIR-1845A [82].

For the NPD method, empirical data is collected for arrival and departure procedures in several aircraft configurations (characterized by flap setting, thrust level, and landing gear configuration). Based on these configurations, noise levels are interpolated as a function of observer distance from the noise source assuming a standard atmosphere and consistent sound energy dissipation with distance. Noise for thrust levels other than those with data available are determined by interpolating

between the available arrival and departure thrust levels. The number of NPD curve sets varies by aircraft type within most of these models, generally ranging from 4 to 12 curves (different power settings or configurations) per engine family. In AEDT, NPD curves are typically provided for aircraft in an approach configuration - to capture aerodynamic source noise with flaps and landing gear extended - and a departure configuration representing a clean aerodynamic configuration.

The NPD approach allows for noise calculation at a single point on the ground given one flight operation (approach, departure, or overflight). The output of the calculation can be a variety of instantaneous or integrated metrics. The process is then repeated for a full grid of observer locations underlying the flight procedure, allowing for the generation of equal-noise contour lines.

While AEDT is an integral component of the environmental regulatory framework, its limited fidelity in aerodynamic noise prevents direct application for the evaluation of advanced operational concepts. Because the NPD approach requires interpolation between a limited set of thrust levels and aircraft configurations, detailed noise changes resulting from aircraft speed or configuration variations cannot be captured. For example, delayed deployment of landing gear and flaps cannot be implemented using standard NPD curve sets, as approach NPD curves assume that the aircraft is in full landing configuration throughout a procedure.

Another limitation of the NPD approach is the limited fidelity of noise shielding and directivity assumptions. The direction of noise propagation from an aircraft depends on the configuration of the aircraft (such as wing and engine geometry), flight attitude (including pitch and bank angle), and the specific source of the noise (e.g., aerodynamic noise from particular structural components or jet mixing noise from the high-speed engine exhaust). A detailed treatment of noise in advanced operational procedures requires a higher-fidelity directivity assessment of noise than can be achieved with a simple single-source distance-based noise attenuation model.

One way to address the limitations of the NPD noise calculation method is to use standalone physics-based noise models. Such models generally include source modeling, shielding, and propagation. The benefit of such a model is higher fidelity for advanced procedures, although the process is not directly compatible with existing NPD-based methods. Approaches are under

development to convert high-fidelity results into a multi-dimensional lookup table similar to the NPD method but incorporating thrust and configuration variables as well [83]. It is expected that such methods could be used to incorporate noise characteristics for advanced procedures into existing tool workflows.

#### **2.4.4 Source-Based Approach (ANOPP)**

To address the limitations in the NPD-based noise modeling, higher-fidelity models can be used to capture various noise sources, shielding, and propagation. This is important for modeling procedures where aerodynamic sources are important, such as modified speed profiles and changes in aircraft configuration scheduling (landing gear and high-lift device deployment).

The outputs of source-based models can be used to directly calculate noise fields from an overflight or calculate higher-fidelity NPD data sets that better capture aircraft configuration, speed, and thrust levels of interest. The Aircraft Noise Prediction Program (ANOPP) is one model that can be used for this purpose. ANOPP is a NASA-developed model that computes noise levels from the airframe and engine components (fan, core, jet, and turbine) at a user-defined observer grid for a single flight procedure. It accounts for propagation through user-defined atmosphere and aircraft component shielding effects.

The methods used in ANOPP for noise computation are semi-empirical, based on historical noise data combined with physical noise models. These models have been improved over time, based on new full-scale and experimental data, but the fundamental noise source models are essentially unchanged. A series of modules take input on aircraft and engine parameters to generate cumulative noise projections for an aircraft configuration and flight procedure. ANOPP is configured primarily for noise prediction on conventional tube and wing aircraft configurations.

#### **2.4.5 Alternative and International Noise Models**

In light of the physical complexity of noise generation, propagation, and perception, there exists a wide range of potential modeling approaches and implementations. While AEDT and ANOPP are the primary tools used for analysis in this thesis, alternative noise models are used for particular applications in both in the US and international settings. These models could serve a similar role to

AEDT and ANOPP in the data-driven procedure design approach described in this thesis, with the caveat that exact contour geometry and recommended design configurations are sensitive to modeling assumptions and results. As discussed in this thesis, the tradeoff between fidelity and runtime means that the noise model of choice for any particular application or procedure may vary based on specific analysis goals, since increased accuracy is overshadowed beyond a certain modeling utility threshold by flight-to-flight randomness and variation in measured noise [84].

Example physics-based or semi-empirical models in use include NOISEMAP, developed by the US Air Force for military aircraft and airport noise studies [85]. Outside of the US, the Parametric Aircraft Noise Analysis Module (PANAM) developed by the German Aerospace Center (DLR) was developed with the intention of accounting for various significant noise sources efficiently and semi-empirically to allow for rapid configuration evaluation in system-level aircraft design analysis [86]. NASA and others have developed higher-fidelity engine noise modeling program for specific applications, such as the FOOTPR framework for jet noise [87]. High-fidelity component noise models with full three-dimensional computational fluid dynamic solutions have been demonstrated for specific components. In one recent NASA study, computational mesh resolutions sufficient to capture high-frequency noise components from landing gear required a runtime upward of two months for a single simulation on a 1,200 core supercomputer [88].

Other noise models have been developed based on lookup table methods and empirical regression. These models have significant run-time benefit at the potential cost of fidelity and modeling capability for non-standard procedures. The original model developed for use in the US regulatory context was the FAA Integrated Noise Model (INM) [89]. This model was an early implementation of the NPD method as outlined in the standard SAE-AIR-1845 [82]. Various additions and integrations using INM have been developed. The Model for Assessing Global Exposure to the Noise of Transport Aircraft (MAGENTA) was developed with INM as a noise core to allow for rapid batched evaluation of noise impact at the regulatory level of significance. Other large-scale reduced order models have been developed for use in large-scale noise evaluation studies in the US, including the Noise Integrated Routing System (NIRS) developed by Metron Aviation between 1998 and 2012.

Beginning in 2012, INM, MAGENTA, and NIRS were superseded by AEDT as the regulatory noise code for noise evaluation of operations.

Other noise models are used for operational noise evaluation. In the UK, ANCON is the primary noise model for calculating noise quota count impacts using an NPD-based approach for determining flight-level SEL impacts [90]. In Switzerland, the FLULA code serves a similar purpose with additional treatment and validation for directivity assumptions [91]. In Germany, the SIMUL model incorporates empirical lookup functions on a source-specific basis with basic physics-driven relationships to generate aeroacoustic predictions [92]. Direct adaptations of INM and/or AEDT are also used in some countries outside of the US.

## 2.5 Noise Metrics

Noise can be quantified using a variety of methods and metrics with the ultimate objective of capturing the acoustic and non-acoustic factors that cause annoyance, complaints, and health impacts. Fundamentally, noise is sound that is unwanted due to its loudness, pitch, or other characteristics. Sound itself is pressure variation relative to steady-state pressure within a medium, normally measured in decibels (dB). Sound pressure level (SPL) is defined based on this concept in Eq. 1.

$$\text{SPL (dB)} = 20 \log \left( \frac{p_{\text{rms}}}{p_{\text{ref}}} \right) \quad \text{Eq. 1}$$

Where:

$p_{\text{rms}}$  = root-mean-square of pressure variation about ambient steady state

$p_{\text{ref}}$  = root-mean-square of minimum audible reference pressure variation

The most straightforward method for comparing noise levels is to compare raw SPL values from background levels to noise-generating events. However, human perception of SPL varies greatly as a function of sound frequency or tone. For example, a mid-frequency noise (e.g., 3,000 Hz) at a fixed SPL is perceived as louder than a low frequency noise (e.g., 50 Hz) at the same SPL. Raw magnitude measurements typically don't capture key elements of sound frequency and tonality that drive human noise perception.

In addition to frequency, several qualities of a sound (sharpness, tonality, roughness, and fluctuation strength) impact perceived noisiness. Most of these effects vary between individuals in absolute terms (total SPL tolerance) as well as relative importance (e.g., frequency vs. sharpness). Therefore, no quantitative metric for noise can correlate to annoyance for all human observers. The methods and metrics most commonly used in industry are based on research performed during the 1970s and before, leading to decades of noise analysis and policy based on a set of common metrics and thresholds. Commonality between metrics and methods across studies and over extended periods of time allows for comparison between different technologies and time periods. The following discussion presents a partial list of metrics currently in use with a discussion of practical limitations and relevant supplemental information to inform procedure design efforts.

Many metrics have been developed to quantify noise for various context and purposes. Broadly speaking, metrics can be divided into two categories: single event and cumulative. Single event metrics quantify the sound exposure from a single overflight and can be used to evaluate specific operational changes or procedure designs on a before-and-after basis. Cumulative metrics incorporate many operations over a representative time interval (such as average annual day, peak day of operations using a particular runway configuration, or peak hour of operations using a particular procedure). These metrics show the impact of operational or procedural changes in the context of the actual operational intensity, procedure sets, and fleet mixes.

### **2.5.1 Frequency Spectrum Weighting**

Human response to a given SPL depends upon the frequency of that sound. A given sound's intensity results in a different perception of noise depending on the frequency of that noise. Scientific exploration of these spectral effects began in the 1930s, with refinements and applications continuing for the next several decades. One strategy to account for spectral noise sensitivity is to apply a masking function that weights high-sensitivity frequencies most heavily. The filter function used most frequently is referred to as A-weighting, which amplifies the intensity from frequencies near the middle of the audible spectrum. The A-weighted filter function is shown in Figure 7.

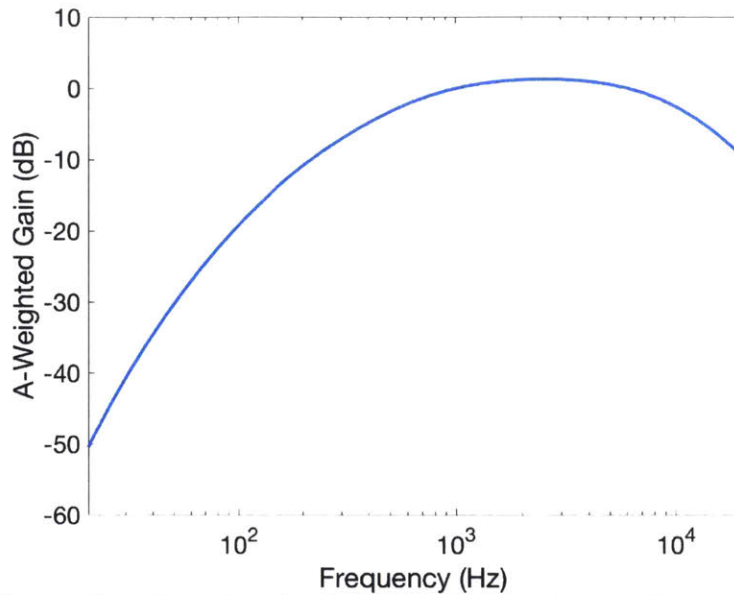


**Figure 7. A-weighting filter function for determining equivalent instantaneous loudness within the frequency range of human hearing**

A-weighted sound pressure level (commonly shortened to dBA) has become the de-facto standard for many noise certification purposes, including applications in transportation and consumer electronics [93]. The filter is effective at emphasizing the frequencies to which humans are most sensitive, translating raw mixed-spectrum sound signatures to levels reflective of psychoacoustic perceived loudness [94].

### 2.5.2 Single Event Metrics

While the aggregate impact of noise on communities depends on the entire daily distribution of flights tracks and operational strategies, each individual flight has an instantaneous impact on community annoyance. A class of “single-event” noise metrics has been established to allow for quantification of each noise event. Aircraft flyover events produce a characteristic rise and fall in SPL as the aircraft nears the observer, passes the point of closest approach, and recedes out of audible range. To the first order, the aircraft is only audible when the SPL rises above the background (or threshold) noise level. These metrics are derived from a typical SPL time history for a single aircraft overflight event, as was shown in Figure 4.

Flyover event measurements and single event metrics can be determined using microphones tuned for the desired spectral weighting (typically A-weighting). Alternatively, spectral gain

functions can be applied in post-processing analysis using data from full-spectrum microphones. While a wide variety of metrics are available that account for tonal components and other specific characteristics of noise events, two primary metrics were analyzed in this thesis for single-event sound exposure:

- $L_{MAX}$ : The simplest metric for single-event noise reporting is the maximum SPL occurring from that event. This metric measures full-spectrum SPL at a single observer location. This is an instantaneous metric that corresponds to the loudest sound level generated by an overflight without accounting for duration.
- SEL: Sound Exposure Level (SEL) accounts for the duration of a noise event by integrating the total sound energy for the time during which the sound level is within 10dB of its peak.

Both  $L_{MAX}$  and SEL can be used as building blocks for analyzing multiple flights in cumulative noise analysis.

### **2.5.3 Cumulative Metrics**

While single-event metrics are meant to describe the instantaneous impact of a single flight in a single location, cumulative metrics aim to assign a single value for overall noise impact at an airport averaged across all operations. Such an averaging allows consideration for fleet mix at an airport and flight time of day distributions. In addition, some cumulative metrics allow quantification of repetitive noise exposure and overflight frequency.

#### **DNL**

DNL is the most commonly-used cumulative metric. DNL is calculated as an average continuous daily A-weighted noise level due to aviation activity. This metric has been the regulatory benchmark in the United States and Europe since airport noise became part of required environmental assessment. Night time activity between 10:00pm and 7:00am is penalized with an additional 10dBA to reflect the lower background noise experienced during those hours as well as the sleep disruption caused by singular loud events. The mathematical formulation for DNL is a logarithmic summation



of SEL levels at each observer location over the course of a 24-hour period with a 10dB penalty applied for all night operations, as shown in Eq. 2.

$$DNL = 10 \log \left[ \frac{1}{86,400} \left( \sum 10^{SEL_{day}/10} + \sum 10^{(SEL_{night}+10)/10} \right) \right] \quad \text{Eq. 2}$$

Where:

SEL<sub>day</sub> = Single-Event Daytime Sound Exposure Level

SEL<sub>night</sub> = Single-Event Daytime Sound Exposure Level

There are several drawbacks to using DNL as the primary noise evaluation metric for airports. First, because the metric averages sound energy over a 24-hour period, the impact of individual overflight events that are highly distressing to communities are not be clearly represented by the metric. Maximum sound level is usually significantly higher than DNL, thus obscuring the true noise impact of an overflying aircraft. Additionally, the night-time penalty of 10 dB is not fully justified by scientific research on lifestyle and health impacts. The time window for which this penalty is effective is also debatable, leading to potential tension between airline schedulers, airport planners, and community members.

65dB is the standard DNL threshold used to determine land use requirements, mitigation funding eligibility, environmental impact compliance, and other important airport economic impacts. Thus, the 65dB geographic DNL footprint has become the primary noise metric reported by airports. Many airports supplement 65dB DNL contours with additional noise thresholds and operational data. In order to minimize noise complaints, many airports invest in noise programs outside the legally-binding footprint. As aircraft technology permits quieter operations, movement to a lower DNL threshold may be feasible.

#### **N<sub>ABOVE</sub>**

The number of noise events above a set threshold is a metric of growing interest among noise analysts and communities inside and outside the US. Research and evaluation of the metric originated in Australia in an effort to address shortcomings of DNL in certain analytical contexts [95]. The metric is a straightforward count of operations louder than a set threshold L<sub>MAX</sub> value, which can be different

for day and night operations (where night is defined as the period from 10pm to 7am). The method used for selecting  $N_{\text{ABOVE}}$  thresholds in this thesis is based on an analysis of geographic location of noise complaints relative to various exposure levels as described in Section 2.7.

#### **2.5.4 Other metrics**

Airport noise offices, development planner, regulators, and communities frequently propose and use alternative noise metrics to those presented here. For example, cumulative metrics specific to the standard school day help airports plan traffic flows around highly-impacted schools where jet noise can significantly impact the teaching environment. Audibility metrics are used to evaluate jet noise impacts in national parks, where background noise is low and noise exposure is unwelcome. The time spent above certain sound intensity levels can also be used to evaluate the impacts of aviation on speech, a factor that heavily influences noise complaint rates.

### **2.6 Noise Management Objectives**

The objective of aircraft noise management programs depends on stakeholder perspective and incentives. Broadly, noise management outcomes can be categorized into three types:

1. Reduction in noise levels generated on a single-event basis for a particular location
2. Reduction in total number of impacted people based on a desired noise metric
3. Reallocation of noise exposure to address perceived equity issues

These objectives may conflict, preventing a simple optimal solution for addressing noise. For example, reduction in population exposure may favor concentration of flight operations over specific low-population areas. Such a strategy reduces noise impact on other populated areas at the expense of the overflowed community. This outcome reduces the number of individuals affected by aircraft noise but does not address noise exposure equity between communities. Therefore, the design of new arrival and departure procedures is strongly influenced by stakeholder negotiations and preferences.

### **2.6.1 Reduction in Single-Event Noise Levels**

The simplest noise management outcome is single-event noise reduction for specific locations on the surface or for all communities underlying a given arrival or departure track. In terms of measurable outcomes, this can consist of quieter measured sound levels at a specific location on the surface or a reduction in overall noise contour area as a result of procedure modification. This objective implies adherence to baseline track locations, relying on flight profile modifications to achieve noise benefits. These modifications may include source noise reduction through improved engine technology and aerodynamics, climb or descent speed adjustments, thrust level adjustments, or other profile-related modifications.

Operational concepts to reduce single-event noise levels through profile modification can alter contour geometry in a way that is beneficial to all underlying communities or creates areas of benefit and disbenefit. For example, a procedure that results in reduced source noise generation throughout an arrival or departure benefits all underlying communities. However, other procedures such as high-thrust departures may have detrimental impacts on communities along the sideline of the initial climb segment and beneficial impacts to communities underlying the departure track farther from the departure runway due to increased overflight altitude. The relationship between specific observer location and procedure definition means that single-event analyses should be evaluated on a runway-specific basis. For example, existing noise abatement departure procedures (NADPs) optimized for close-in noise reduction (NADP-1) and mid-distance noise reduction (NADP-2) were tailored to benefit populations at specific distances from the departure runway [96].

### **2.6.2 Population Exposure Reduction**

Total population exposure reduction is one possible objective for noise management. Given a noise metric and threshold of interest, procedures or operational strategies can be implemented to minimize the total number of people exposed to that level or higher. Total population exposure is widely reported for the purposes of environmental reporting and accounting for progress in noise over time. For example, the population within the 65dB DNL contour is widely available on an airport-by-airport basis through FAA Part 150 studies and resulting Noise Exposure Maps.

Minimizing total population exposure numbers does not guarantee desired system configuration. Population exposure counts do not typically account for the magnitude of exposure for those communities falling within the impacted area. An observer exposed to an integrated noise level barely above the threshold value is counted the same as an observer with significantly higher overflight volume and noise impact. Once an observer location falls within a noise tabulation contour, additional noise exposure at that location does not increase the overall population count. Therefore, the objective of minimizing noise exposure population count incentivizes the concentration of noise over a small geographic area. Furthermore, net population exposure reduction may be achieved by relocating noise from one high-population region to a different low-population region. While the total number of people exposed to noise is reduced, the introduction of noise to a previously unimpacted area may generate new and disproportionate annoyance among the newly-impacted community.

### **2.6.3 Equity**

Minimizing impacted population counts does not account for potential equity factors between communities. An alternative noise management objective is to increase equity between communities based on noise exposure, or alternatively stated, to "spread the pain" of noise exposure. At the most basic level, the concept is that people should share the burden of negative noise impacts along with the benefits arising from air transportation.

There are two key problems with equity as a noise management objective. The first is that, regardless of technical innovation, airplanes make noise and must operate at low altitudes in the vicinity of airports in order to take off and land. Runways are built in fixed locations and operational patterns are dictated by wind direction. Technical constraints on arrival and departure procedures mean that the initial climb and final approach segments of flight are aligned with runways according to prevailing use patterns. Communities in the vicinity of airports, particularly along the extended runway centerline for aircraft on approach, are therefore bound to experience higher overflight concentration than other communities (including communities located an equal distance from the airport in a direction not aligned with an approach or departure runway). Despite the physical constraint on flight track redistribution imposed by runway infrastructure, there are areas located further from the airport where equity considerations may be taken into account.

The second key problem with equity as a noise management objective is the lack of clear definition of equity. Assuming that the objective is equitable noise exposure, the choice of measurement metric is one key consideration. Multiple metrics, such as DNL and  $N_{\text{ABOVE}}$ , may be used to evaluate differences in noise exposure between communities. A proposed solution may be considered "equitable" under one metric and threshold but not under another. An alternative definition of noise equity involves equalizing annoyance or other secondary impacts between communities. This definition is fundamentally subjective and variable between individuals. Non-acoustic factors, such as number of flights visible from a particular location, may play a role in addition to annoyance dose-response functions. In practice, community desires may include elements of equal noise distribution as well as equal annoyance/perception. Designing an equitable solution requires preliminary concurrence between communities on what constitutes equity, a fundamentally political process involving negotiations and tradeoffs outside the scope of this thesis.

## **2.7 Environmental Regulations**

In the US, changes to flight procedures are subject to federal environmental review. The National Environmental Policy Act (NEPA) of 1969 established new environmental assessment requirements for Federal agencies undertaking development work. The act provides a legal structure by which stakeholders evaluate and communicate environmental impacts prior to and during major federal projects, also outlining requirements for reporting and mitigation of any adverse effects. NEPA established the Council on Environmental Quality (CEQ) within the Executive Branch in order to ensure compliance with the Act by all federal agencies. In compliance with NEPA and CEQ guidelines, the FAA provides specific environmental policy guidance in the form of the Airport Environment Program (AEP). This program addresses environmental impacts in many categories including air quality, wildlife impact, land use, and sustainability. Guidance and requirements on airport noise are also provided under the AEP. This section describes some of the legal reporting requirements related to airport noise as well as special categorical exclusions for certain types of improvements.

### **2.7.1 FAA Order 1050.1: Environmental Impacts, Policies and Procedures**

Infrastructure development projects proposed by the FAA, a federal agency, are subject to the requirements of NEPA as well as guidelines and regulations from the CEQ contained in 14 CFR parts 1500-1508. FAA Order 1050.1F provides detailed guidance for airport, airspace, and procedure projects with respect to environmental impact assessment and reporting. In terms of noise evaluation, Order 1050.1F prescribes the types and scope of analysis required, metrics to be reported, and thresholds for significant impact determination. This includes specific requirements and best practices for initial environmental review and the preparation of Environmental Assessment (EA) and Environmental Impact Statement (EIS) analyses and documentation. The guidelines help ensure that FAA actions comply with federal guidance and that environmental assessment is executed consistently across the NAS.

### **2.7.2 14 CFR Part 150: Noise Compatibility Planning**

In 1979, Congress enacted the Aviation Safety and Noise Abatement Act with a series of new requirements for the interface between community and airport. 14 CFR Part 150 was adopted in 1981 to provide key definitions, reporting requirements, metrics, and thresholds for use in airport environment analysis around the NAS. Part 150 established annual average DNL as the legal standard metric for evaluating noise impacts. It also establishes INM or FAA-approved equivalent (e.g., AEDT) as the standard tool for generating annual average DNL noise exposure contours. The law prescribes the methods by which airports should prepare noise exposure maps, calculate population noise exposure, and establish Noise Compatibility Programs (NCPs) to lessen noise issues in areas of significant exposure. These include appropriate land use and zoning in high-noise areas, as well as mitigations such as sound insulation for qualifying homes [97].

Participating in the Part 150 program is voluntary, but the benefits of doing so are potentially quite large [98]. Once a Part 150 noise study is accepted by the FAA, the airport authority may recommend two types of programs. The first are operational mitigations, including flight path adjustments and runway use guidelines. Once an NCP is accepted, the FAA has 180 days to implement the operational guidelines. The second type of program involves land use, so areas within high-noise DNL contours may be rezoned (such as industrial or agricultural use). Existing residences and other

noise-sensitive structures may qualify for federally-funded noise insulation as well. Both of these land-use mitigations benefit airports by reducing noise complaints in the short term. In the long term, appropriate zoning prevent development in noise-sensitive areas.

## **2.8 Capturing Annoyance from Overflight Frequency**

Section 2.2.1 introduced the background and scientific underpinning of annual-average DNL as the regulatory metric for noise impact evaluation in the US. The metric was effective for capturing the effects of high noise levels in the immediate vicinity of airports, particularly given the high source noise levels of early jet aircraft. However, the noise complaints around the NAS are now occurring well outside the 65 dB annual average DNL contour. An example of this was shown in Figure 2 from BOS, where over 95% of complaint locations fall occurred outside of the official annual average 65 dB DNL “significant noise” contour between August of 2015 and July of 2016. This trend is repeated across the NAS, with complaints occurring further from the airport and with greater frequency in locations where single-event and integrated noise levels are lower than in prior years. This suggests a need for alternative metrics to supplement annual average DNL in order to capture contemporary annoyance effects.

Complaints do not serve as a direct proxy for annoyance or population impact due to sociopolitical factors that may influence who complains and with what frequency. Lack of information, political organization, communication channels, and other factors may prevent people impacted by aircraft noise from complaining. Any equitable procedure modification for noise reduction must take into account all impacted people regardless of ability to complain. Nonetheless, complaint locations do provide high-level information about the geographic extent of airport noise impacts. Information derived from complaint location data about annoyance factors and thresholds can be applied to all procedures that impact nearby communities.

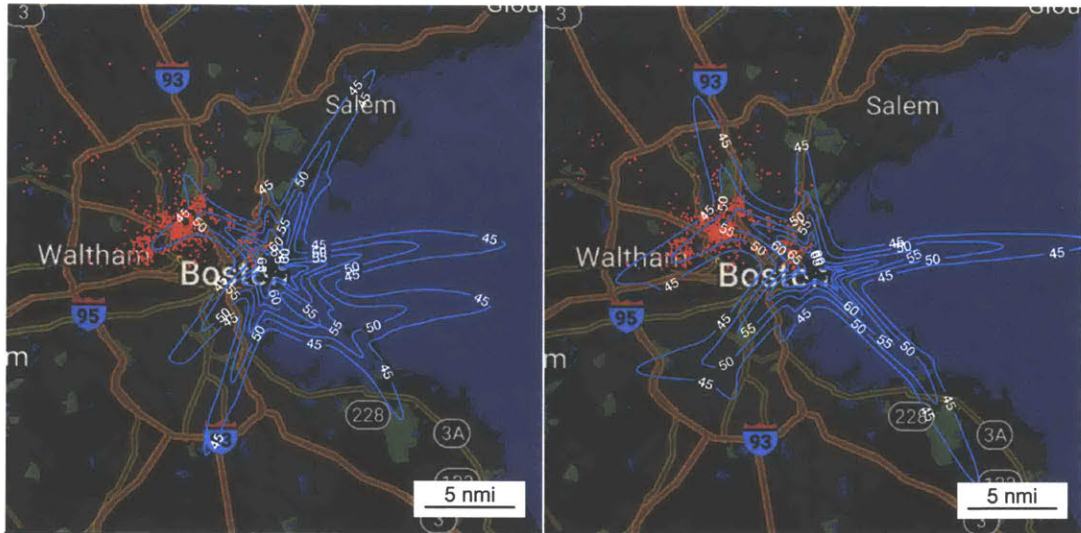
Alternate metrics have been studied in the literature, although the longstanding regulatory status of DNL as the principal analysis method for formal environmental studies has prevented widespread adoption of these alternates in the US. For example, in an effort to determine appropriate metrics and thresholds for analysis of candidate PBN arrivals and departure procedures at BOS,

Brenner evaluated the potential impact of calculating DNL and  $N_{\text{ABOVE}}$  for peak day and peak hour traffic levels corresponding to a specific departure runway configuration rather than annual average day for all runway configurations [99]. The research used complaint data provided by Massport, operator of Boston Logan Airport, to evaluate the percentage of complaints contained by noise contours generated using the two metrics and assumptions.

Figure 8 shows the impact of using annual average day traffic levels compared to a peak day of use for the procedure being analyzed. In this analysis, Brenner isolated complaint data geographically that appeared to be associated with Runway 33L departures. It was demonstrated that contours generated with annual average day traffic assumptions captured a relatively small percentage of complaints, with a 54.2% complaint capture at a low 45dB DNL level. Complaint capture values were higher when a peak day of runway 33L departures was used for the traffic baseline, raising complaint capture to 87.3% for the 45dB DNL contour. This suggests the potential utility of considering peak day traffic for individual procedures when evaluating annoyance rather than averaging results to include days when that procedure is not in use.

Qualitative feedback from communities indicates that overflight frequency is an important factor driving annoyance.  $N_{\text{ABOVE}}$  captures overflight frequency effects directly, essentially counting the number of qualifying events experienced by a surface observer over the period of interest. Figure 9 shows analysis that aimed to establish an adequate threshold for the  $N_{\text{ABOVE}}$  metric based on complaint capture. Based on the BOS case study shown here with a peak day flight procedure assumption, the appropriate threshold for qualifying events appears to be 60dB  $L_{\text{MAX}}$  for daytime overflights and 50dB  $L_{\text{MAX}}$  for nighttime overflights. At a 25 flight per day overflight frequency assuming these threshold values, the complaint capture was 84.3%. At a 50 flight per day overflight frequency, the complaint capture was 77.5%.

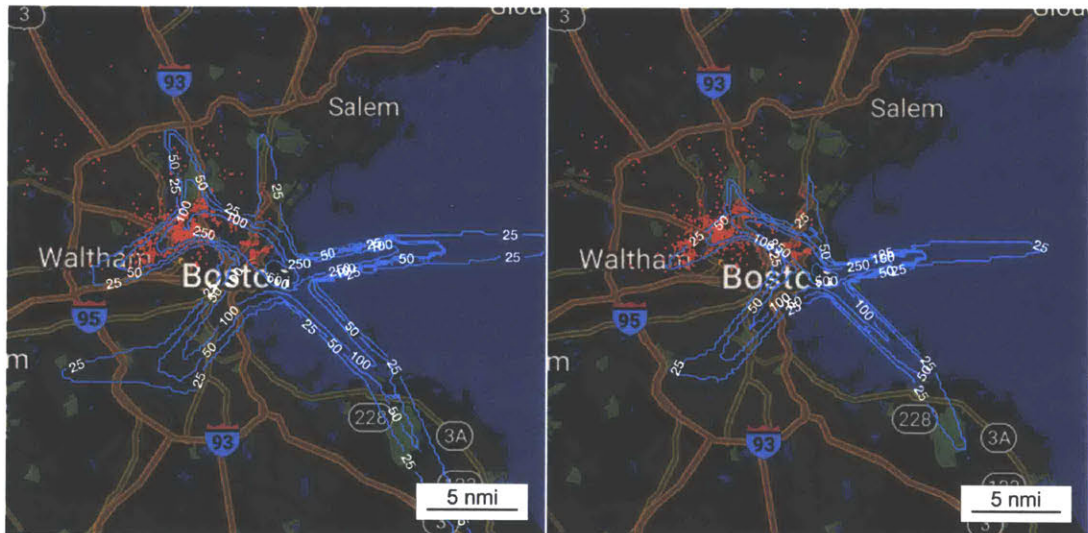




Contour Level (DNL)	Annual Average Day DNL Contours	33L Peak Day DNL Contours
45dB	54.2%	87.3%
50dB	14.7%	66.1%
55dB	8.1%	21.3%
60dB	3.5%	8.5%
65dB	0.1%	5.17%

Figure 8. BOS 33L departures complainant coverage for all scenarios by DNL contour level

Source: Brenner 2017

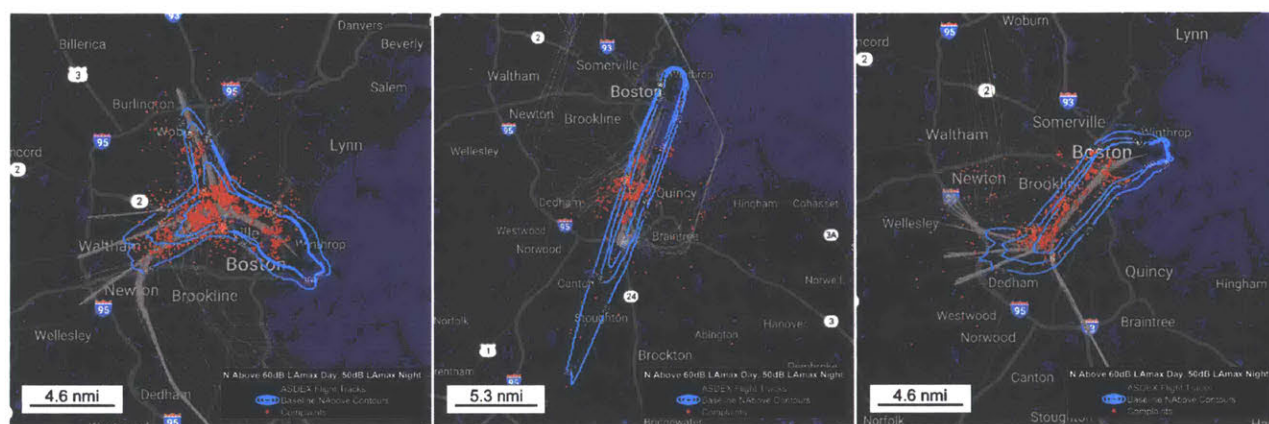


Contour Level (Flights/Day)	33L Peak Day $N_{\text{ABOVE}}$ 60dB Day, 50dB Night Contours	33L Peak Day $N_{\text{ABOVE}}$ 65dB Day, 55dB Night Contours
25	84.3%	67.1%
50	77.5%	47.6%
100	55.5%	17.0%
250	20.3%	9.7%
500	0.0%	0.0%

Figure 9. BOS 33L departures complainant coverage for peak day by  $N_{\text{ABOVE}}$  thresholds

Source: Brenner 2017

In 2018, Yu extended the  $N_{ABOVE}$  thresholds identified in the preliminary results above to additional runway ends at BOS [100]. In Yu’s analysis, complaints were grouped using a K-means clustering approach to correlate geographic complaint locations with specific arrival and departure runways. Three procedures with readily-identifiable complaint clusters were identified: Runway 33L departures, runway 27 departures, and runway 4L/R arrivals. Peak days of utilization for each of these procedures were identified using radar data corresponding to the period of complaints (August 2015– July 2016) for the purpose of generating  $N_{ABOVE}$  contours for complaint capture analysis. Results are shown in Figure 10.



BOS Rwy33L Departures		BOS Rwy4L/R Arrivals		BOS Rwy27 Departures	
Daily Overflights	Complaint Capture	Daily Overflights	Complaint Capture	Daily Overflights	Complaint Capture
25	96.9%	25	83.6%	25	92.2%
50	90.8%	50	67.9%	50	82.5%
100	59.0%	100	43.8%	100	60.5%

**Figure 10. Complaints captured by peak-day  $N_{ABOVE}$  contours at BOS (60dB day, 50dB night)**  
Source: Yu 2018

Results from Brenner and Yu provide preliminary support for using peak day traffic for specific procedures to evaluate the potential for noise annoyance rather than limiting analysis to traditional annual average day DNL contour generation. While additional work is required to determine whether the specific results from this study are generalizable to other runways and airports in the NAS, it appears that  $N_{ABOVE}$  thresholds of 25 or 50 flights daily at a daytime level of 60dB  $L_{MAX}$  and a nighttime level of 50dB  $L_{MAX}$  are appropriate for preliminary analysis of flight procedures and operational strategies. The analysis in this thesis uses an annoyance threshold of 25 daily flights at the 60dB (day) and 50dB (night) level.

## 2.9 Multi-Stakeholder System Modeling Literature Review

Group decision making in the context of environmental policy has been the subject of several papers and dissertations. At a broad level, policy planning problems have been established as “wicked” problems characterized by a lack of singular formulation, stopping rules, or evaluation criteria. Wicked problems are uncertain, complex, and involve divergent values from involved stakeholders. The general concept of handling such problems in system design have been addressed in broad systems (e.g. [101], [102]) as well as in the specific context of environmental planning (e.g. [103], [104]). The majority of literature on wicked problems focuses on formulation and characterization rather than evaluating a solution space. The problem of airport noise falls under the category of wicked problems due to the lack of clear objective function or stopping criteria. This leads to difficulty implementing an optimization scheme in the design space. Rather, a multi-stakeholder framework to assist in a negotiation process through informed impact analysis appears to best suit the analytical needs for the airport noise problem.

Communities impacted by environmental effects comprise one of the many stakeholder groups in the air transportation system. Fraser et al framed the problem of environmental policy-making as a balance between bottom-up engagement and top-down decisions [105], indicating that environmental policy issues must involve significant interaction between communities and authorities. By its nature, this leads to negotiations between stakeholders. Gregory et. al introduced a method to make environmental decisions incorporating community input without requiring consensus among all stakeholders [106]. Van den Hove argued that collaborative environmental policy solutions require equal measures of negotiation and consensus building due to fundamental divergence in value structures that prevent optimal solution generation [107].

Multi-stakeholder evaluation models may be used to evaluate simplified versions of wicked problems. By definition, these problems cannot be fully enumerated or expressed in closed analytic form. O’Neill presented a generalized framework for valuing multi-stakeholder engineering systems with variable cost and utility structures [108]. This framework primarily focused on calculating and evaluating system output state vectors and applying a valuation structure to determine the utility of system modifications. The framework required analyst assumption of stakeholder valuation in order

to generate a value proposition from a proposed system change. Figure 11 shows a schematic of O'Neill's multi-stakeholder valuation model.

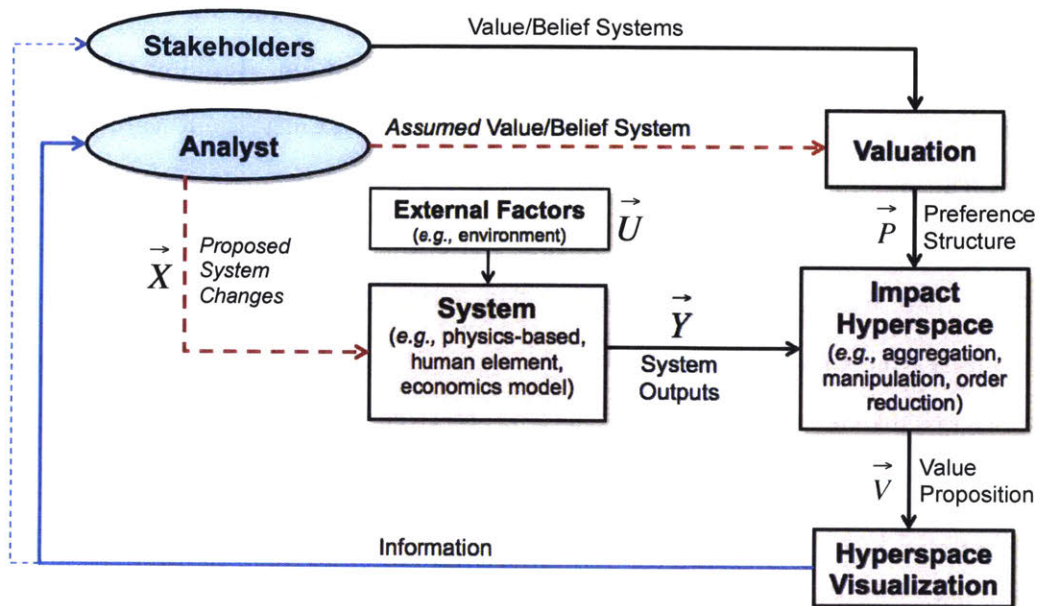


**Figure 11. Multi-stakeholder system transformation model developed by O'Neill [108]**

Cho et. al applied this framework to an approach procedure optimization problem for noise minimization with a simplified treatment of procedure design constraints and stakeholder preference in terms of fuel and noise exposure [109]. Regan et. al also developed a stakeholder consensus model using a linear programming formulation with user-defined weighting functions [110]. This analytical approach is an application of the general iterative weighting and valuation procedure outlined by the analytic hierarchy process [111], generating numeric utility values for complex systems using subjective stakeholder input for weighting functions on many sub-problems within a decomposed system. Hajkowicz demonstrated the use of multiple criteria analysis (MCA), an alternative analytic utility weighting approach, in multi-stakeholder environmental decision making [112].

One key component of multi-stakeholder consensus building and decision making around technical topics is effective visualization of model results. Non-technical stakeholders can only evaluate proposals effectively with access to the same information baseline available to technical designers. Visualization techniques for general trade space exploration have been developed for use

in multi-stakeholder settings [113] with some prior research aiming to develop novel visualization methods for aircraft noise specifically (e.g. [114]). The decision-making process itself can also be tracked visually to ensure concurrent understanding of negotiation progress [115].

## 2.10 Change Propagation in Air Transportation Systems

Air transportation systems are dynamic, technology-intensive, and heavily regulated. A framework developed by Mozdzanowska demonstrated that technology transition in the air transportation system requires an interconnected feedback process between stakeholders and processes [116]. The framework, shown in Figure 12, consists of an awareness-building process around the need for change, a change process with potential internal refinement and feedback loops, an implementation process, and system behavior propagation into the national airspace system. In this framework, the trigger for initiating a change process may occur due to a catalytic event (such as an accident or new technology introduction) or due to gradual changes in the system or stakeholder preference structures.

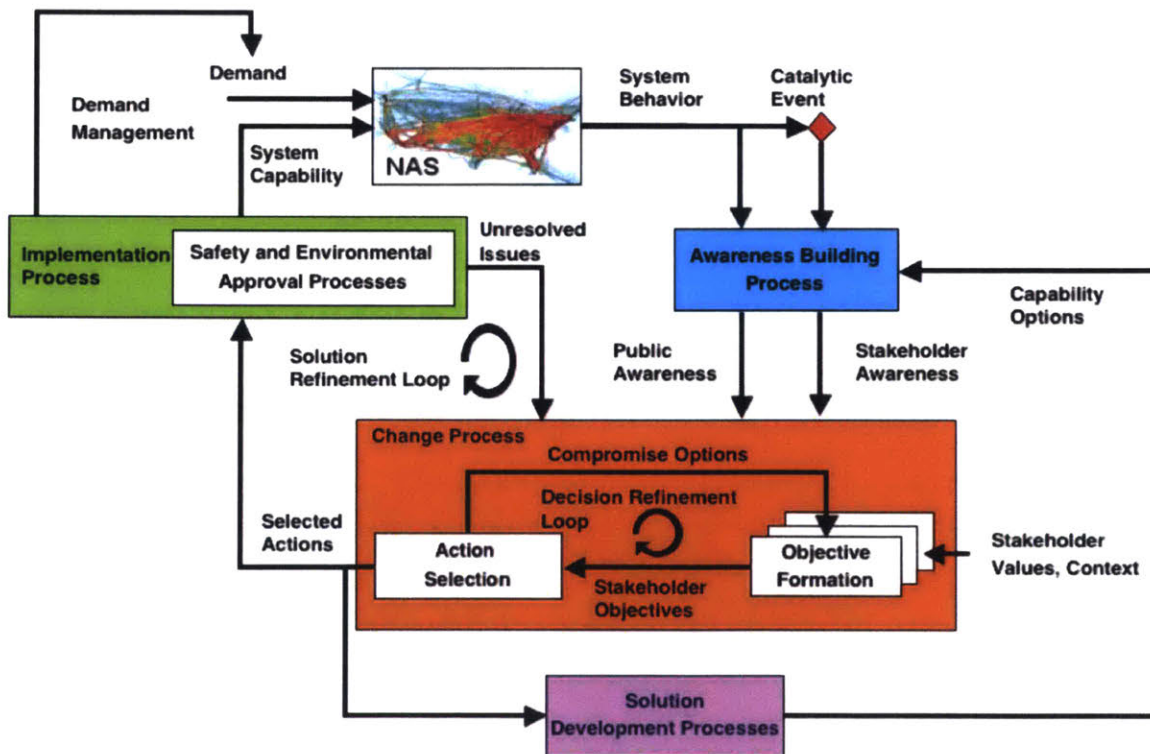
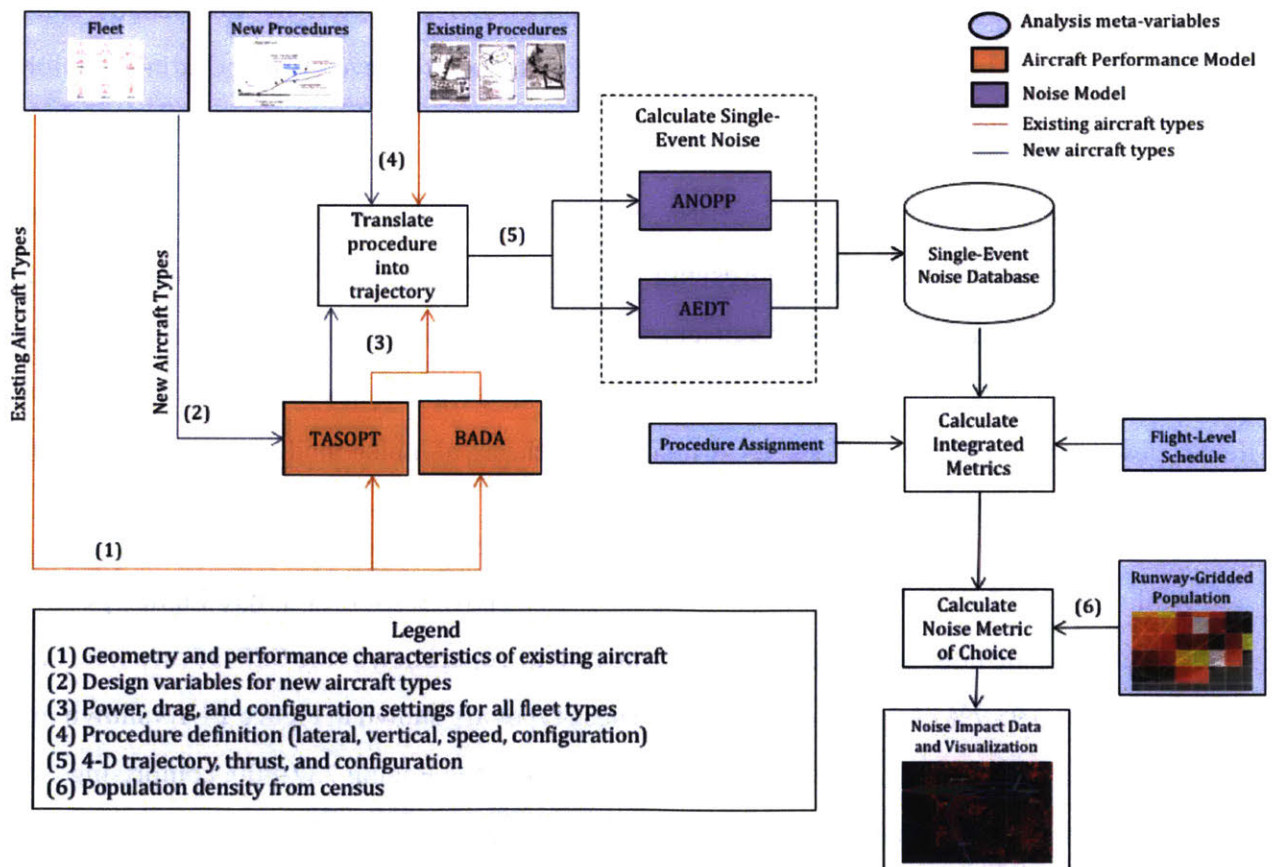


Figure 12. System dynamic transition model developed by Mozdzanowska [116]

One key component to this analysis is defining the set of relevant stakeholders and their relative influence in a given system, as described by Mitchell et. al [117]. Allen et. al. described the economic drivers behind these complex system transitions in the context of Air Traffic Management (ATM) [118]. These challenges result in constraints on implementation of many of the PBN procedures envisioned as part of modernized systems, preventing straightforward procedure adoption timeline assumptions [119]. In order to evaluate noise implications within dynamic system change models, multi-stakeholder system valuation models are required.

# Chapter 3. Noise Analysis Methods

The method used in this thesis for noise evaluation is applicable to existing and novel aircraft and procedures. It was developed to be useful for rapid single-airport analysis as well as system-level studies of benefit potential from modified procedures and fleet composition [120]. The procedure involves pre-calculation of single-event noise grids on a generic basis. These generic results are maintained in a database, allowing rapid rotation and superposition to determine airport-specific integrated noise impacts including DNL and  $N_{ABOVE}$  for different airports and traffic assumptions. Figure 13 shows a flowchart representation of this noise analysis method. This chapter presents more detail on individual components of the noise analysis framework.



**Figure 13. Noise analysis flowchart for single-event and cumulative impact evaluation of new procedures**

### **3.1 Fleet Development**

The fleet of aircraft types that serves an airport has a fundamental impact on single-event and integrated noise levels. Older generations of aircraft have significantly louder engines and aerodynamic surfaces than modern types with similar performance. In addition, for a set engine and airframe technology level, large and heavy aircraft are typically louder due to increased total thrust requirements (increased engine noise) and larger aerodynamic surfaces and exposed components (increased airframe noise). Therefore, total noise exposure is highest for airports with frequent service from older and/or larger aircraft.

In the analysis method shown in Figure 13, noise levels can be modeled for existing or novel aircraft types. This allows for analysis of noise exposure levels for baseline fleet conditions as well as hypothetical fleet evolution scenarios. This is an important capability for evaluation of procedure development proposals, which may have both short term and longer-term implementation objectives. Short-term noise benefits may be captured assuming baseline fleet mixes and existing aircraft types, while longer-term exposure is based on potential fleet evolution including technology evolution and insertion into the fleet.

Noise modeling may be performed through direct exposure calculations for every fleet type serving an airport or by identifying representative aircraft types for subsets of the operational mix. Representative fleet modeling groups subsets of aircraft types with similar noise and performance characteristics in order to reduce computational cost proportional to the number of representative fleet types selected. For the analysis performed in this thesis, all noise modeling is performed for a representative fleet mix to reduce computational cost.

While the 2017 FAA Aviation System Performance Metrics (ASPM) single-flight operational records database includes 509 unique aircraft type codes in operation at the OEP-35 airports, the top 40 types make up 94.7% of the total operations. These types are shown in Figure 14. As shown in this chart, the most frequent aircraft type by frequency share is the Boeing 737-800, comprising 11.7% of total movements. For this reason, the Boeing 737-800 was selected as the primary representative aircraft type used in this thesis for single-event analysis.



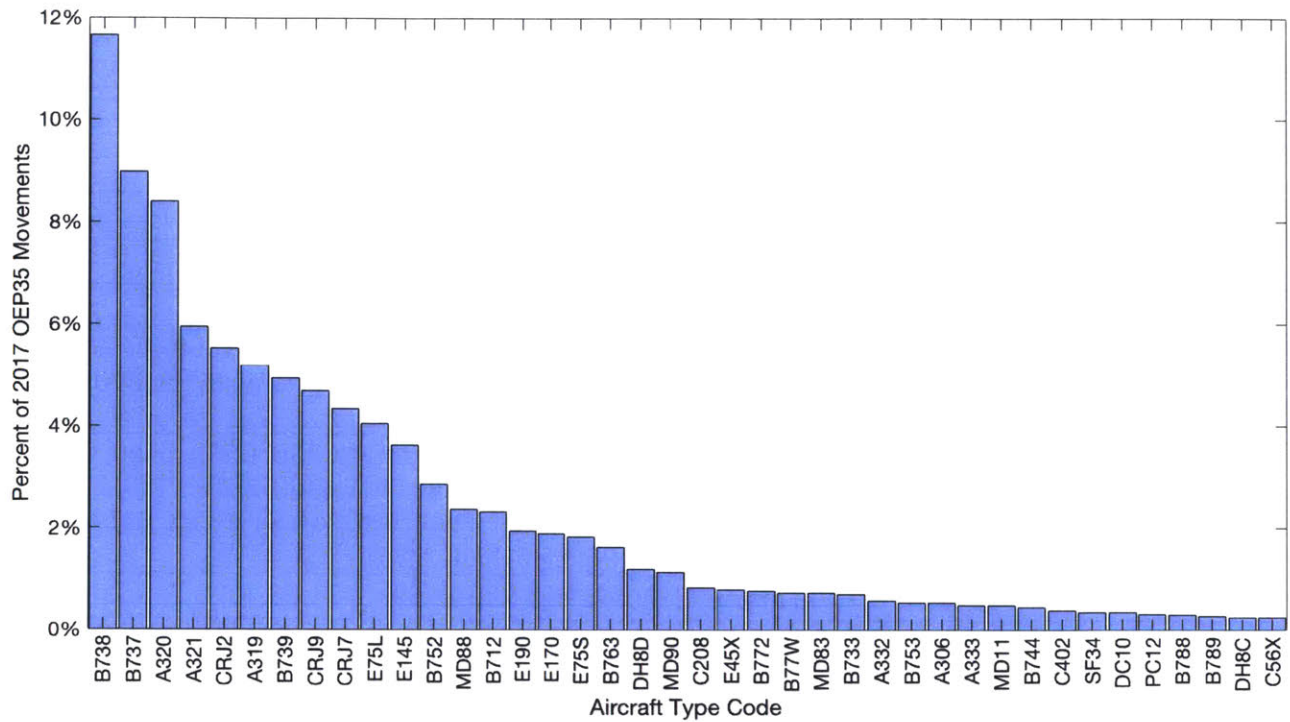


**Figure 14. Top 40 aircraft types by movement count at the OEP-35 airports in 2017**

In terms of developing a representative fleet mix for noise modeling, seven aircraft types were selected to capture the performance and noise characteristics of the broader fleet without requiring high-fidelity modeling of individual sub-fleets. The mapping of aircraft types as defined in ASPM to representative fleet families for the purpose of analysis in this thesis is shown in Table 1.

**Table 1. Fleet Type Mapping of Top 100 Types by OEP-35 Movement Share to Representative Fleet Types**

<b>Representative Type</b>	<b>Share of OEP-35 Movements</b>	<b>Included Types</b>
<b>B738</b>	26.6%	<b>737 Family:</b> B733, B734, B735, B736, B737, B738, B739
<b>A320</b>	19.5%	<b>A320 Family:</b> A319, A320, A321
<b>B752</b>	3.4%	<b>757 Family:</b> B752, B753
<b>B777</b>	7.8%	<b>Widebody:</b> A306, A310, A332, A333, A343, A346, A359, A388, B744, B748, B762, B763, B764, B772, B77L, B77W, B788, B789, DC10, MD11
<b>E145</b>	21.1%	<b>Regional and Business Jets:</b> BE40, C25A, C25B, C550, C560, C56X, C680, C68A, C750, CL30, CL35, CL60, CRJ1, CRJ2, CRJ7, CRJ9, E135, E145, E45X, E50P, E55P, F2TH, F900, GALX, GL5T, GLEX, GLF4, GLF5, H25B, J328, LJ35, LJ45, LJ60, LJ75
<b>E170</b>	9.7%	<b>E170 Family:</b> E170, E190, E75L, E75S
<b>MD88</b>	6.8%	<b>DC-9 Family and Low-Bypass Narrowbody:</b> B712, B732, MD82, MD83, MD88, MD90
<b>Omit</b>	5.1%	<b>Propeller &amp; uncommon types:</b> AT43, AT45, AT73, B190, B350, BE20, BE30, BE65, BE99, BE9L, C208, C402, DH8A, DH8B, DH8C, DH8D, E120, PA31, PC12, SF34, SH36, SW4, <b>All Others</b>

### 3.2 Procedure Development

Procedures in the noise analysis method refer to existing or novel definitions for aircraft trajectories during approaches and departures. The trajectory includes a lateral component (ground track), vertical component (altitude profile or climb gradient target), speed component (through speed constraints or other guidance), and/or configuration component (landing gear extension, guidance on flap settings, and speed brake use). Existing flight procedures are typically published as instrument flight procedures, as described in more detail in Section 7.2.1. This definition may include a sequence of waypoints and leg types as well as speed guidance and altitude constraints. These procedures are published graphically as well as textually in the Coded Instrument Flight Procedures (CIFP) product.

### 3.2.1 Coded Instrument Flight Procedures

The FAA CIFP database was used to evaluate the geometry and characteristics for existing instrument approach procedures in the US. The CIFP is a textual listing of procedures, runways, navigation aids, waypoints, and other relevant aeronautical data encoded in ARINC-424-18 format. This format is typically used to translate procedure designs into machine-readable code for use in flight management systems. It is a flexible data format intended for efficient parsing by cockpit computer systems. Table 2 shows the information provided in the CIFP for RNAV and RNP procedures. However, the limited bandwidth and character fields included in the ARINC-424-18 code prevents inclusion of relevant data such as approach categories, minimums, fixed-wing vs. helicopter procedure designation, controlling obstacle data, visual depictions, and plain-text procedure names. Therefore, CIFP processing provides useful high-level procedure geometry without full operational context or applicability. The CIFP is updated in 28-day distribution cycles and available for public download from the FAA Aeronautical Information Services website.<sup>2</sup>

**Table 2. RNAV and RNP approach parameter information contained in CIFP**

<b>Data Category</b>	<b>Information in CIFP (ARINC-424-18)</b>
Location	Region, Airport, and Runway
Procedure Definitions	Procedure Type, Segment Count
Waypoint Designation	Fly-by, Fly-over, Initial Approach Fix (IAF), Intermediate Fix (IF), Precision Final Approach Fix (PFAF), Missed Approach Point (MAP)
Leg Geometry	Course, Distance
Final Approach Geometry	Glidepath Angle, Threshold Crossing Height

CIFP procedure geometries must be translated into detailed lateral tracks for noise analysis. A translation program was developed for this noise analysis framework that builds flight track centerlines from an input list of fly-by waypoints, fly-over waypoints, and other leg types. The translation from CIFP database format to waypoint listing to smoothed lateral trajectory centerline

---

<sup>2</sup> [https://www.faa.gov/air\\_traffic/flight\\_info/aeronav/digital\\_products/cifp/](https://www.faa.gov/air_traffic/flight_info/aeronav/digital_products/cifp/)

is shown conceptually in Figure 15. The smoothed procedure centerline generation process assumes a turn radius based on groundspeed and bank angle that may be dependent on the phase of flight or specific procedure assumptions.

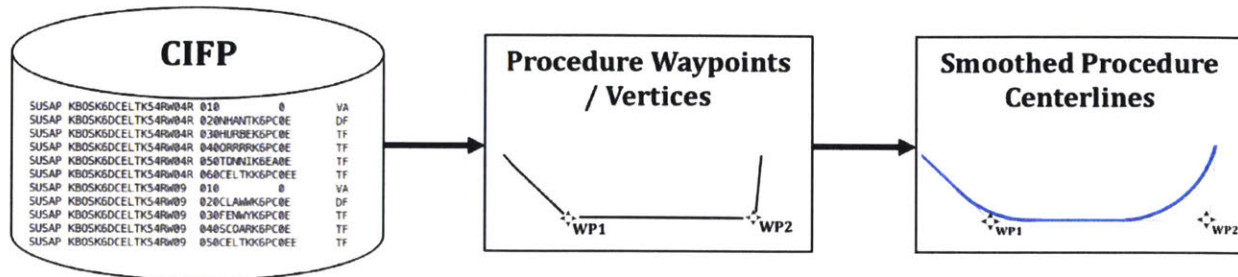


Figure 15. CIFP translation to trajectory centerline for noise analysis

### 3.2.2 Procedure Generation from Radar Data

An alternative to procedure-based methods is to use historical radar data for identification of representative trajectories. Specific flights can be used as input for noise models or sets of radar data can be processed using statistical clustering methods, filtering, and averaging methods to determine “centroid” procedures representative of a broad operational set. These data-driven profile generation methods have the added benefit of providing altitude and speed trajectory information based on actual flight conditions rather than aircraft performance assumptions. Naturally, data-driven methods require access to high-fidelity historical radar data to operations representing those to be modeled in the noise analysis process.

## 3.3 Aircraft Performance Models

Two aircraft performance models are used in this noise analysis method, depending on the objective of the analytical framework: the Eurocontrol Base of Aircraft Data (BADA) [121] and The Transport Aircraft System OPTimization (TASOPT) [122]. For this noise analysis method, BADA is used as the primary aircraft performance data source when all aircraft in the analysis are existing aircraft types, while TASOPT is used for any analysis involving novel or modified aircraft types.

### **3.3.1 BADA 4**

The BADA 4.0 model is used for modeling scenarios which incorporate only existing aircraft types. The dataset is maintained in partnership with airlines and aircraft manufacturers, who provide and validate the data. BADA uses a mass-varying kinetic approach to calculate aircraft performance, summing forces about the aircraft which is modeled as a point mass. The aerodynamic and engine parameters for each aircraft are modeled as polynomial functions, with the coefficients for each aircraft type validated by flight test data from aircraft manufacturers. The model includes separate drag polynomial functions for clean configurations as well as different flap and landing gear settings. The drag and thrust models account for altitude changes assuming standard atmospheric temperature and pressure lapse rates [123].

For noise analysis in this thesis, the BADA model is used to calculate thrust requirements for arrival and departure procedures as well as deceleration profiles in various flap configurations for each available aircraft type. Weight assumptions based on flight distance are used to determine climb gradient as well as thrust for individual missions.

### **3.3.2 TASOPT**

TASOPT jointly optimizes the airframe, engine, and full flight trajectory of a “tube and wing” transport aircraft using physics-based computations to predict aircraft weight, aerodynamics and performance without the need for traditional empirical regression methods. The tool incorporates fundamental low-order models for structures, aerodynamics, and engine performance to generate optimized aircraft designs given a set of mission constraints [122]. Existing aircraft can be modeled approximately by incorporating geometric constraints to match fuselage, wing, tail, and engine size as well as mission capabilities. These aircraft are then validated against the actual baseline aircraft in terms of structural weight and total trip fuel burn compared to data provided by manufacturers and airlines.

The strength of the TASOPT model relative to empirical models such as BADA is the capability of modeling notional or future aircraft types. This is important for evaluating future scenarios. For this analysis, TASOPT is used to calculate thrust and drag for existing and future fleet types for

scenarios involving aircraft types not covered by the BADA dataset. By modeling both existing and future aircraft types with TASOPT, consistency between baseline and experimental results is assured.

### 3.4 Detailed Trajectory Generation

While the procedure development phase of the noise modeling process defines aircraft track and altitude profiles, noise models also require thrust and aerodynamic configuration data for each segment of a procedure in order to calculate total noise signature. Thrust levels are a key input requirement for engine noise estimation. Detailed speed and aircraft configuration data provide input to aerodynamic noise modules and duration-based noise exposure corrections. Because neither procedure interpretation methods nor radar-based representative trajectory selection methods provide thrust levels directly, a thrust calculation method is required to generate all required inputs for noise modeling.

This procedure is based on a force-balance kinematics model as shown in Figure 16. In this model, one of the aircraft performance models described in Section 3.3 is used to determine total drag and thrust available based on aircraft configuration, weight, speed, and altitude. Aircraft flight path angle can then be calculated for scenarios with fixed thrust or thrust can be calculated for scenarios with fixed flight path angle. The full set of variables treated as inputs and outputs for each segment is summarized in Table 3.

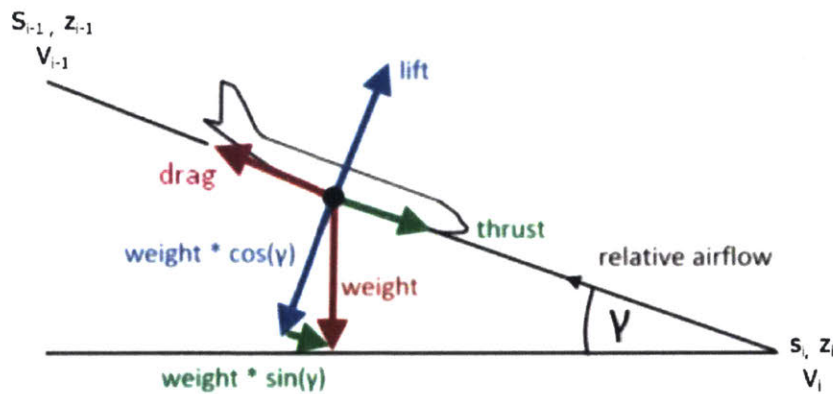


Figure 16. Force-balance approach used to calculate thrust and drag for profile definitions

[124]

**Table 3. Kinematics equations used to calculate arrival and departure profiles**

User Inputs for Given Procedure Segment	Procedure Generator Outputs
<p><i>Aircraft configuration and speed:</i></p> <ul style="list-style-type: none"> <li>• Flap, Landing Gear, Speedbrake setting</li> <li>• True airspeed</li> </ul> <p><i>And any two of the following:</i></p> <ul style="list-style-type: none"> <li>• Required altitude change, segment length, flight path angle, thrust</li> </ul>	<p>Two remaining variables are calculated using the following kinematics equations:</p> <ol style="list-style-type: none"> <li>1. <math>a = \frac{\Sigma F}{m} = \frac{T+W \sin \gamma - D}{W/g}</math></li> <li>2. <math>\frac{\Delta V^2}{2a} = \Delta S = \frac{\Delta z}{\sin \gamma}</math></li> <li>3. <math>D = \frac{1}{2} \rho V^2 S C_D (\delta_{flap}, \delta_{gear}, C_L)</math></li> <li>4. <math>C_L = \frac{2W \cos \gamma}{\rho V^2 S}</math></li> </ol>

### 3.5 Noise Modeling

Two noise models were used in for analysis in this thesis. The FAA AEDT is used for procedures using standard speed and configuration profiles (such as RNAV waypoint relocation or other lateral track modifications). NASA's ANOPP is used for procedures involving modified speed, thrust, or configuration because it accounts for changes in noise components sensitive to specific aircraft state.

#### 3.5.1 AEDT

AEDT is the primary analysis package used in the US to evaluate community noise impacts near airports. AEDT uses NPD lookup tables to calculate noise from data generated through flight test and/or analysis. A functional relationship between engine throttle setting and source-to-observer slant distance yields noise estimates for specific locations on the surface. The noise frequency spectrum is obtained empirically from representative aircraft families at set power levels and aircraft configurations. This analysis method results in a simple and computationally tractable noise estimation capability for engine noise sources. Aerodynamic noise contributions, however, are not fully incorporated into the model. For instance, total noise, including both engine and aerodynamic (airframe) noise, is derived empirically for a reference speed of 160 knots. For speeds outside of 160 knots, AEDT accounts for speed in terms of duration changes for a noise event but not in terms of changes to airframe source noise [76]. Therefore, any speed difference from this reference value results in potential inaccuracies in airframe noise estimates.

### **3.5.2 ANOPP**

To address the limitations of NPD-based noise modeling, higher-fidelity models can be used to capture various noise sources, shielding, and propagation. Such models can be used to directly calculate source noise throughout an overflight event or to calculate higher-fidelity NPD data sets that capture configuration and speed effects. ANOPP is one model that can be used for this purpose. ANOPP was originally developed by NASA in the 1970s to provide predictive capabilities in individual aircraft studies and parametric multivariable environmental evaluations. The program was developed with a modular framework and open documentation to allow for interface development with other tools and software. The tool is designed to evaluate noise for a single flight procedure but also satisfies objectives beyond single-procedure noise analysis. ANOPP uses a semi-empirical model, incorporating both historical noise data and physics-based acoustics models. It computes noise levels from multiple sources, both airframe and engine (fan, core, and jet), for a three-dimensional observer grid based on user-defined arrival and departure procedures [78]. The tool also accounts for propagation through a customizable atmospheric model and aircraft component shielding effects. A series of modules take input on aircraft and engine parameters to generate cumulative noise projections. Specific modules within ANOPP have been improved over time based on new full-scale and experimental data.

### **3.5.3 Simplified Contour Generation Method**

A simplified noise contour generation method was developed to evaluate changes arising from lateral track modification, a capability that is useful for the evaluation of large parametric track definitions studies and optimization frameworks. The purpose of this method is to enable rapid application of modeled noise results to a broad set of track geometries that would be impractical for direct modeling with one of the higher-fidelity models due to run time. Vertical trajectory, configuration, and thrust are assumed constant across each of the generated contour sets in this method.

Noise contours are generated for a generic straight-in or straight-out flight procedure using AEDT or ANOPP, as appropriate for the proposed modification. In general, AEDT is appropriate for any procedure involving lateral track modification only, while ANOPP is appropriate for procedures



involving changed in speed profile or configuration (landing gear and high-lift device) scheduling. Raw noise model outputs are converted into contour half-width lookup tables as a function of distance to touchdown (approach noise) or distance from start of takeoff roll (departure noise). The contours that serve as the source of these half-width functions may be generated using either AEDT or ANOPP. Figure 17 shows an example 60dB  $L_{MAX}$  contour for a Boeing 737-800 on a standard 3° approach profile generated using AEDT with orthogonal distance chord lines illustrated at intervals of 0.25 NM for graphical clarity. The contour half-width functions used for all actual analysis in this thesis are generated at intervals of 0.05 NM

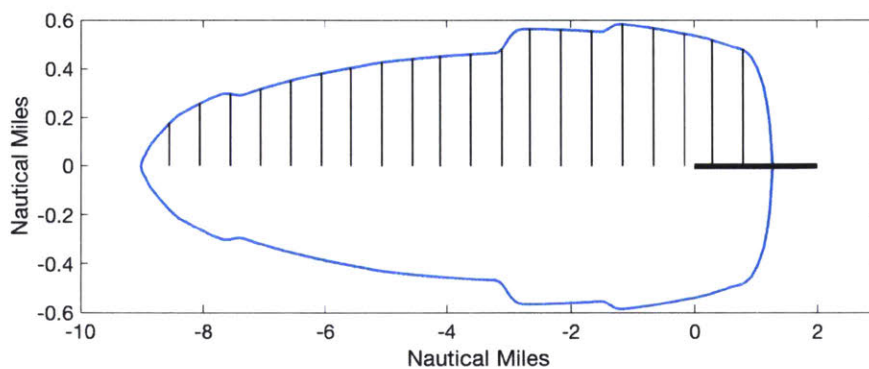


**Figure 17. 60dB  $L_{MAX}$  contour for a Boeing 737-800 on a straight-in final approach segment with resulting contour half-width function shown in black.**

Contour half-width lookup functions are generated and stored for the noise metrics ( $L_{MAX}$  or SEL) and threshold levels of choice. The source contours must be generated using vertical profile and thrust assumptions consistent with the desired analysis. For example, evaluation of customized departure procedures using the rapid contour generation method may use radar-derived climb gradients on an aircraft-specific basis, while analysis of RNAV approach procedures may assume a standard 3° glideslope for the sake of consistency between airports and arrival geometries.

Contour half-width functions generated with this method can be used to rapidly calculate contours for user-defined lateral ground tracks. For each along-track segment interval along a procedure centerline, a contour gridpoint is generated orthogonally to the left and right of the centerline at the distance determined from the contour half-width function. This is shown for an example procedure centerline in Figure 18. This process may be repeated to generate contour

geometry for each lateral track definition, aircraft type, and metric level necessary for a desired analysis.

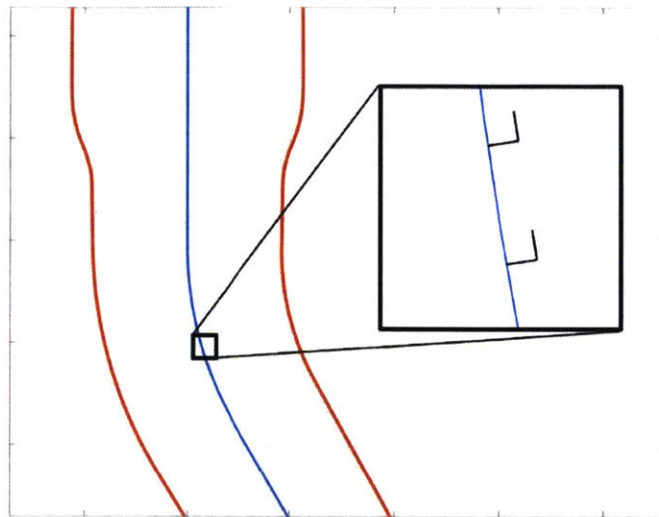


**Figure 18. Contour generated by applying the half-width functions orthogonal to an RNAV procedure centerline**

The contour half-width function method results in small differences compared to a direct AEDT or ANOPP runs for the same lateral profile. That is, running a custom arrival or departure profile in a noise model directly may result in slightly different contour geometry than the simplified method introduced here. This effect is due to differences in shielding assumptions for turning aircraft as well as exposure duration effects. To illustrate this effect, Figure 19 shows a set of three Boeing 737-800 arrivals that were evaluated directly in AEDT. Each of these uses the default vertical and thrust profile included in AEDT. The figure shows  $L_{MAX}$  and SEL contours for a straight-in arrival as well as alternative lateral profiles with 30° and 60° final approach interception angles 2 NM from touchdown. This is not intended to represent an actual arrival procedure recommendation but is intended to illustrate the effect of turns on noise contour geometry in noise model outputs.

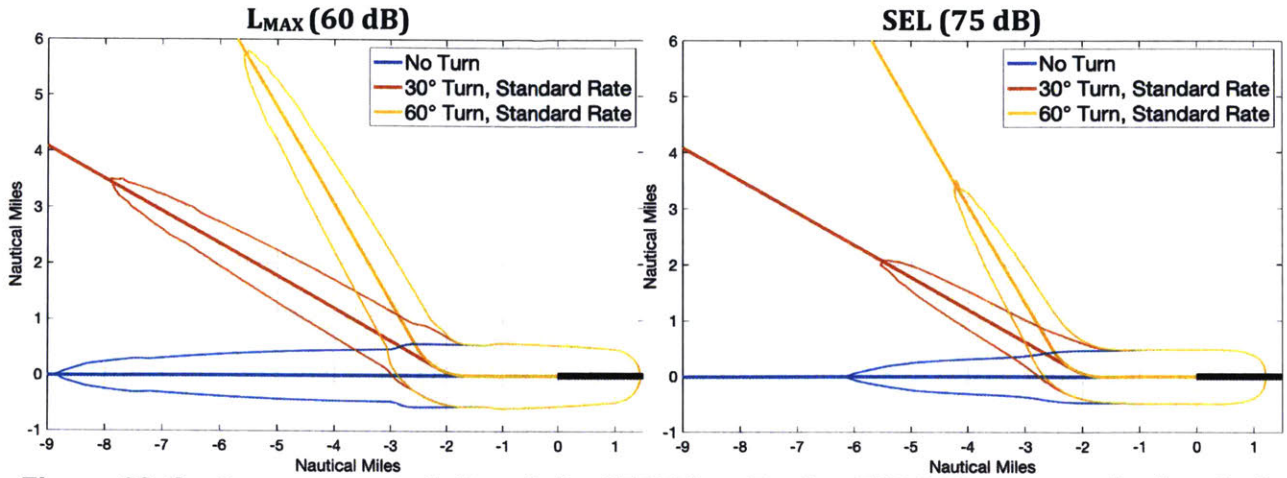


**Figure 19. Contours generated directly by AEDT for a Boeing 737-800 on a standard arrival profile with a turn of 0°, 30°, or 60° on the final approach segment**

Including a turn segment in the lateral track definition introduces slight differences in contour width on the inside and outside of the turn. Figure 20 shows the contour half-width function in the vicinity of the turn for the three scenarios shown in Figure 19. Away from the vicinity of the turn, the half-width functions re-converge to the straight-in baseline.

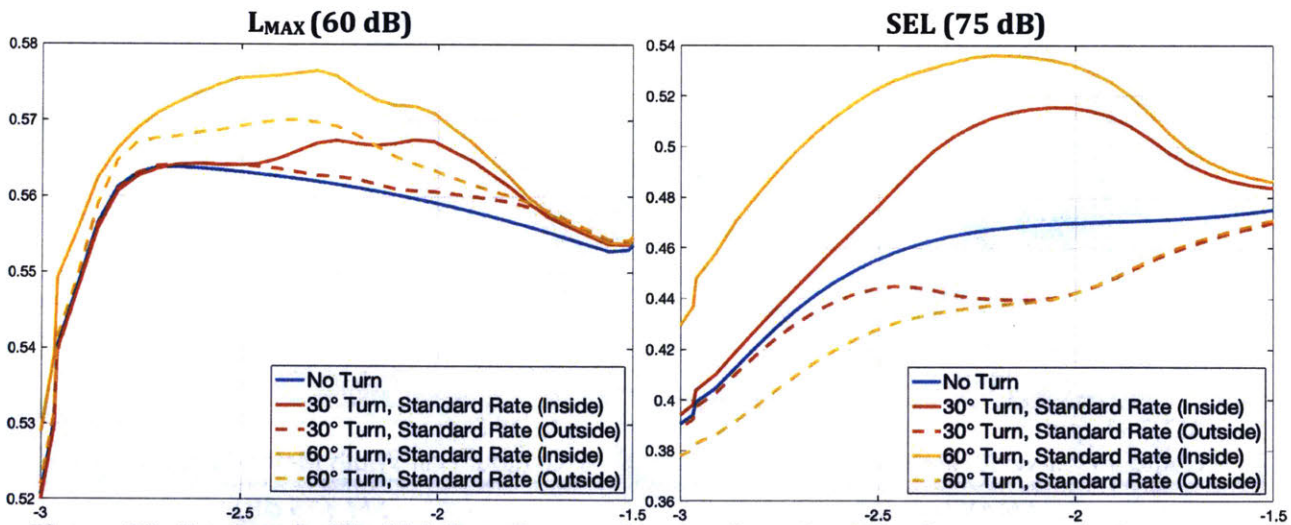


**Figure 20. Contour half-width functions at the turn location based on contours from AEDT for a Boeing 737-800 on a standard arrival profile with a turn of 0°, 30°, or 60° on the final approach segment**

Figure 20 shows that including turns leads to a variation of  $L_{MAX}$  contour width of less than 0.02 NM from the straight-in baseline for  $L_{MAX}$  at the 60dB contour level. The variation in contour width for SEL is larger, with a difference between the straight-in width and 60° turn width as large as 0.06 NM. This figure shows that the error introduced by assuming straight-in contour geometry for

turning procedures is larger for SEL than for  $L_{MAX}$  but that the error is smaller than the population exposure resolution of 0.1 NM used in this thesis in both cases. SEL contour with is more sensitive to turn geometry due to the increased duration of exposure to observers located on the inside of the turn and decreased duration of exposure to observers located on the outside of the turn. This has no effect on  $L_{MAX}$  because the peak noise level is not affected by the change in exposure duration. Figure 21 shows a comparison of noise contours generated by AEDT and the rapid contour generation method for a hypothetical B737-800 approach to runway 4R at BOS including a 60° turn into the final approach segment. The figure illustrates that the rapid contour generation method results in negligible geometry differences for  $L_{MAX}$  contours relative to direct AEDT outputs. The differences between the rapid contour generation method and AEDT are slightly larger for SEL results, although still below the 0.1NM resolution of the underlying population grid.

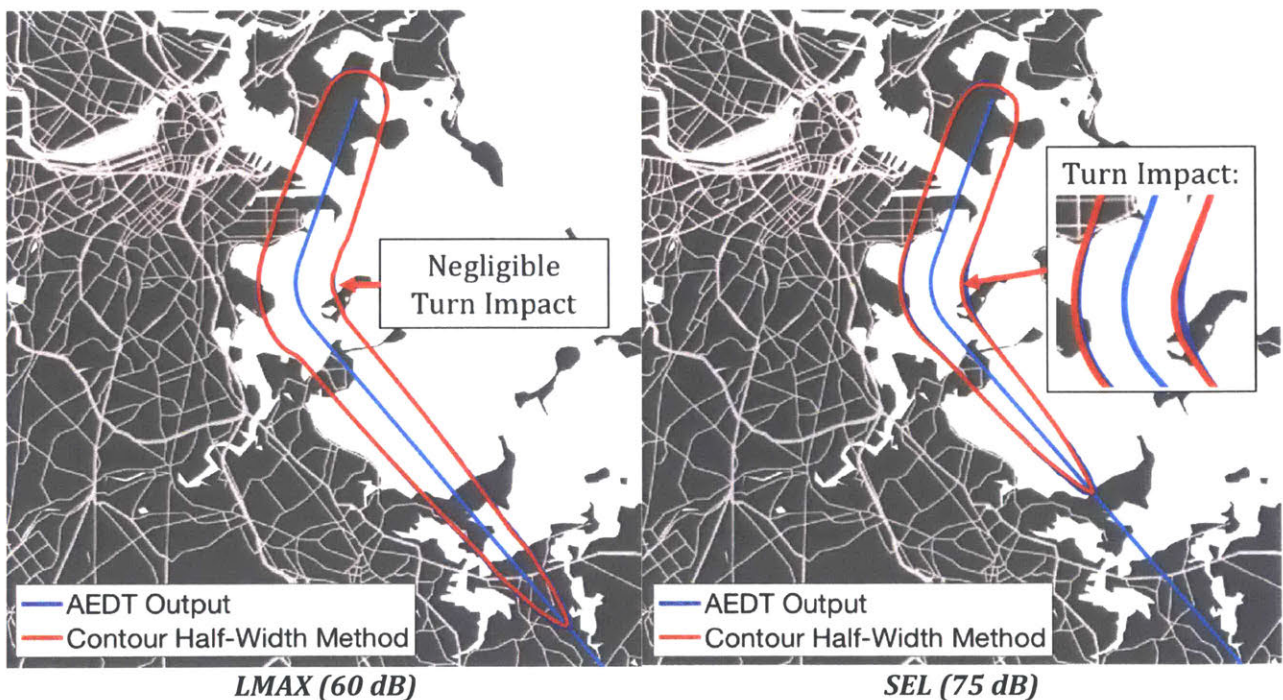


**Figure 21. Full contour comparison between AEDT output and rapid contour generation method for a 737-800 approach procedure to Runway 4R at BOS containing a 60° turn**

While it is clear that small errors in contour width for turning profiles are introduced by assuming straight-in contour geometry for all procedures, the differences are small enough to allow meaningful differentiation between procedures at the scale of population analysis performed in this thesis. In addition, all noise analysis performed using this method in this thesis uses the  $L_{MAX}$  metric,

thus minimizing potential error from the rapid contour generation method relative to SEL as shown in the left panel of Figure 21.

### **3.6 Flight-Level Schedule Development**

Flight-level schedules can be developed using two high-level processes under this noise analysis method. In the first, aircraft arrivals and departures are allocated to runways and procedures based on historical radar data. This is the most direct method available for reconstructing historical runway use as there are no embedded assumptions about runway preference by aircraft type, equipage and availability for particular procedures, or daily variation in active procedure sets. Historical radar data can be used directly (by modeling noise for each individual trajectory) or indirectly (by allocating operations appearing in the radar data to representative trajectories on a one-to-one basis). This method relies on availability of high-fidelity low altitude radar data for the airport of interest and requires significant pre-processing of trajectories to provide a usable catalog of arrivals and departures by runway end as a function of time.

The second method of flight-level schedule development uses the FAA Aviation System Performance Metrics (ASPM) database on the airport level and the single-flight level.<sup>3</sup> Flight-level data is available for arrivals and departures, including actual off and on times and aircraft type codes. An example of this data is shown in Table 4. Using this data, a list of arrival and departure counts by aircraft type was developed for each of the OEP-35 airports for the full year of 2017 operations. These counts were segregated by hour to allow for determination of daytime and nighttime noise metrics as well as for accurate allocation of operations by runway configuration.

---

<sup>3</sup> <https://aspm.faa.gov/>

**Table 4. Example flight-level data from ASPM**

Carrier	Flight Number	Tail Number	ACID	Departure	Arrival	ETMS Equipment Code	Scheduled Gate Out	Flight Plan Gate Out	Actual Gate Out	Scheduled Gate In	Flight Plan Gate In	Actual Gate In
NA	0	CFMFL	CFMFL	CCR3	BOS	FA50	11:15	11:15	10:57	11:32	11:32	11:06
NA	0	LN901LM	LN901LM	BGR	BOS	BE20	15:30	15:30	15:31	16:31	16:31	16:38
NA	0	LN988QC	LN988QC	SLN	BOS	LJ35	15:00	15:00	15:02	19:13	19:13	19:24
AAL	29	N925AN	AAL29	MIA	BOS	B738	12:28	12:28	12:32	15:50	15:50	16:01
AAL	146	N990NN	AAL146	LAX	BOS	B738	08:40	08:40	08:34	17:32	17:32	17:22
AAL	200	N111ZM	AAL200	JFK	BOS	A321	07:44	07:44	07:36	09:00	09:00	08:37
AAL	202	N993NN	AAL202	LAX	BOS	B738	13:45	13:45	13:46	22:23	22:23	22:08
AAL	226	N874NN	AAL226	ORD	BOS	B738	06:00	06:00	05:50	09:18	09:18	09:08
AAL	252	N948NN	AAL252	ORD	BOS	B738	09:55	09:55	09:53	13:14	13:14	13:04
AAL	746	N575UW	AAL746	PHL	BOS	A321	17:30	17:30	17:26	18:59	18:59	18:53
AAL	815	N559UW	AAL815	DFW	BOS	A321	20:20	20:20	20:17	01:00	01:00	00:58

The ASPM airport efficiency database also includes runway configuration at each major airport in the NAS in hourly and 15-minute increments, with an example day of data for Boston Logan Airport shown in Table 5. For each hourly time increment, the corresponding hour of arrival and departure counts by aircraft type are allocated proportionally to the active runways. For example, flights were assumed to be equally split between runways when the airport efficiency report table indicates that two arrival runways were active. This assumption results in inaccurate allocation in some cases, as arrivals and departures often favor one runway over another (for example, runway 33R at BOS is shown as an active runway for portions of the day in Table 5, but this runway is a mere 2,557 ft in length and is only used for certain propeller aircraft arrivals). However, it accounts for large-scale traffic allocation by runway at an airport, particularly when averaged over a full year of operations.

**Table 5. Example airport efficiency data from ASPM**

Airport	Scheduled Departure Date	Local Hour	Scheduled Departures	Scheduled Arrivals	Actual Departures	Actual Arrivals	Actual Total	ADR+ Cap AAR	Runway Configuration (Arr Dep)
BOS	05/01/2018	0	1	16	3	22	25	80	4R   4L, 4R, 9
BOS	05/01/2018	1	1	6	1	4	5	80	4R   4L, 4R, 9
BOS	05/01/2018	2	0	0	0	1	1	80	4R   4L, 4R, 9
BOS	05/01/2018	3	0	0	0	0	0	80	4R   4L, 4R, 9
BOS	05/01/2018	4	0	0	0	3	3	80	4R   4L, 4R, 9
BOS	05/01/2018	5	18	9	17	14	31	80	33L   27, 33L
BOS	05/01/2018	6	50	9	44	14	58	82	33L, 33R   27, 33L
BOS	05/01/2018	7	43	29	41	38	79	82	33L, 33R   27, 33L
BOS	05/01/2018	8	33	27	44	33	77	82	33L, 33R   27, 33L
BOS	05/01/2018	9	40	23	42	29	71	82	33L, 33R   27, 33L
BOS	05/01/2018	10	33	26	36	32	68	82	33L, 33R   27, 33L
BOS	05/01/2018	11	29	24	35	28	63	82	27, 32   33L
BOS	05/01/2018	12	27	31	28	37	65	80	27, 32   33L
BOS	05/01/2018	13	26	41	35	38	73	80	27, 32   33L
BOS	05/01/2018	14	36	31	29	42	71	80	27, 32   33L
BOS	05/01/2018	15	27	31	41	31	72	80	27, 32   33L
BOS	05/01/2018	16	33	34	31	43	74	80	27, 32   33L
BOS	05/01/2018	17	39	45	44	45	89	80	27, 32   33L
BOS	05/01/2018	18	37	38	38	43	81	81	22L   22L, 22R
BOS	05/01/2018	19	40	34	41	38	79	81	22L   22L, 22R
BOS	05/01/2018	20	21	28	27	33	60	81	22L   22L, 22R
BOS	05/01/2018	21	20	23	20	30	50	81	22L   22L, 22R
BOS	05/01/2018	22	9	29	20	27	47	81	22L   22L, 22R
BOS	05/01/2018	23	2	25	8	27	35	81	22L   22L, 22R
<b>Total</b>			<b>565</b>	<b>559</b>	<b>625</b>	<b>652</b>	<b>1277</b>	<b>1938</b>	

In terms of procedure allocation, the baseline chosen for comparative analysis in a noise study depends on the specific airport and procedure set available at that airport. For example, some airports may have baseline traffic footprints that are accurately modelled by straight-in arrivals to all runways. Others may have location-specific or time-specific procedures that must be incorporated into the baseline noise model. Heuristic procedure allocation schemes for arrivals and departures for specific runway ends can be specified by the analyst during the flight-level schedule generation process, or straight-in and straight-out assumptions may be used for simplified analysis.

### **3.7 Calculating Integrated Impacts**

Integrated impacts are calculated through a single-event superposition method based on gridded population exposure metrics. For this method to be computationally efficient, it is important that all noise results are computed and saved on a consistent observer grid. Either DNL or  $N_{\text{ABOVE}}$  can be calculated through summation of gridded single-event data. In the case of DNL, exposure is calculated using Eq. 2. For calculating  $N_{\text{ABOVE}}$ , the observer grid locations impacted by noise above a set  $L_{\text{MAX}}$  (day and night) threshold are catalogued for each single-flight noise event. For each observer location, the corresponding  $N_{\text{ABOVE}}$  value is simply the number of operations where the noise level was above the set threshold.

### **3.8 Population Impact Modeling**

The ultimate objective of noise analysis is to evaluate population impact, including annoyance, exposure numbers, and potential consideration of equity metrics. This requires population data analysis on a location-specific basis. Such analysis can be accomplished using raw US Census population counts, although these data are provided on an irregular grid defined by census block geometry (the finest resolution available from the US Census for population counts). Additional demographic data is also provided on a coarser grid (at the block group level) – these data are required for equity and environmental justice assessment studies. The scope of this thesis is limited to population exposure metrics without consideration of supplemental demographic data.

In order to allow for rapid population assessment for a wide range of airports across the NAS, a population re-gridding method was developed for this framework. The re-gridding method ingests raw block-level census data at the from the US Census Bureau. Population counts are converted to densities by pre-calculating the land area of each census tract. Figure 22 shows an example of raw census block data, with absolute population count shown for each geospatial region as well as calculated block area.



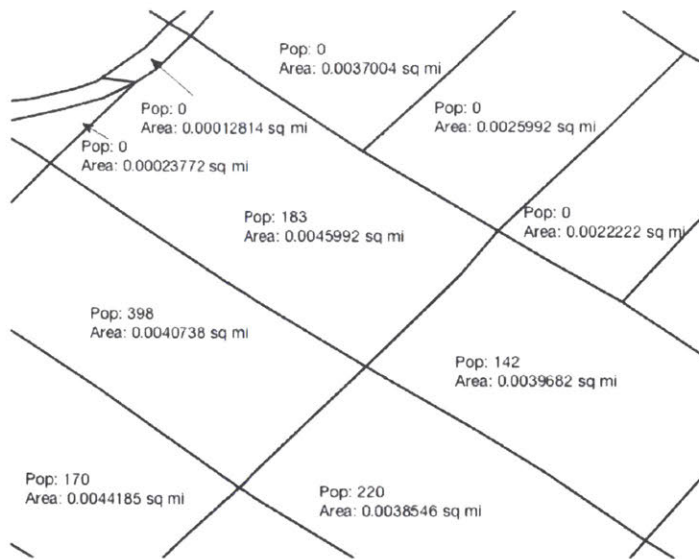


**Figure 22. Representative census blocks and population counts with calculated areas**

In traditional noise impact studies, population counts are retained in this irregularly-spaced format and all impact variables are calculated at the centroid location for a given block. However, the gridded noise impact method for rapid impact analysis at multiple airport and runway ends required further processing. Population density is calculated for each block. The method assumes uniform distribution of population throughout census-designated geospatial regions. Resulting population densities are shown in Figure 23 for a 1 NM square region of Boston and Cambridge, MA.

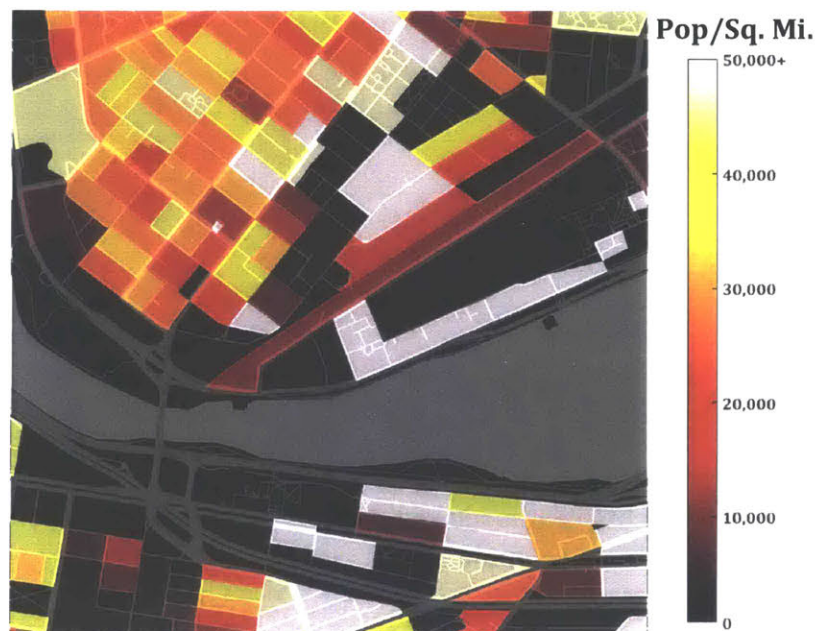


**Figure 23. 2010 US Census block-level absolute population counts converted to geospatial population density**

A regular grid is then superimposed and the overlap percentage of each grid cell with nearby census regions is calculated. Figure 24 shows an example of grid coverage calculation for a single census block. The population count for each block is redistributed to the regular 0.1 NM x 0.1 NM grid based on the population density and overlap percentages. The population allocated to each square grid cell is the summation of constituent population contributions from each census block partially or fully overlapping that cell.

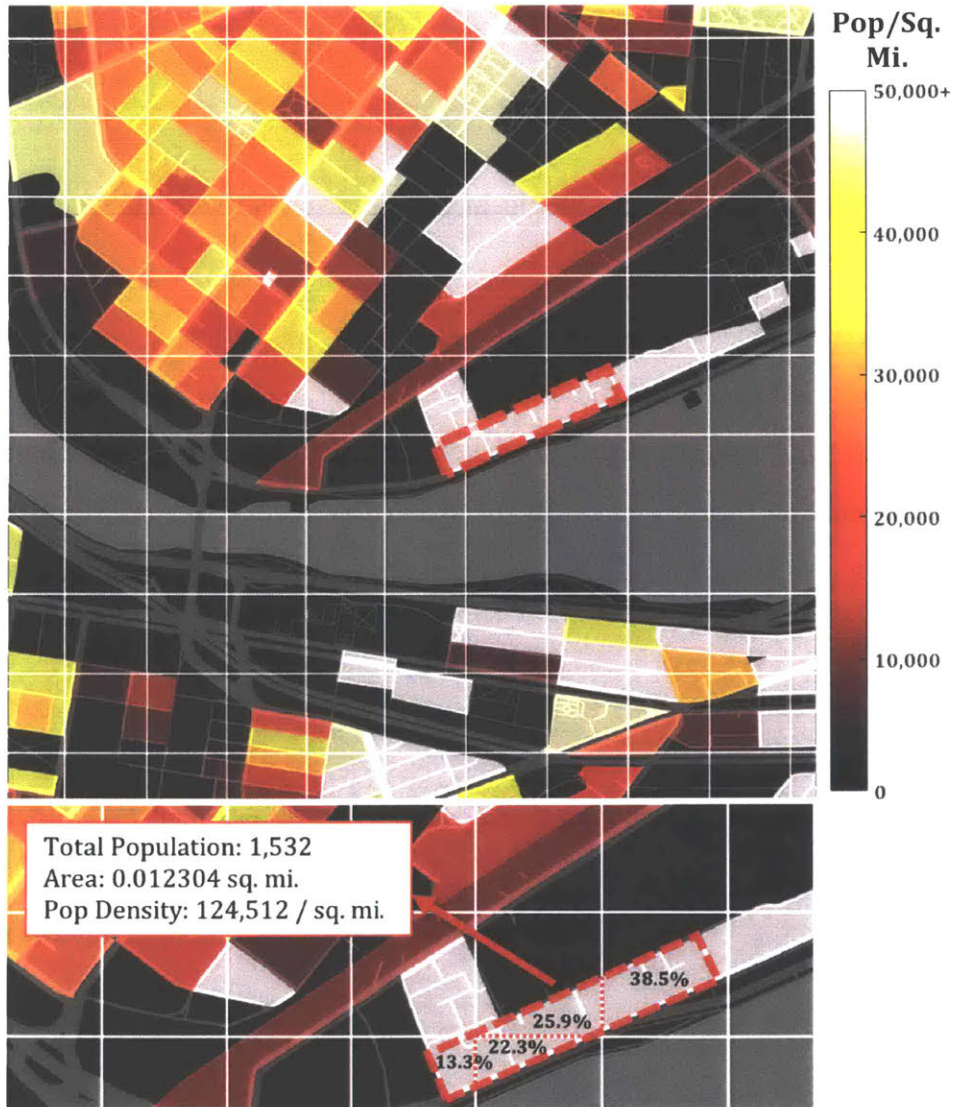


**Figure 24. Demonstration of area-based census data redistribution method for gridded population calculation**

A complete example of re-gridded population data from 2010 Census block-level counts onto to a regular 0.1 NM square grid over a 1 NM square region is shown in Figure 25.

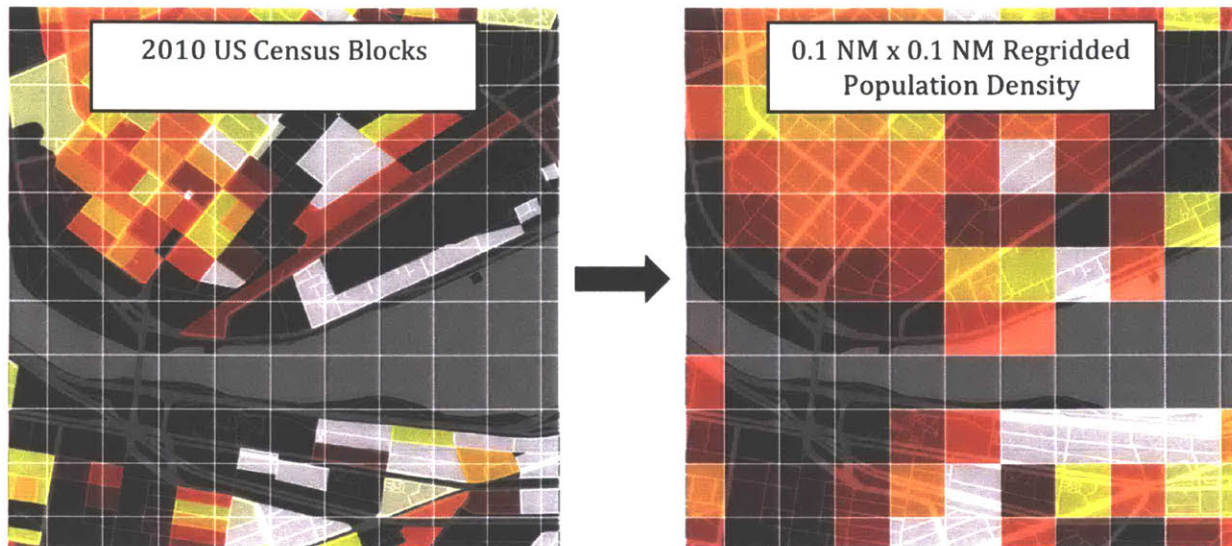


**Figure 25. Re-Gridded 2010 Block-Level US Census Population Data**

Population re-gridding saves computational expense because noise results and population numbers are saved on a consistent grid on an airport-by-airport basis. As a result, population exposure can be calculated simultaneously with noise levels in this method. The re-gridding method can be applied in a cartesian North-up reference frame (as shown in Figure 25) or in a runway oriented track-up frame. Both methods have potential computation benefits depending on the desired noise analysis and metrics. North-up grid generation centered around a common airport point allows single-event noise results for an airport to be compiled in a consistent reference frame. Combination of these procedures into cumulative metric is then a simple exercise of pointwise arithmetic (such as logarithmic summation of SEL results to generate DNL contours). Runway oriented track-up population gridding allows noise assessment to be performed once for a procedure concept on a gridpoint basis and applied to each runway end of interest without requiring re-generation of noise contours.

Both north-up and runway-aligned noise grids were pre-calculated for each of the OEP-35 airports in the United States. Six example processed population density maps are shown in Figure 26.

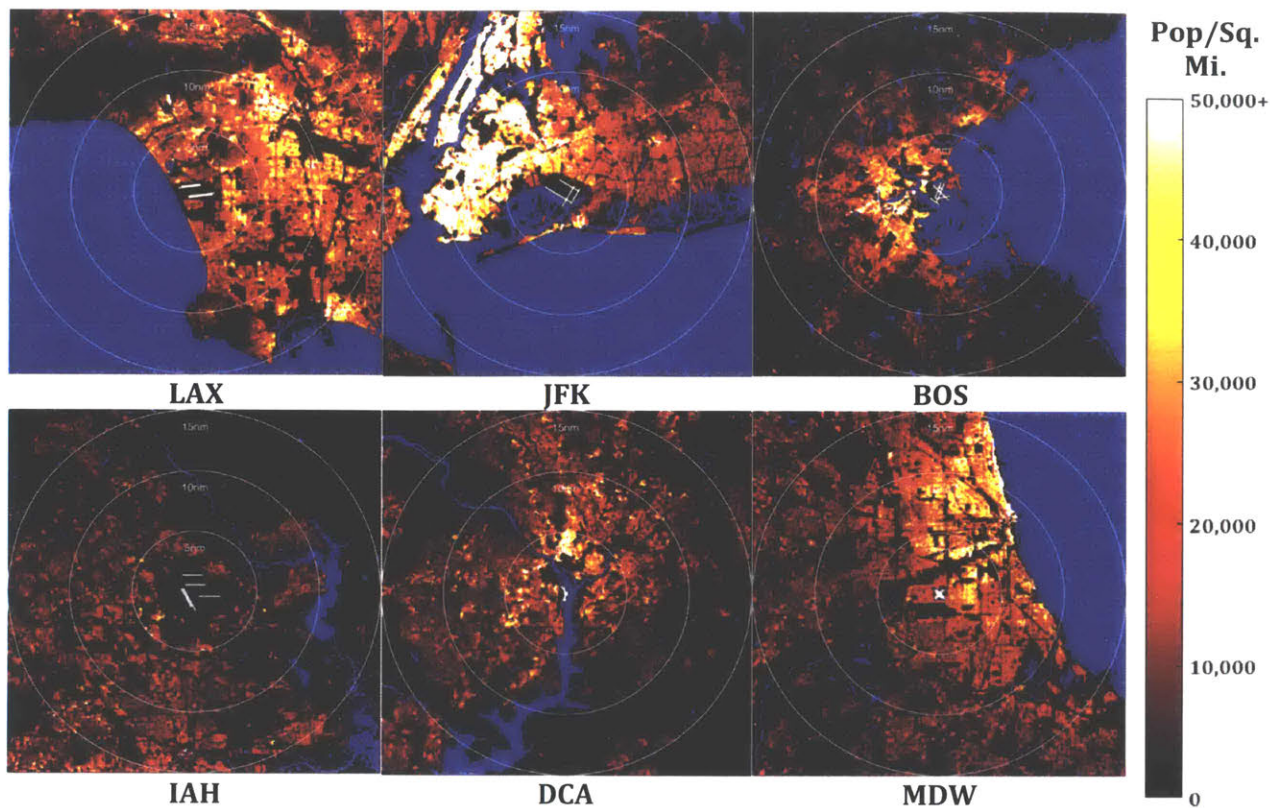


Figure 26. Re-gridded population data for six examples from the OEP-35 airports

### 3.9 Noise Impact Reporting and Visualization

The final output of the noise analysis method is data and impact visualization. Due to the complex nature of noise metrics, flight procedure design and allocation, timetable assumptions, and impact analysis, it is important to select effective data and graphics to convey results to a wide range of stakeholders. Typically, quantitative results are presented in terms of total population impacted positively and negatively by a proposed procedure change according to a set noise metric and threshold level. This may be presented in tabular format, further broken down by locality and/or demographic impacts, or graphically as annotations on contour diagrams.

In terms of graphical result presentation, most noise impact analyses result in contour diagrams overlaid on maps showing communities in the vicinity of airports. Metadata on these graphics may include population density, noise-sensitive areas (schools, hospitals, places of worship), and other relevant cartographic features. In most cases, the objective of a noise visualization is to demonstrate the change in exposure expected to occur from a proposed change. This change may be demonstrated

with a binary representation (i.e. graphical depiction of areas that are “better” and “worse” compared to a baseline metric) or with a nuanced depiction showing magnitude of change.

One of the key challenges of noise visualization is that impact analysis typically depends on both baseline noise exposure levels as well as expected change due to an operational change. For example, an increase in  $N_{\text{ABOVE}}$  of 20 operations per day is significantly more perceptible from a baseline of 0 daily operations than from a high starting baseline of 100 or more operations per day. Therefore, graphics must depict in some manner both the baseline impact level in a region of interest as well as expected changes. While past regulation, research, and best practice has resulted in typical contour formats for NEPA and FAA Part 150 DNL noise exposure maps and impact reporting, there is potential for improvement and standardization for noise studies involving alternative metrics such as  $N_{\text{ABOVE}}$ . The details of effective noise impact visualization characteristics are outside the scope of this thesis.



## Chapter 4. Characteristics and Constraints for RNAV and RNP Approaches

RNAV and RNP procedures provide increased precision relative to conventional radio-based procedures such as Instrument Landing System (ILS), Localizer, and VHF Omnidirectional Range (VOR) approaches. Figure 27 shows the high-level conceptual difference between conventional, RNAV, and RNP procedures. These procedures are defined using GPS-based waypoints and leg types, allowing increased flexibility relative to conventional guidance. Implementation to date has focused on safety and efficiency benefits from RNAV and RNP. From a noise perspective, PBN procedures provide increased flexibility relative to conventional navigation guidance in terms of lateral and vertical path constraints. For approaches, the increased flexibility of RNAV and RNP may allow for shortened final approach segment lengths and steeper final approach intercept angles compared to conventional procedures. In addition, GPS or barometric vertical guidance allows for simpler adjustment of glide path angle on final approach relative to conventional ground-based vertical guidance systems such as the ILS glideslope.

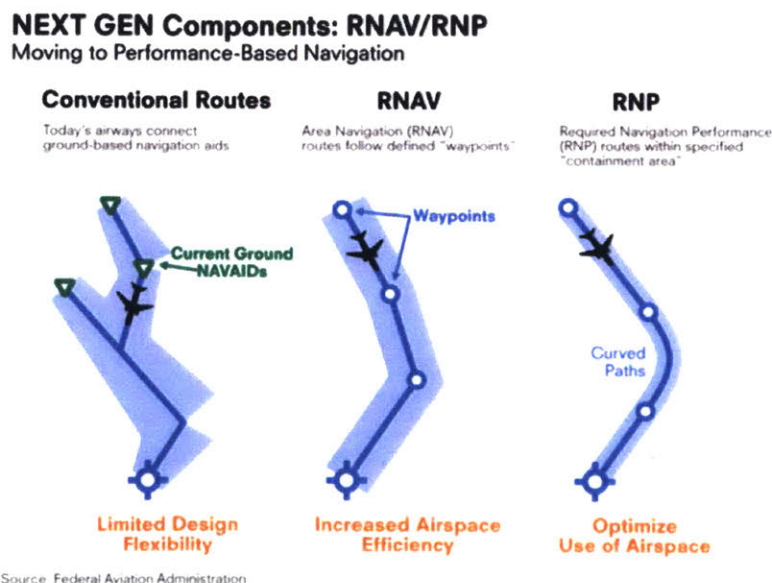
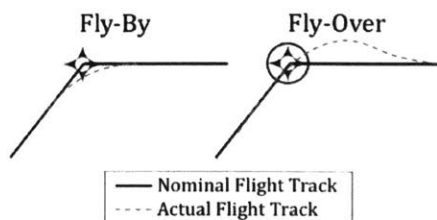


Figure 27. Conceptual difference between conventional navigation, RNAV, and RNP

Procedure definitions are encoded and stored in cockpit flight management system databases, allowing pilots to load and activate the desired trajectory into guidance displays and autoflight systems. RNAV and RNP procedure definitions have the potential to increase predictability for pilots and ATC while reduce workload for both groups. While both RNAV and RNP procedures can incorporate either straight track-to-fix (TF) or curved radius-to-fix (RF) segments, RF legs in RNAV procedures require advanced equipage compared to typical TF-based procedures and are more characteristic of RNP procedures<sup>4</sup>.

### 4.1 RNAV Approach Design Parameters and Criteria

RNAV approach procedures enable navigation between arbitrary points in space without the use of ground-based navigation aids. Typically, RNAV procedures are executed using GPS navigation guidance. While several leg types are permitted in RNAV procedure definitions, the most common constituent leg type for arrivals is the “track to fix” or TF legs. These legs connect waypoints in sequential order. For waypoints designated as “fly-by”, the flight management system on the aircraft anticipates an upcoming waypoint and initiates a turn prior to arrival, placing the aircraft track inside the turn. For waypoints designated as “fly-over”, the aircraft overflies the waypoint prior to initiating a turn, placing the aircraft track outside the turn. Figure 28 shows the difference in ground track for an aircraft passing a fly-by and a fly-over waypoint. Fly-by waypoints are more commonly used in arrival and departure procedures than fly-over waypoints. The following criteria discussion focuses on sequences of fly-by waypoint connected by TF legs.



**Figure 28. Flyby vs. flyover waypoints**

---

<sup>4</sup> FAA Order 8260.58A PBN Design: 1-2-5(d)(3)



The cross-track tolerance for RNAV procedures during the approach phase (other than the final approach course) and during departures is 1 NM, referred to as RNP-1. In the final approach segment of an approach, the RNP level may be specified in the procedure depending on obstacle clearance or other operational requirements. Typical cross-track tolerance in the final approach course for current RNP procedures is 0.3 NM, although procedures may have reduced RNP tolerances to enable reduced minimums. Minimums refer to the lowest altitude to which an aircraft may descend during the final approach segment without visual acquisition of the runway environment. As a result, lower minimums enable landings in worse weather conditions. Figure 29 shows an example RNP approach profile view for Runway 19 at Washington National Airport with both RNP 0.11 and RNP 0.30 minimums, showing the benefit of higher precision in terms of reduced minimums. Future procedures may be able to utilize similar variable RNP levels to enable specific operational and noise-related goals.

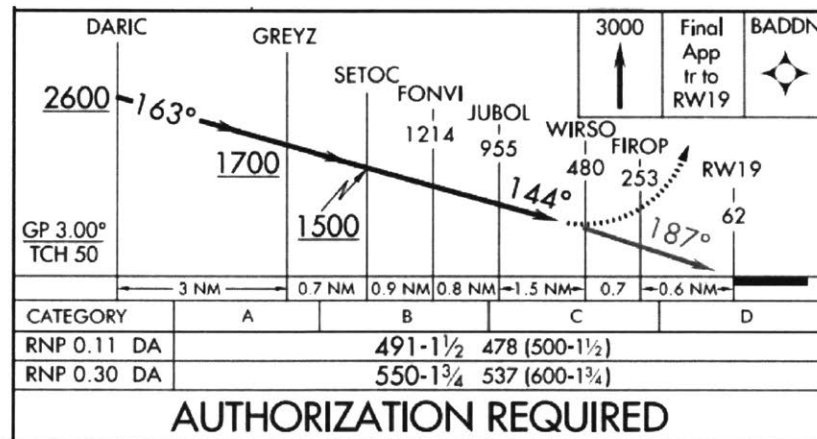


**Figure 29. Profile view for RNP Runway 19 approach at DCA with variable minimums depending on RNP level on the final approach segment**

While navigation accuracy is generally better than the required performance, the width of the obstacle protected area around an RNAV procedure centerline allows a wide variety of navigation systems and aircraft types to utilize the procedure without special aircrew training or software modifications.

In order to obtain maximal noise benefits from RNAV approach procedures, aggressive procedures may be designed within the confines of operational limitations and design criteria imposed by the FAA. These criteria are in place to ensure consistency across the NAS, repeatability

of ground tracks on an individual procedure, flyability by all necessary aircraft types in worst-case wind conditions, and safe obstacle clearance throughout the procedure. General procedure design criteria are outlined in the same document used for conventional procedure criteria, the US Standard for Terminal Information Procedures (TERPS) [125]. Criteria specific to publicly-available RNAV and RNP arrival and departure procedures are published separately in the US Standard for PBN Instrument Procedure Design [126]. The design criteria that are most relevant for noise-reduction approach procedure design are discussed in more detail below.

#### **4.1.1 Fix-to-Fix Leg Length**

In terms of flyability, procedures are constrained by vertical path angle, leg alignment constraints, and minimum leg lengths between waypoints. Vertical path constraints are intended to enable the aircraft types expected to use an approach or departure to execute the procedure in a stabilized manner given aircraft performance and anticipated weather conditions. Minimum leg length constraints are intended to provide adequate distance for aircraft to physically turn onto successive procedure segments given anticipated speeds and bank angles while also allowing cockpit flight management systems to cycle between waypoints.

Speed assumptions for leg length calculations are based on aircraft approach category. Aircraft are divided into approach performance categories based on approach reference speed ( $V_{REF}$ ):

$$V_{REF} = 1.3 \times V_{SO}$$

Where  $V_{SO}$  is the stall speed for the aircraft at maximum landing weight in landing configuration. 14 CFR 97.3 defines  $V_{REF}$  thresholds for approach categories. Most transport category jet aircraft fall into approach category C and D. While approach procedures can be designed with different minimums and visibility requirements for different approach category aircraft, procedures for use at major airports intended to address noise from jet airliners must use assumptions and thresholds for category D aircraft.

Minimum leg length is driven by navigational accuracy as well as aircraft maneuverability and flyability. For navigation accuracy purposes, the minimum leg length between any two waypoints on a straight approach segment is 1 NM or twice the cross-track tolerance (XTT) of the approach

segment, whichever is smaller. For RNAV approaches, where the XTT is 1 NM<sup>5</sup>, the minimum leg length is therefore 1 NM. For flyability purposes, the minimum leg length must allow for turn anticipation leading into and out of the segment. The distance of turn anticipation (DTA) depends on aircraft speed as well as bank angle. The indicated airspeed assumptions for DTA calculation are shown in Table 6.

**Table 6. Aircraft Approach Categories and Procedure Design Speed Assumptions**

Approach Category and V <sub>REF</sub> Range (KIAS) <sup>6</sup>	Procedure Design Speed Assumptions Below 10,000 ft <sup>7</sup> (KIAS)		
	Initial and Intermediate Approach Segment	Final Approach Segment	Missed Approach and Departure
<b>A:</b> V <sub>REF</sub> < 91 kts	150	90	110
<b>B:</b> 91 ≤ V <sub>REF</sub> < 121 kts	180	120	150
<b>C:</b> 121 ≤ V <sub>REF</sub> < 141 kts	250	140	240
<b>D:</b> 141 ≤ V <sub>REF</sub> < 166 kts	250	165	265
<b>E:</b> V <sub>REF</sub> ≥ 166 kts	310	250	310

Turn radius and DTA are a function of groundspeed and bank angle. In order to determine groundspeed, the assumed indicated airspeed (V<sub>KIAS</sub>) must be converted to true airspeed (V<sub>KTAS</sub>) and further corrected for assumed worst-case tailwinds. For the purpose of procedure design, V<sub>KTAS</sub> is calculated using Eq. 3:<sup>8</sup>

$$V_{KTAS} = \frac{V_{KIAS} \times 171233 \times \sqrt{303 - 0.00198 \times \text{alt}}}{(288 - 0.00198 \times \text{alt})^{2.628}} \quad \text{Eq. 3}$$

Where:

alt = Altitude above sea level (ft)

V<sub>KIAS</sub> = Indicated airspeed (knots)

V<sub>KTAS</sub> = True airspeed (knots)

<sup>5</sup> FAA Order 8260.58A PBN Design: Table 1-2-1

<sup>6</sup> 14 CFR 97.3

<sup>7</sup> FAA Order 8260.58A PBN Design: Table 1-2-2

<sup>8</sup> FAA Order 8260.58A PBN Design: Formula 1-2-7

True airspeed is then corrected for worst-case tailwinds. A tailwind of 30 knots is assumed at or below 2,000 ft above ground level (AGL). Above 2,000 ft AGL, the tailwind is calculated using Eq. 4.<sup>9</sup> The tailwind assumption may be augmented or replaced with a retrospective wind study to enable either higher or lower minimum leg lengths, depending on operational needs and prevailing wind conditions at specific airports. For example, airports with strong seasonal winds may require increased wind assumptions to ensure that published procedures are flyable by all anticipated aircraft types and Flight Management Systems (FMS) in worst-case weather conditions.

$$V_{KTW} = 0.00198 \times \text{alt} + 47 \quad \text{Eq. 4}$$

Where:

alt = Altitude above sea level (ft)

$V_{KTW}$  = Tailwind speed (knots)

Groundspeed ( $V_{\text{ground}}$ ) is the sum of  $V_{KTAS}$  and  $V_{KTW}$ . For RNAV procedures with an XTT of 1 NM, bank angle ( $\phi$ ) is assumed to be 3° below 500 ft AGL. Above 500 ft AGL, bank angle is assumed to be the lesser of 5° or one-half the track change of the turn ( $\beta$ ), to a maximum of 25°. Given bank angle and groundspeed, the turn radius may then be calculated using Eq. 5.<sup>10</sup>

$$R = \frac{V_{\text{ground}}^2}{\tan \phi \times 68625.4} \quad \text{Eq. 5}$$

Where:

R = Turn radius (NM)

$V_{\text{ground}}$  = Groundspeed (knots)

$\phi$  = Bank angle (degrees)

---

<sup>9</sup> FAA Order 8260.58A PBN Design: Formula 1-2-8

<sup>10</sup> FAA Order 8260.58A PBN Design: Formula 1-2-10

The DTA associated with a turn at a waypoint may then be calculated using Eq. 6.<sup>11</sup>

$$DTA = R \times \tan \frac{\beta}{2} \quad \text{Eq. 6}$$

Where:

DTA = Distance of Turn Anticipation (NM)

R = Turn radius (NM)

$\beta$  = Magnitude of heading change (degrees)

The minimum segment length between two fly-by RNAV waypoints is the sum of the DTA from the turn leading into the segment (“DTA<sub>1</sub>”) and the DTA from the turn exiting the segment (“DTA<sub>2</sub>”) as illustrated in Figure 30. Because the minimum segment length is a function of turn anticipation distance from multiple waypoints, each with potentially different speed and wind assumptions, criteria-compliant procedure design requires an iterative analysis strategy that captures leg-to-leg variability.

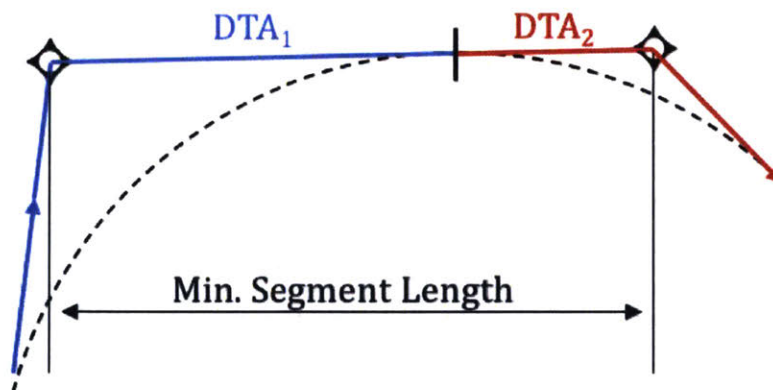


**Figure 30. Illustration of minimum segment length between two fly-by RNAV waypoints**

Any turn with a magnitude less than or equal to 10° is assigned a DTA of 0. This allows shallow turns to be incorporated in procedures without incurring an increase in minimum leg length. For certain turn geometries, the lack of turn anticipation requirement for shallow turns allows a cumulative heading change to be split between multiple track segments in order to reduce total

---

<sup>11</sup> FAA Order 8260.58A PBN Design: Paragraph 1-2-5 (b) 1-a(1)

along-track distance required for that change. This effect is shown in Figure 31, where a 2-segment 45° total heading change requires less along-track distance using a shallow secondary turn (shown in black) relative to a similar procedure where both turns involve greater than 10° of total heading change.

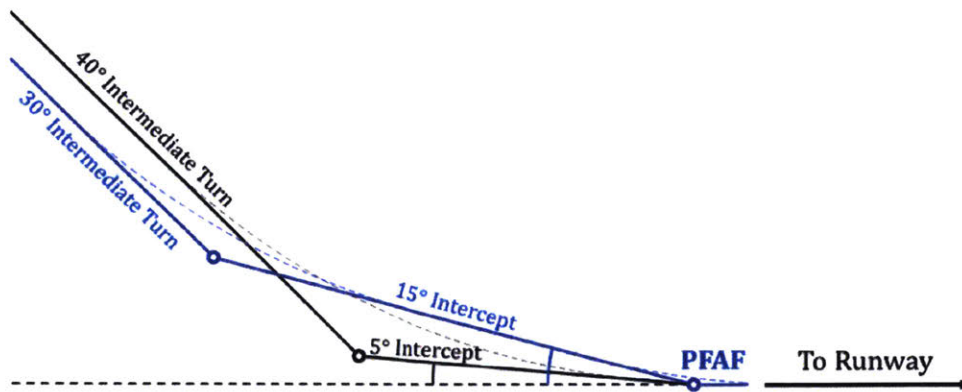


**Figure 31. 2-segment RNAV approach segment with 45° total heading change distributed between final turn and intermediate turn**

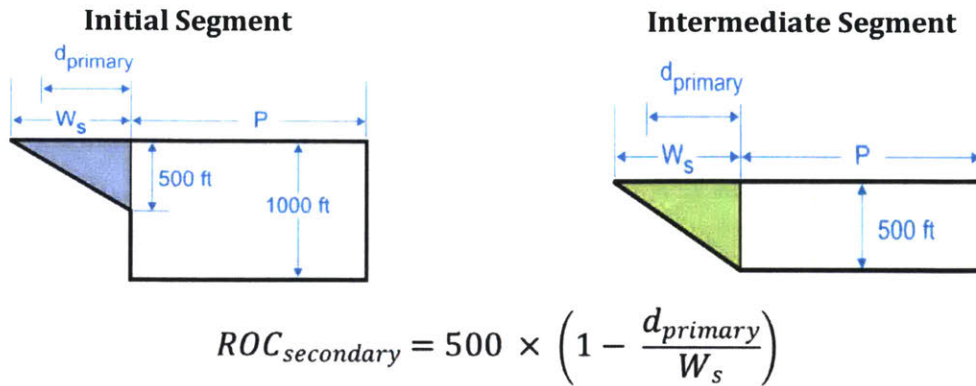
#### 4.1.2 Required Obstacle Clearance

The general principal of procedure design criteria is to ensure flyability and safe obstacle avoidance margins for arriving aircraft in instrument meteorological conditions. These conditions must be met for all aircraft types, assuming worst-case wind conditions and aircraft maneuverability. Required obstacle clearance (ROC) is the fundamental driver for minimum altitude constraints. The ROC depends on the designation of the procedure leg. For example, ROC values are smaller during final approach than during procedure segments farther from the airport.

A buffer zone is built around a procedure centerline depending on the cross-track accuracy of the underlying navigation system as well as procedure-specific geometry. For approach and procedures, there are typically two buffer zones: an inner “primary area” and an outer “secondary area”. The primary area may have different ROC values from the secondary area.

For straight segments within procedures connecting fly-by waypoints, the ROC value within the primary area of the procedure is 1000 ft for initial segments and 500 ft for intermediate segments. The secondary area for both initial and intermediate segments consists of a linearly-tapering obstacle

protection surface from 500 ft ROC at the inside boundary of the secondary area to 0 ft ROC at the outside boundary. The cross-sectional geometry of RNAV leg ROC values is shown in Figure 32.



Where:

$d_{primary}$  = Perpendicular distance (feet) from primary area edge

$W_s$  = Total width of the secondary area (feet)

**Figure 32. Required Obstacle Clearance for initial and intermediate straight RNAV approach segments connecting fly-by waypoints<sup>12</sup>**

For the final approach segment of a vertically-guided RNAV procedure, ROC is provided through the use of a sloping Obstacle Clearance Surface (OCS). No obstacle may penetrate the OCS along the final approach segment. If obstacles do penetrate the OCS, minimums and/or glide path angle must be increased. The geometry of the OCS depends on the source of vertical guidance on the final approach segment. Figure 33 shows the OCS geometry for Lateral/Vertical Navigation (LNAV/VNAV) and Localizer Performance with Vertical Guidance (LPV) or Ground-Based Augmentation System (GBAS) Landing System (GLS) final approach guidance. LNAV/VNAV procedures use onboard barometric readings to calculate vertical guidance (Baro-VNAV). In some cases, GPS signals with Wide Area Augmentation Systems (WAAS) can be used in lieu of Baro-VNAV to supply vertical guidance on LNAV/VNAV final approach segments. LPV/GLS final approaches use ground-based augmented GPS signals to provide vertical guidance.

<sup>12</sup> FAA Order 8260.3D TERPS: Figure 2-4-2 and 2-5-2; Formula 2-4-1 and 2-5-1

For final approach segments without vertical guidance, the ROC for the full length of the final approach segment is 250 ft in the primary area, tapering from 250 ft to 0 ft in the secondary area. Because the obstacle protection surface is not sloped for procedures without vertical guidance, obstacles for the full length of the final approach segment dictate minimums for the approach.

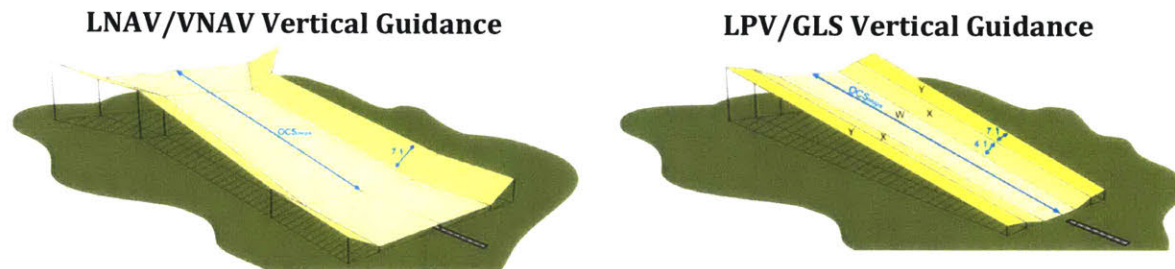


**Figure 33. Obstacle clearance surface for vertically-guided RNAV final approach segments<sup>13</sup>**

In order to determine the minimum height for specific segments of an RNAV procedure other than the final approach, the ROC for the primary and secondary area of each segment must be compared with underlying obstacle and terrain databases. Any location 20,000 ft or further from the nearest runway at an airport is also required to consider a 200 ft Adverse Assumption Obstacle (AAO) to account for potential unreported and unsurveyed construction away from the immediate airport vicinity.<sup>14</sup> The ROC for the segment type (i.e. 500 ft for the primary area of an intermediate segment) is then added to the height of the controlling obstacle and rounded to the next highest 100 ft increment. The obstacle that drives the level segment minimum altitude is that which results in the largest sum of obstacle height and ROC and is referred to as the “controlling obstacle”. For example, the minimum intermediate segment altitude at the PFAF is 500 ft above the top of the controlling obstacle or AAO, whichever is higher, rounded to the next highest 100 ft.

#### **4.1.3 Final Approach Segment Length and Glide Path Angle**

Many noise-motivated procedure design efforts seek to shorten the final approach segment to allow for lateral track movement away from the extended runway centerline. For RNAV approaches,

---

<sup>13</sup> FAA Order 8260.58A PBN Standards: Figure 3-3-1 and 3-4-3

<sup>14</sup> FAA Order 8260.19H Flight Procedures and Airspace: Section 2-11-5(b)



the minimum distance from the threshold to the PFAF is defined by the location where the barometric glide path angle (GPA) for approaches with vertical guidance or visual descent angle (VDA) for approaches without vertical guidance intersects the minimum intermediate segment altitude. This distance is calculated using Eq. 7.<sup>15</sup>

$$d_{\text{Baro}} = \ln \frac{r + \text{alt}_e}{r + \text{alt}_b} \times \frac{r}{\tan \theta} \quad \text{Eq. 7}$$

Where:

$d_{\text{Baro}}$  = Distance along barometric glidepath (ft)

$\text{alt}_b$  = Altitude at beginning of segment (ft AGL)

$\text{alt}_e$  = Altitude at end of segment (ft AGL)

$\theta$  = GPA/VDA (degrees)

$r$  = Mean radius of Earth (20,890,537 ft per FAA convention)

The maximum glide path angle for the final approach segment is dependent on the approach category of the aircraft, as shown in Table 7. For procedures intended to serve transport-category jet aircraft which are typically in approach category C or D, the maximum permissible glide path angle with or without vertical guidance is 3.50°.

**Table 7. Maximum Glide Path Angle by Approach Category**

<b>Approach Category and V<sub>REF</sub> Range (KIAS)<sup>16</sup></b>	<b>Maximum GPA/VDA Angle<sup>17</sup></b>
<b>A:</b> V <sub>REF</sub> ≤ 80 kts	6.40°
<b>A:</b> 81 ≤ V <sub>REF</sub> < 91 kts	5.70°
<b>B:</b> 91 ≤ V <sub>REF</sub> < 121 kts	4.20°
<b>C:</b> 121 ≤ V <sub>REF</sub> < 141 kts	3.77°
<b>D:</b> 141 ≤ V <sub>REF</sub> < 166 kts	3.50°
<b>E:</b> V <sub>REF</sub> ≥ 166 kts	3.10°

Figure 34 shows a schematic of the final approach segment geometry relative to controlling obstacles at the PFAF. The minimum final approach segment length is a function of minimum PFAF

<sup>15</sup> FAA Order 8260.58A PBN Design: Formula 1-3-3

<sup>16</sup> 14 CFR 97.3

<sup>17</sup> FAA Order 8260.3D TERPS: Table 2-6-1

altitude as well as procedure glidepath angle. Table 8 shows the resulting minimum final approach segment length for Category C aircraft assuming a threshold crossing height of 50 ft.

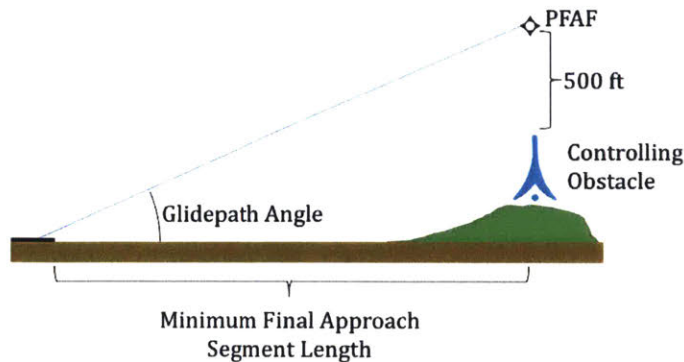


**Figure 34. Schematic of final approach segment geometry for RNAV procedures**

**Table 8. Minimum Final Approach Segment Length for RNAV procedures**

PFAF Altitude \ GPA	3.0°	3.1°	3.2°	3.3°	3.4°	3.5°
	Min. Final Approach Length (Nautical Miles)					
<b>800 ft</b>	2.36	2.28	2.21	2.14	2.08	2.02
<b>1,000 ft</b>	2.98	2.89	2.80	2.71	2.63	2.56
<b>1,200 ft</b>	3.61	3.49	3.39	3.28	3.19	3.09
<b>1,400 ft</b>	4.24	4.10	3.97	3.85	3.74	3.63
<b>1,600 ft</b>	4.87	4.71	4.56	4.42	4.29	4.17
<b>1,800 ft</b>	5.50	5.32	5.15	5.00	4.85	4.71
<b>2,000 ft</b>	6.12	5.93	5.74	5.57	5.40	5.25

## 4.2 RNP Approach Design Parameters and Criteria

RNP procedures are characterized by reduced cross-track tolerances and the availability of curved radius-to-fix (RF) legs for procedure construction. Because they are defined precisely and not calculated by onboard flight management systems, RF legs result in more predictable ground tracks than the fly-by waypoints typically used in RNAV procedures. TF legs may also be used in RNP approach procedure. The challenge of RNP procedures lies primarily with equipment and training, as onboard monitoring and alerting systems are required as well as special airline and pilot authorization to use a procedure. RNP equipment is expected to grow over time, allowing greater utilization of approach and departure procedures in the NAS.

### **4.2.1 Fix Geometry**

The fix-to-fix length requirements for TF legs are the same for RNP procedures as for RNAV. Construction of the procedures are similar to RNAV procedures with reduced cross-track tolerances and correspondingly increased flexibility with respect to obstacle avoidance. Due to increased automation and conformance monitoring in both straight segments and turns, shortened leg lengths are allowed relative to RNAV procedures. The minimum leg length is 0.2 NM with a maximum of three waypoints located in any 1 NM subsegment of the approach<sup>18</sup>. This increased flexibility may be used to connect multiple RF segments using short TF straight segments, for example.

For RF turns, the minimum radius is driven by aircraft airspeed (see Table 6), altitude, wind (see Eq. 4), and bank assumptions. For procedures with cross-track tolerances less than 1 NM (such as RNP 0.3 approach segments), the maximum bank angle is 20°<sup>19</sup>. The resulting minimum turn radius may be calculated using Eq. 5.

### **4.2.2 Required Obstacle Clearance**

The minimum altitude at the PFAF is determined by the controlling obstacle height along the intermediate segment. This altitude is calculated using the same method applied for RNAV approaches described in Section 4.1.2. For required obstacle clearance along the final approach segment, an obstacle clearance surface is constructed from the 250 ft height along the glidepath to the PFAF. The lowest permitted minimums for “Authorization Required” RNP approaches (RNP-AR) is 250 ft on the barometric glidepath. The actual height above the surface of the barometric glidepath is affected by temperature, with reduced temperatures resulting in reduced absolute aircraft altitude. For this reason, a critical low temperature value is specified for each approach. An additional margin is calculated as a “vertical error budget” (VEB) to account for altitude uncertainty on the final approach arising due to several factors. These include actual navigation performance error, waypoint

---

<sup>18</sup> FAA Order 8260.58A PBN Design: 4-1-1 (a)(3)

<sup>19</sup> FAA Order 8260.58A PBN Design: 1-2-5 (c)(3)(b)

precision error, flight technical error, altimetry system error, vertical angle error, and reported pressure level error.<sup>20</sup>

### **4.2.3 Final Approach Segment Length and Glide Path Angle**

For RNP-AR procedures, RF turns are allowed in the final approach segment. This allows the procedure to include a turning segment from the PFAF that continues to a lower final rollout point (FROP). The FROP is located along the final approach segment, which must be aligned within 3° of the extended runway centerline. The minimum distance from the threshold to the FROP is either the point where the glidepath reaches 500 ft above touchdown elevation or the point where the aircraft is 15 seconds from the decision altitude point assuming the fastest approach speed for the approach category with a 15-knot margin, whichever is greater.<sup>21</sup>

Glide path angle criteria for RNP approaches are the same as for RNAV approaches, as shown in Table 7. The standard glidepath is 3.0°. As for RNAV approaches, the steepness of the glidepath influences the minimum final approach segment length. Increasing the glidepath angle decreases the minimum final approach segment length and FROP distance, both of which are driven primarily by altitude constraints and obstacle clearance rather than waypoint cycling. Table 9 shows the distance from the FROP to the runway threshold as a function of approach category and glidepath angle for an RNP procedure to a sea-level runway with a decision height of 250 ft and threshold crossing height of 50 ft. These values assume a missed approach segment with cross track tolerance of 1 NM or greater.

For approaches with an RF turn in the final approach segment, the decision altitude may occur during a turning segment. If the runway environment is not in sight and a missed approach is initiated using take-off/go-around mode during a turn, some autoflight systems require additional mode changes so the aircraft remains in the turn during the missed approach initiation. This may be

---

<sup>20</sup> FAA Order 8260.58A PBN Design: 4-2-4 (a)(2)

<sup>21</sup> FAA Order 8260.58A PBN Design: 4-2-2 (b)

rectified with approved operational procedures, additional training, and/or FMS software modifications. Considerations such as these motivate the requirement for aircraft and crew authorization on certain RNP procedures in current operations, although standardization is expected with more widespread development and implementation of procedures over time.

**Table 9. Minimum Distance from FROP to Threshold for RNP procedures assuming a 50 ft threshold crossing height**

Appch. Cat.	GPA	3.0°	3.1°	3.2°	3.3°	3.4°	3.5°
		Min. FROP Distance (Nautical Miles)					
A: 90 K <sub>IAS</sub>		1.41	1.37	1.32	1.28	1.25	1.21
B: 120 K <sub>IAS</sub>		1.41	1.37	1.32	1.28	1.25	1.21
C: 140 K <sub>IAS</sub>		1.41	1.37	1.32	1.28	1.25	1.21
D: 165 K <sub>IAS</sub>		1.41	1.39	1.37	1.35	1.33	1.32
E: 250 K <sub>IAS</sub>		1.78	1.75	1.74	1.72	1.70	1.69

### 4.3 Implications of RNAV and RNP Approach Design Parameters

In order to modify procedures to reduce community noise, it is often desirable to shorten the minimum final approach segment length as much as possible given safety and procedure design constraints. Shortened final approaches allow greater flexibility for procedure designers to avoid overflight of communities located on the extended runway centerline. As shown in Table 8 and Table 9, RNP procedures can be designed with shorter straight-in segments than RNAV procedures. For Approach Category D aircraft used in airline operations, the minimum straight final approach segment ranges from 1.32 NM to 1.41 NM depending on glidepath angle. This distance is independent of minimum PFAF altitude. For RNAV procedures, the minimum straight final distance is longer and depends directly on minimum PFAF altitude. Therefore, for locations where shortening the final approach segment as much as practical is advantageous, RNP procedures have greater flexibility than RNAV procedures.

For RNAV procedures, the maximum final approach intercept angle is determined by whether the procedure has vertical guidance. Procedures with vertical guidance have a maximum intercept angle of 15°, while those without vertical guidance have a larger limit of 30°. This difference means that approaches without vertical guidance have more flexibility in terms of leg geometry in the vicinity of the PFAF, potentially allowing noise-sensitive communities to be avoided.

The vertical profile followed by an arriving aircraft has a large impact on noise due to both altitude and thrust effects. Procedures with vertical guidance provide greater consistency and predictability for aircraft altitude above specific surface locations and reduce the incidence of level-offs with resulting temporary thrust increases. RNP procedures or RNAV procedures with vertical guidance (LPV or LNAV/VNAV) provide this consistency. From a single-event noise exposure standpoint, approaches with vertical guidance are preferable to those without.

One key factor that determines the practical utility of an approach procedure are its minimums, or the lowest altitude to which an aircraft may descend without visual acquisition of the runway environment. Minimums are driven by obstacles along the final approach segment and the obstacle protection area defined for the specific final approach guidance technology. Approaches with vertical guidance typically have the lower minimums than those without vertical guidance. Among approaches with vertical guidance, RNP approaches typically have the lower minimums than LNAV/VNAV or LPV RNAV approaches. Reducing the approach minimums increases the utility of a procedure by maximizing the percentage of time when weather conditions permit utilization. Operators and air traffic controllers prefer procedures with consistent utility across the broadest possible range of weather conditions.

Equipage is a major constraint on potential utilization for PBN procedures. Different procedure types have different requirements in terms of cockpit avionics. RNAV approaches without vertical guidance are the least restrictive and are flyable by most transport-category jet aircraft. RNAV approaches with vertical guidance require additional equipage. LPV approaches require a GPS receiver capable of receiving Wide Area Augmentation System (WAAS) signals, while LNAV/VNAV approaches require either WAAS or barometric VNAV systems. Equipage levels for certain types of vertical guidance are more stringent than those for lateral-only RNAV, so not all fleet types are capable of flying all types of RNAV procedures. RNP procedures require onboard monitoring and alerting systems, pilot training, and authorization requirements for airlines and aircraft fleets depending on RNP tolerances for the procedure. These requirements add cost and complexity for airline operators, reducing overall equipage and ability to fly RNP procedures relative to RNAV.

Air traffic control operates most effectively when the majority of traffic uses consistent routes and procedures. In order for PBN procedures to achieve consistent utilization, the traffic flows using these procedures must be compatible with overall procedures and ATC norms. For example, lower equipage levels for RNP procedures requires additional ATC workload to differentiate equipped aircraft from non-equipped aircraft, segregate traffic flows between the various navigation types, and ensure separation between aircraft with different equipage levels. This discourages the widespread adoption of navigation technologies without critical-mass adoption in the airline fleet.

#### **4.4 RNAV and RNP Characteristics for Existing Procedures**

RNAV and RNP procedures provide greater flexibility than conventional radio-based navigation in terms of approach guidance. While noise reduction is one potential benefit of modified RNAV and RNP procedure implementation, other potential benefits mechanisms include lower approach minimums for runways in challenging terrain, procedural separation for arrivals and departures, and other operational objectives. This section examines the degree to which existing RNAV and RNP procedures leverage the design criteria flexibility afforded by advanced PBN technology. It is important to note that most procedures are designed without noise as a key design consideration, so tend to use conservative design standards (i.e. straight-in geometry) to minimize pilot workload and potential for navigation error. The purpose of this analysis is to explore the set of current procedures for existence-cases of procedures with potential noise benefits at other airports.

In order to evaluate the current state of RNAV and RNP procedures in the NAS, the CIFP distribution dated March 29, 2018 was processed to extract parameters on final approach segment geometry and intermediate approach intercept angles. For this CIFP cycle, there were 6,041 total RNAV (GPS) approach procedures designated for a runway and 393 total public RNP approach procedures in the US. These were not further differentiated into procedures intended for use by air carrier jet aircraft (approach categories C & D), so statistics include procedures usable only by light general aviation aircraft as well.

#### 4.4.1 Current Procedure Characteristics

##### FINAL APPROACH LENGTH AND INTERCEPT GEOMETRY

The general configuration for the final approach segment of RNAV and RNP procedures are shown in Figure 35.



**Figure 35. Intermediate and final approach geometry for RNAV and RNP procedures**

In terms of noise impact, the length of the final straight approach segment is a key indicator of the aggressiveness of an approach design. For RNAV (GPS) approach procedures, the straight-in final approach leg connects the PFAF to the MAP. The intermediate segment prior to the PFAF may also be aligned with the runway. For RNAV (RNP) approach procedures, the turn onto the final straight approach segment may occur after passing the PFAF at the FROP. The final straight approach segment may refer to the entire final approach segment if it is aligned with the runway, or the segment from the FROP to the missed approach point if the final approach segment includes turns. Table 10 shows the final straight segment length and intercept geometry for all public RNAV (GPS) procedures in the US as of March 29, 2018.

**Table 10. Final approach geometry for RNAV (GPS) procedures in the NAS as of March 29, 2018**

Final Approach Length			Intercept Angle at PFAF		
<b>Total Procedures (with and without vertical guidance): 6,047</b>					
<b>≤ 3.0 NM</b>	42	0.7%	<b>≤ 1.0°</b>	5,746	95.0%
<b>3.1-4.0 NM</b>	224	3.7%	<b>1.1°-15.0°</b>	196	3.3%
<b>4.1-5.0 NM</b>	2327	38.5%	<b>15.1°-30.0°</b>	105	1.7%
<b>5.1-6.0 NM</b>	2659	44.0%			
<b>6.1-7.0 NM</b>	517	8.6%			
<b>&gt; 7.0 NM</b>	277	4.6%			

Table 10 shows an apparent scarcity of aggressive final approach geometry in currently published RNAV procedures. 95.0% of procedures do not include a turn at the final approach fix, indicating that a strong majority of procedures are designed with traditional conservative straight-



in alignment of the final and intermediate segments. In addition, 95.6% of RNAV procedures have a final approach segment length of 4.1 NM or greater. Both of these parameters indicate that RNAV procedures are typically designed with conservative final approach segment geometry that does not utilize the full design opportunity space allowed by RNAV criteria but is consistent with conventional straight-in approach design standards and norms.

Table 11 shows the distribution of key final approach parameters in public RNP approach procedures as of March 29, 2018. The table shows that the majority of RNP procedures currently in public distribution do not utilize the full capability and flexibility contained in the design standards. 11.7% of procedures include RF turns in the final approach segment, one of the key capabilities afforded by RNP relative to RNAV procedures. Using a straight final approach segment reduces track design flexibility and resulting noise reduction potential. This is corroborated by the small percentage (13.2%) of RNP procedures with a straight final segment length shorter than 3.0 NM. Broadly speaking, final approach segments longer than 3.0 NM can be achieved with RNAV guidance, again indicating that current RNP implementation is not benefiting from the full potential of precise guidance in the final approach phase.

**Table 11. Final Approach Geometry for RNP procedures in the NAS as of March 29, 2018**

Straight Final Approach			RF Leg in Final Approach Segment		
<b>Total Procedures: 393</b>					
<b>≤ 3.0 NM</b>	52	13.2%	<b>Yes</b>	46	11.7%
<b>3.1-4.0 NM</b>	103	26.2%	<b>No</b>	347	88.3%
<b>4.1-5.0 NM</b>	86	21.9%			
<b>5.1-6.0 NM</b>	98	24.9%			
<b>6.1-7.0 NM</b>	40	10.2%			
<b>&gt; 7.0 NM</b>	14	3.6%			

**GLIDEPATH ANGLE**

Table 12 shows the glidepath angle for all public PBN procedures in the US as of March 29, 2018. The table shows that the majority of procedures are designed with a standard glidepath angle of 3.0° or less. However, the prevalence of steeper approaches with PBN technology is striking. 21.1% of RNAV (GPS) approaches with vertical guidance have a glidepath angle steeper than 3.0°, while 6.4% of RNAV (RNP) procedures have the same characteristic. While the CIFP does not include notations

or justifications for steep glidepath angles on approach, the glidepath angle is currently changed from standard for operational need only (obstacle and terrain avoidance). However, the availability of these steeper approaches in the NAS may indicate potential feasibility of similar procedures motivated by noise considerations.

**Table 12. Glidepath angle for RNAV and RNP procedures in the NAS as of March 29, 2018**

Proc. Type GPA	RNAV (GPS) with Vertical Guidance		RNAV (RNP)	
	Total Procedures: 5,781		Total Procedures: 393	
GPA ≤ 3.0°	4,556	78.9%	368	93.6%
3.0° < GPA ≤ 3.1°	875	15.1%	9	2.3%
3.1° < GPA ≤ 3.2°	54	0.9%	3	0.8%
3.2° < GPA ≤ 3.3°	51	0.9%	2	0.5%
3.3° < GPA ≤ 3.4°	43	0.7%	0	0%
3.4° < GPA ≤ 3.5°	119	2.1%	5	1.3%
GPA > 3.5°	83	1.4%	6	1.5%

The operational community has historically expressed concern with widespread adoption of steeper approach path angles driven by factors other than safety, terrain, or airport access. This is due to the increase in energy level on final approach and corresponding risk for runway overrun accidents. Modern aircraft with clean aerodynamic configurations are less capable of reliably executing steep approach paths without the use of speed brakes, themselves a contributor to increased noise. Therefore, although there are potential noise reduction benefits from steeper approach procedures, they are not considered as an analysis parameter in this thesis due to potential operational hurdles.

#### 4.4.2 Existence Cases for Novel RNAV and RNP Procedure Design

A limited set of procedures that exercise the criteria limits of RNAV and RNP have already been published. The approach procedures shown in Figure 36 are existence cases for advanced procedures such as those explored in this thesis. Figure 36(a) shows the RNAV (GPS) X approach to Runway 29 at Newark Liberty International Airport. This approach includes a final approach segment length of 3.1 NM, a final approach intercept angle of 27°, and a final approach course offset from the extended runway centerline by 12.68°, and a glide path angle of 3.5°. The procedure has minimum descent altitude of 510 ft AGL, allowing utilization of Runway 29 in weather conditions lower than possible

with visual approaches (there are no conventional instrument approach procedures to Runway 29). Figure 36(b) shows the RNAV (RNP) approach to Runway 26L at Honolulu International Airport. This approach includes a final rollout distance of 1.33 NM preceded by an RF turn in the final approach segment. This final rollout distance is slightly less than the minimum value presented in Table 9 because the threshold crossing height in Figure 36(b) is raised 25 ft for obstacle clearance (HNL), thus moving the 500 ft rollout altitude closer to the threshold while maintaining a standard 3.0° glide path angle. Procedures similar to those shown in Figure 36 have potential to be applied at other runways in the NAS with noise issues not addressable through conventional approach procedure design.

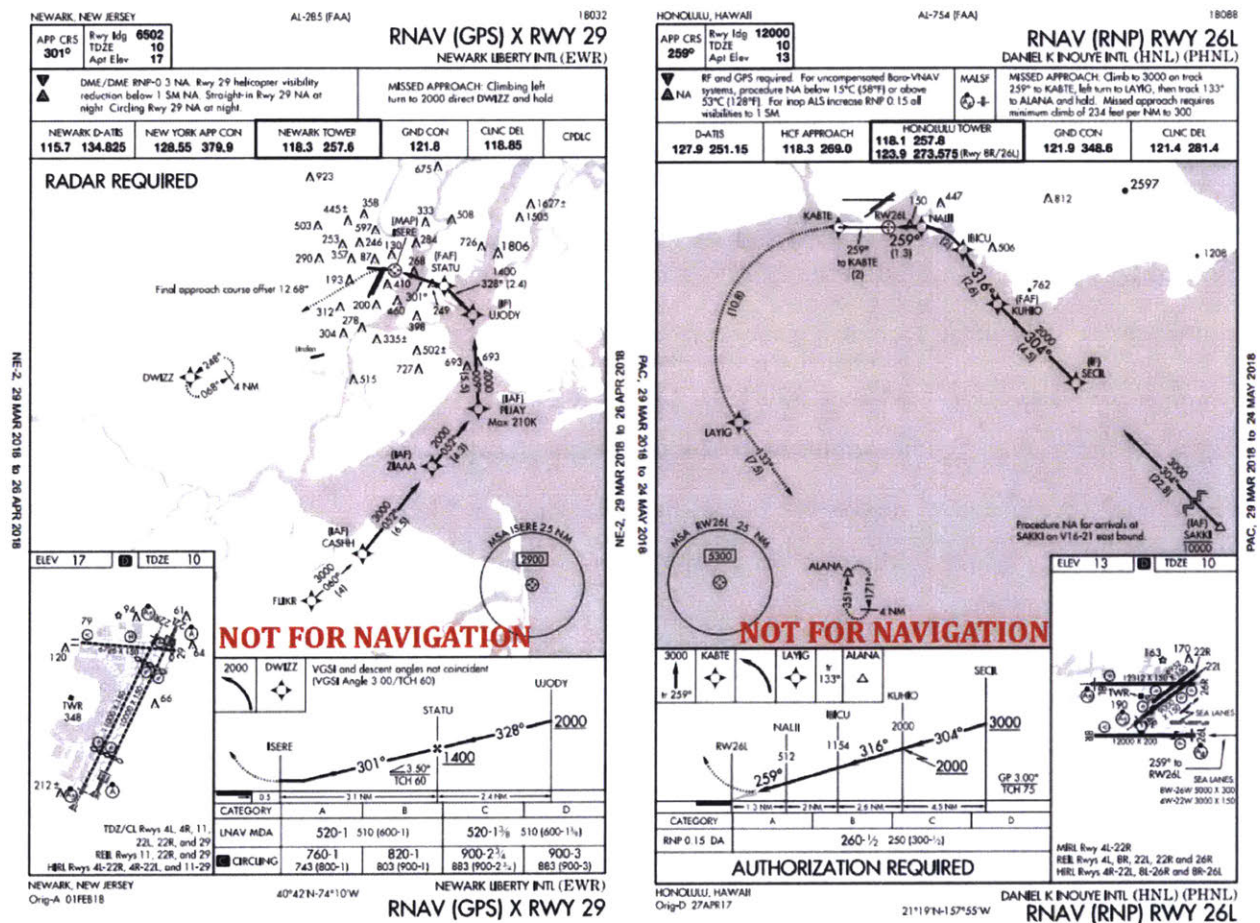


Figure 36. Example published RNAV (left) and RNP (right) instrument approach procedures with waypoint geometry near criteria limits

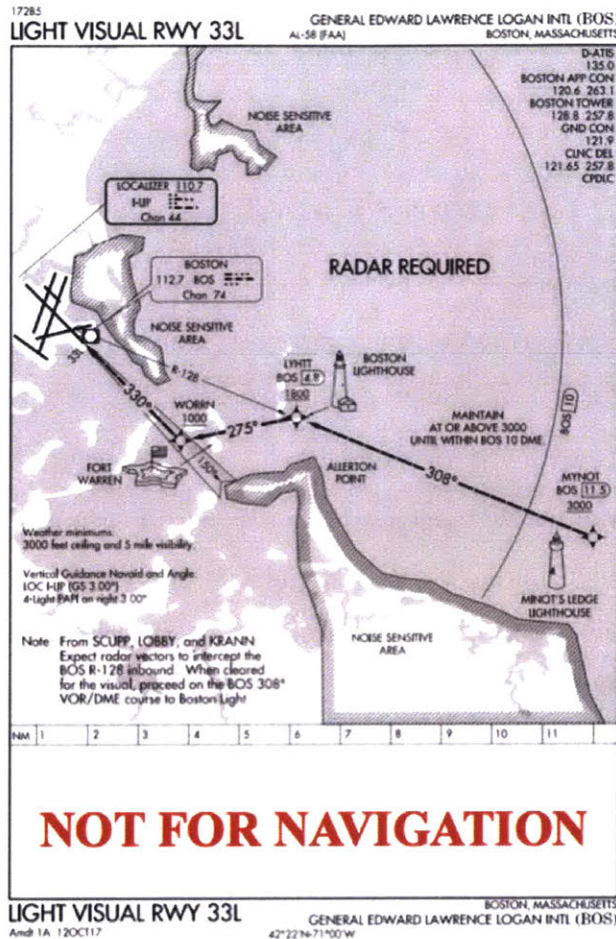
## 4.5 RNAV Visual Flight Procedures

Instrument approach procedures (IAPs) designed under PBN criteria are subject to stringent design limitations due to the requirement for reliability and repeatability in poor weather conditions. The procedures are designed for use in zero-visibility conditions throughout the approach until the minimum descent height on the final approach course. However, this level of guidance is not always necessary, presenting an opportunity for flexible RNAV guidance at a lower level of stringency that provides useful information to pilots and allows for more accurate navigation on non-instrument approach procedures.

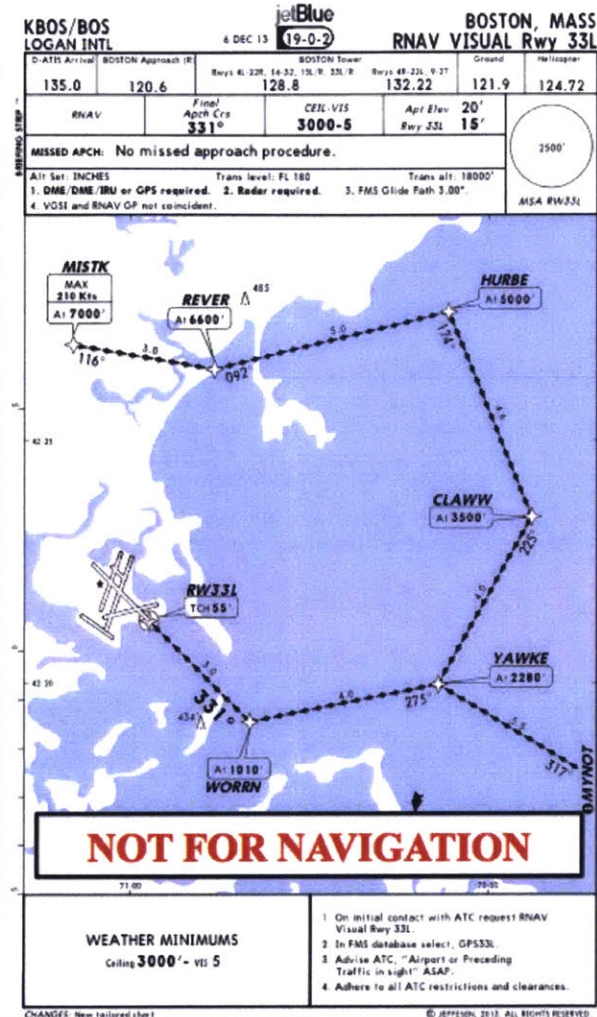
An alternative flight guidance technology has been developed for arrival procedures operated in visual meteorological conditions. The RNAV Visual Flight Procedure (RVFP) is a sequence of waypoints that is preloaded into an aircraft flight management system to allow for navigation guidance as a backup for visual obstacle and terrain avoidance during the approach phase. The RVFP concept was originally intended to replicate the operational and noise benefits obtained from using traditional charted visual approach procedures. For example, Figure 37(a) shows the published Light Visual to Runway 33L at BOS. This procedure is primarily intended for use at night, reducing overflight noise impacted on populated areas under the straight-in final approach course. However, a lack of overwater visual references made the procedure challenging to fly precisely with outside references alone. Therefore, jetBlue Airways developed and received approval for an RVFP version of the procedure shown in Figure 37(b). This RVFP allows pilots to operate the procedure in visual conditions with positive navigation guidance on the primary flight display and to the autoflight system. Because RNAV Visual approaches must be flown in visual meteorological conditions, they are not required to be flight inspected as instrument approach, significantly reducing the development cost relative to standard instrument approach procedures. Operators must demonstrate flyability of proposed procedures with expected fleet types and conditions rather than meeting specific approach design criteria [127].

RVFPs provide significant flexibility for procedure design due to the lack of set criteria. This allows for sharper intermediate-to-final segment intercept angles, shortened final approach segment lengths, and reduced leg length requirements as appropriate for the operator and fleet types

expected to operate the procedure. Because of this flexibility, it is feasible to design RVFPs with greater noise benefit than RNAV IAPs either with or without vertical guidance, in some cases approaching the flexibility and noise benefit level provided by RNP.



(a) BOS "Light Visual" Runway 33L



(b) BOS RNAV Visual Runway 33L

Reproduced with permission of jetBlue Airways

Figure 37. Example of a charted visual procedure and RNAV Visual serving the same runway

The primary drawback of RVFPs is that there is no mechanism for publication or public distribution of charted procedures or FMS databases. Procedures are developed by an operator who must demonstrate flyability, establish operational agreements with ATC, and maintain the procedure charts and databases. The existence of RVFPs is not advertised publicly, nor are provisions included to allow the use of RVFPs by other operators without significant transfer cost in terms of database upgrades and operational capability. Most FMS database subscriptions include updates with

published procedures only, requiring incremental subscription costs and update processes for operator-specific procedures even if the carrier who creates and maintains the procedure wishes to make it available for others. Therefore, adoption of RVFPs to date has been limited to several specific airports and operators. The potential for noise reduction from this highly-flexible procedure option suggests an opportunity for expanded development, public availability, and utilization of RVFPs when weather conditions permit visual operations.

## **4.6 Nonstandard Instrument Flight Procedures and Waivers**

In certain situations, the procedure design criteria set forth by FAA guidance documents may not provide adequate flexibility to enable necessary arrival or departure procedures at specific runways or airports. One key element of system safety is consistency of procedures between airports, runways, and aircraft types. Therefore, compliance with criteria standards is strongly encouraged when operationally feasible. However, considerations for obstacles, navigation information, or traffic levels may motivate a waiver application for nonstandard procedures<sup>22</sup>. Waiver applications are reviewed by the FAA Flight Standards Service branch (AFS).

As shown in Section 4.4.1, most current procedures do not take maximum advantage of design flexibility already available in RNAV and RNP criteria, indicating that potential benefits may be realized without requiring waiver applications. Chapter 5 analyzes potential noise reductions that could be achieved for all runways the OEP-35 airports leveraging current design criteria without the use of waivers.

---

<sup>22</sup> FAA Order 8260.3D TERPS: 1-4-2

# Chapter 5. System Noise Reduction Potential of RNAV and RNP Approaches

While it is generally understood that RNAV and RNP procedures allow greater flexibility than conventional procedures in terms of track geometry, the noise exposure reduction potential available on a runway-specific basis at major airports throughout the NAS have not been quantified. Such a quantification could inform FAA screening and prioritization of NextGen rollout in terms of procedure technology and target locations for implementation with the highest potential environmental benefit.

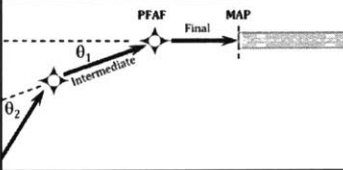
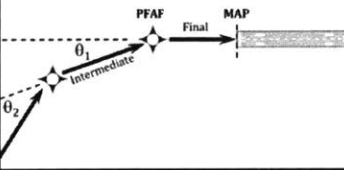
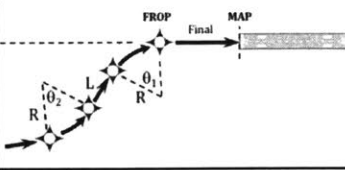
This analysis assumes criteria constraints only for each runway. This results in a best-case scenario for PBN design where procedure design is unconstrained by airspace, obstacle clearance requirements, interactions with arrivals and departures at other runways, and interface requirements with standard terminal arrival routes. The analysis is intended to demonstrate the potential benefits arising from shortened final approach segment lengths and increased use of turning legs in the intermediate and final segment of the approach. For this reason, the candidate procedure designs evaluated in this study represent “best-case” procedure designs permitted by TERPS and PBN design criteria (e.g. minimum leg lengths are used for RNAV legs). Detailed design and validation for each candidate procedure was not performed.

## 5.1 Track Generation Method

For each PBN procedure concept, a set of candidate procedures was developed for a generic north-oriented runway. The lateral tracks for these procedures were developed by varying two or more parametric values within the intermediate and final segment for the specified navigation technology. Those parametric values also have a direct effect on other design features within each procedure. For example, leg lengths for the RNAV procedures were determined by calculating the distance of turn anticipation between each turn as described in Section 4.1.1 In all cases, the

procedures were developed for Approach Category D aircraft to enable potential procedure use by the full fleet mix at air transportation hubs. Table 13 shows the range of parameters that were used to develop the procedure geometry for each of the three study cases for PBN procedure concepts.

**Table 13. Parameter Ranges for RNAV and RNP Procedure Evaluation Study**

	<b>RNAV: Vertical Guidance</b>	<b>RNAV: No Vertical Guidance</b>	<b>RNP</b>
Illustration			
Fixed Parameters	PFAF Altitude: 800 ft Glidepath Angle: 3.0° Final Approach Segment Length: 2.51 NM	PFAF Altitude: 800 ft Glidepath Angle: 3.0° Final Approach Segment Length: 2.51 NM	FROP Altitude: 500 ft Glidepath Angle: 3.0° Straight Final Approach Segment Length: 1.41 NM
Varied Parameters	$\theta_1$ : 0° to $\pm 15^\circ$ by 1° $\theta_2$ : 0° to $\pm 90^\circ$ by 5° $\theta_3$ (not shown above): 0° to $\pm 90^\circ$ by 5°	$\theta_1$ : 0° to $\pm 15^\circ$ by 1° $\pm 16^\circ$ to $30^\circ$ by 2° $\theta_2$ : 0° to $\pm 90^\circ$ by 5° $\theta_3$ (not shown above): 0° to $\pm 90^\circ$ by 5°	$\theta_1$ : 0° to $\pm 90^\circ$ by 5° $\theta_2$ : 0° to $\pm 90^\circ$ by 5° R: 1.26 (minimum) or 2NM L: 0 to 3NM by 0.2NM
Dependent Parameters	Segment Lengths	Segment Lengths	N/A
Total Tracks Generated	42,439	64,343	43,808

It is important to note that the PFAF or FROP location was held constant at a minimum value assuming a rollout height of 800 ft for RNAV and 500 ft for RNP procedures. An 800 ft PFAF altitude is only possible for runway ends without significant obstacle constraints along the first 3 miles of the extended runway centerline. For the purpose of this broad parametric benefits case evaluation, obstacle clearance criteria were not evaluated against terrain and obstruction databases for each runway in the NAS. Further validation would be necessary to confirm that a PFAF altitude of 800 ft AGL is attainable for each specific runway end. It should also be noted that a turn is not mandatory at either the PFAF or FROP in this formulation. Longer straight-in final segments are permitted by setting  $\theta_1$  and/or  $\theta_2$  to 0°.

Noise is driven by actual flown ground track rather than by waypoint location directly. This is particularly important for fly-by waypoints at the location of a track course change. The onboard



flight management computer calculates a turn trajectory based on actual flight conditions and aircraft-specific assumptions. These may be different from the worst-case assumptions assumed in the procedure design process, such as in the calculation of the DTA. For the purposes of this approach procedure analysis, turn geometry for fly-by waypoints was calculated assuming a true airspeed of 180 knots and a bank angle of 15°. The resulting turn radius is 1.76 NM. This is consistent with observed turn radius values for maneuvering aircraft on arrival from radar data at Boston Logan Airport. An example of fly-by turn geometry used to connect two fly-by waypoints for use in noise modeling is shown in Figure 38.

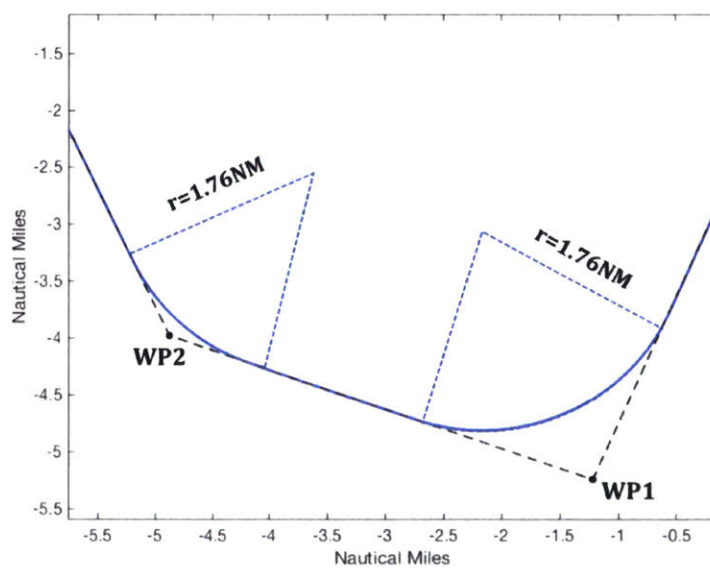


**Figure 38. Assumed as-flown turn anticipation geometry for FB waypoints**

Detailed lateral tracks were generated by applying the parametric procedure design values given in Table 13 with the turn anticipation assumptions for FB waypoints shown in Figure 38. Over 100,000 total lateral path definitions were calculated in this manner. Figure 39 shows the resulting ground tracks for a random subset of 40 examples from each procedure type.

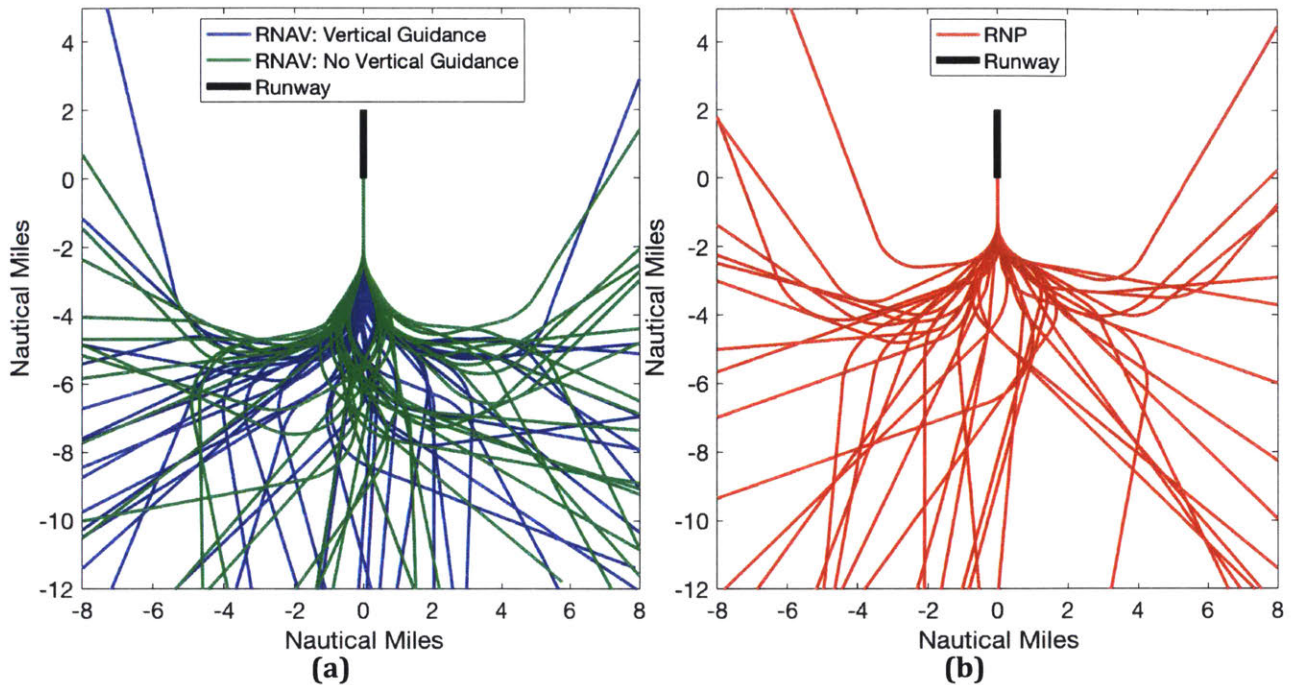


**Figure 39. Example lateral tracks for RNAV (a) and RNP (b) arrival procedures**

## 5.2 Noise Contour Generation

The simplified noise contour evaluation method introduced in Section 3.5.3 was used to evaluate arrival noise for the procedure set generated in this study. Single-event  $L_{MAX}$  noise grids were calculated using AEDT for a set of seven representative aircraft types as listed in Table 14. These aircraft were selected based on representation within the US air carrier fleet as well as the availability of high-resolution historical radar data for arrivals and departures in order to determine representative altitude profiles.

**Table 14. Representative Aircraft Types Used in Noise Study**

Aircraft Type	Representing Types
Airbus A320	Airbus Narrowbody
Boeing 737-800	Boeing Narrowbody
Boeing 757-200	Large Narrowbody/Small Widebody
Boeing 777-300	Large Widebody
Embraer 145	Small Regional Jet
Embraer 170	Large Regional Jet
McDonnell Douglas MD-88	Older Low-Bypass Engine Narrowbody

In terms of altitude, the baseline straight-in noise calculations assumed vertical profiles based on 20 days of radar data from 2015 and 2016 recorded by the Airport Surface Detection Equipment X (ASDE-X) system at BOS. Altitude tracks were analyzed as a function of distance to touchdown. The median profile was selected to represent an “average” profile on a type-by-type basis. This median profile was further processed to remove minor altitude fluctuations, as such fluctuations would propagate to variations in thrust on the final approach segment. Thrust was calculated for each representative profile using the BADA 4 aircraft performance model. Weight was assumed to be 75% of maximum gross takeoff weight for each aircraft type. Landing gear extension was assumed at 1,700 ft AGL with a flap extension schedule based on airspeed thresholds included in BADA 4. The landing gear extension altitude assumption corresponds to the ILS glideslope intercept altitude on the Boston ILS Runway 4R approach.

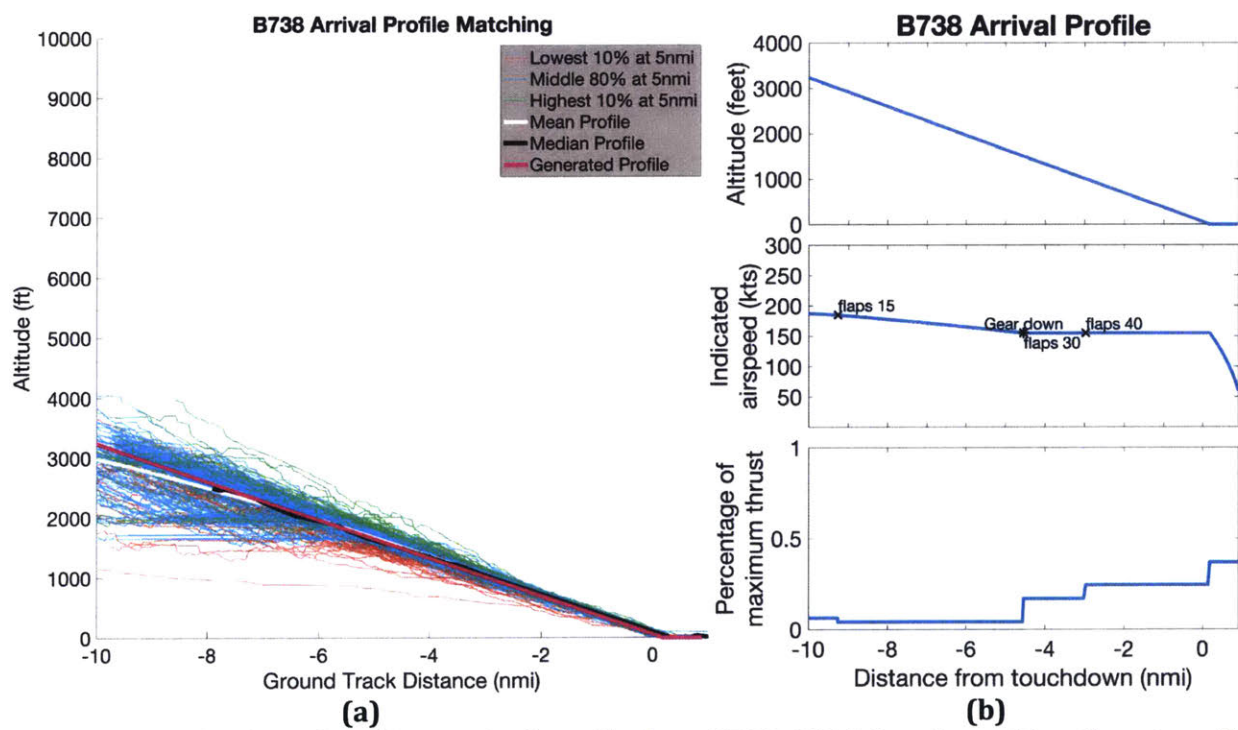


**Figure 40. Radar-based median arrival profile for a B737-800 (a) and resulting thrust profile calculated using BADA-4 (b)**

A full  $L_{MAX}$  noise grid was calculated for a straight-in arrival by each of the representative aircraft types. Noise contours were generated at the 50dB and 60dB  $L_{MAX}$  levels for each aircraft type. These contour levels were selected for analysis in order to enable further post-processing of results into  $N_{ABOVE}$  contours for the 50dB night level and 60dB day level. AEDT straight-in arrival  $L_{MAX}$  contours

were used to determine contour half-width as a function of distance to touchdown for each aircraft type, with resulting half-width functions shown in Figure 41. As expected, for the arrival phase - where aerodynamic sources makes up a significant portion of the total noise signature - the ordering of contour size corresponds to the order of aircraft size.

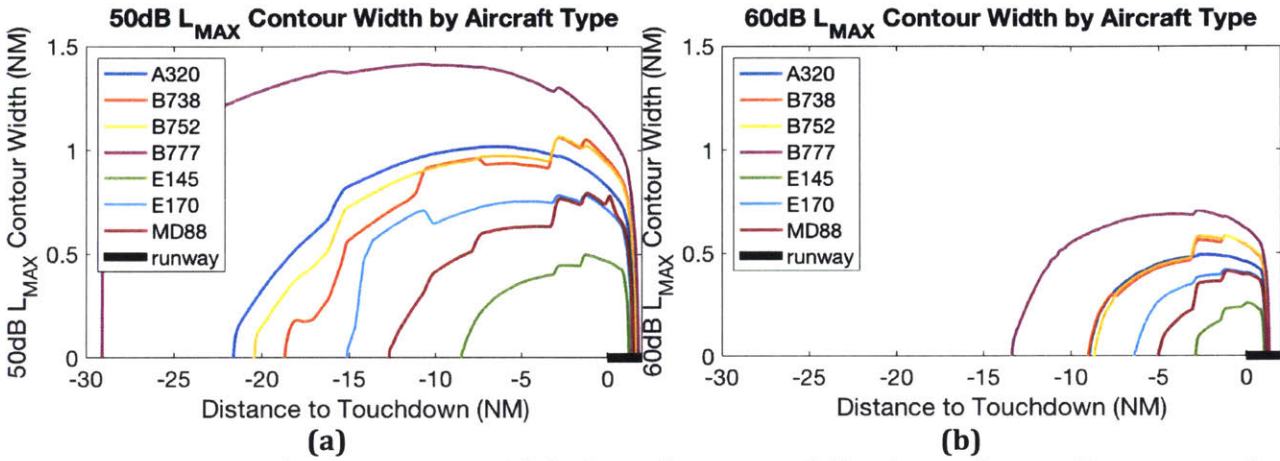


**Figure 41. Approach  $L_{MAX}$  contour widths for 7 fleet types following radar median approach profiles**

### 5.3 Population Exposure Calculation

Rapid noise analysis for multiple runways is achieved by calculating all noise contours on a common grid relative to an arbitrary north-oriented runway and pre-calculating population and demographic data on the same grid. For the purpose of this analysis, all data were calculated on a  $30 \times 30$  NM grid at a 0.1 NM square resolution. This method allows for computation of population noise impact by locating the index of grid points inside the contour level of interest and summing those indices in the desired runway's population matrix.

In order to compute noise for the 282 runway ends at the OEP-35 airports, population grids were pre-computed for each runway end such that the runway heading was aligned to the top of the grid and the runway threshold was the origin. Figure 42 shows an example of the runway-specific analysis process at New York La Guardia Airport (LGA). The figure shows the north-oriented population data

and runway layout, a desired noise contour for evaluation on each runway end, and the noise contour superimposed on runway-up population grids for each of the four runway ends at LGA.

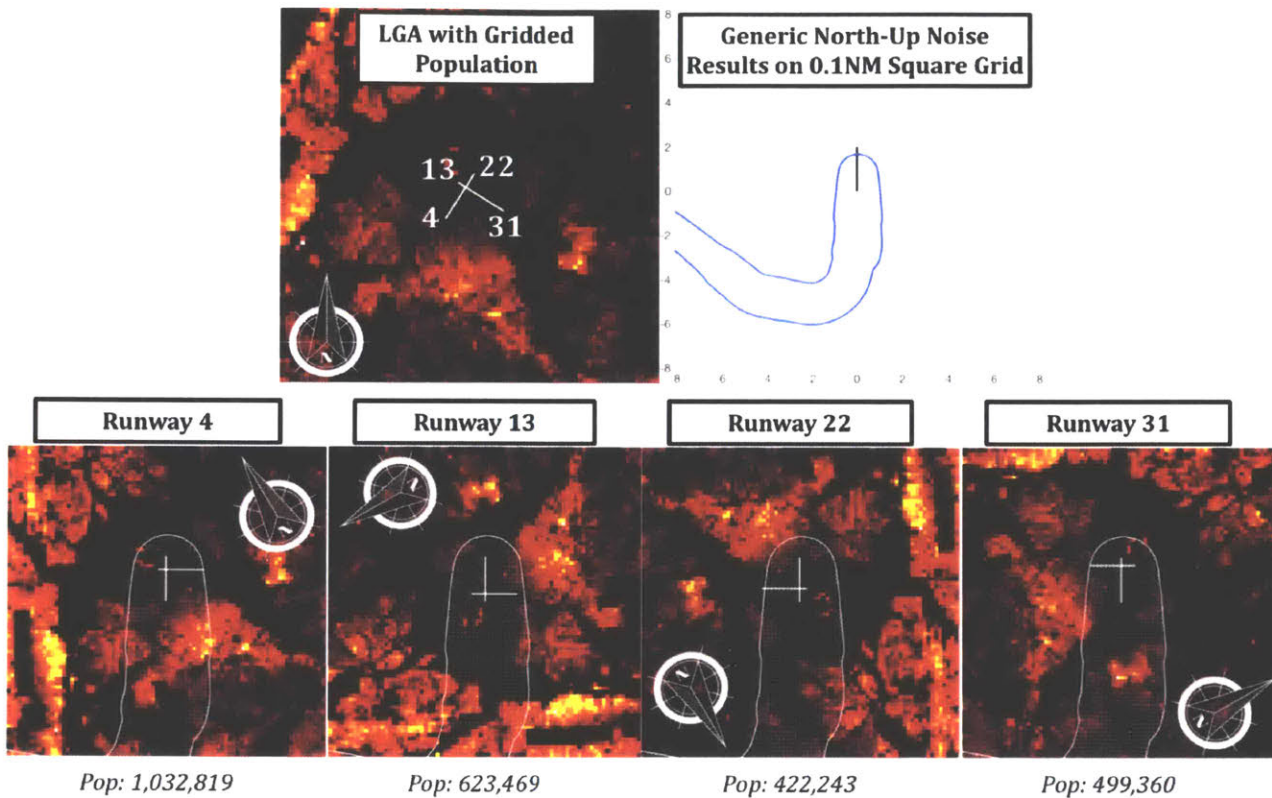


**Figure 42. Illustration of population grid rotation at LGA airport showing the baseline north-oriented airport layout, a generic noise contour, and runway-aligned population grids**

The pre-calculation of rotated population data is significantly more computationally efficient than rotating the noise contours themselves to match the north-up population data. In essence, noise contour results may be applied directly to underlying population grids using a “cookie-cutter” mask to rapidly evaluate net population impact. This computational efficiency allows for rapid evaluation of each runway end in the analysis for any candidate procedure. This is important due to the number of total population summations included in this analysis: With 108,151 RNAV and RNP procedure definitions, 7 aircraft types, 2 metrics levels, and 282 runway ends, the total number of population exposure calculations in this analysis is nearly 427 million. Total runtime for the analysis was 4 days on a desktop workstation computer.

## **5.4 Average Hourly and Daily Schedule Generation**

In order to compare benefits levels across runways, it is important to consider the total number of arrivals as well as the expected population exposure reduction for each arrival. Total benefits from PBN procedure implementation are largest for noise-optimal arrivals on traffic-intensive runways. For each runway in the NAS, jet arrival rates were determined from FAA ASPM flight-level records on an hour-by-hour basis for the full year of 2017. Arrival runway configuration records were also retrieved from the ASPM hourly airport-level efficiency database. For hours with multiple active arrival runways, jet arrivals were allocated equally to each active runway. Arrivals occurring between 7:00am and 10:00pm (local time) were tabulated as day operations, while those occurring outside those hours were tabulated as night operations. Ultimately, the average hourly daytime and nighttime runway utilization rates represent the average rate for the corresponding time of day taken from a full year of data. Average daily runway utilization was calculated using a similar method, averaging arrivals over all of 2017 into an annual average day.

For runway-level analysis shown in Section 5.5 through Section 5.8, the Boeing 737-800 was used as the single example aircraft type for consistency between runway ends and procedure modifications. This aircraft was chosen because it was the most common type by movement count at the OEP-35 airports in 2017, as shown in Figure 14. The average hourly operation counts corresponding to each runway are for all turbojet types, not the B737-800 alone. Net population benefit calculations make the simplifying assumption that every arrival is a B737-800 for the purpose of ranking runway end population results. This allows for consistency between tabulated and graphical results when comparing runway ends.

By contrast, the system-level roll-up analysis in Section 5.9 includes treatment of the actual fleet mix at each airport for estimating total system-level benefits. Each arrival from the flight-level database was assigned to one of seven representative types for noise analysis according to the mapping shown in Table 1, and population impact numbers were calculated using noise contours for that representative aircraft type. The system-level roll-up analysis does not include runway-level graphical presentation, preventing any inconsistency between tabulated and graphical results.

## 5.5 RNAV Procedures with Vertical Guidance

In order to evaluate the noise reduction potential from RNAV procedures with vertical guidance, the 42,439 candidate procedures described in the first column of Table 13 were evaluated at each of the 282 runway ends in the OEP-35 airports. The procedure (or set of procedures) with the minimum population exposure was selected from this set of candidate options. For simplicity, all candidate procedures were compared to a straight-in baseline. This is a reasonable approximation for most runways in the NAS, although benefits may not be representative of actual baseline operations at specific locations with terrain, airspace, or procedural constraints dictating nonstandard arrival configurations in the conventional baseline.

### 5.5.1 Runway-level results

Figure 43 shows an example runway end in the NAS with high population exposure reduction potential, Los Angeles International (LAX) runway 25L. This result is based on 60dB  $L_{MAX}$  exposure levels for the Boeing 737-800, corresponding to the daytime  $N_{ABOVE}$  threshold discussed in Section **Error! Reference source not found.** This figure shows the baseline straight-in procedure noise contour, lowest-noise RNAV procedure with vertical guidance, and population impact summary.

The noise benefits for this runway are large due to the density of the population underlying the straight-in arrival track. By altering the procedure centerline to avoid these high-density areas, the net population exposure is reduced by 53,058. This net change in exposure arises due to a reduction in noise at the 60dB level for 80,998 people but a corresponding increase in noise at the same level for 27,940 people due to the track relocation. Therefore, while the net population impact of this procedure is large, a substantial number of people are exposed to new noise as a byproduct of reducing net impact. This effect is discussed in more detail in Section 5.10.

Any lateral track modifications over populated land areas results in redistribution of noise. The magnitude of this redistribution varies by location and underlying population configuration (the number of people benefited relative to the number of people newly impacted). Some runways have favorable geographic location allowing purely beneficial population impact, such as runway 33L at BOS as shown in Figure 44.

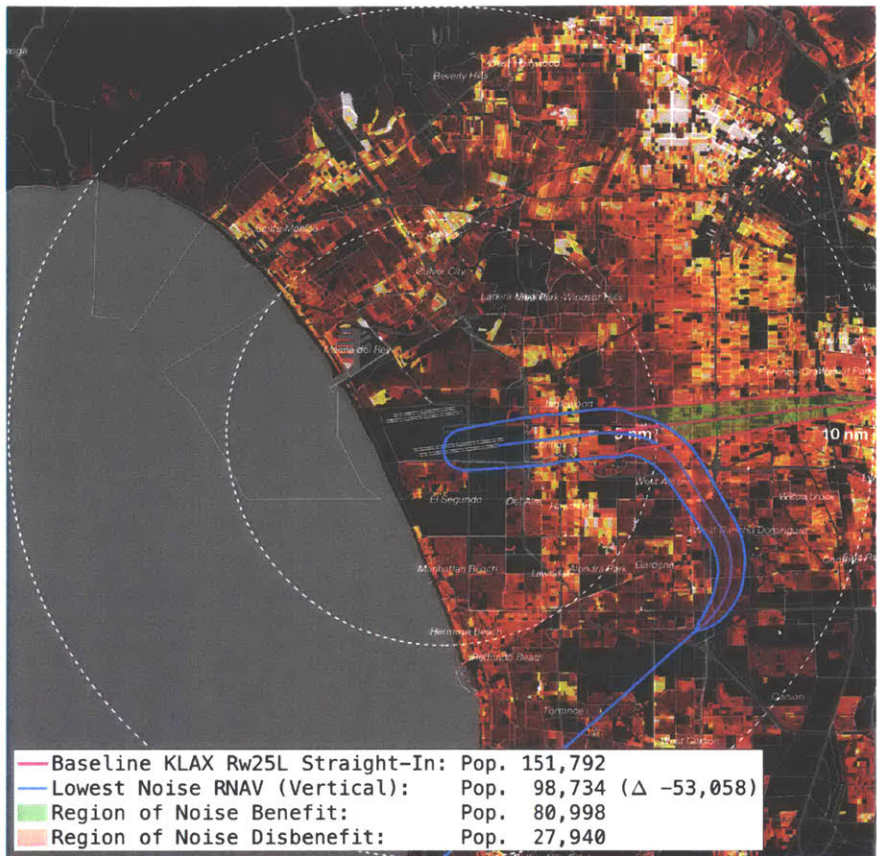


**Figure 43. Noise-minimal RNAV approach with vertical guidance for LAX runway 25L (B737-800 60dB L<sub>MAX</sub>)**

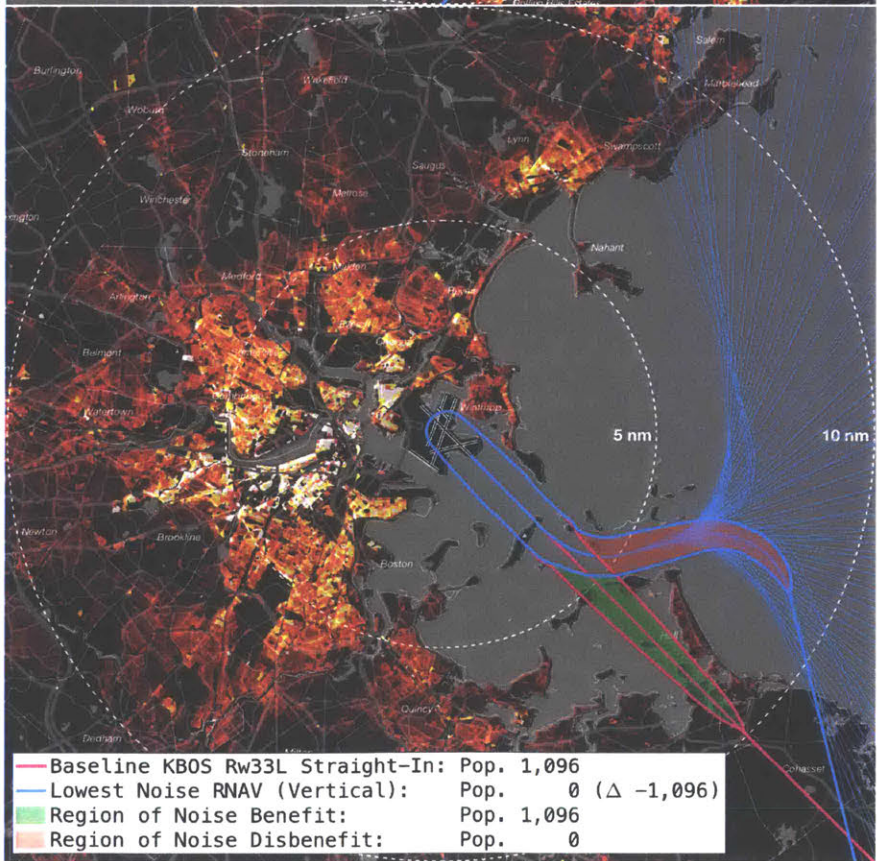


**Figure 44. Noise-minimal RNAV approach with vertical guidance for BOS runway 33L (B737-800 60dB L<sub>MAX</sub>)**



Population reduction potential was also evaluated on each runway end at the 50dB level, corresponding to the nighttime  $N_{\text{ABOVE}}$  sensitivity level. These results were tabulated and ranked separately from the 60dB results. An example Boeing 737-800 arrival noise contour at the 50dB level is shown in Figure 45 for Chicago O'Hare Airport (ORD) runway 10L.

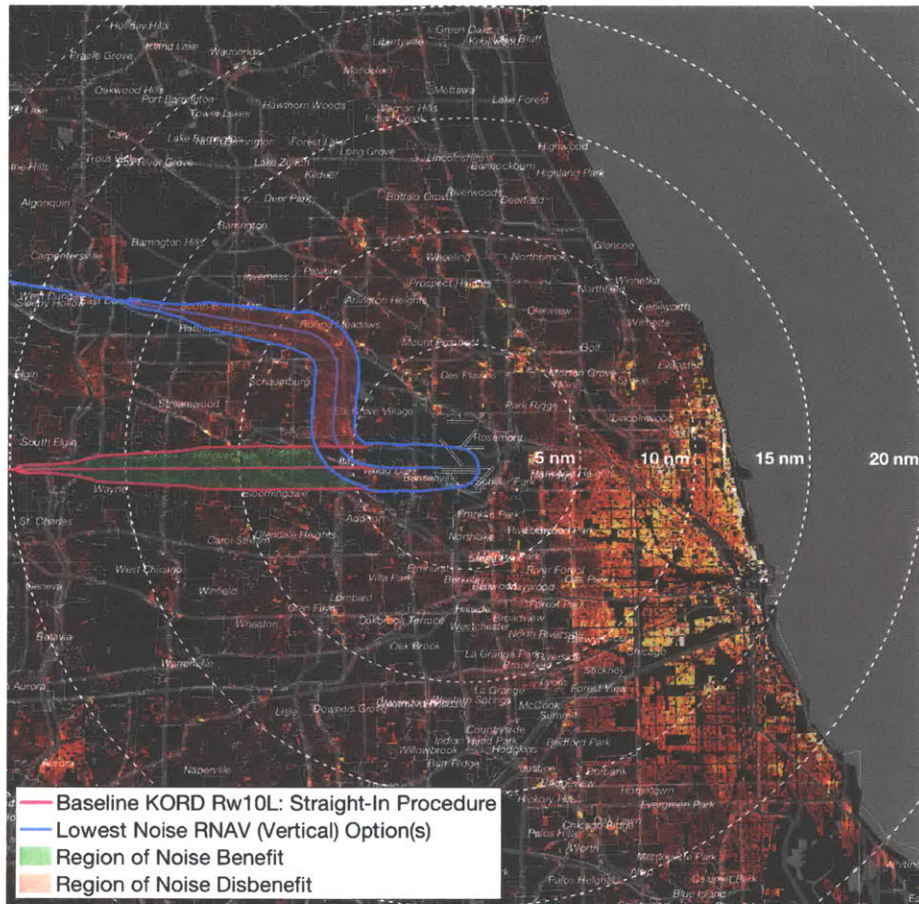


**Figure 45. Noise-minimal RNAV approach with vertical guidance for ORD runway 10L (B737-800 50dB  $L_{\text{MAX}}$ )**

The geographic extent of the contour is significantly larger than that for 60dB contours (note that the night exposure map in Figure 45 shows range rings to 20NM rather than 10NM, as shown for 60dB contours). It stands to reason that the noise-preferred procedure definition may vary depending on the target  $L_{\text{MAX}}$  threshold level. Community annoyance thresholds and time-of-day considerations can directly impact the preferred solution. Community sensitivity to noise changes at night. For the  $N_{\text{ABOVE}}$  metric, this is reflected in a lowered  $L_{\text{MAX}}$  impact level from 60dB to 50dB between the hours of 10pm and 7am. Because contours are both longer and wider at the 50dB level

relative to the 60dB level, the procedure centerline that minimizes noise is often different for the lower threshold. For example, Figure 46 shows the noise-minimal RNAV track at the 50dB and 60dB levels for a Boeing 737-800 arrival at Baltimore Washington Airport (BWI) runway 33R. The preferred procedure converges on the final approach course from opposite directions depending on which noise threshold is selected. It should be noted that preferred procedures for different noise thresholds are sometimes aligned. Figure 47 shows the noise-minimal solution for Runway 10 at the same airport, where the 50dB and 60dB procedure solutions are aligned.

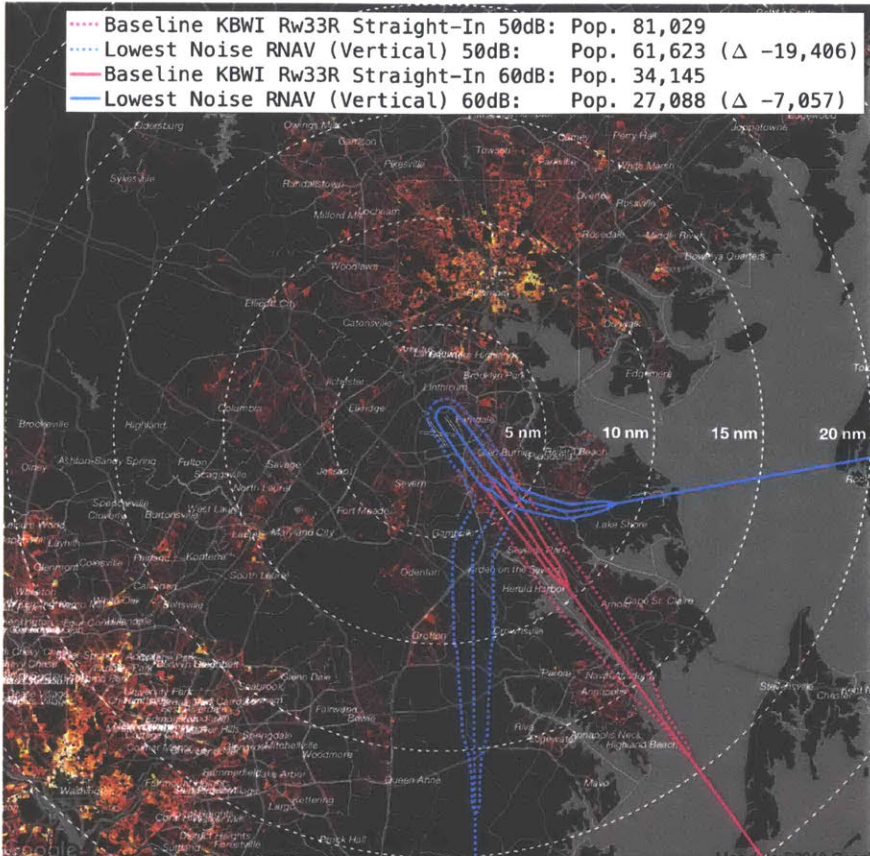


**Figure 46. Threshold Sensitivity of Noise-Minimal RNAV Approach with Vertical Guidance for KBWI Runway 33R (B737-800 50dB vs. 60dB L<sub>MAX</sub>)**

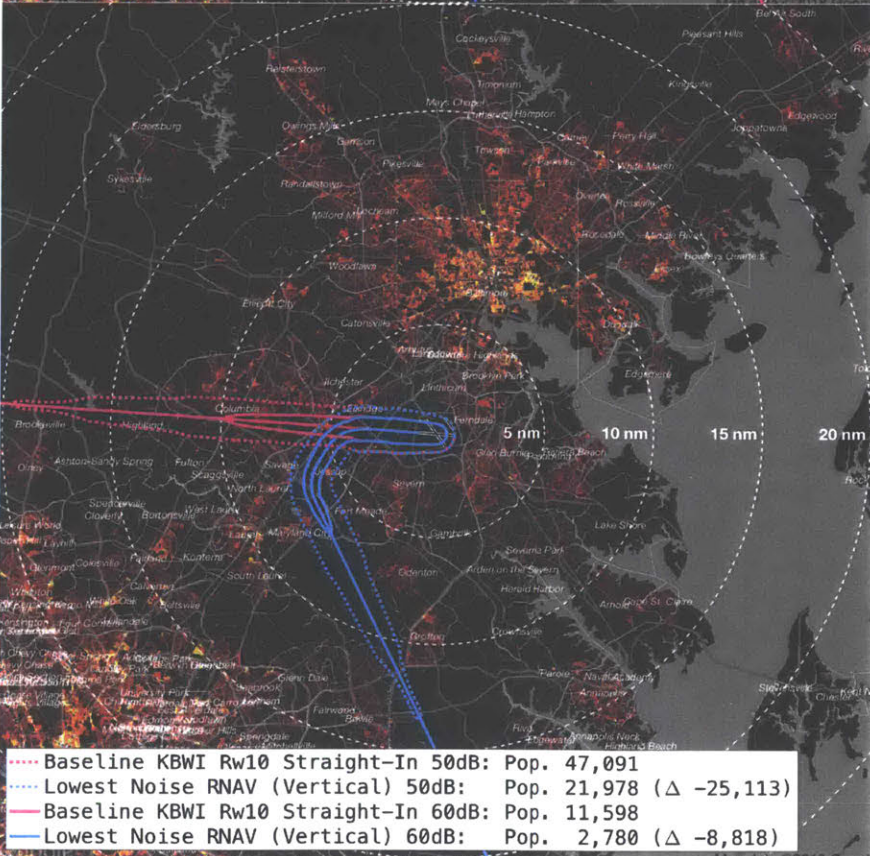


**Figure 47. Threshold Sensitivity of Noise-Minimal RNAV Approach with Vertical Guidance for KBWI Runway 10 (B737-800 50dB vs. 60dB L<sub>MAX</sub>)**

### 5.5.2 Results for all OEP-35 runway ends

The population benefit evaluation illustrated in Section 5.5.1 for specific runways was repeated for each of the 282 runways at the OEP-35 airports. A simple metric for total noise benefit potential for a modified procedure is the noise intensity on a runway, defined here as the product of population impact at a target noise level on a per-arrival basis and the average arrival rate for the corresponding runway. For example, a new procedure used 10 times per hour on average with a per-flight population reduction of 50,000 people would have a total impact reduction of 500,000 noise events per hour. This metric can be used for high-level comparison of runway ends in the NAS.

Figure 48 shows population exposure reduction at the 60dB  $L_{MAX}$  level as a function of daytime jet arrival rate for each runway end in the OEP-35 airports. The markers in the figure corresponds to one runway in the OEP-35 airport set. The population exposure reduction shown in the figure is the difference between a straight-in baseline and the lowest-noise RNAV procedure with vertical guidance for a Boeing 737-800 arrival. Isolines for hourly noise intensity reduction are also shown to enable comparison between different runway ends in terms of cumulative impact. This metric is analogous to the Person-Events Index used as one component of noise assessment in Australia aviation infrastructure projects, and serves as a simple surrogate for absolute noise impact experienced from a full set of flights using a runway and/or procedure [128]. The metric is the product of runway arrival volume and population reduction and represents the total population benefit expected from implementation of a modified procedure at specific runway ends. Traffic volumes for day and night periods are averaged over the full operational year of 2017.

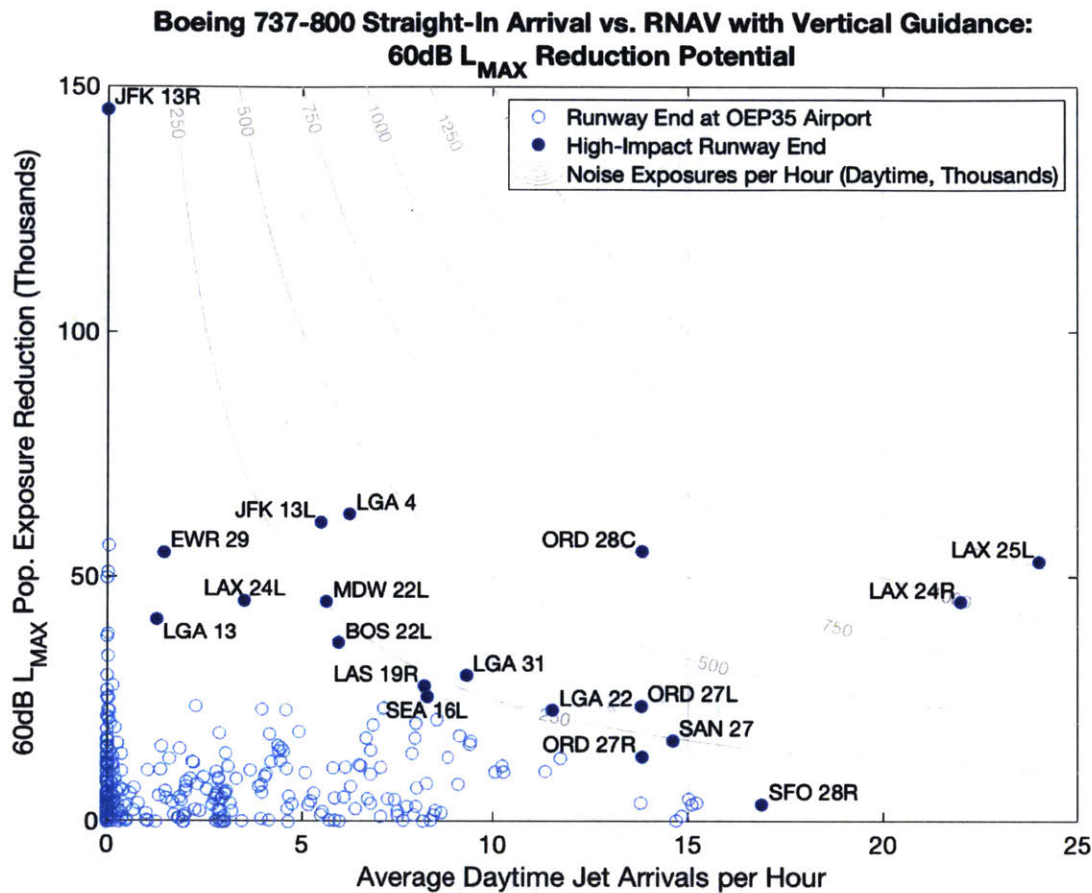


**Figure 48. 2017 Daytime 60dB L<sub>MAX</sub> noise reduction potential from RNAV procedures with vertical guidance for all OEP-35 runways**

The figure illustrates several characteristics of noise reduction potential from RNAV procedures in the NAS. First, population impact reduction is a function of single-flight noise reduction as well as the operational volume associated with a given procedure. Specific high-impact procedures may be characterized by either or both of these properties. The 50 runway ends in the OEP-35 with the largest daytime population exposure reduction potential ranked by hourly noise impact are listed in Table 15. This subset of runway ends includes 23 unique airports, broadly characterized by their location in or near densely-populated urban areas.

**Table 15. Highest benefit opportunities for RNAV procedures with vertical guidance at the 60dB level (B737-800)**

Rank	Airport	Rwy	Avg Day Jet Arrs/Hr (2017)	B738 Straight-In 60dB Pop.	Baseline Hourly Noise Intensity	B738 RNAV (Vert) 60dB Pop.	60dB Pop. Δ	Hourly Noise Intensity Reduction
1	KLAX	25L	24.01	151,792	3,643,873	98,734	-53,058	1,273,694
2	KLAX	24R	21.99	130,022	2,859,541	85,132	-44,890	987,255
3	KORD	28C	13.83	106,520	1,473,462	51,310	-55,210	763,705
4	KLGA	4	6.24	353,298	2,204,739	290,602	-62,696	391,251
5	KJFK	13L	5.5	232,171	1,276,479	171,110	-61,061	335,714
6	KORD	27L	13.81	66,189	914,340	42,535	-23,654	326,758
7	KLGA	31	9.34	202,103	1,887,113	172,277	-29,826	278,497
8	KLGA	22	11.55	79,129	913,980	56,351	-22,778	263,098
9	KMDW	22L	5.64	130,040	733,654	85,191	-44,849	253,027
10	KSAN	27	14.62	87,083	1,272,919	70,498	-16,585	242,428
11	KLAS	19R	8.21	92,313	758,040	64,697	-27,616	226,772
12	KBOS	22L	5.96	62,240	371,174	25,857	-36,383	216,973
13	KSEA	16L	8.29	43,378	359,714	17,946	-25,432	210,896
14	KORD	27R	13.84	51,388	710,991	38,132	-13,256	183,407
15	KSEA	16R	8.54	44,009	376,042	23,283	-20,726	177,097
16	KPHL	27R	7.15	24,412	174,538	1,236	-23,176	165,701
17	KPHX	25L	9.17	27,740	254,327	10,295	-17,445	159,940
18	KLAS	19L	7.99	87,767	701,021	67,755	-20,012	159,842
19	KLAX	24L	3.5	128,037	448,195	82,958	-45,079	157,800
20	KDFW	17L	9.45	18,053	170,539	1,663	-16,390	154,829
21	KMIA	9	11.74	36,040	423,226	23,119	-12,921	151,734
22	KDFW	17C	9.43	17,871	168,484	2,118	-15,753	148,516
23	KDCA	19	6.87	88,703	609,500	68,955	-19,748	135,693
24	KORD	9L	7.97	30,755	245,260	13,774	-16,981	135,417
25	KEWR	4R	11.37	39,412	448,034	29,135	-10,277	116,829
26	KDTW	22R	10.25	29,449	301,832	18,121	-11,328	116,104
27	KDFW	18R	8.83	15,620	137,997	2,580	-13,040	115,203
28	KMDW	31C	6.68	92,518	617,967	75,526	-16,992	113,497
29	KJFK	31R	7.88	34,473	271,777	20,674	-13,799	108,788
30	KMIA	12	10.3	19,608	201,996	9,468	-10,140	104,459
31	KPHL	9R	4.59	24,873	114,082	2,275	-22,598	103,648
32	KDTW	21L	10.06	27,319	274,886	17,203	-10,116	101,788
33	KMSP	12R	6.8	49,092	333,950	34,596	-14,496	98,610
34	KPHL	26	4.94	28,608	141,269	10,377	-18,231	90,026
35	KSEA	34R	3.96	48,100	190,237	25,341	-22,759	90,013
36	KEWR	29	1.43	87,766	125,771	32,812	-54,954	78,750
37	KJFK	31L	7.06	34,145	241,079	23,056	-11,089	78,293
38	KPHX	7R	6.5	18,589	120,755	7,141	-11,448	74,367
39	KIAH	27	6.55	17,343	113,518	5,999	-11,344	74,252
40	KSEA	34L	4.16	35,705	148,604	17,991	-17,714	73,726
41	KSFO	28L	15.04	4,955	74,522	260	-4,695	70,611
42	KPHX	26	9.13	12,664	115,654	5,037	-7,627	69,653
43	KSLC	34R	4.38	29,757	130,286	14,261	-15,496	67,847
44	KIAH	26L	6.14	17,634	108,267	6,587	-11,047	67,825
45	KIAD	1C	4.47	17,829	79,622	2,938	-14,891	66,501
46	KMSP	12L	6.8	46,900	319,106	37,330	-9,570	65,114
47	KIAH	9	4.53	27,368	123,919	13,074	-14,294	64,722
48	KBWI	33L	8.28	34,006	281,591	26,238	-7,768	64,324
49	KMCO	17L	5.81	34,141	198,526	23,248	-10,893	63,342
50	KSLC	34L	4.41	31,373	138,243	17,071	-14,302	63,021

As discussed above, the noise-optimal procedure may be different for daytime and nighttime operations. Figure 49 shows population exposure reduction at the 50dB L<sub>MAX</sub> level as a function of nighttime runway utilization for each runway end in the study in conjunction with the average 2017 nighttime jet arrival rate for the runway. Each marker in the figure again corresponds to a single candidate RNAV procedure modification for the associated runway end.

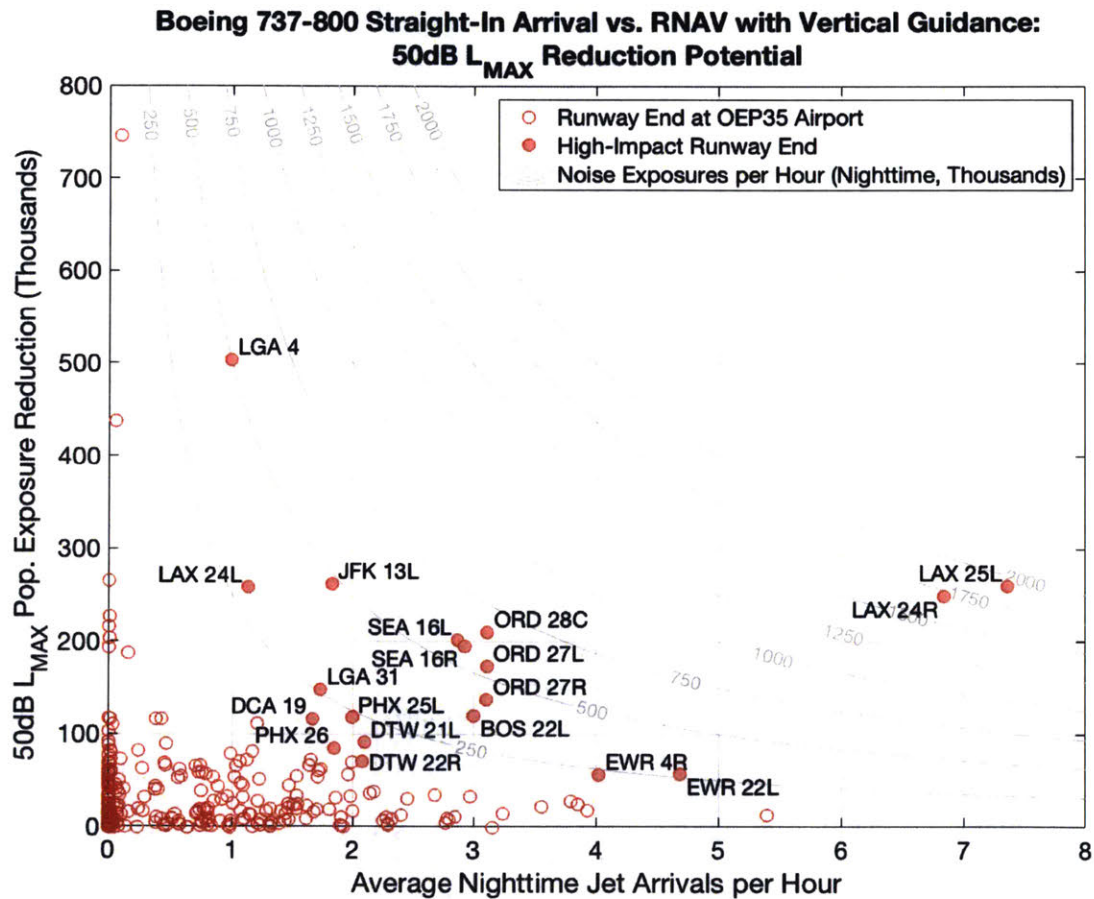


**Figure 49. 2017 Nighttime 50dB L<sub>MAX</sub> noise reduction potential from RNAV procedures with vertical guidance for all OEP-35 runways**

While many of the same runways appear in the highest-benefit set, the exact magnitude and ranking of potential benefits is different than for the daytime case. As for the daytime operations, the largest potential single-event noise reductions occur around major airports located in congested metropolitan areas. One consideration for procedure noise evaluation at the 50dB level relative to the 60dB level is the larger total noise footprint and correspondingly larger population impact numbers. The 50 runway ends in the OEP-35 with the largest nighttime population exposure reduction potential ranked by hourly noise impact are listed in Table 16.

**Table 16. Highest benefit opportunities for RNAV procedures with vertical guidance at the 50dB level (B737-800)**

Rank	Airport	Rwy	Avg Night Jet Arrs/Hr (2017)	B738 Straight-In 50dB Pop.	Straight-In Hourly Noise Intensity	B738 RNAV (Vert) 50dB Pop.	50dB Pop. Δ	Hourly Noise Intensity Reduction
1	KLAX	25L	7.36	515,405	3,793,643	254,780	-260,625	1,918,333
2	KLAX	24R	6.84	500,693	3,422,846	251,243	-249,450	1,705,294
3	KORD	28C	3.11	358,306	1,116,077	148,004	-210,302	655,064
4	KSEA	16L	2.87	263,118	756,083	61,160	-201,958	580,337
5	KSEA	16R	2.93	257,059	753,020	61,475	-195,584	572,937
6	KORD	27L	3.11	300,660	935,507	126,814	-173,846	540,924
7	KLGA	4	0.99	1,270,806	1,261,617	766,918	-503,888	500,244
8	KJFK	13L	1.83	895,514	1,637,002	633,293	-262,221	479,341
9	KORD	27R	3.11	249,407	775,343	111,513	-137,894	428,677
10	KBOS	22L	3.01	168,934	507,876	48,741	-120,193	361,343
11	KLAX	24L	1.13	503,362	569,880	244,812	-258,550	292,717
12	KEWR	22L	4.69	164,488	771,075	106,902	-57,586	269,947
13	KLGA	31	1.73	531,549	920,852	382,790	-148,759	257,709
14	KLGA	22	2	297,617	595,335	178,589	-119,028	238,096
15	KPHX	25L	2	147,380	294,198	29,140	-118,240	236,029
16	KEWR	4R	4.02	150,787	606,707	93,970	-56,817	228,609
17	KDCA	19	1.67	313,754	523,816	196,734	-117,020	195,366
18	KDTW	21L	2.1	158,700	332,817	67,320	-91,380	191,637
19	KPHX	26	1.85	115,782	214,045	30,830	-84,952	157,050
20	KDTW	22R	2.08	145,605	303,293	75,349	-70,256	146,342
21	KORD	9L	2	120,727	241,153	51,038	-69,689	139,204
22	KMDW	22L	1.21	325,785	394,696	214,278	-111,507	135,093
23	KSEA	34L	1.65	114,353	189,176	42,424	-71,929	118,993
24	KMCO	17L	1.97	111,381	218,922	55,272	-56,109	110,284
25	KSEA	34R	1.64	120,613	198,026	54,186	-66,427	109,062
26	KPHL	27R	1.74	104,975	182,652	43,110	-61,865	107,643
27	KSAN	27	3.8	209,364	795,516	181,678	-27,686	105,198
28	KDFW	17C	1.72	72,526	124,642	12,164	-60,362	103,737
29	KMEM	27	2.98	99,751	297,059	67,018	-32,733	97,479
30	KPIT	28L	1.17	102,869	120,148	21,581	-81,288	94,942
31	KJFK	31L	3.86	81,487	314,189	56,903	-24,584	94,788
32	KBWI	33L	2.68	84,773	227,451	49,964	-34,809	93,395
33	KDFW	17L	1.71	65,538	112,170	11,804	-53,734	91,967
34	KDFW	18R	1.54	66,276	101,832	11,125	-55,151	84,739
35	KLAS	19L	2.18	201,570	439,041	163,560	-38,010	82,790
36	KEWR	22R	1.12	191,927	215,560	119,735	-72,192	81,081
37	KLAS	19R	2.15	194,392	417,283	157,694	-36,698	78,776
38	KJFK	31R	3.56	82,594	293,879	60,483	-22,111	78,673
39	KIAD	1C	0.99	88,815	87,979	9,491	-79,324	78,577
40	KPHL	9R	1.06	83,845	89,285	13,228	-70,617	75,199
41	KMEM	18R	2.45	90,502	222,165	59,953	-30,549	74,992
42	KSFO	28L	3.93	24,871	97,730	6,481	-18,390	72,263
43	KEWR	29	0.09	853,007	79,719	106,617	-746,390	69,755
44	KSFO	28R	5.4	15,626	84,363	2,809	-12,817	69,198
45	KPDx	28L	1.04	87,591	90,761	22,327	-65,264	67,626
46	KMCO	18R	1.98	118,943	235,847	85,582	-33,361	66,150
47	KMDW	31C	1.47	248,107	365,394	203,502	-44,605	65,691
48	KPHL	26	1.23	104,080	127,905	52,353	-51,727	63,568
49	KCLE	24R	1.86	114,438	212,689	83,162	-31,276	58,128
50	KIAD	1R	1.02	99,043	101,449	45,097	-53,946	55,256



## **5.6 RNAV Procedures without Vertical Guidance**

RNAV procedures without vertical guidance have similar design criteria to those with vertical guidance with the key distinction occurring where there is a turn at the PFAF. For procedures with vertical guidance, the maximum intercept angle is 15°. For procedures without vertical guidance, this is relaxed to 30°. The additional flexibility in this turn allows for additional track movement in the vicinity of the PFAF relative to the straight-in baseline, allowing for population exposure reduction for runways with population centers in the impacted region. While there are other differences in terms of obstacle clearance requirements as discussed in Section 4.1.2, the fundamental geometric constraints prior to the final approach segment are the same for RNAV procedures with and without vertical guidance.

### **5.6.1 Runway-level results**

Any procedure geometry allowed under vertical guidance criteria is also allowed under non-vertical criteria. Therefore, the benefit derived from removing vertical guidance is purely a byproduct of steeper approach intercept capability. Due to the similarities between RNAV procedures with and without vertical guidance, only one example is presented. Among the OEP-35 runway ends examined in this study, BOS runway 9 had the largest incremental noise benefit from non-vertically guided RNAV. However, this runway is not used for jet arrivals. The location with the second-largest potential benefit is LGA runway 4, which is used heavily for jet arrivals and illustrated in Figure 50.

It is important to recognize that the greater flexibility afforded by the removal of vertical guidance is accompanied by a reduction in approach precision as well as higher approach minimums in most cases. Operators typically prefer approaches with vertical guidance due to higher precision and utility. Therefore, overall operational utilization of non-vertically guided procedures may be lower than for other types of PBN procedures, limiting the potential benefits from the greater lateral track design flexibility from a noise standpoint.

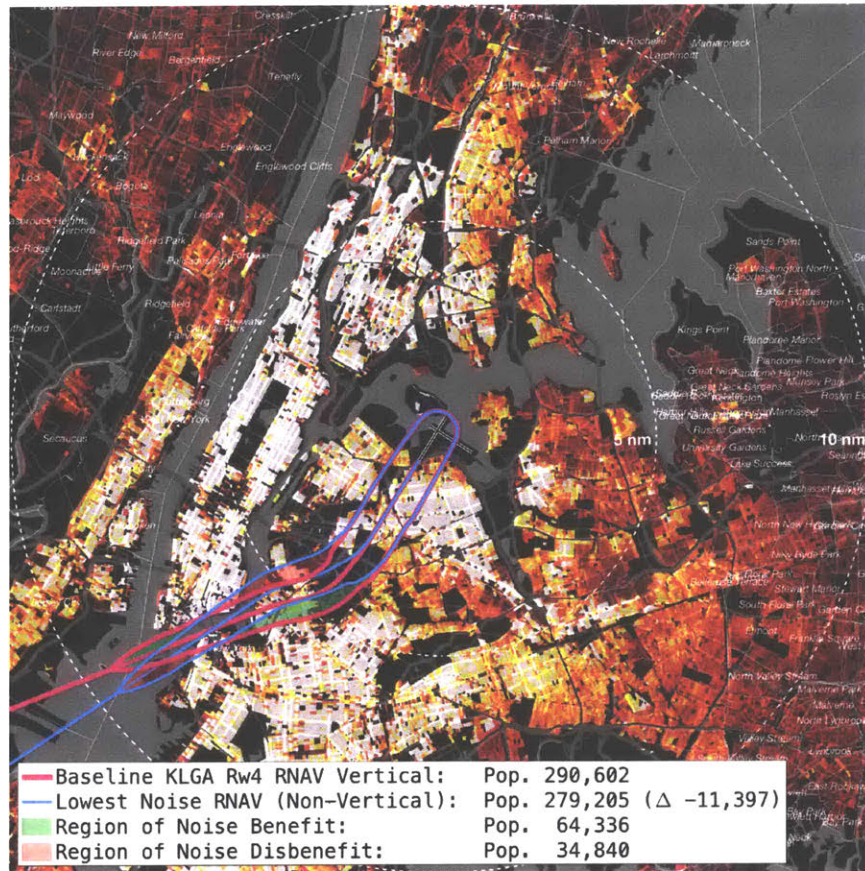


**Figure 50. Comparison between noise-minimal RNAV approach with and without vertical guidance at LGA runway 4**

### 5.6.2 Results for all OEP-35 runway ends

The noise reduction potential from RNAV approaches without vertical guidance were calculated for all the runway ends in the OEP-35 airports for daytime and nighttime  $L_{MAX}$  threshold levels. Results are shown as a function of day and night average jet arrival volume from 2017 for the corresponding runway. Figure 51 shows the daytime results and Figure 52 shows the nighttime results for each runway end. The impact figures also show isolines for noise intensity reduction, the product of runway arrival volume and population reduction. This metric represents the total population benefit level expected from implementation of a modified procedure at specific runway ends. Traffic volumes for day and night periods are averaged over the full operational year of 2017. Table 17 shows the 50 procedures that have the highest noise intensity reduction for daytime operations. Table 18 shows the same data for the 50 procedures having the highest nighttime benefit.

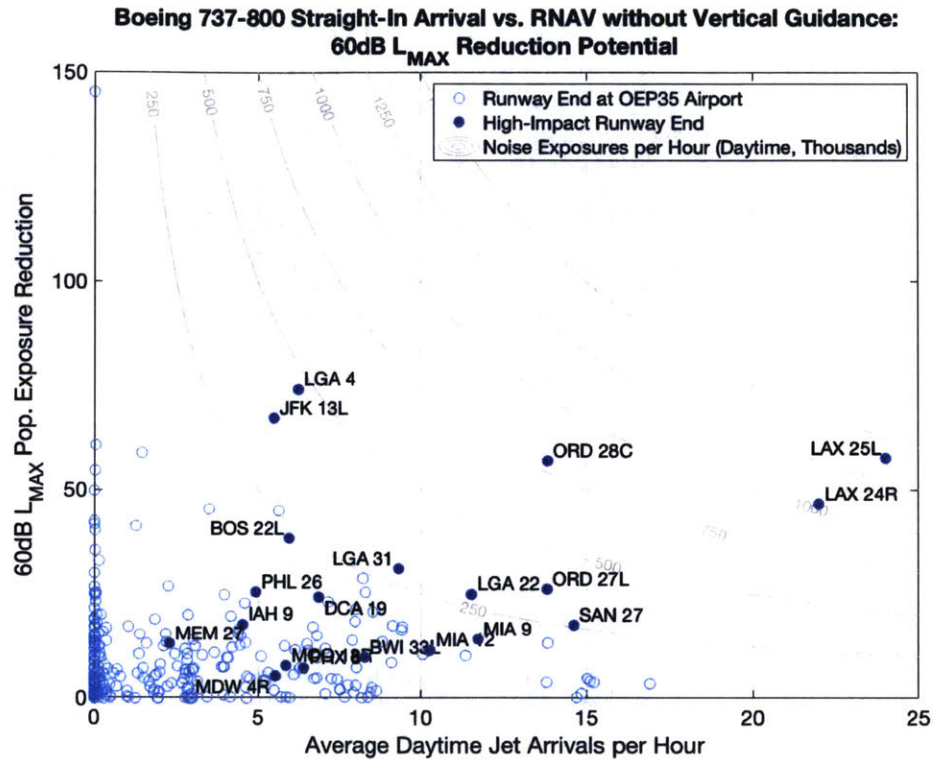


**Figure 51. 2017 Daytime 60dB  $L_{MAX}$  noise reduction potential from RNAV procedures without vertical guidance for all OEP-35 runways**

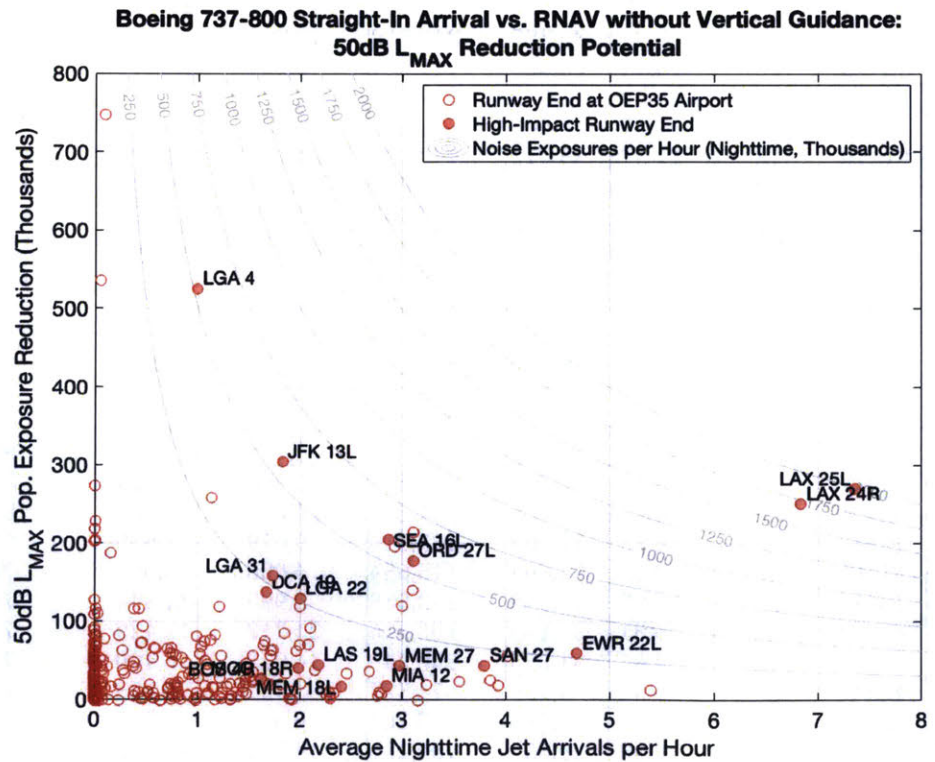


**Figure 52. 2017 Nighttime 50dB  $L_{MAX}$  noise reduction potential from RNAV procedures without vertical guidance for all OEP-35 runways**

**Table 17. Highest benefit opportunities for RNAV procedures without vertical guidance at the 60dB level (B737-800)**

Rank	Airport	Rwy	Avg Day Jet Arrs/Hr (2017)	B738 Straight-In 60dB Pop.	Baseline Hourly Noise Intensity	B738 RNAV (Vert) 60dB Pop.	60dB Pop. Δ	Hourly Noise Intensity Reduction
1	KLAX	25L	24.01	151,792	3,643,873	94,210	-57,582	1,382,296
2	KLAX	24R	21.99	130,022	2,859,541	83,435	-46,587	1,024,576
3	KORD	28C	13.83	106,520	1,473,462	49,587	-56,933	787,539
4	KLGA	4	6.24	353,298	2,204,739	279,205	-74,093	462,374
5	KJFK	13L	5.5	232,171	1,276,479	165,053	-67,118	369,016
6	KORD	27L	13.81	66,189	914,340	39,968	-26,221	362,219
7	KLGA	31	9.34	202,103	1,887,113	171,063	-31,040	289,832
8	KLGA	22	11.55	79,129	913,980	54,078	-25,051	289,352
9	KSAN	27	14.62	87,083	1,272,919	69,511	-17,572	256,855
10	KMDW	22L	5.64	130,040	733,654	85,191	-44,849	253,027
11	KLAS	19R	8.21	92,313	758,040	63,554	-28,759	236,158
12	KBOS	22L	5.96	62,240	371,174	23,945	-38,295	228,375
13	KSEA	16L	8.29	43,378	359,714	17,946	-25,432	210,896
14	KORD	27R	13.84	51,388	710,991	38,132	-13,256	183,407
15	KSEA	16R	8.54	44,009	376,042	23,283	-20,726	177,097
16	KLAS	19L	7.99	87,767	701,021	66,426	-21,341	170,457
17	KDCA	19	6.87	88,703	609,500	64,419	-24,284	166,861
18	KMIA	9	11.74	36,040	423,226	21,929	-14,111	165,709
19	KPHL	27R	7.15	24,412	174,538	1,236	-23,176	165,701
20	KDFW	17L	9.45	18,053	170,539	885	-17,168	162,179
21	KPHX	25L	9.17	27,740	254,327	10,295	-17,445	159,940
22	KLAX	24L	3.5	128,037	448,195	82,660	-45,377	158,843
23	KDFW	17C	9.43	17,871	168,484	1,464	-16,407	154,682
24	KORD	9L	7.97	30,755	245,260	12,388	-18,367	146,470
25	KPHL	26	4.94	28,608	141,269	3,167	-25,441	125,630
26	KDFW	18R	8.83	15,620	137,997	2,105	-13,515	119,400
27	KMIA	12	10.3	19,608	201,996	8,036	-11,572	119,211
28	KEWR	4R	11.37	39,412	448,034	29,135	-10,277	116,829
29	KDTW	22R	10.25	29,449	301,832	18,121	-11,328	116,104
30	KMDW	31C	6.68	92,518	617,967	75,526	-16,992	113,497
31	KJFK	31R	7.88	34,473	271,777	20,674	-13,799	108,788
32	KDTW	21L	10.06	27,319	274,886	16,795	-10,524	105,893
33	KPHL	9R	4.59	24,873	114,082	2,119	-22,754	104,363
34	KMSP	12R	6.8	49,092	333,950	34,164	-14,928	101,548
35	KSEA	34R	3.96	48,100	190,237	23,295	-24,805	98,105
36	KEWR	29	1.43	87,766	125,771	28,943	-58,823	84,295
37	KJFK	31L	7.06	34,145	241,079	22,308	-11,837	83,575
38	KPHX	7R	6.5	18,589	120,755	5,726	-12,863	83,559
39	KSEA	34L	4.16	35,705	148,604	15,986	-19,719	82,070
40	KBWI	33L	8.28	34,006	281,591	24,243	-9,763	80,844
41	KIAH	9	4.53	27,368	123,919	9,679	-17,689	80,094
42	KPHX	26	9.13	12,664	115,654	4,058	-8,606	78,594
43	KIAH	27	6.55	17,343	113,518	5,999	-11,344	74,252
44	KMCO	17L	5.81	34,141	198,526	21,712	-12,429	72,273
45	KSLC	34L	4.41	31,373	138,243	14,973	-16,400	72,266
46	KSFO	28L	15.04	4,955	74,522	232	-4,723	71,032
47	KIAH	26L	6.14	17,634	108,267	6,094	-11,540	70,852
48	KSLC	34R	4.38	29,757	130,286	14,261	-15,496	67,847
49	KIAD	1C	4.47	17,829	79,622	2,938	-14,891	66,501
50	KMSP	12L	6.8	46,900	319,106	37,330	-9,570	65,114

**Table 18. Highest benefit opportunities for RNAV procedures without vertical guidance at the 50dB level (B737-800)**

Rank	Airport	Rwy	Avg Night Jet Arrs/Hr (2017)	B738 Straight-In 50dB Pop.	Straight-In Hourly Noise Intensity	B738 RNAV (Vert) 50dB Pop.	50dB Pop. Δ	Hourly Noise Intensity Reduction
1	KLAX	25L	7.36	515,405	3,793,643	245,346	-270,059	1,987,772
2	KLAX	24R	6.84	500,693	3,422,846	249,587	-251,106	1,716,615
3	KORD	28C	3.11	358,306	1,116,077	144,052	-214,254	667,374
4	KSEA	16L	2.87	263,118	756,083	57,983	-205,135	589,466
5	KSEA	16R	2.93	257,059	753,020	61,346	-195,713	573,315
6	KJFK	13L	1.83	895,514	1,637,002	590,842	-304,672	556,941
7	KORD	27L	3.11	300,660	935,507	122,832	-177,828	553,314
8	KLGA	4	0.99	1,270,806	1,261,617	745,381	-525,425	521,626
9	KORD	27R	3.11	249,407	775,343	109,236	-140,171	435,756
10	KBOS	22L	3.01	168,934	507,876	48,741	-120,193	361,343
11	KLAX	24L	1.13	503,362	569,880	244,651	-258,711	292,899
12	KEWR	22L	4.69	164,488	771,075	104,762	-59,726	279,979
13	KLGA	31	1.73	531,549	920,852	373,165	-158,384	274,384
14	KLGA	22	2	297,617	595,335	168,055	-129,562	259,168
15	KPHX	25L	2	147,380	294,198	28,668	-118,712	236,971
16	KDCA	19	1.67	313,754	523,816	176,613	-137,141	228,958
17	KEWR	4R	4.02	150,787	606,707	93,970	-56,817	228,609
18	KDTW	21L	2.1	158,700	332,817	67,210	-91,490	191,868
19	KSAN	27	3.8	209,364	795,516	165,108	-44,256	168,159
20	KPHX	26	1.85	115,782	214,045	30,830	-84,952	157,050
21	KDTW	22R	2.08	145,605	303,293	75,349	-70,256	146,342
22	KMDW	22L	1.21	325,785	394,696	206,890	-118,895	144,044
23	KORD	9L	2	120,727	241,153	51,038	-69,689	139,204
24	KMEM	27	2.98	99,751	297,059	56,010	-43,741	130,261
25	KSEA	34L	1.65	114,353	189,176	39,237	-75,116	124,265
26	KMCO	17L	1.97	111,381	218,922	49,272	-62,109	122,077
27	KSEA	34R	1.64	120,613	198,026	50,542	-70,071	115,045
28	KPHL	27R	1.74	104,975	182,652	40,722	-64,253	111,798
29	KDFW	17C	1.72	72,526	124,642	9,237	-63,289	108,768
30	KLAS	19L	2.18	201,570	439,041	156,523	-45,047	98,117
31	KBWI	33L	2.68	84,773	227,451	48,280	-36,493	97,913
32	KPIT	28L	1.17	102,869	120,148	19,329	-83,540	97,572
33	KJFK	31L	3.86	81,487	314,189	56,326	-25,161	97,013
34	KDFW	17L	1.71	65,538	112,170	9,506	-56,032	95,900
35	KDFW	18R	1.54	66,276	101,832	10,075	-56,201	86,352
36	KEWR	22R	1.12	191,927	215,560	115,622	-76,305	85,701
37	KJFK	31R	3.56	82,594	293,879	58,801	-23,793	84,658
38	KMEM	18R	2.45	90,502	222,165	56,454	-34,048	83,581
39	KLAS	19R	2.15	194,392	417,283	156,376	-38,016	81,605
40	KMCO	18R	1.98	118,943	235,847	78,196	-40,747	80,796
41	KIAD	1C	0.99	88,815	87,979	7,458	-81,357	80,591
42	KPHL	9R	1.06	83,845	89,285	9,264	-74,581	79,420
43	KSFO	28L	3.93	24,871	97,730	6,043	-18,828	73,984
44	KSFO	28R	5.4	15,626	84,363	2,366	-13,260	71,589
45	KPDx	28L	1.04	87,591	90,761	19,490	-68,101	70,566
46	KEWR	29	0.09	853,007	79,719	105,305	-747,702	69,878
47	KPHL	26	1.23	104,080	127,905	47,670	-56,410	69,323
48	KMDW	31C	1.47	248,107	365,394	201,660	-46,447	68,404
49	KMIA	9	3.24	77,108	249,874	57,268	-19,840	64,293
50	KCLE	24R	1.86	114,438	212,689	80,842	-33,596	62,440

## **5.7 RNP Procedures**

RNP procedures allow precise RF turns in the final approach segment of an approach, allowing for rollout on a straight-in segment closer to the runway than permitted in an RNAV approach. There is no maximum angle for this final turn, allowing for much greater flexibility in terms final runway alignment in the intermediate and final segments of the procedure. Traditional flyby and flyover waypoints are also permitted in RNP procedures, meaning that any lateral procedure design that can be designed under RNAV criteria can also be designed under RNP criteria. Therefore, the noise benefit possible with RNP is always at least as high as RNAV with or without vertical guidance. While RNP procedures are associated with increased monitoring and conformance requirements, lower minimums, and greater predictability than RNAV procedures, the principal benefit in terms of noise arises because of this increased lateral route flexibility.

### **5.7.1 Runway-level results**

Runways with the greatest incremental benefit from RNP are those with population centers in the immediate vicinity of the runway end. Close-in turns to final and precise RF turning segments have the greatest potential to reduce population impact by precision avoidance of these high-impact areas. Figure 53 shows the highest-benefit RNP approach procedure candidate to ORD runway 28C. This approach definition uses a short final segment to enable a close-in turn from a base leg to the south of the airport where population density is lower than along the straight-in approach path.

Figure 54 shows the highest-benefit RNP approach procedure to DCA runway 19. This runway is served by a published RNP procedure, as shown in the right panel of the figure. The existing procedure uses a waiver to reduce the minimum final approach segment length in order to avoid prohibited airspace along the final approach path. However, it is interesting to note that the overall geometry of the published procedure is consistent with the output from the procedure selection model used in this analysis.

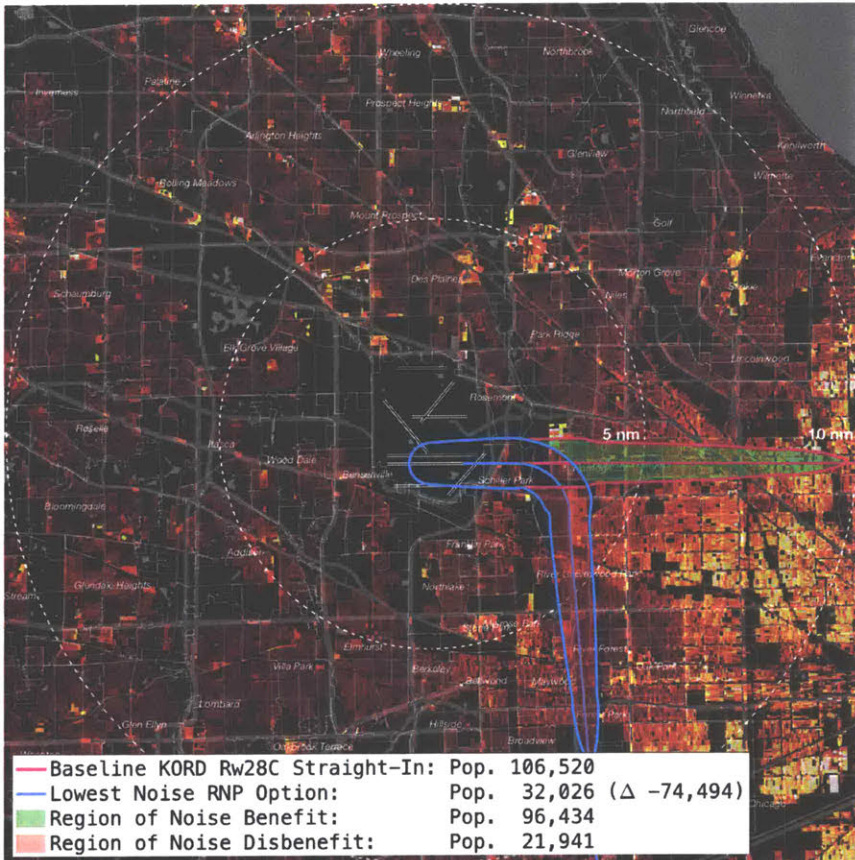
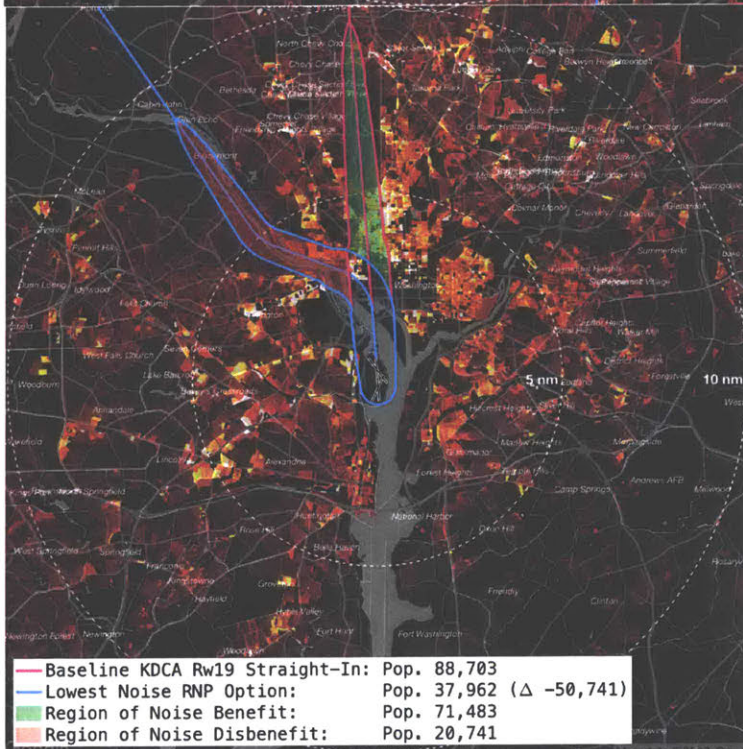
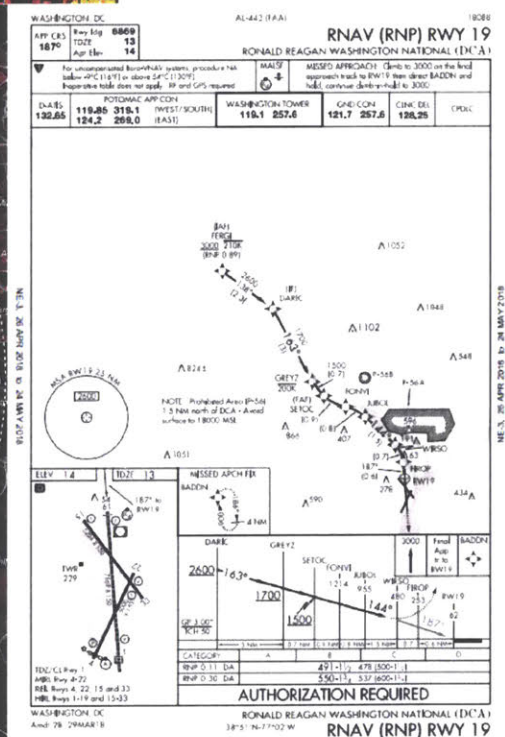


Figure 53. ORD Runway 28C noise-minimal RNP procedure relative to a straight-in baseline (Boeing 737-800, 60dB L<sub>MAX</sub>)



(a) Noise-minimal RNP result



(b) Published RNP runway 19

Figure 54. DCA runway 19 noise-minimal RNP procedure relative to a straight-in baseline (Boeing 737-800, 60dB L<sub>MAX</sub>) compared with published RNAV (RNP) to the same runway

### **5.7.2 Results for all OEP-35 runway ends**

The runways with the highest potential benefit from RNP procedures are similar to the high-benefit RNAV runways, although the precise ranking and magnitude of benefit varies. The noise reduction potential from RNP approaches were calculated for all the runway ends in the OEP-35 airports for daytime and nighttime  $L_{MAX}$  threshold levels using the same methods and reporting used for the RNAV approach criteria options. Results are shown as a function of day and night average jet arrival volume from 2017 for the corresponding runway. Figure 55 shows the daytime results and Figure 56 shows the nighttime results for each runway end. Table 19 shows the 50 procedures that have the highest noise intensity reduction for daytime operations. Table 20 shows the same data for the 50 procedures having the highest nighttime benefit.

The overall noise benefit from RNP approaches is higher than for either version of RNAV in all cases. As discussed in prior sections, RNP criteria can be used to overlay the track geometry of any RNAV procedure. Therefore, the noise benefits from RNAV are matched at a minimum. The benefits of RNP with respect to close-in maneuvering and precise turn segments throughout the approach results in additional incremental benefits.



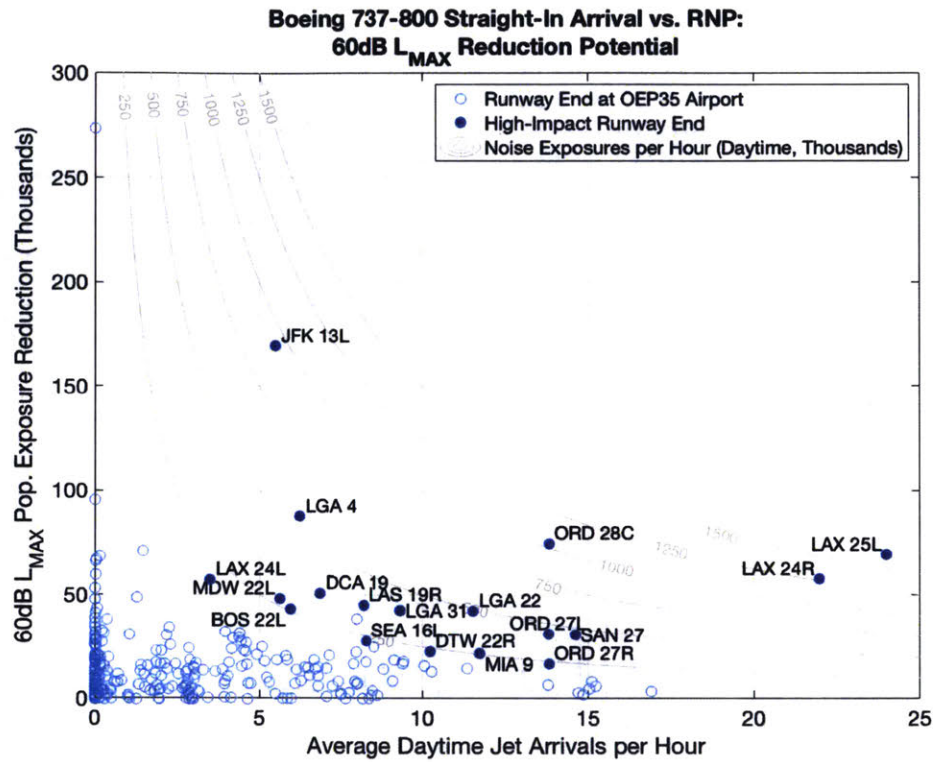


**Figure 55. 2017 Daytime 60dB  $L_{MAX}$  noise reduction potential from RNP procedures for all OEP-35 runways**

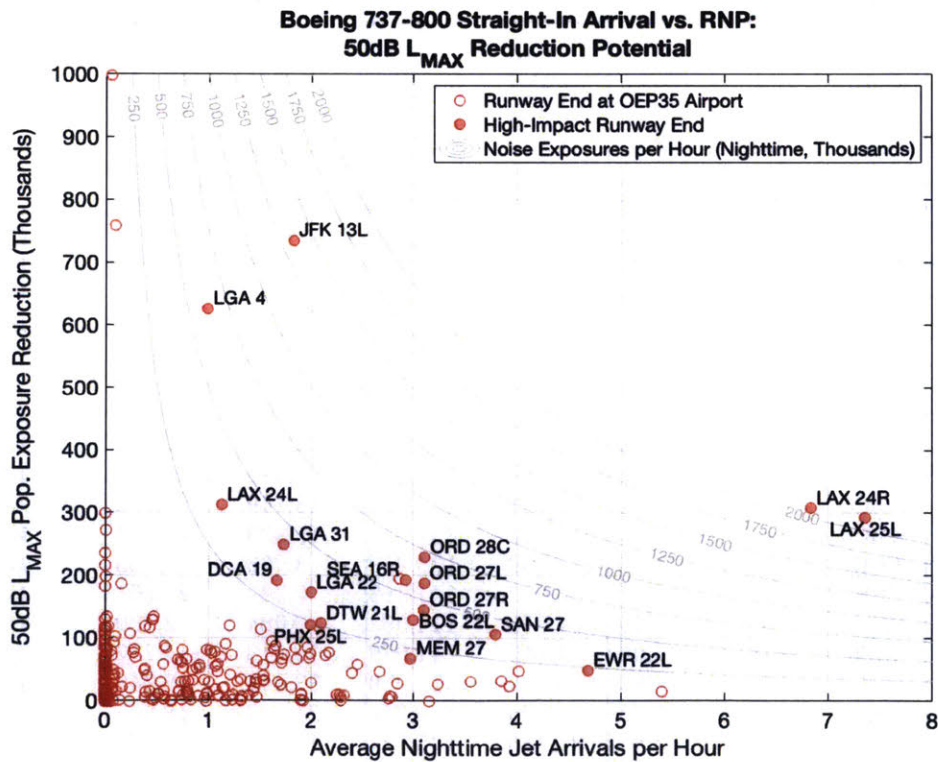


**Figure 56. 2017 Nighttime 50dB  $L_{MAX}$  noise reduction potential from RNP procedures for all OEP-35 runways**

**Table 19. Highest benefit opportunities for RNP procedures at the 60dB level (B737-800)**

Rank	Airport	Rwy	Avg Day Jet Arrs/Hr (2017)	B738 Straight-In 60dB Pop.	Baseline Hourly Noise Intensity	B738 RNAV (Vert) 60dB Pop.	60dB Pop. Δ	Hourly Noise Intensity Reduction
1	KLAX	25L	24.01	151,792	3,643,873	82,490	-69,302	1,663,643
2	KLAX	24R	21.99	130,022	2,859,541	72,208	-57,814	1,271,489
3	KORD	28C	13.83	106,520	1,473,462	32,026	-74,494	1,030,455
4	KJFK	13L	5.5	232,171	1,276,479	62,745	-169,426	931,506
5	KLGA	4	6.24	353,298	2,204,739	265,813	-87,485	545,946
6	KLGA	22	11.55	79,129	913,980	36,891	-42,238	487,870
7	KSAN	27	14.62	87,083	1,272,919	56,175	-30,908	451,792
8	KORD	27L	13.81	66,189	914,340	34,989	-31,200	430,999
9	KLGA	31	9.34	202,103	1,887,113	159,623	-42,480	396,652
10	KLAS	19R	8.21	92,313	758,040	47,292	-45,021	369,695
11	KDCA	19	6.87	88,703	609,500	37,962	-50,741	348,654
12	KLAS	19L	7.99	87,767	701,021	49,490	-38,277	305,730
13	KMDW	22L	5.64	130,040	733,654	81,836	-48,204	271,955
14	KBOS	22L	5.96	62,240	371,174	18,993	-43,247	257,907
15	KMIA	9	11.74	36,040	423,226	14,212	-21,828	256,331
16	KDTW	22R	10.25	29,449	301,832	6,591	-22,858	234,278
17	KORD	27R	13.84	51,388	710,991	34,610	-16,778	232,136
18	KSEA	16L	8.29	43,378	359,714	15,576	-27,802	230,549
19	KSEA	16R	8.54	44,009	376,042	19,104	-24,905	212,805
20	KLAX	24L	3.5	128,037	448,195	70,742	-57,295	200,562
21	KORD	9L	7.97	30,755	245,260	8,488	-22,267	177,571
22	KPHX	25L	9.17	27,740	254,327	9,227	-18,513	169,732
23	KDFW	17L	9.45	18,053	170,539	118	-17,935	169,424
24	KEWR	4R	11.37	39,412	448,034	24,756	-14,656	166,609
25	KDFW	17C	9.43	17,871	168,484	949	-16,922	159,537
26	KDTW	21L	10.06	27,319	274,886	11,514	-15,805	159,031
27	KPHL	27R	7.15	24,412	174,538	3,463	-20,949	149,779
28	KBWI	33L	8.28	34,006	281,591	16,305	-17,701	146,575
29	KSLC	34L	4.41	31,373	138,243	7	-31,366	138,212
30	KJFK	31R	7.88	34,473	271,777	17,557	-16,916	133,362
31	KMIA	12	10.3	19,608	201,996	6,747	-12,861	132,490
32	KSLC	34R	4.38	29,757	130,286	2	-29,755	130,278
33	KSEA	34R	3.96	48,100	190,237	16,011	-32,089	126,913
34	KDFW	18R	8.83	15,620	137,997	1,256	-14,364	126,900
35	KCLE	24R	5.1	48,831	248,838	23,953	-24,878	126,776
36	KATL	27L	15.12	14,047	212,396	5,696	-8,351	126,270
37	KMDW	31C	6.68	92,518	617,967	73,830	-18,688	124,825
38	KSLC	35	4.21	29,517	124,362	86	-29,431	124,000
39	KJFK	22L	4.45	111,173	495,066	83,435	-27,738	123,520
40	KIAD	1R	4.6	30,116	138,574	3,379	-26,737	123,026
41	KMCO	17L	5.81	34,141	198,526	13,749	-20,392	118,577
42	KMCO	18R	5.86	34,410	201,544	15,839	-18,571	108,773
43	KIAH	9	4.53	27,368	123,919	3,903	-23,465	106,247
44	KPHL	26	4.94	28,608	141,269	7,347	-21,261	104,989
45	KPHL	9R	4.59	24,873	114,082	2,084	-22,789	104,524
46	KJFK	31L	7.06	34,145	241,079	19,413	-14,732	104,015
47	KMSP	12R	6.8	49,092	333,950	33,844	-15,248	103,725
48	KMDW	4R	5.53	39,805	220,268	21,263	-18,542	102,606
49	KEWR	29	1.43	87,766	125,771	16,775	-70,991	101,732
50	KSEA	34L	4.16	35,705	148,604	11,691	-24,014	99,946

**Table 20. Highest benefit opportunities for RNP procedures at the 50dB level (B737-800)**

Rank	Airport	Rwy	Avg Night Jet Arrs/Hr (2017)	B738 Straight-In 50dB Pop.	Straight-In Hourly Noise Intensity	B738 RNAV (Vert) 50dB Pop.	50dB Pop. Δ	Hourly Noise Intensity Reduction
1	KLAX	25L	7.36	515,405	3,793,643	222,456	-292,949	2,156,254
2	KLAX	24R	6.84	500,693	3,422,846	192,379	-308,314	2,107,701
3	KJFK	13L	1.83	895,514	1,637,002	160,159	-735,355	1,344,231
4	KORD	28C	3.11	358,306	1,116,077	128,868	-229,438	714,670
5	KLGA	4	0.99	1,270,806	1,261,617	644,153	-626,653	622,122
6	KORD	27L	3.11	300,660	935,507	113,079	-187,581	583,661
7	KSEA	16R	2.93	257,059	753,020	64,224	-192,835	564,884
8	KSEA	16L	2.87	263,118	756,083	67,873	-195,245	561,047
9	KORD	27R	3.11	249,407	775,343	104,189	-145,218	451,446
10	KLGA	31	1.73	531,549	920,852	282,194	-249,355	431,981
11	KSAN	27	3.8	209,364	795,516	103,464	-105,900	402,386
12	KBOS	22L	3.01	168,934	507,876	40,320	-128,614	386,660
13	KLAX	24L	1.13	503,362	569,880	190,450	-312,912	354,263
14	KLGA	22	2	297,617	595,335	124,787	-172,830	345,719
15	KDCA	19	1.67	313,754	523,816	121,774	-191,980	320,513
16	KDTW	21L	2.1	158,700	332,817	35,259	-123,441	258,874
17	KDTW	22R	2.08	145,605	303,293	27,744	-117,861	245,502
18	KPHX	25L	2	147,380	294,198	26,804	-120,576	240,692
19	KEWR	22L	4.69	164,488	771,075	115,571	-48,917	229,310
20	KMEM	27	2.98	99,751	297,059	31,867	-67,884	202,159
21	KEWR	4R	4.02	150,787	606,707	102,970	-47,817	192,397
22	KJFK	22R	1.51	274,030	413,863	160,376	-113,654	171,650
23	KMCO	17L	1.97	111,381	218,922	26,536	-84,845	166,765
24	KLAS	19L	2.18	201,570	439,041	125,042	-76,528	166,686
25	KPHX	26	1.85	115,782	214,045	31,769	-84,013	155,314
26	KLAS	19R	2.15	194,392	417,283	122,060	-72,332	155,268
27	KJFK	22L	1.62	259,806	421,737	165,468	-94,338	153,137
28	KORD	9L	2	120,727	241,153	46,465	-74,262	148,339
29	KMDW	22L	1.21	325,785	394,696	205,897	-119,888	145,247
30	KSEA	34L	1.65	114,353	189,176	27,324	-87,029	143,973
31	KMEM	18R	2.45	90,502	222,165	32,569	-57,933	142,214
32	KMCO	18R	1.98	118,943	235,847	50,386	-68,557	135,939
33	KSEA	34R	1.64	120,613	198,026	38,814	-81,799	134,300
34	KPHL	27R	1.74	104,975	182,652	30,936	-74,039	128,825
35	KBWI	33L	2.68	84,773	227,451	38,077	-46,696	125,288
36	KJFK	31L	3.86	81,487	314,189	49,315	-32,172	124,046
37	KCLE	24R	1.86	114,438	212,689	48,461	-65,977	122,622
38	KDFW	17C	1.72	72,526	124,642	5,743	-66,783	114,772
39	KJFK	31R	3.56	82,594	293,879	51,495	-31,099	110,654
40	KBOS	4R	1.62	89,427	144,484	21,333	-68,094	110,017
41	KMEM	18L	2.4	79,615	191,288	35,551	-44,064	105,871
42	KPIT	28L	1.17	102,869	120,148	12,479	-90,390	105,573
43	KDFW	17L	1.71	65,538	112,170	5,643	-59,895	102,512
44	KMDW	31C	1.47	248,107	365,394	184,805	-63,302	93,226
45	KSFO	28L	3.93	24,871	97,730	1,715	-23,156	90,991
46	KPHL	26	1.23	104,080	127,905	31,700	-72,380	88,949
47	KDFW	18R	1.54	66,276	101,832	9,836	-56,440	86,719
48	KMIA	9	3.24	77,108	249,874	50,599	-26,509	85,904
49	KPHL	9R	1.06	83,845	89,285	5,685	-78,160	83,231
50	KSFO	28R	5.4	15,626	84,363	440	-15,186	81,988

## 5.8 Comparison of PBN Approach Guidance Methods for Noise Reduction

This analysis identified noise-minimizing approach designs at both the 50dB and 60dB level for RNAV (with and without vertical guidance) as well as RNP guidance technologies. In all cases, RNAV approaches with vertical guidance have the least lateral track flexibility and the corresponding lowest population benefit. RNAV approaches without vertical guidance have incrementally greater track flexibility and larger population benefit levels. RNP procedures have the greatest lateral flexibility and largest population benefit. However, the incremental benefit level for each level of guidance varies dramatically between runways depending on underlying population configuration.

Figure 57 shows the population benefit levels for all three PBN guidance technologies evaluated in this study for the top 75 runway ends in the OEP-35 airports as ranked by maximum single-event noise reduction at the 60dB level for a B737-800 arrival. There are two clear takeaways from the figure. First, specific runway ends account for a large portion of projected population exposure reduction on a system scale. Airports in the major metropolitan areas of New York, Los Angeles, and Chicago comprise a major portion of total projected noise benefits due to the density of the population centers in the vicinity of the airports. Second, the benefit of RNP appears to be the largest when the reduced final approach segment length allows for turns onto final from an intermediate segment overlying water bodies or sparsely-populated areas.

The largest RNP population benefit in absolute as well as incremental terms occurs at Runway 13L and 13R at New York JFK Airport (JFK), as shown in figure Figure 57. These runways are characterized by dense populations on the runway centerlines and opportunities for low-noise overwater approaches from the southeast given sufficiently short final approach segments. The procedure geometry for all three PBN guidance options are shown in Figure 58 (runway 13R) and Figure 59 (runway 13L). Figure 60 shows the example of Minneapolis-St. Paul Airport (MSP) runway 35, where RNP and RNAV without vertical guidance allow for interception of the final approach course from a low-noise approach corridor over the Minnesota River. Figure 61 shows the procedure geometry outputs for Seattle-Tacoma Airport (SEA) runway 34L, where the Puget Sound provides a low-impact overwater approach corridor. Figure 62 shows results for Tampa International Airport

(TPA) runway 19L where all procedures are over land but take advantage of regions of varying population density depending on maneuver capability in the three criteria levels. Figure 63 shows results for LGA runway 4, where RNP criteria allows a shortened final approach segment length which eliminates the need to overfly the densely-populated borough of Brooklyn.

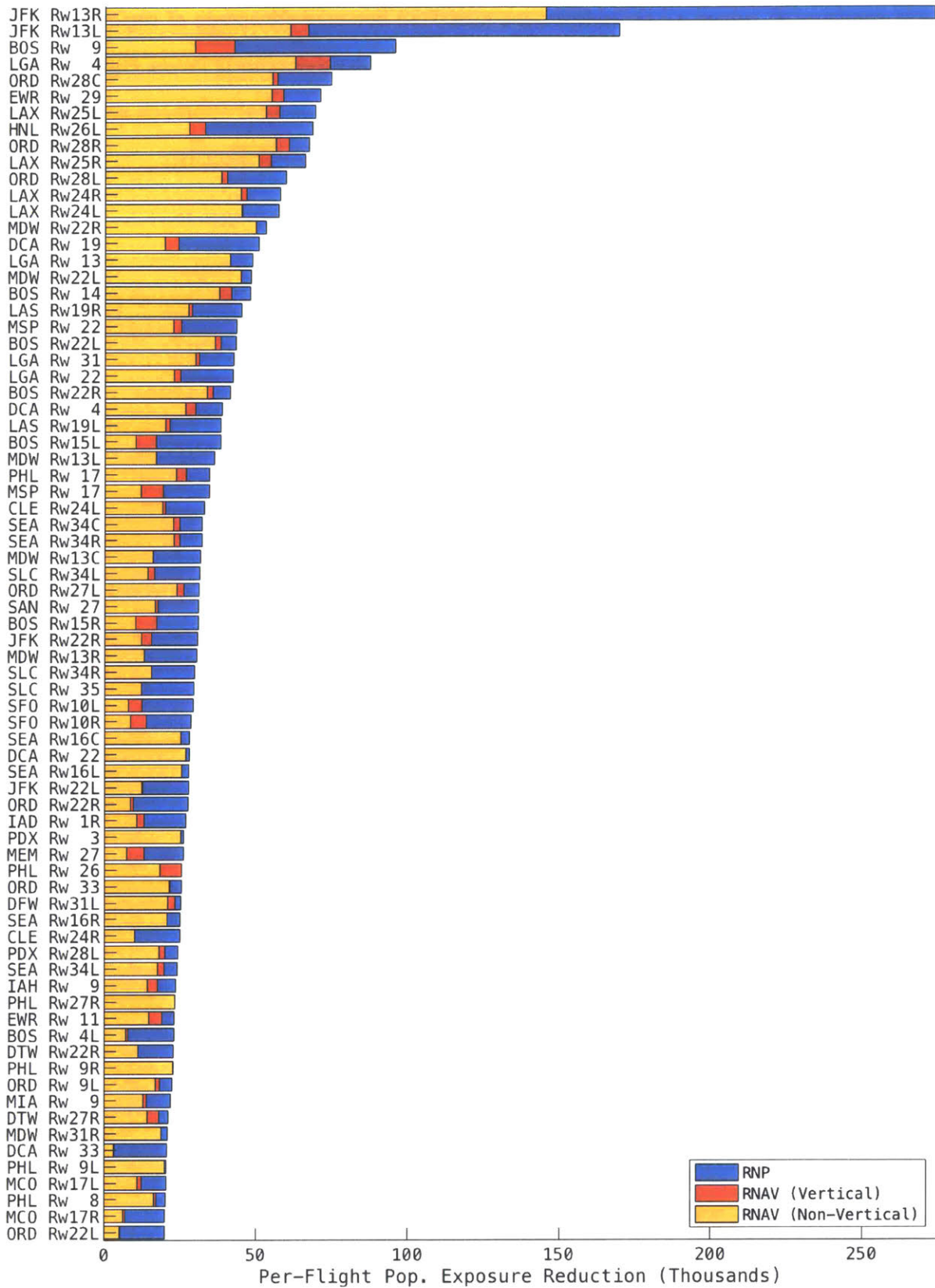
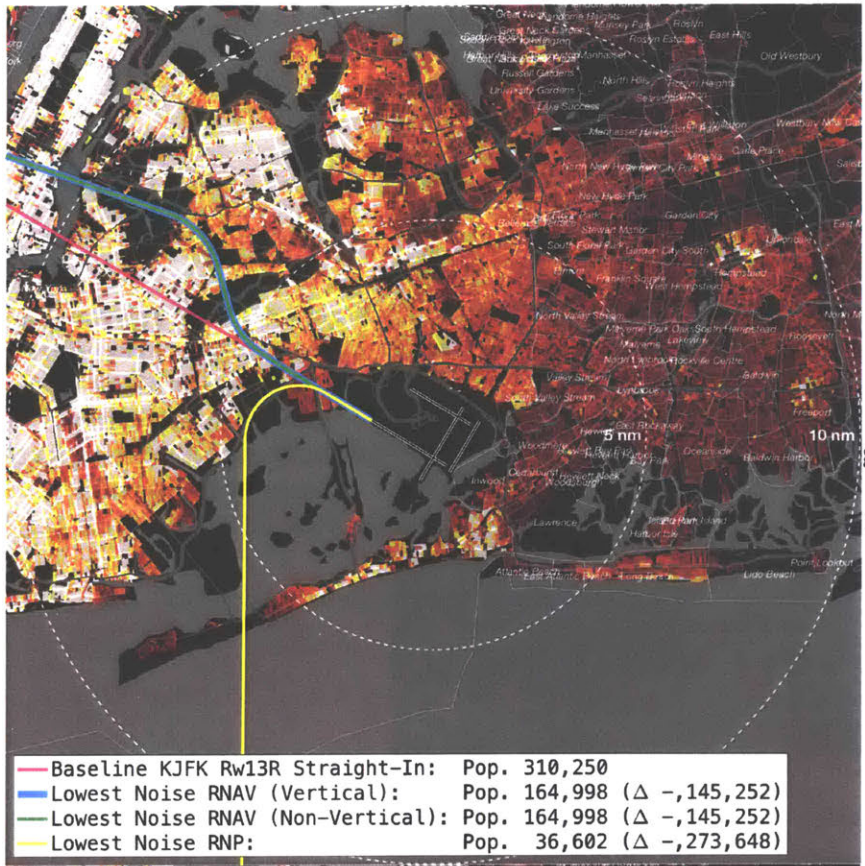
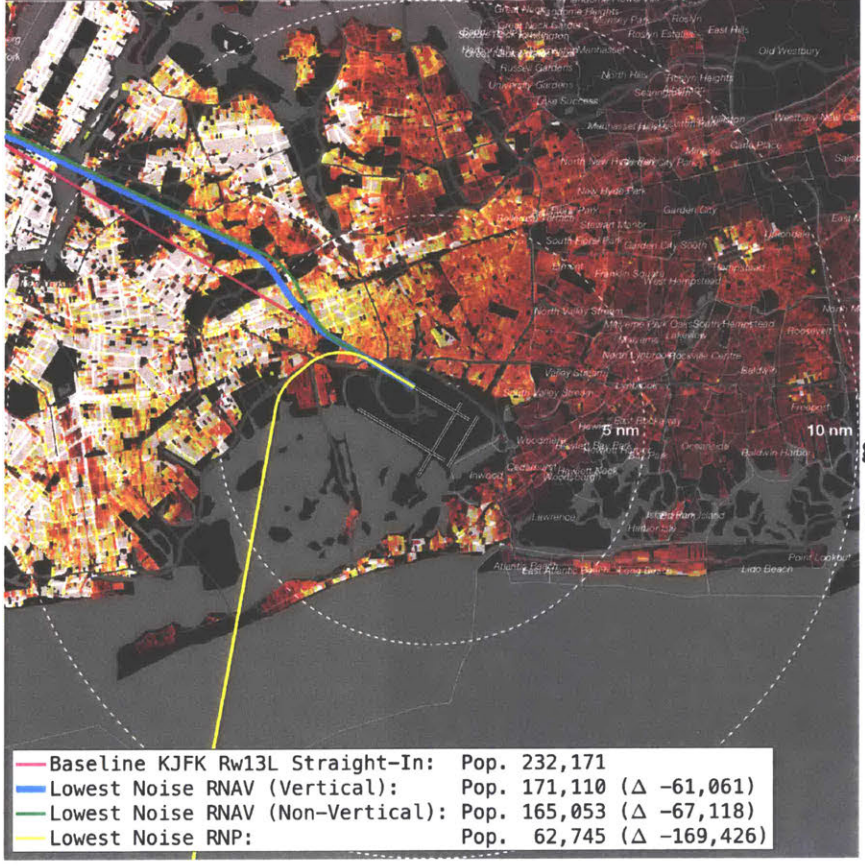


Figure 57. Population exposure reduction (B737-800, 60dB L<sub>MAX</sub>) for PBN procedures at the highest-benefit 75 runways in the OEP-35



**Figure 58. JFK runway 13R noise-minimal procedure centerlines for RNAV with and without vertical guidance and RNP relative to a straight-in baseline (Boeing 737-800, 60dB L<sub>MAX</sub>)**



**Figure 59. JFK runway 13L noise-minimal procedure centerlines for RNAV with and without vertical guidance and RNP relative to a straight-in baseline (Boeing 737-800, 60dB L<sub>MAX</sub>)**

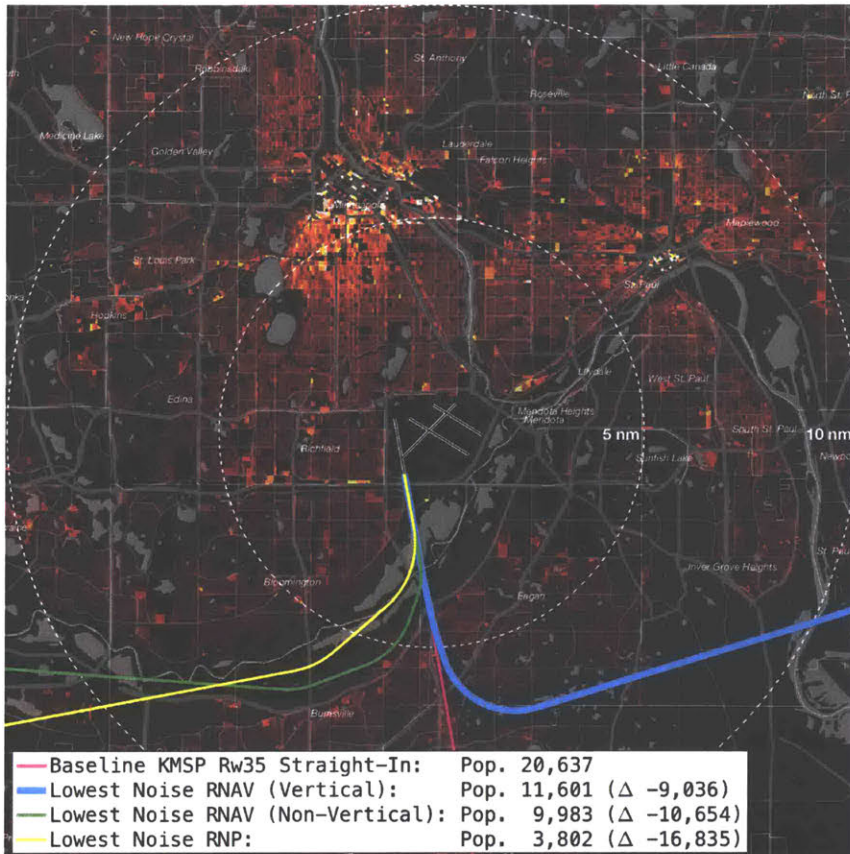


**Figure 60. MSP runway 35 noise-minimal procedure centerlines for RNAV with and without vertical guidance and RNP relative to a straight-in baseline (Boeing 737-800, 60dB L<sub>MAX</sub>)**

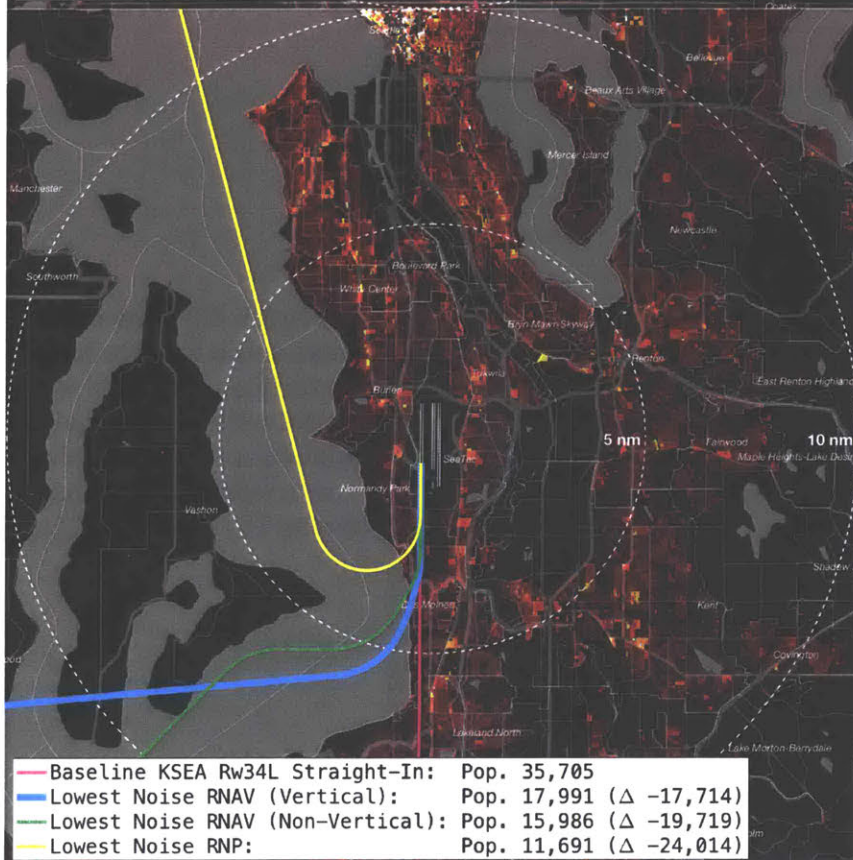


**Figure 61. SEA runway 34L noise-minimal procedure centerlines for RNAV with and without vertical guidance and RNP relative to a straight-in baseline (Boeing 737-800, 60dB L<sub>MAX</sub>)**



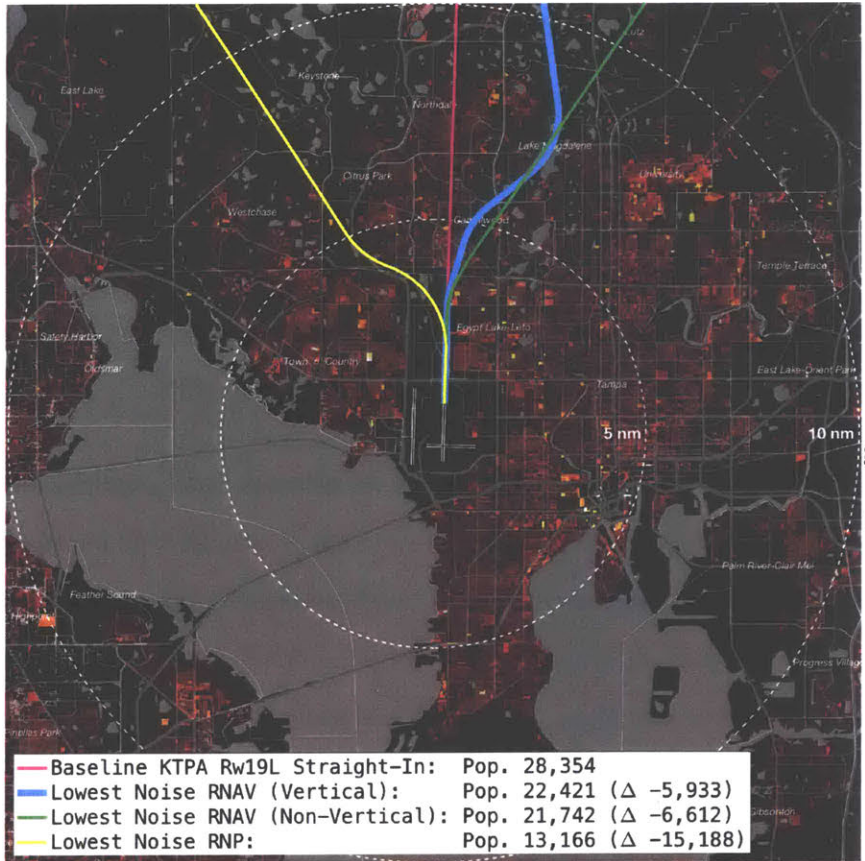


**Figure 62. TPA runway 19L noise-minimal procedure centerlines for RNAV with and without vertical guidance and RNP relative to a straight-in baseline (Boeing 737-800, 60dB L<sub>MAX</sub>)**

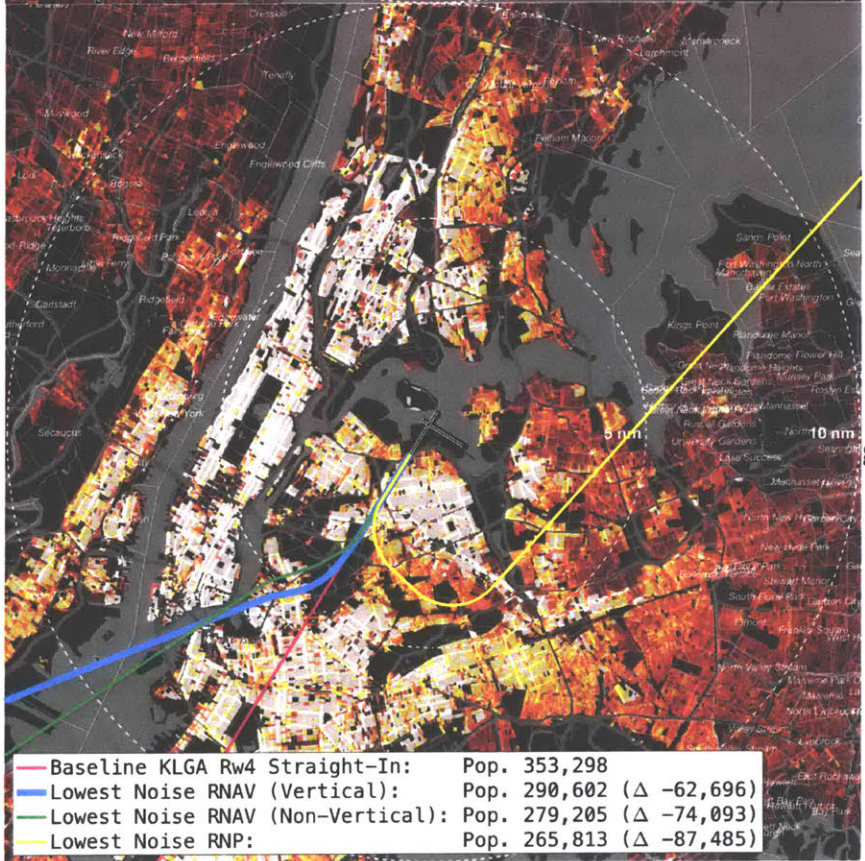


**Figure 63. LGA runway 4 noise-minimal procedure centerlines for RNAV with and without vertical guidance and RNP relative to a straight-in baseline (Boeing 737-800, 60dB L<sub>MAX</sub>)**

## 5.9 Evaluating System-Level Population Exposure Rollup

A first-order estimate of system-level benefit potential from PBN arrivals can be obtained by summing best-case population reduction potential for every jet operation at the OEP-35 airports over the period of a year relative to a straight-in baseline for each runway. This method does not account for operational constraints such as runway interactions, mixed equipage, and airspace integration. However, evaluating impact-reduction potential using actual operational counts and runway use statistics gives a preliminary best-case estimate for potential noise reduction from PBN.

In order to develop a cumulative benefit estimate for the OEP-35 airports, total daytime and nighttime operational counts for each airport were tabulated as a function of aircraft type based on ASPM single-flight records for the full year of operations. Each arrival was assigned to one of seven representative types according to the mapping shown in Table 1. Non-jet aircraft were omitted from the study. Runways were assigned based on ASPM hourly airport configuration records. For time periods with multiple active arrival runways, operations were assumed to split equally between active runways.

The metric used for evaluating system noise effects was the average daily person-event impact (PEI) reduction. This metric represents the net reduction in the number of noise exposure events above a target threshold (60dB daytime, 50dB nighttime) due to the implementation of modified procedures. The metric is the product of operation count and single-flight population reduction, as shown in Eq. 8.

$$PEI = \sum_{\text{airports}} \sum_{\text{runways}} \sum_{\text{aircraft}} \sum_{\text{ops}_{\text{day}}} \Delta P_{60} + \sum_{\text{airports}} \sum_{\text{runways}} \sum_{\text{aircraft}} \sum_{\text{ops}_{\text{night}}} \Delta P_{50} \quad \text{Eq. 8}$$

Where:

PEI = Total Person-Event Noise Impact

$\Delta P_n$  = Change in single-event population exposure at  $n$  dB  $L_{MAX}$  level for given airport, runway, and representative aircraft type

Summing PEI over all airports in the NAS for the full year of operations in 2017 normalized to an annual average day, the relative maximum noise benefits from PBN procedure implementation for all jet arrivals in the OEP-35 airports is shown in Figure 64.

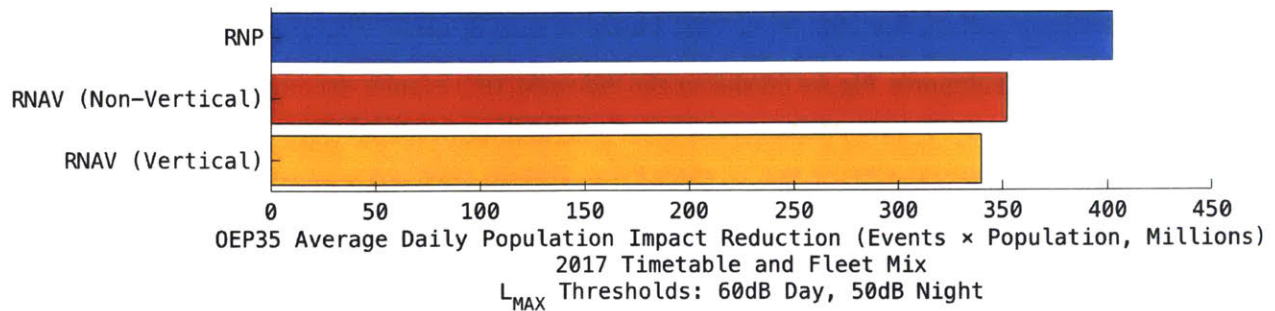


**Figure 64. System-level change in Person-Event Impact from implementing noise-preferred PBN procedures for every jet arrival at the OEP-35 airports in 2017**

This figure represents the hypothetical noise benefit that could be achieved if all aircraft flew noise-optimal approach procedures in the absence of any operational constraints or procedural interference considerations. It is important to note that operationally feasible noise reduction levels are smaller than what is shown in the figure due to the lack of non-criteria constraints imposed in this analysis.

The baseline system-level noise impact assuming straight-in arrivals at the OEP-35 airports is 691.9 million daily person-event impacts. Therefore, the reduction potential shown in this rollup analysis is very significant relative to the baseline. RNAV procedures with vertical guidance provide an overall PEI reduction potential of 49.1% relative to the baseline straight-in assumption. RNAV procedures without vertical guidance provide incremental benefits in terms of approach track flexibility, with an overall PEI reduction potential of 50.9% relative to the baseline. RNP procedures provide the most potential benefit, with a PEI reduction potential of 58.2% relative to the baseline.

From the results presented above, it is clear that the largest benefit on a system level can be achieved through the use of RNAV procedures with vertical guidance. This is encouraging from an implementation standpoint due to the high equipage and operational capability for these procedures in today's system. The incremental benefit occurring from sharper final approach intercept turns in procedures without vertical guidance is relatively small, with a larger jump in benefits occurring for RNP approach procedures.

The best-case roll-up benefits from PBN implementation occur disproportionately at several specific high-benefit airports. Figure 65 shows the PEI reduction results decomposed for each airport in the OEP-35.

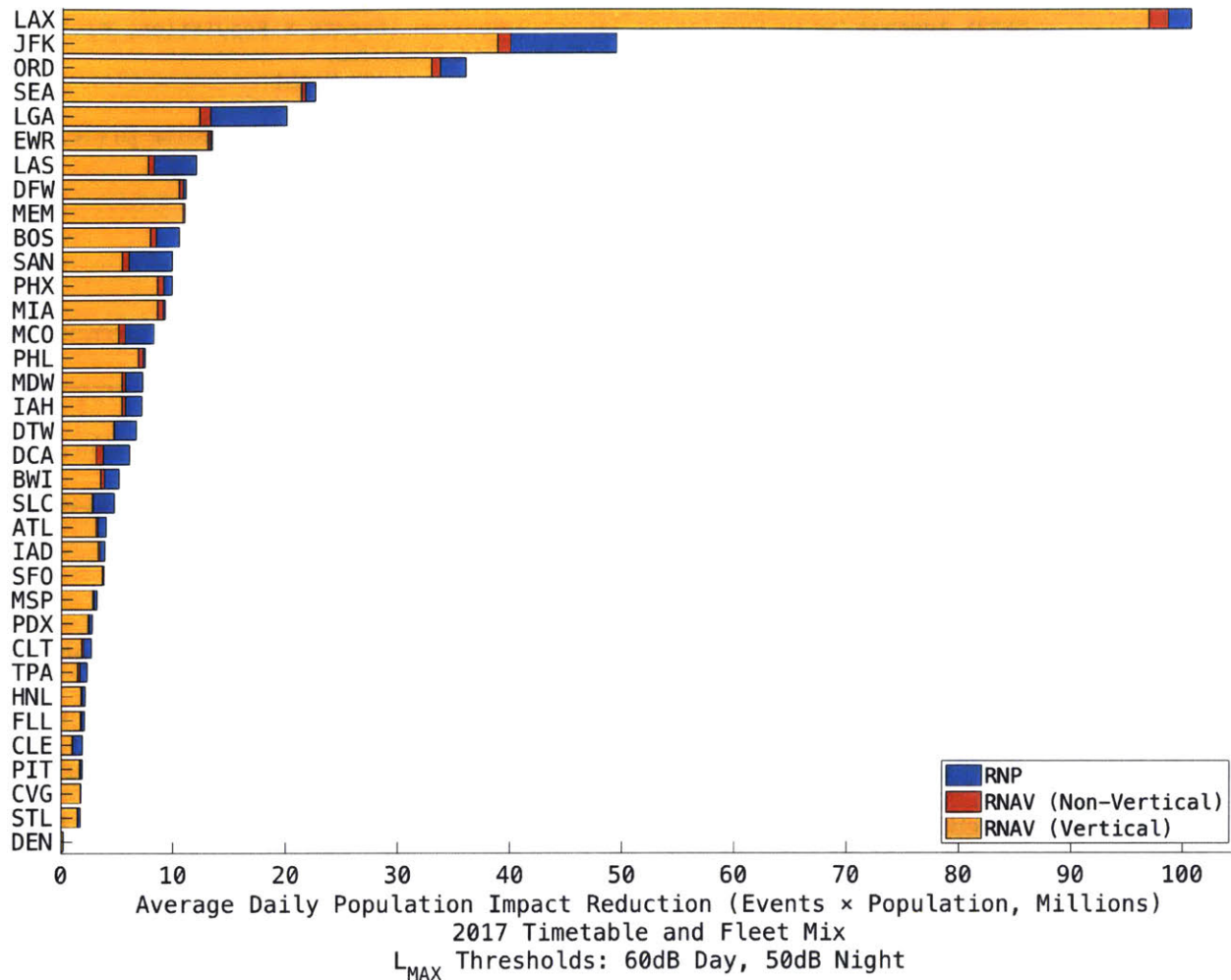


**Figure 65. Airport-level change in PEI from implementing noise-preferred PBN procedures for every jet arrival at the OEP-35 airports in 2017**

The noise reduction benefits are clustered at several specific airports. In terms of the RNP impact reduction metric shown in Figure 65, the top 4 airports alone account for 51.8% of the total benefit: 25.0% at LAX, 12.3% at JFK, 9.0% at ORD, and 5.6% at SEA. This large benefit arises because of a combination of the high volume of jet arrivals as well as magnitude of benefits on a per-flight basis. The policy implications of this ranking indicate system-level population impact reduction could be achieved most readily by focusing on several high-impact airports and runway ends. However, Figure 65 does emphasize that there are at least small potential benefits at all of the OEP-35 airports. Some

airports achieve the majority of potential benefit from RNAV alone (such as EWR), while others see large incremental benefits from RNP (such as JFK and LGA).

## **5.10 Approach to Tradeoff Evaluation in Procedure Selection**

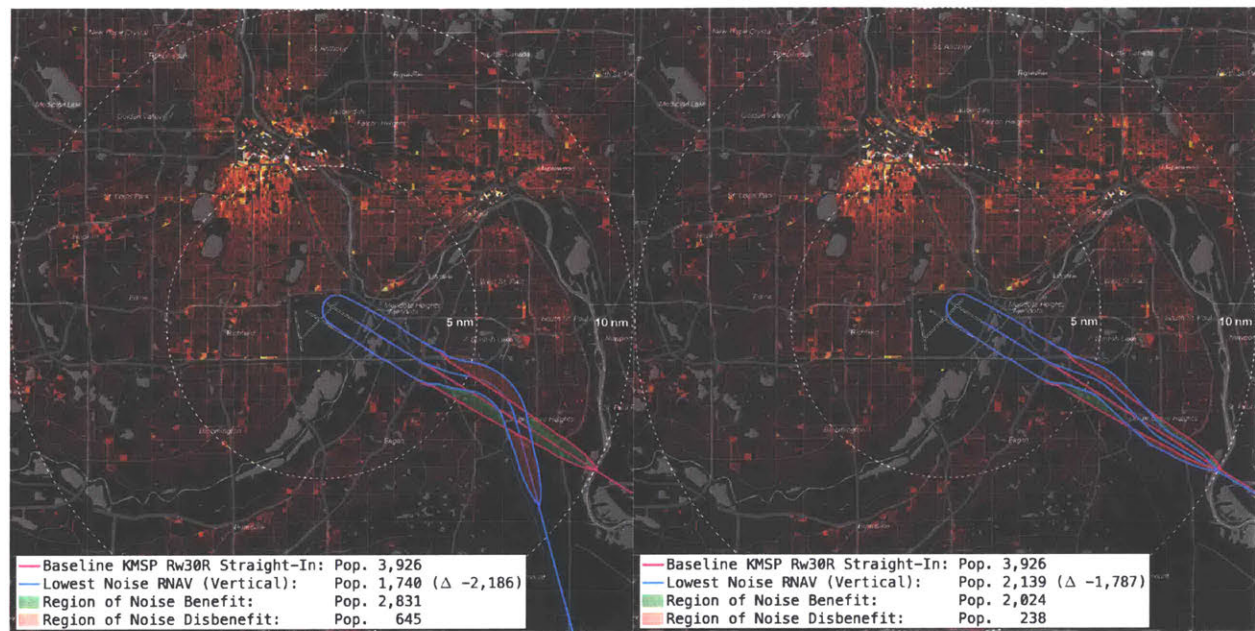
### **5.10.1 Population Benefit and Disbenefit**

The analysis presented thus far has used net population exposure reduction as the sole objective function. Of the set of possible procedure designs, the option with the lowest total population exposure is considered to be the preferred solution. However, in many cases the proposed modification results in new communities being exposed to noise. While the net impact may be beneficial because the number of people benefited by the change (i.e. those underlying the baseline straight-in procedure) are more numerous than those newly impacted, any noise shift has the potential to generate issues of equity.

It is desirable to consider the relationship between population benefit and disbenefit in the procedure design process. One metric for this purpose is the ratio of population count benefitted to the population count disbenefited by the procedure change. This ratio is a representation of population “leverage” – leverage ratios greater than one indicate that each newly-impacted person corresponds to at least one person benefited elsewhere. In order for a procedure modification to have a net benefit on population impact count, the leverage ratio must always be greater than 1. For a procedure with no newly-impacted population as a function of a procedure change, the leverage ratio is undefined.

Figure 66 shows an example of the impact of maximizing net population reduction compared to maximizing the benefit leverage ratio using the same guidance technology. The figure shows two approach procedure designs using RNAV with vertical guidance to MSP runway 30R. Figure 66(a) shows the procedure definition for maximum net population benefit, with a total population reduction of 2,186. This net benefit is comprised of 2,831 people who no longer receive noise at or above 60dB  $L_{MAX}$  compared to the baseline and 645 newly-impacted people. The corresponding population benefit leverage ratio is 4.39, meaning that each newly-impacted person corresponds to 4.39 people who benefit from the change. Figure 66(b) shows the procedure definition for maximum

population benefit leverage ratio, with a total population reduction of 1,787. This net benefit is comprised of 2,024 people who no longer receive noise at or above 60dB L<sub>MAX</sub> compared to the baseline and 238 newly-impacted people. The corresponding population benefit leverage ratio is 8.50, meaning that each newly-impacted person corresponds to 8.50 people who benefit from the change. The figure illustrates that it is possible in some cases to identify alternative PBN procedure designs with reduced net population benefit in exchange for an improvement in a secondary and desirable population impact metric.



**(a) Best for Net Population Reduction**      **(b) Best for Benefit Leverage Ratio**  
**Figure 66. Impact of maximizing net population reduction vs. benefit leverage ratio using RNAV procedures with vertical guidance for MSP runway 30R**

As could be reasonably inferred from the discussion above, some runway ends have a tradeoff continuum between net population impact reduction and benefit leverage. This tradeoff can be visualized as a Pareto set as shown in Figure 67 for MSP runway 30R. Dominant design points are highlighted in the figure. For each dominant design point, there is no alternative procedure that is preferable in terms of both net population reduction and population benefit leverage ratio. The highlighted Pareto optimal point #1 corresponds to Figure 66(a) while point #11 corresponds to Figure 66(b). Every marker shown on the scatter plot corresponds to a possible criteria-compliant RNAV approach procedure with vertical guidance for that runway.

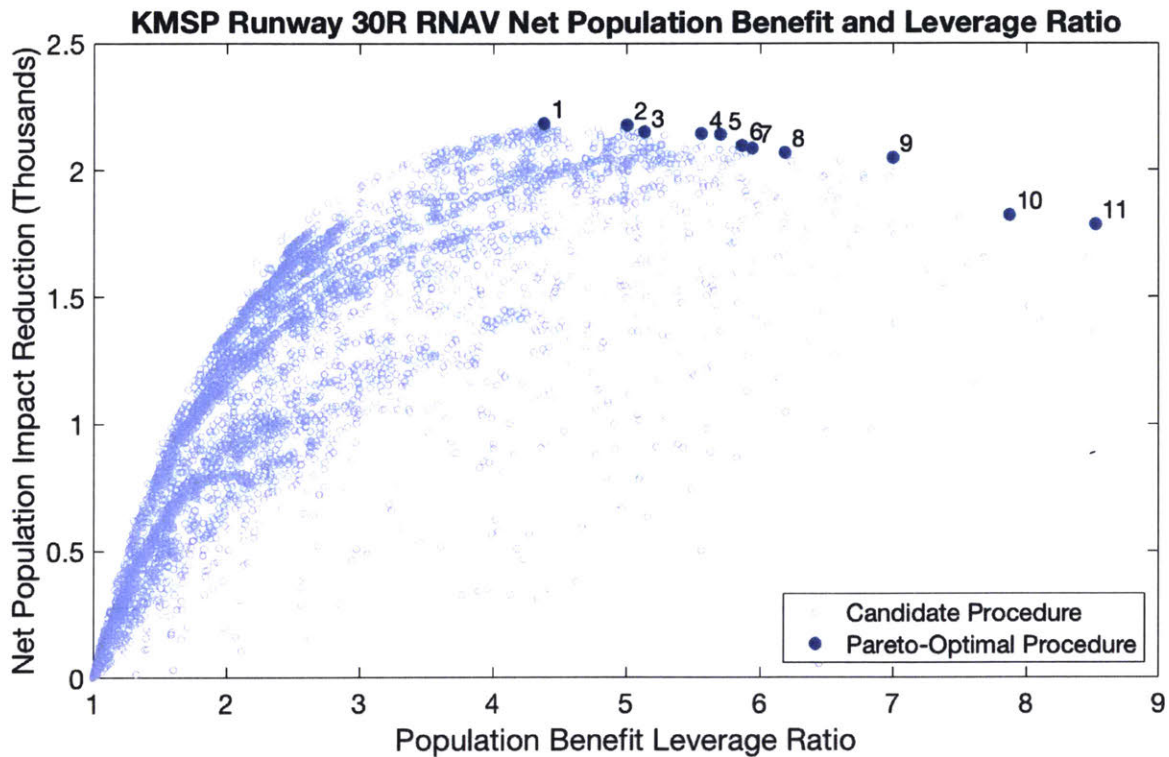


**Figure 67. Pareto set for the objectives of net population reduction and benefit leverage ratio for RNAV approaches with vertical guidance for MSP Runway 30R**

Figure 68 depicts each of the 11 members of the Pareto set for this runway. In this case, all of the Pareto set solutions involve a general track layout that crosses the extended final approach course from the left prior to an ultimate intercept from the right. The procedures with the greatest net population benefit are shown with thick lines, while those with the highest population benefit leverage are shown as thinner lines. While the procedure definitions in the Pareto set are similar, small changes in approach parameters do lead to tradeoffs in terms of population exposure redistribution. In general, the procedures with the highest population benefit leverage for this runway are those that do not differ drastically from the baseline straight-in configuration but instead use minor tweaks to avoid particularly noise-sensitive regions on the extended runway centerline.

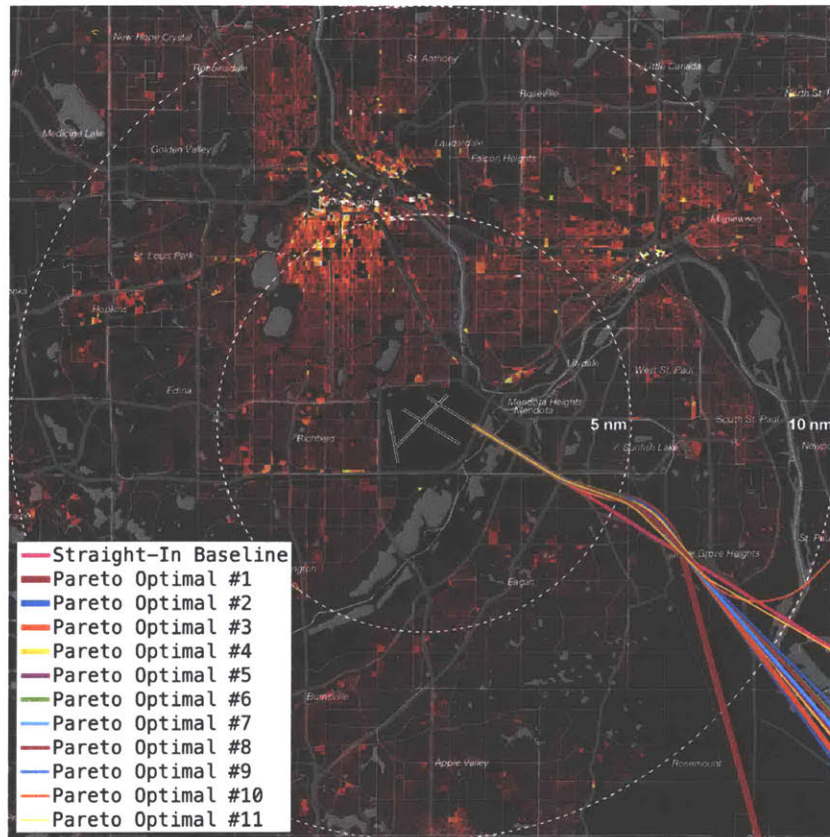


**Figure 68. Map view of set for the objectives of net population reduction and benefit leverage ratio for RNAV approaches with vertical guidance for MSP runway 30R**

Not all runway ends have a Pareto set of candidate procedures. In some cases, the same procedure definition maximizes both population reduction potential and population leverage for impacted populations. One such example is Runway 1L at Washington Dulles Airport. The full set of possible procedures with noise benefits is shown in Figure 69, along with the optimal procedure highlighted as Point #1. Figure 70 shows a map view of the procedure corresponding to Point #1.

The tradeoff figures shown below provide examples of visualizations that could potentially inform the procedure design process in the presence of uncertain or variable stakeholder objectives. When evaluating total population impacts, communities affected both positively and negatively by proposed changes can evaluate proposed solutions as well as feasible alternatives in the design space. Rather than an analyst presenting a single “best” solution based on assumed community preferences, presenting Pareto sets of candidate procedures allow for more comprehensive and balanced evaluation and screening process based on location-specific noise reduction objectives and political realities.



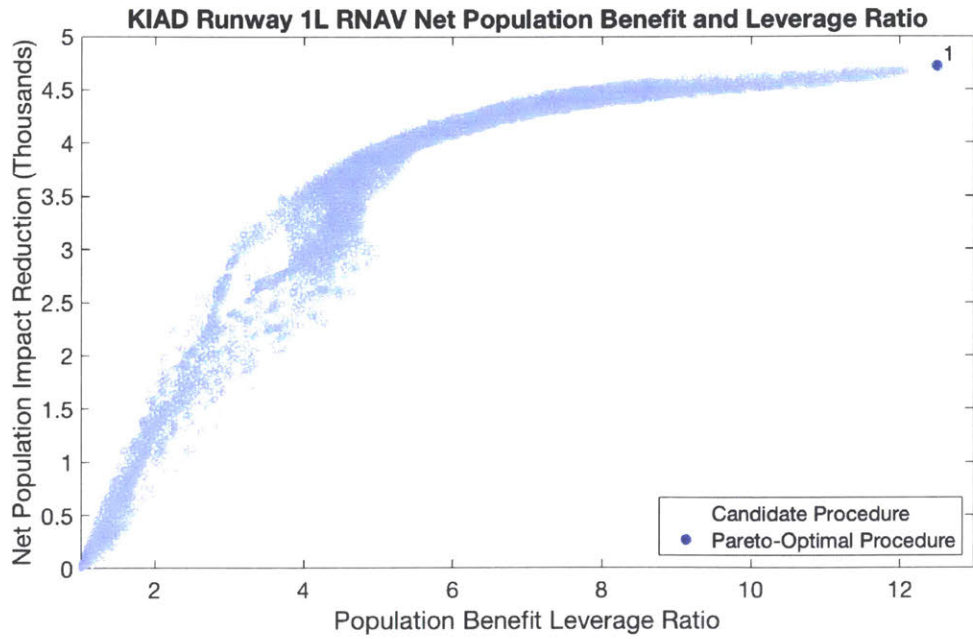


Figure 69. Pareto set for the objectives of net population reduction and benefit leverage ratio for RNAV approaches with vertical guidance for IAD runway 1L

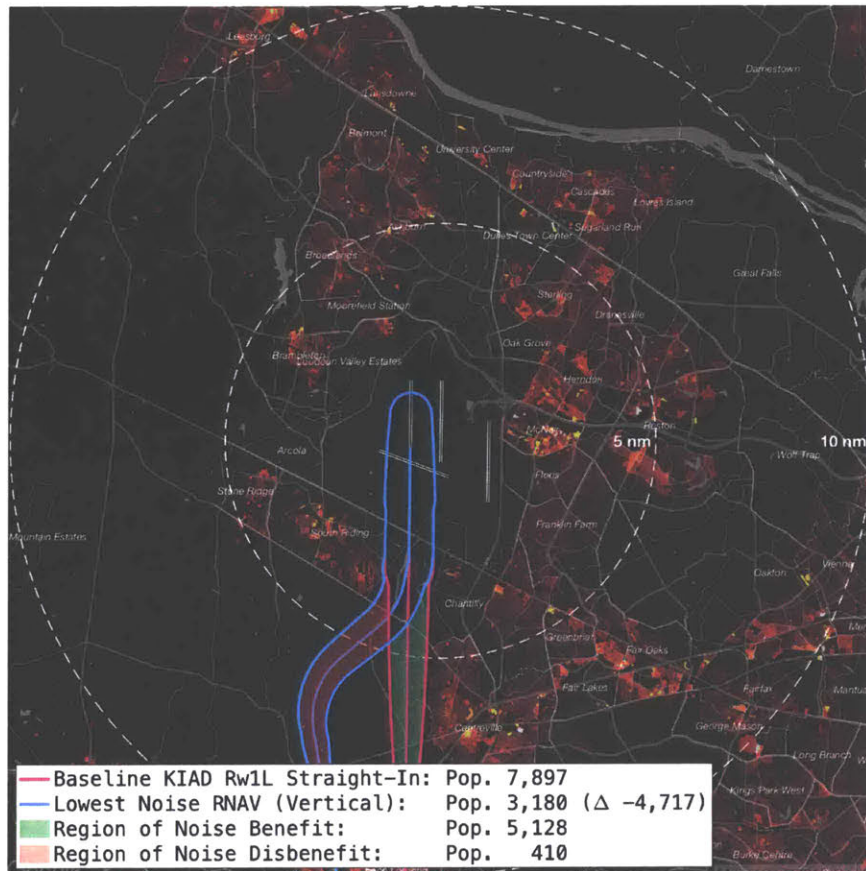


Figure 70. Map view of population and benefit leverage-preferred RNAV procedure at IAD runway 1L

### **5.10.2 Track Length Implications**

For operators, one of the key design objectives for PBN procedures is to reduce track length. Shorter track lengths result in reduced fuel consumption and flight time, both of which reduce total operating cost to airlines. In addition, reducing fuel burn provides environmental benefit in terms of emission reduction, reducing the overall climate impact on a flight-by-flight basis. Therefore, there may be a direct tradeoff between environmental objectives. Reducing noise at the expense of increased fuel burn has implications for air quality and climate change emissions. This illustrates the complexity of procedure design due to multiple competing objectives that may be mutually exclusive in terms of environmental and economic impact. Therefore, in noise-motivated procedure design efforts, analysis and consideration of competing tradeoffs is an important component of a multi-stakeholder procedure design framework.

Procedure track length is sensitive to the direction of a flight to the enroute transition waypoint. For example, an approach procedure that is optimized for arrivals from the south may be highly inefficient for arrivals from the north. In general, any new approach procedure interfaces with the enroute environment through standard terminal arrival routes (STARs) with one or more transition waypoints. At the airport system level, track length analysis requires data on the operational frequency for each STAR and transition. However, the types of issues that arise related to track length tradeoffs with noise can be illustrated using simplified hypothetical arrival transition waypoints. An example of such a tradeoff evaluation and visualization is provided in this section.

RNAV approaches with vertical guidance to MSP runway 30R are used below as an illustrative example of track-length tradeoff analysis. The same concept is readily applicable to other runways in the OEP-35. For this runway, arrivals from the east are generally aligned with the intended landing direction while arrivals from the west require a course reversal. Figure 71 shows the track length implications of RNAV redesigns for arrivals from two notional transition waypoints located 50 NM to the west and east of the airport. The notional transition waypoints are not intended to represent actual STAR waypoints, but rather to serve as illustrative examples of track length implications. For simplicity, the straight-in baseline is assumed to have a 15-mile final approach length preceded by a direct vector segment from the transition waypoint. Each candidate RNAV procedure is created with

the track generation method described in Section 5.1 and uses the same transition waypoint as its starting point. The result of this method is that each candidate procedure begins at the same location, diverges based on the parametric design space developed for noise reduction, and re-converges for the final approach segment prior to landing. Total track length is recorded for the baseline and each candidate procedure.

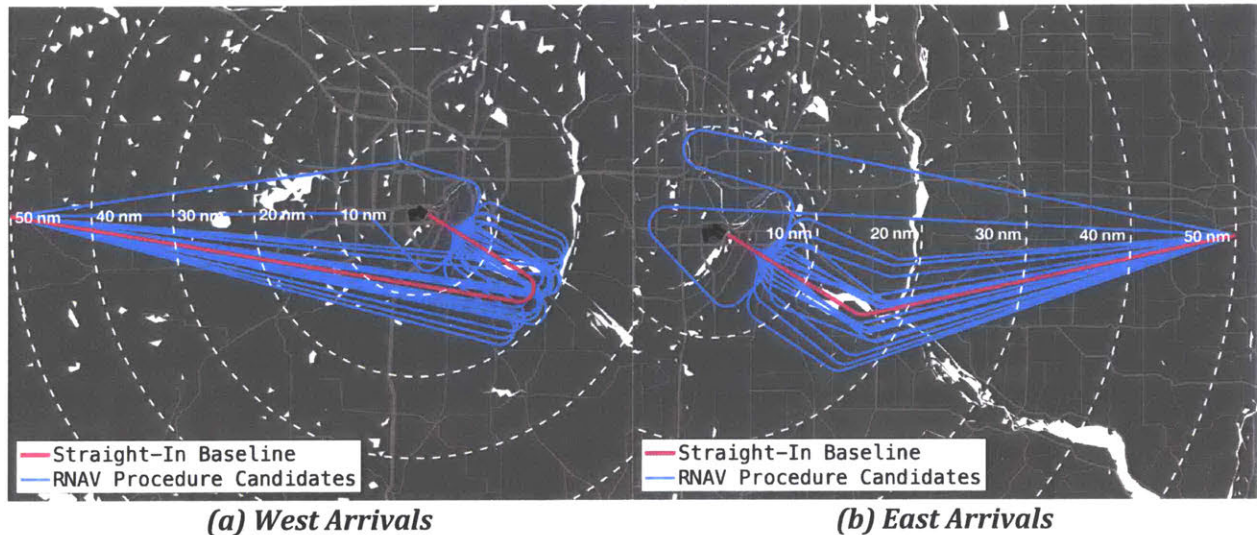


**Figure 71. Subset of RNAV procedure designs showing notional track length implications for lateral track redesign relative to a straight-in baseline**

The tradeoff between track length and noise exposure for MSP runway 30R for arrivals from the west can be visualized using a plot such as the one shown in Figure 72. Each marker represents an RNAV procedure candidate with noise reduction potential. Net population exposure reduction at the 60dB  $L_{MAX}$  level is shown on the vertical axis. Track distance in NM relative to the straight-in baseline is shown on the horizontal axis, where negative numbers indicate a track length reduction relative to the baseline. The Pareto set is shown with solid blue markers, representing procedures where no alternative exists with both lower noise and shorter track distance. Noise-beneficial RNAV approaches to MSP runway 30R have track length reduction potential as high as 17.8 NM if track length is the primary objective, corresponding to the leftmost Pareto set marker in Figure 72. The noise-optimal solution results in a track length reduction of 5.9 NM, corresponding to the rightmost Pareto set marker. The lateral tracks corresponding to the Pareto set in Figure 72 are shown in Figure 73. Each of the track definitions in the Pareto set is shown in blue, with the track length-optimal procedure definition highlighted in red and the noise-optimal procedure highlighted in yellow.

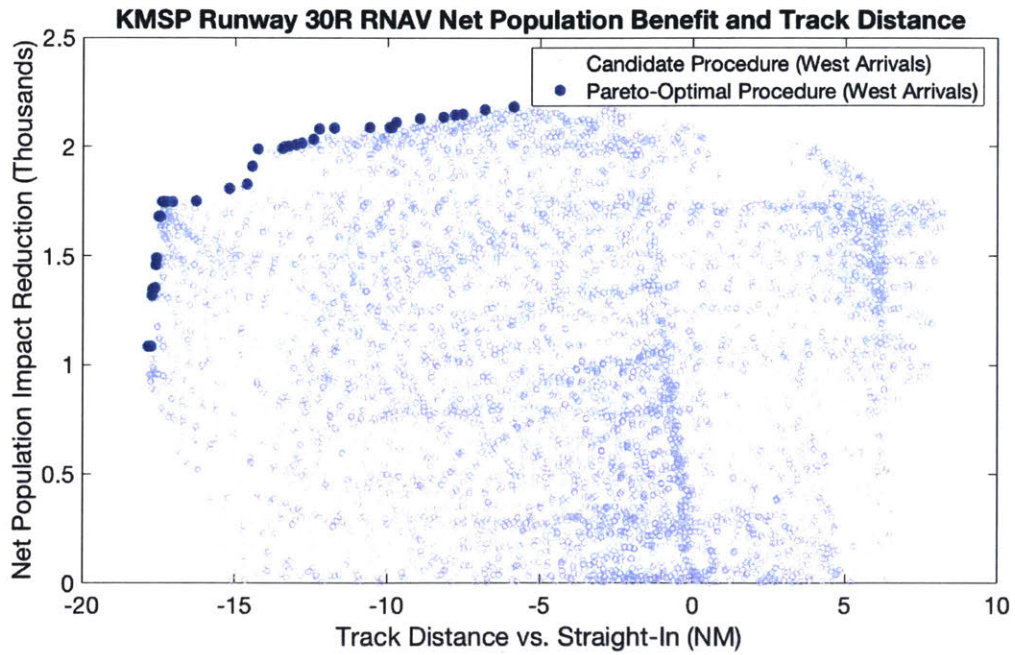


**Figure 72. Pareto set trading net population reduction (60dB L<sub>MAX</sub>) and track length reduction for RNAV approaches with vertical guidance for MSP Runway 30R (west arrivals)**

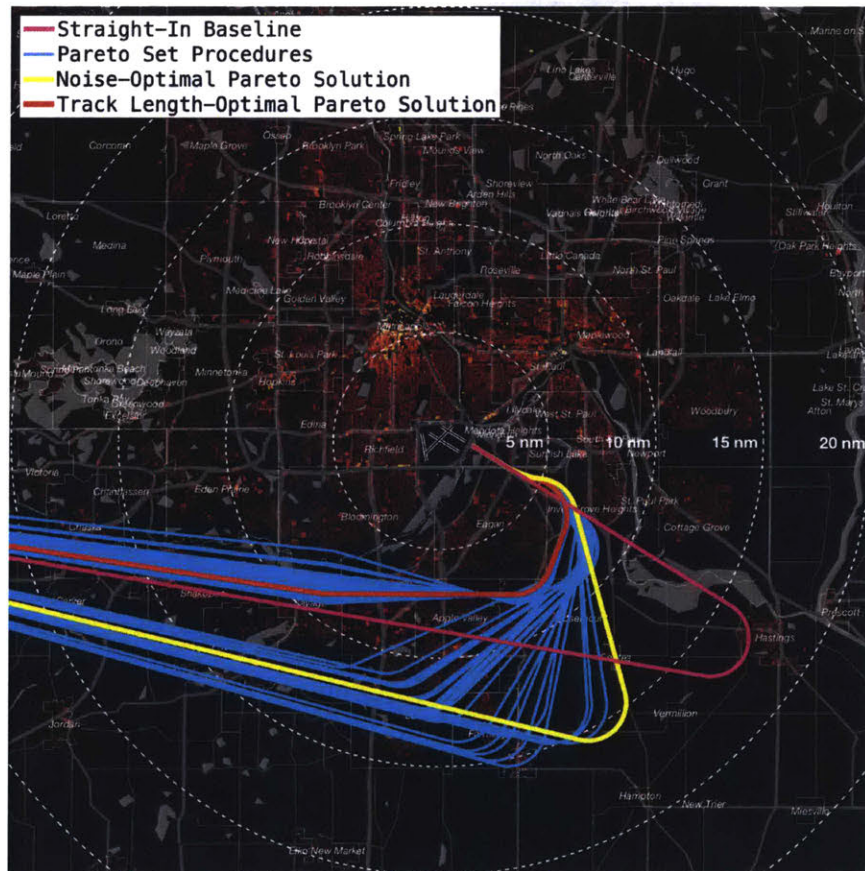


**Figure 73. Pareto set tracks for RNAV approaches with vertical guidance for MSP Runway 30R trading net population reduction (60dB L<sub>MAX</sub>) and track length reduction (west arrivals)**

Approaches from the east have lower track length reduction potential because the straight-in baseline is already near alignment with the arrival direction in that case. The maximum possible track length reduction without incurring a noise penalty is 2.6 NM. The noise-optimal solution requires a track length increase of 7.1 NM. The tradeoff scatter plot between track length and noise exposure for MSP runway 30R arrivals from the east is shown in Figure 74. While the figure shows that less track length benefit can be realized for easterly arrivals compared to westerly arrivals, it is clear that an opportunity exists to design procedures at this runway that have significant population exposure reduction without incurring a track length penalty compared to the baseline. The lateral tracks corresponding to the Pareto set in Figure 74 are shown in Figure 77. As for the westerly arrivals, each of the track definitions in the Pareto set is shown in blue, with the track length-optimal procedure definition highlighted in red and the noise-optimal procedure highlighted in yellow.

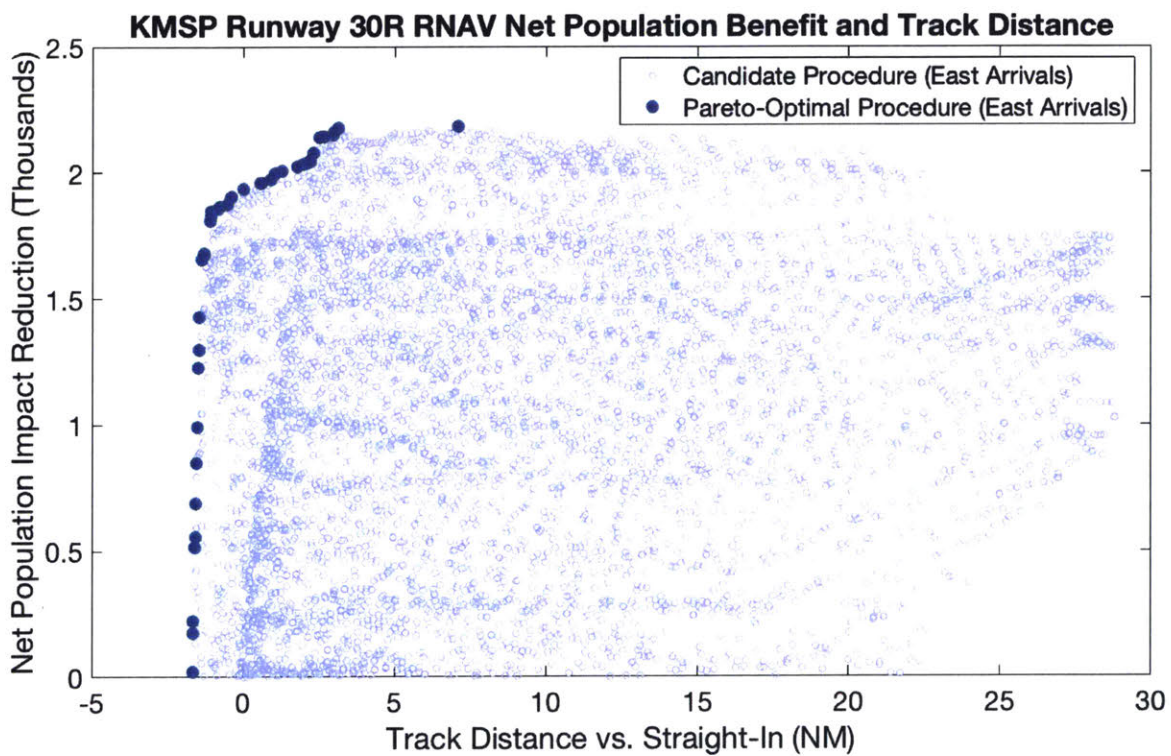


**Figure 74. Pareto set trading net population reduction (60dB  $L_{MAX}$ ) and track length reduction for RNAV approaches with vertical guidance for MSP Runway 30R (east arrivals)**

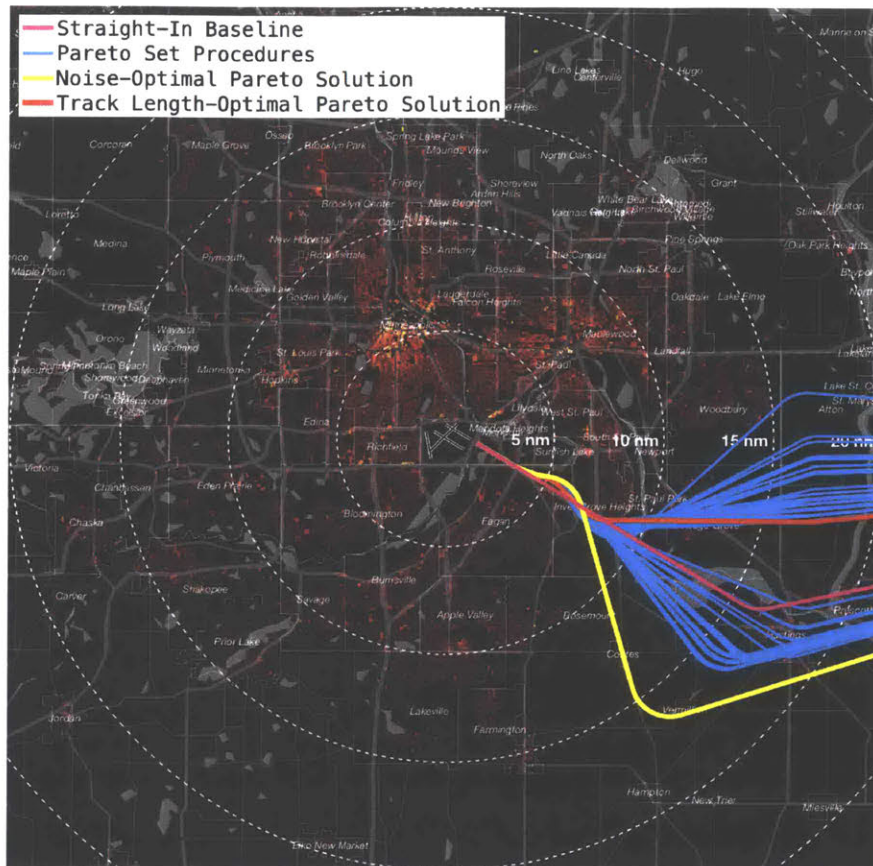


**Figure 75. Pareto set tracks for RNAV approaches with vertical guidance for MSP Runway 30R trading net population reduction (60dB L<sub>MAX</sub>) and track length reduction (east arrivals)**

The figures shown in this section for MSP runway 30R are illustrative examples, but the precise shape and characteristics of the Pareto set may vary substantially between runways depending on airspace configuration, procedure interactions, underlying population density, and STAR geometry for each airport. It is useful to present the array of potential solutions to impacted stakeholders on a location-specific basis to provide increased transparency on tradeoffs in the feasible design space.

Ultimately, it is evident that moving away from the absolute optimal solution based on one metric may yield substantial benefits in terms of another metric. This is a key component for effective procedure design evaluation and negotiation in a multi-stakeholder system. The tradeoff visualization methods introduced in this section also have potential application for metrics beyond population leverage and track length. Potential examples include trades between different noise metrics/thresholds, equity considerations, demographic data, emissions, procedure complexity, and runway throughput.

## **Chapter 6. System Noise Reduction Potential for Reduced Speed Departures**

Typical jet aircraft departures involve an acceleration to 250 knots shortly after takeoff. At this speed, the NASA ANOPP noise model indicates that, for modern aircraft, airframe noise dominates engine noise. By reducing departure climb speed to a level where airframe noise is similar to engine noise, total source noise can be minimized. Preliminary ANOPP results by Thomas (2017) indicate that the airframe/engine noise equivalence speed is in the vicinity of 220 knots for typical jet aircraft [129]. This result is highly sensitive to a clean-wing aerodynamic noise correction factor in ANOPP, which is based primarily on noise data collected from overflight measurement campaigns conducted by NASA in the 1970s. Therefore, the appropriate value of this correction factor may be different for modern airliners. The value of the clean-wing coefficient impacts the viability of speed control as a noise reduction technique, suggesting the need for experimental validation of modeled results. However, the physical drivers of speed-based noise reduction are clear – any uncertainty lies in the magnitude of the effect and the transition speed at which the effect becomes perceptible.

### **6.1 Technical Basis for Reduced Speed Departures**

Aircraft noise is generated by a combination of engine and airframe sources. Improvements in materials and engine design over the past several decades have significantly reduced engine noise. In older generations of aircraft, engines were the dominant noise source during departure. As engine noise has decreased, airframe noise has become more perceptible from the ground. Airframe noise arises due to turbulence in the airflow around components such as flaps and landing gear. Airframe noise is highly dependent on aircraft speed, with higher speeds resulting in higher noise levels. Airframe noise also increases when flaps are extended, speed brakes are used, and/or the landing gear is deployed [6].

In a typical jet departure, the aircraft accelerates on the runway and performs its initial climb segment at a predetermined takeoff thrust. The initial thrust level may vary based on aircraft weight, runway length, weather conditions, and other variables. During this initial segment, the aircraft climbs at an initial climb speed dependent on aircraft weight. Upon reaching a transition altitude, typically between 1,000 ft and 1,500 ft, the thrust is reduced to a climb setting and the aircraft accelerates to a target climb speed. The target climb speed is typically 250 knots, which is the maximum speed permitted below 10,000 ft in the United States. As the aircraft accelerates, the flaps are incrementally retracted until the wing is in its clean configuration [130]. Figure 76 shows a schematic of a typical departure profile.

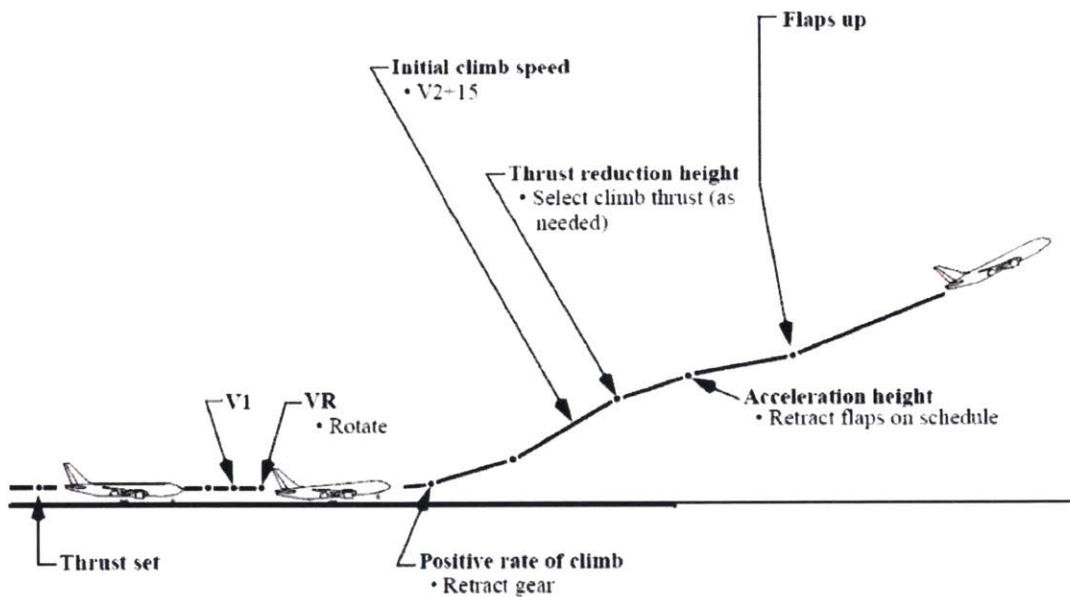


**Figure 76. Standard jet departure profile**

Noise model results indicate a strong interaction between aircraft speed and airframe noise. To demonstrate this effect, the departure profile shown in Figure 76 was modeled with a variable target climb speed ranging from 160 knots to 250 knots. For modeling purposes, thrust levels were held constant for each departure speed. Flaps were assumed to be configured as required for the target speed.

$L_{MAX}$  noise contours for the variable-speed departure profiles for a Boeing 737-800 are shown in Figure 77, illustrating the contribution of engine and airframe sources to the total noise contour at a range of climb speeds. At 160 knots, noise is dominated by engine sources. As the target climb speed



increases, airframe noise becomes more pronounced. At 220 knots, engine and airframe noise sources are similar under the departure path. At 250 knots, airframe noise is the dominant source. The transition from engine-dominated to airframe-dominated noise occurs in the range of 210 knots to 230 knots for each of three aircraft types examined in this analysis (Boeing 737-800, Boeing 777-300, and Embraer 170).

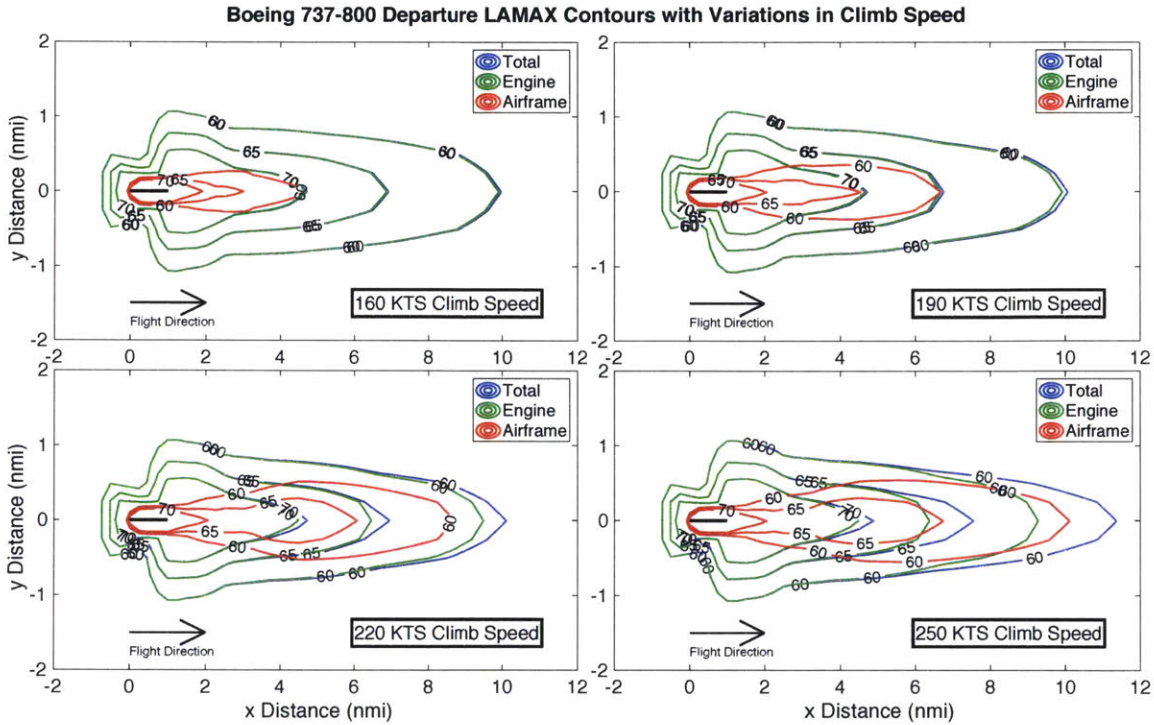


**Figure 77.  $L_{MAX}$  noise contours for a 737-800 departure with target climb speeds varying from 160 knots to 250 knots**

Figure Source: Thomas 2017 [129]

For an aircraft operating in the airframe-dominated noise regime, speed reduction results in a reduction of total noise. This presents an opportunity to reduce total noise for departing jet aircraft by setting a target climb speed that is lower than 250 knots, ideally near the transition speed where airframe and engine noise sources are of similar magnitude. Climbing near this transition speed provides the majority of the noise reduction benefit from reduced airframe source while minimizing operational impact.

The benefits from reducing departure speed occur from the initial climb thrust cutback point approximately 5 miles from departure to the point where the aircraft reaches 10,000 ft. This noise

reduction occurs primarily underneath the centerline of the departure flight track, which is where the RNAV track concentration effects are most pronounced.

The results in this chapter represent a system-level implementation of a 220-knot speed constraint on all jet departures following RNAV SIDs. For aircraft not capable of safe operation at 220 knots in a clean configuration, the minimum safe airspeed may be used.

## **6.2 Speed Limitations for Existing Departure Procedures**

Speed constraints are permitted in existing RNAV departure procedures “when necessary to ensure obstacle clearance, airspace efficiency during turns, or when necessary to achieve an operational advantage [131].” Speed constraints are sometimes applied to the first leg of a departure procedure to constrain obstacle protection area assumptions during the initial climb from the runway to a turn-at-altitude point. In other cases, the constraint applies beyond the initial climb segment of the procedure. A listing of existing RNAV departure procedures with speed constraints below 250 knots beyond the initial climb is shown in Table 21 based on an analysis of the May 2018 CIFP (see Section 3.2.1 for method). In some cases, the speed constraint applies only to specific runways or for specific waypoint sequences within a procedure.

**Table 21. Existing RNAV DPs with Speed Constraints**

<b>Airport</b>	<b>RNAV SID</b>	<b>Speed Restriction (Kts)</b>	<b>Airport</b>	<b>RNAV SID</b>	<b>Speed Restriction (Kts)</b>
102	LAKPT3	175	KGPI	KILLY1	230
KABQ	GRZZZ3	230	KIAH	GUMBY3	230
KABQ	JEMEZ3	230	KJYO	PTOMC2	210
KABQ	RDRNR3	230	KLAS	STAAV8	220
KBWI	CONLE3	230	KLAS	BOACH8	230
KBWI	FIXET2	230	KLAS	SHEAD1	230
KDAL	RAMBL5	230	KLGA	GLDMN5	220
KDAL	SNSET4	230	KLGA	HOPEA3	220
KDAL	EMMTT4	240	KLGA	JUTES3	220
KDAL	ESNYE4	240	KLGA	NTHNS4	220
KDCA	BOOCK3	220	KLGA	TNNIS6	220
KDCA	CLTCH2	220	KLGB	TOPMM3	210
KDCA	DOCTR4	220	KMMH	CROLI1	230
KDCA	HORTO3	220	KMMH	OENNS1	230
KDCA	JDUBB2	220	KPHX	IZZZO6	220
KDCA	REBLL4	220	KPHX	JUDTH6	220
KDCA	SCRAM4	220	KPHX	ZIDOG1	230
KDCA	SOOKI4	220	KSAN	ZZOOO2	230
KDCA	WYNGS4	220	KSBA	GAUCH1	210
KDFW	AKUNA7	240	KSFO	WESLA3	230
KDFW	ALIAN2	240	KSJC	TECKY3	230
KDFW	ARDIA6	240	KSLC	EDETH5	230
KDFW	BLECO8	240	KSLC	LEETZ6	230
KDFW	DARTZ7	240	KSLC	NSIGN5	230
KDFW	FORCK2	240	KSLC	PECOP5	230
KDFW	GRABE8	240	KSLC	TWF4	230
KDFW	HRPER3	240	KSNA	HOBOW2	210
KDFW	HUDAD2	240	KSNA	MIKAA1	210
KDFW	JASPA5	240	KSNA	PIGGN2	210
KDFW	KATZZ2	240	KSNA	STAYY1	220
KDFW	LOWGN8	240	KUKI	RONHU1	230
KDFW	MRSSH2	240	KUKI	RYPAX1	230
KDFW	NELYN5	240	L08	KUMBA1	220
KDFW	TRYTN3	240	L08	ZUNGU1	220
KDFW	WSTEX2	240	P13	IZTIR2	200
KDFW	ZACHH3	240	PANC	NOEND4	230
KELP	ATKNN5	220	TJPS	WLFRD2	230
KEWR	PORTT4	220	W43	LLADN1	230

Speed constraints are typically included in departure as a written notation on the chart, a graphical notation next to impacted waypoints on the plan-view depiction of a procedure, and as a flight management system database flag associated with the procedure. Examples of these notations are shown in Figure 78. Speed restrictions are typically motivated by minimum RNAV TF leg length

design criteria associated with assuming worst-case speed and wind conditions (see Section 4.1.1). However, similar constraints could be applied for noise mitigation reasons. For rapid implementation (or implementation on a trial basis), the speed constraint could be assigned by the tower controller as part of the takeoff clearance or the departure controller as part of the initial climb clearance.

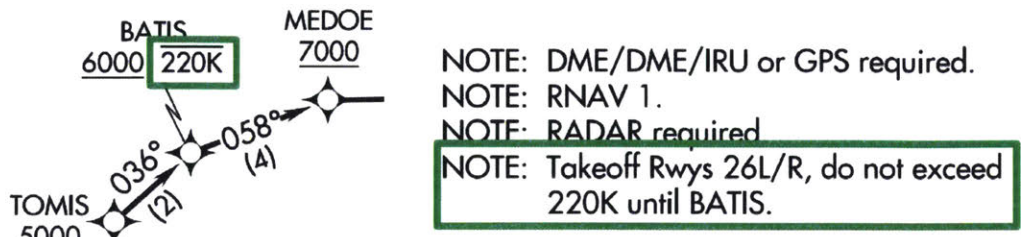


**Figure 78. Speed constraint notations on Las Vegas STAAV Eight RNAV SID**

The set of procedures with speed restrictions in current published departures indicates that reduced speeds are operationally feasible. While existing implementations of reduced speed departures appear to be motivated by minimum leg length considerations within RNAV design criteria rather than noise concerns, broader implementation for noise reasons have not been thoroughly evaluated in terms of implementation considerations or evaluated in actual operations.

### 6.3 Noise Modeling Approach for Reduced Speed Departures

The noise impacts of reduced-speed departures were evaluated using the rapid noise evaluation framework introduced in Chapter 3. Because any noise reduction from this procedure arises from speed-dependent aerodynamic source noise, NPD-based noise models such as AEDT cannot capture the relevant effects because they assume constant speed for the purpose of airframe noise modeling. This motivates the use of ANOPP as the noise model for reduced-speed departure analysis.

Reduced-speed departures were evaluated for noise impact on a straight-out climb procedure for three aircraft types representing a small jet (Embraer 170), medium-range narrowbody (Boeing 737-800), and heavy widebody (Boeing 777-300). The E170 and B737-800 were modeled at a 220-knot reduced speed climb, while the B777-300 was modeled at a 240-knot reduced speed climb due to performance constraints on that aircraft. All three aircraft types were also modeled with a 250-

knot baseline climb for comparison. The departure target speeds were selected such that each aircraft was in a clean configuration during climb.

The vertical profiles and thrust levels for each departure were calculated using the kinematic model introduced in Section 3.4. Figure 79 shows the climb profile modeled for the E170, Figure 80 shows the profile for the B737-800, and Figure 81 shows the climb profile for the B777-300. In all cases, the output noise contours from ANOPP were processed using the contour half-width method described in Section 3.5.3 to enable rapid noise evaluation on multiple track centerlines throughout the NAS. This analysis was conducted for contours at the 60dB  $L_{MAX}$  noise level to capture annoyance at a representative level for daytime departure procedures, consistent with the discussion of other procedures in this thesis.

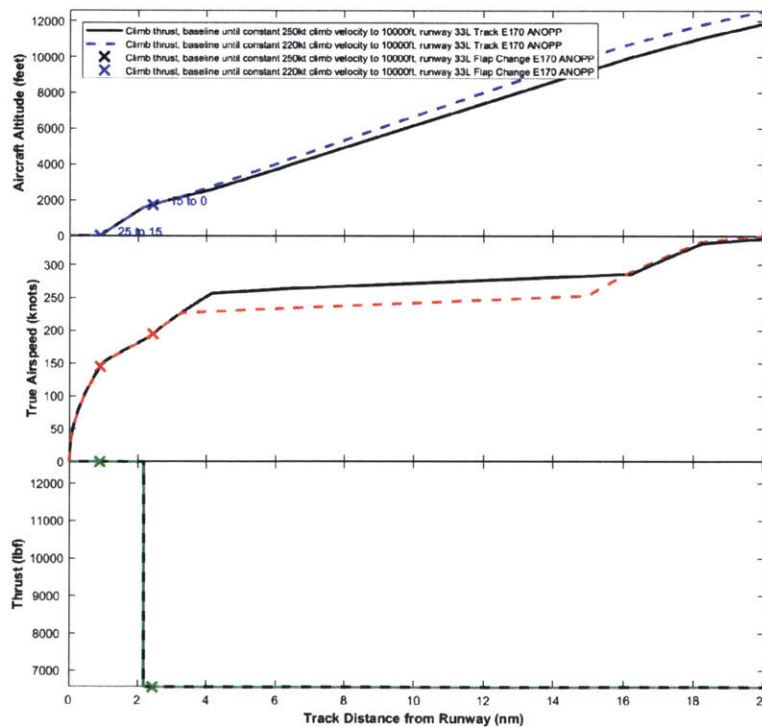


**Figure 79. Reduced speed departure profile for the Embraer 170 with speed target of 220 Knots Indicated Airspeed**

Figure Source: Thomas 2017 [129]

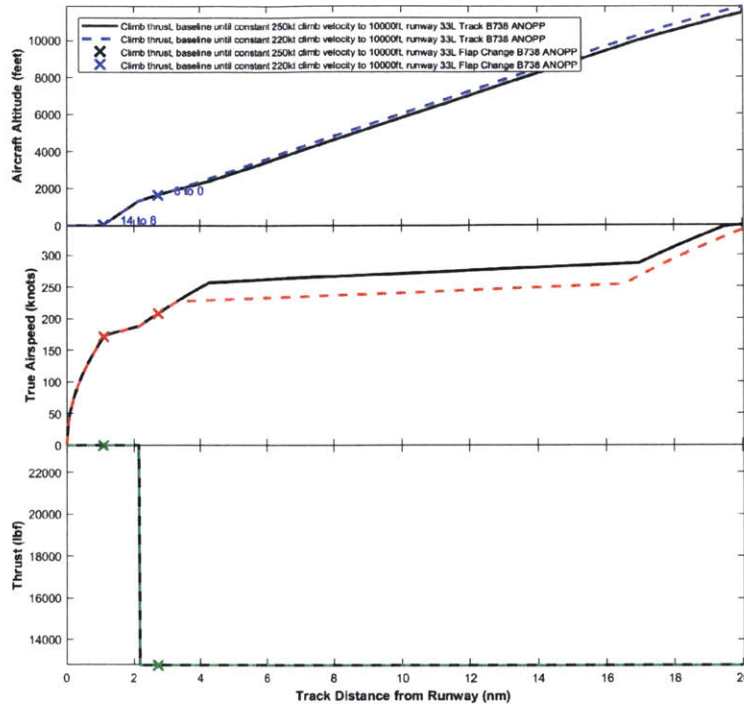


**Figure 80. Reduced speed departure profile for the Boeing 737-800 with speed target of 220 Knots Indicated Airspeed**  
 Figure Source: Thomas 2017 [129]

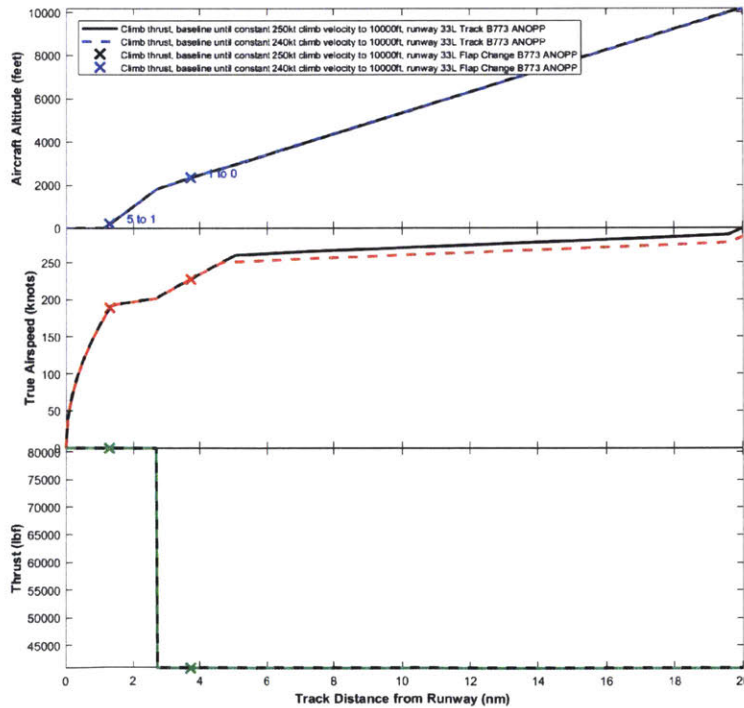


**Figure 81. Reduced speed departure profile for the Boeing 777-300 with speed target of 240 Knots Indicated Airspeed**  
 Figure Source: Thomas 2017 [129]

Noise contour half-widths for the 60dB  $L_{MAX}$  level are shown in Figure 82. The primary benefits occur under the centerline of the departure flight track. Benefits at the 60dB level occur between 5 NM and 20 NM from the start of takeoff roll, depending on the aircraft type. Under a reduced-speed departure, contour width remains constant or is reduced while contour length is contracted relative to the baseline case. Noise is unchanged in the first several miles of the climb procedure because the initial acceleration profile from liftoff speed to target climb speed is the same for both standard and modified procedures.

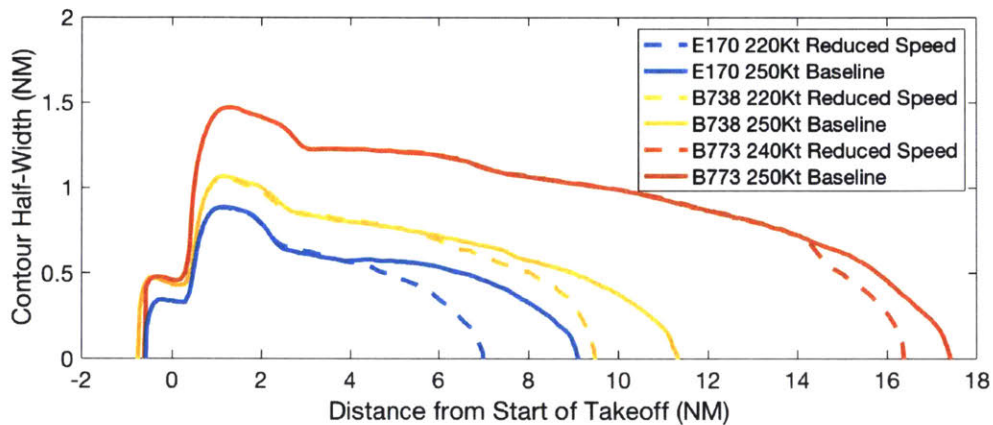


**Figure 82. 60dB  $L_{MAX}$  contour half-widths for reduced speed departures**

ANOPP outputs indicate that the procedure modification is either noise-neutral or beneficial at all  $L_{MAX}$  levels, including thresholds higher and lower than the 60dB  $L_{MAX}$  value used for impact analysis in this thesis. The benefits for 70dB  $L_{MAX}$  are shown in Figure 83. Noise contour geometry is unchanged for the E170 at the 70dB  $L_{MAX}$  level because the aircraft is still below 220 knots at that early stage of the climb profile for both baseline and modified speed concepts.

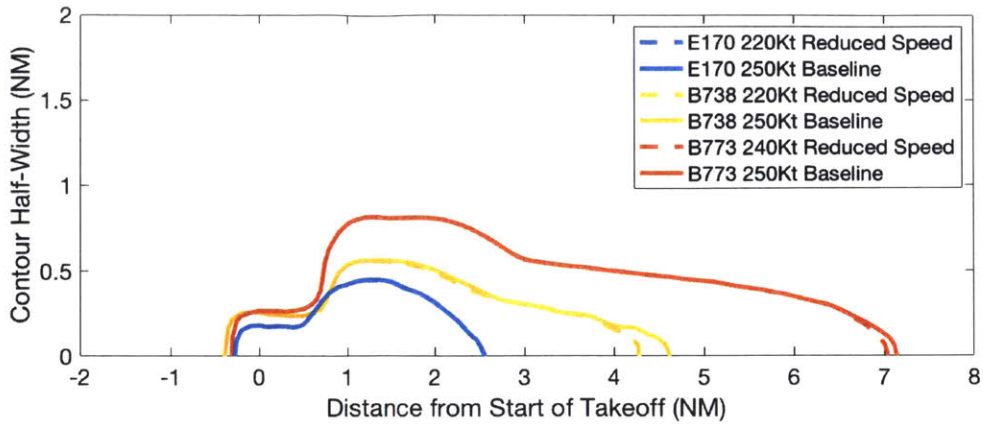


**Figure 83. 70dB L<sub>MAX</sub> contour half-widths for reduced speed departures**

The reduced-speed departure contours were evaluated in comparison to the 250-knot baseline departures for each published RNAV SID in the NAS. The procedure centerlines were derived from the May 2018 CIFP. Each enroute transition route was evaluated to ensure full coverage of all departure routes used by jet aircraft at airports where RNAV SIDs are implemented. In some cases, multiple transitions share the same common initial procedure definition. Noise results for procedure sharing common initial routes are reported as single unit to prevent redundancy.

## 6.4 System Noise Reduction Analysis for Reduced Speed Departures

The reduced-speed departures were applied to all RNAV SID procedures currently published in the NAS assuming a baseline speed of 250 knots for comparison purposes. The highest-benefit procedure identified using this method was the GLDMN Five RNAV SID from Runway 13 at LGA, shown in Figure 84. The procedure serves as an example of the analysis method and potential noise benefits for densely-populated areas, although the baseline procedure already contains a 220 knot speed restriction for operational reasons so the noise-related advantages of reduced speed are already realized in this case. The noise benefits relative to a 250-knot baseline are shown in Figure 85.



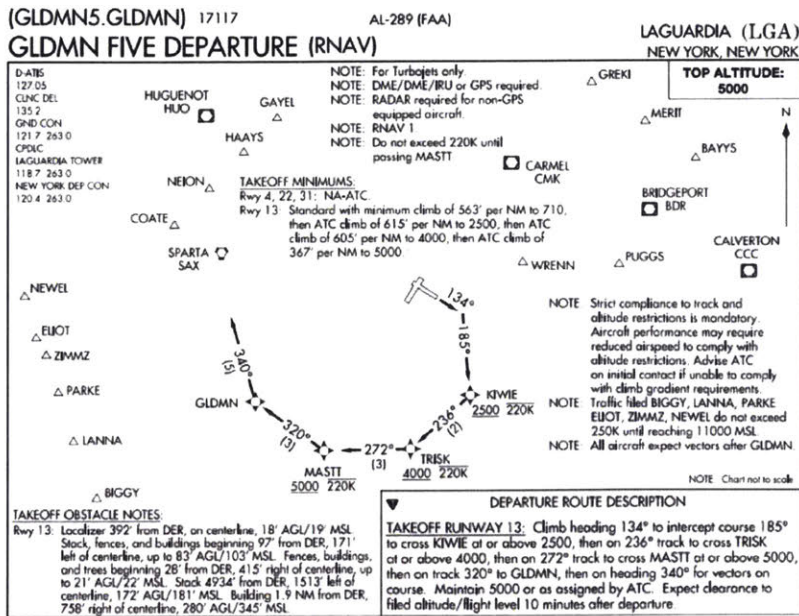


Figure 84. GLDMN Five RNAV SID from Runway 13 at LGA



Figure 85. B737-800 noise benefits from a reduced-speed departure on the GLDMN Five RNAV SID from LGA runway 13 (60dB L<sub>MAX</sub>)

While the reduced-speed departure principle could be applied to any departure, benefits may be the most apparent underlying published RNAV SID procedures. Because of the higher navigation

precision enabled by RNAV guidance, track concentration is highest under this type of procedure relative to other conventional and vector-based departures. Therefore, benefits on a single-flight basis are compounded for communities underlying the track centerline of RNAV SIDs.

Aside from the high outlier benefit level for the GLDMN Five RNAV SID at LGA with an impact level of nearly 1.4 million fewer noise impacts per day, the next tier of procedures cluster at benefit levels between 100,000 and 300,000 noise impacts per day. In all cases, the noise benefit from reduced-speed departures depends on population density underlying the track centerline at track distances between 5 NM and 20 NM. For example, most of the New York area departures that involve over-land departure routing (in addition to the GLDMN Five already shown in in Figure 85) have significant potential benefit from reduced-speed departure. Figure 86 shows the PORTT Four RNAV SID from EWR runway 22R following the ELIOT transition. This departure procedure overflies the densely-populated suburbs of northern New Jersey, so the contraction of the 60dB  $L_{MAX}$  contours results in a single-flight population reduction of 11,113 people at this level.

If the modeled noise benefits are proven accurate through flight trial validation, the implications are particularly useful for locations where lateral track modifications would shift noise onto other sensitive communities. Reduced speed departures have noise benefit under the baseline flight track centerline without increasing noise for other nearby communities, resulting in a situation where no population is exposed to new noise as a result of the change. Therefore, the concept has particularly strong application potential for communities where shifting flight tracks is politically difficult. For example, departures from BOS runway 33L overfly noise-sensitive areas with dense populations regardless of track selection. Figure 87 shows that 220-knot B737-800 reduced-speed departures on the PATSS5 RNAV SID from Runway 33L have single-flight population reduction benefits of 23,114 people without any communities adversely impacted.

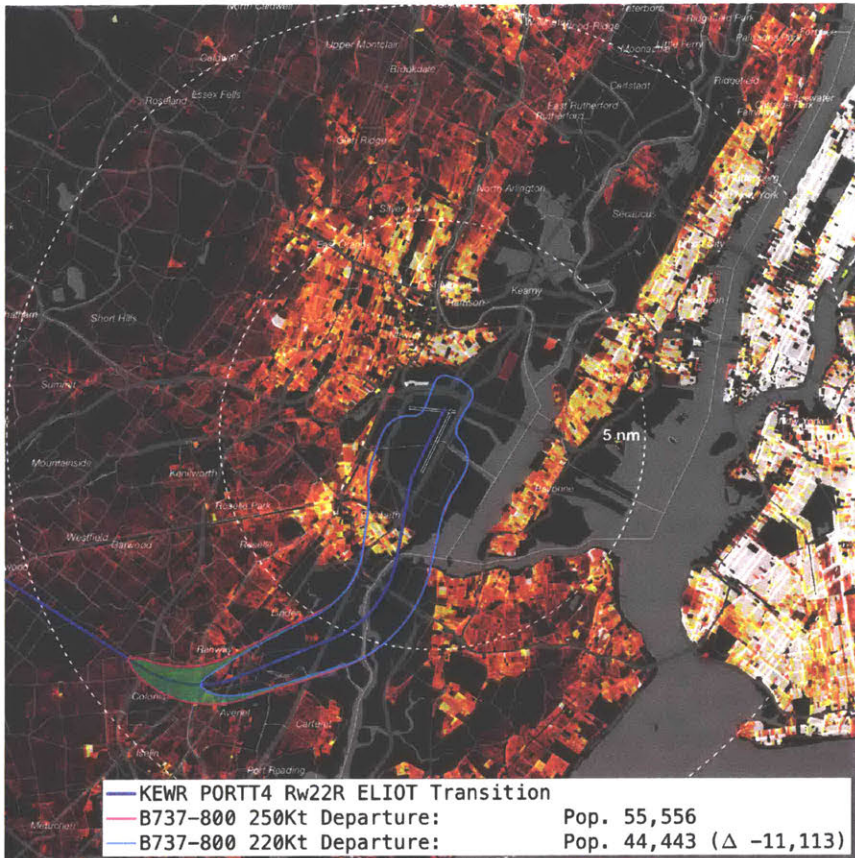


**Figure 86. B737-800 noise benefits from a reduced-speed departure on the PORTT4 RNAV SID from EWR runway 22R, ELIOT Transition (60dB L<sub>MAX</sub>)**

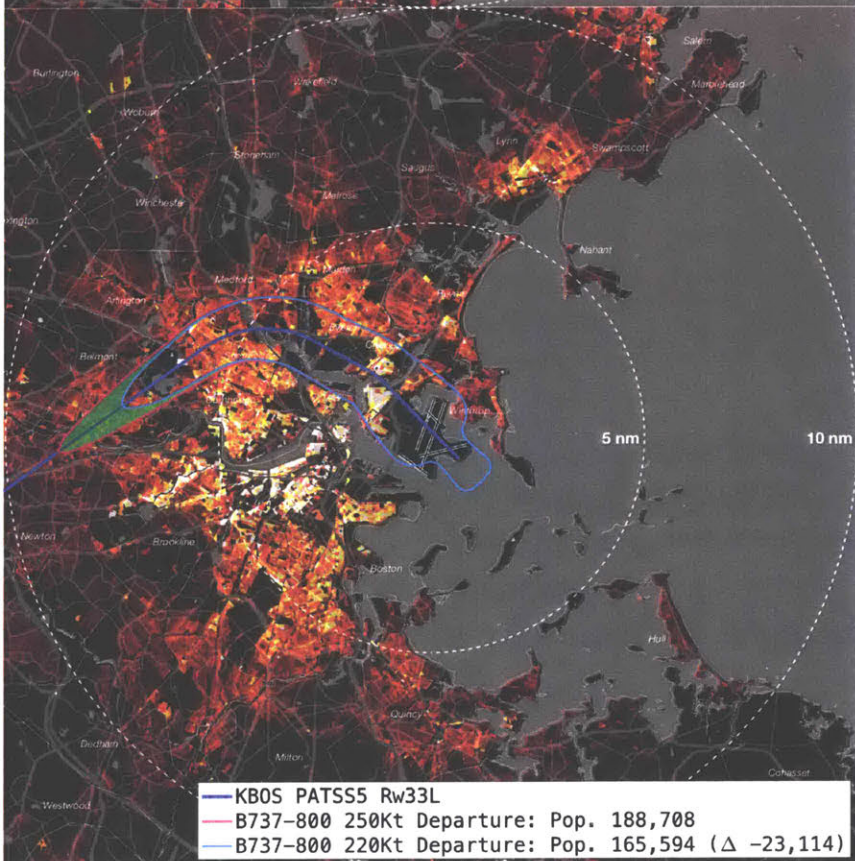


**Figure 87. B737-800 noise benefits from a reduced-speed departure on the PATSS5 RNAV SID from BOS runway 33L (60dB L<sub>MAX</sub>)**

In order to evaluate the potential system-level application for reduced-speed departures, the lateral track for each RNAV SID published for the OEP-35 airports was determined from the May 2015 Coded Instrument Flight Procedures as described in Section 3.2.1. Tracks were considered for every departure runway and enroute transition waypoint to ensure full analysis coverage of RNAV departure routes. This results in 1590 total departure tracks for noise evaluation.

Figure 88 shows distribution of population reduction at the 60dB level for the B737-800 as a function of the total departure rate from the runway designated for that SID. No attempt was made to quantify the exact number of aircraft using each SID or transition. The raw noise results for the 200 highest-benefit procedures in terms of PEI reduction for the B737-800 at the 60dB level are tabulated in Appendix C.

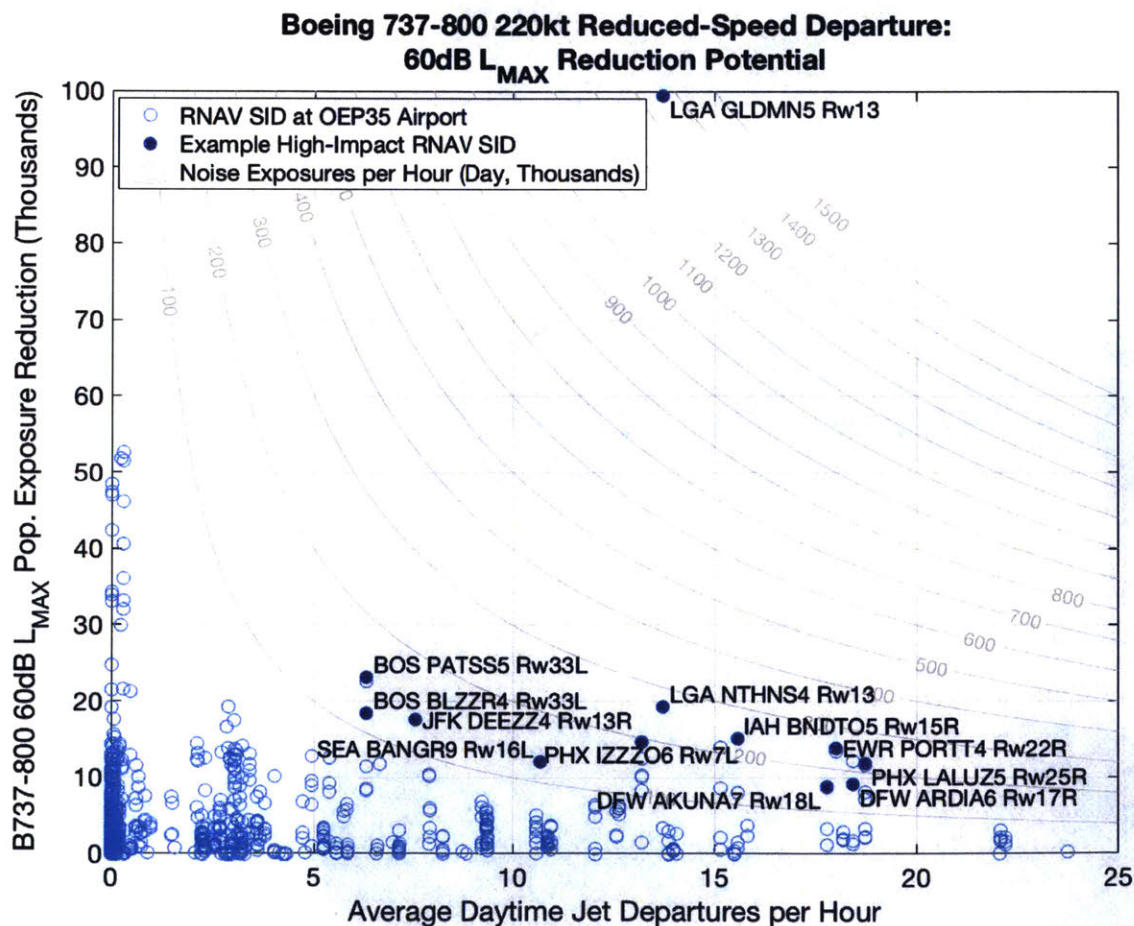


**Figure 88. B737-800 60dB  $L_{MAX}$  noise reduction potential from reduced speed departures as a function of average 2017 daytime jet departure frequency from the associated runway**

## **Chapter 7. Framework for Noise-Reduction Procedure Development**

According to modeling and analysis, there are clear potential noise benefits from the implementation of advanced operational procedures at airports in the NAS. However, operational implementation of these procedure concepts requires consideration of the concept system dynamics underlying procedure implementation in the NAS. This implementation process must consider constraints, objectives, and values for a variety of system stakeholders, including communities, airlines, air traffic controllers, airport operators, and regulators. The analyst must integrate the complex, and often inconsistent, objective set to present coherent and useful information for both communities and operational stakeholders.

This chapter presents a framework that describes the sociotechnical system dynamics involved with flight procedure modification motivated by noise reduction objectives. The framework involves modeling baseline procedure and noise conditions, community reaction and organization processes, proposed action development and refinement, and implementation procedures. Arrival and departure procedure design involves many stakeholders whose objectives must be incorporated into proposed actions by an analyst, who also serves the role of communicating impacts of proposed actions and incorporating feedback. The system involves interacting components that are both technical and political. It is an example of a multi-stakeholder system subject to multiple stakeholder desires and no singular objective function or end state.

This framework illustrates the role of the noise and procedure analyst in the iterative design process as integrator of stakeholder objectives. The objectives and constraints emphasized by each stakeholder group may be unclear or inaccessible to others. In many cases, there is no direct line of communication allowing input and feedback during the design process. For example, community noise groups may be unaware of detailed design parameter restrictions or aircraft performance limitations that influence the solution space while detailed procedure designers may not be aware of

community flexibility of or sensitivity to potential modifications for operational reasons. For the procedure analyst in this framework, feedback from the community, regulators, operational stakeholders, and baseline physical environment provide insight in generating an assumed design objective. This assumed design objective drives each iteration of procedure design.

This framework builds on past work developing models and frameworks for multi-stakeholder system dynamics and air transportation system modeling. Growing concern with the procedure development process and the impact of new PBN procedures on the airport noise environment suggest that current information flows do not sufficiently integrate stakeholder objectives in this process. In short, existing system dynamic models do not address the need for stakeholder input and integration in the specific constraint space of flight procedure design. The conceptual framework introduced in this chapter serves as an aspirational model for the integration of community input with technical design constraints to harness the potential flexibility of RNAV, RNP, and other advanced procedures in a manner that includes and incorporates feedback from all involved parties.

## **7.1 System Dynamic Model for Noise-Motivated Procedure Development**

The airport noise problem incorporates elements of both change propagation models and multi-stakeholder system dynamic models. An integrated framework incorporating the key processes and constraints for noise-motivated procedure development is shown in Figure 89.

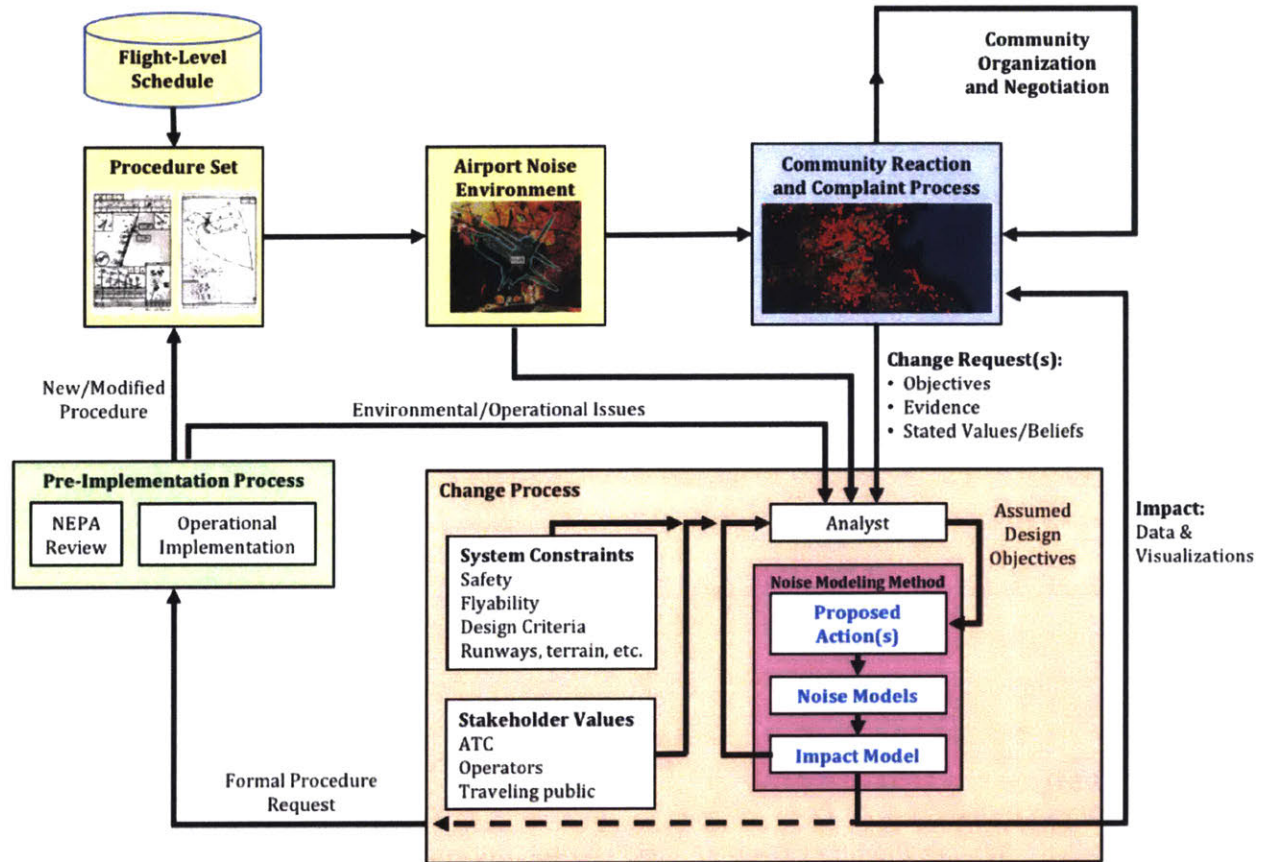


**Figure 89. System dynamic model for noise-motivated procedure development**

The complexity of the procedure design and evaluation process prevents efficient closed-form optimization formulations, particularly due to the lack of clear equity and desirability metrics for all impacted communities. Proposed procedure designs must comply with design constraints and remain operationally compatible with existing procedures. Noise results from this candidate set feed forward to impact quantification and visualization for use by impacted stakeholders, allowing iterative evaluation and feedback from communities rather than assuming *a priori* valuation schemes. Such a framework, if applied in a manner transparent to all stakeholders, can be used as a central component of a consensus-based procedure redesign process.

There are four key elements of the framework presented in this chapter:

1. The baseline noise environment around the airport, itself a function of the flight procedures in use as well as the flight-level schedule (number of flights, timetable, aircraft types, and other factors that impact flight volume on each runway)

2. Community reaction to the airport noise environment, including perception, annoyance, organization, and negotiation functions within community sub-groups
3. Change development process, where an analyst integrates objectives and feedback from a diverse set of stakeholders in the context of community noise concerns to develop noise reduction operational modifications
4. Pre-implementation process where formal development of operational procedure definitions and environmental regulation compliance checks are performed. This process leads to procedure implementation and use.

The next sections of this chapter present context for operations in the NAS and the opportunity space for procedure designers. The processes within the procedure design framework shown above are presented in this context.

## **7.2 Baseline Conditions**

Community requests for flight track review and modification may arise from repeated noise exposure due to flight procedure location, operational volume, runway and procedure use, and other factors impacting flight patterns at an airport. Change requests can be associated with general noise impact (“too many airplanes”) or may consist of specific operational requests regarding the baseline conditions (specific procedure definitions, flight-level schedule and/or times of operation, or runway utilization).

### **7.2.1 Operational Procedures**

Baseline operational procedures are defined by a combination of ATC and airline standard operating procedures (SOPs), letters of agreement (LOAs) between ATC facilities, and published approach and departure procedures. SOPs may be company-specific or facility-specific. For airlines, SOPs cover a broad array of operational elements such as standard takeoff thrust selection, landing gear extension altitude on approach, minimum stabilization altitude, or autopilot engagement altitude guidance. For ATC, SOPs may include standard vectoring patterns, clearance sequences, runway allocations, etc. LOAs establish expected interactions and flows between neighboring ATC



facilities and sectors, intended to simplify handoffs, increase throughput, and ensure safety as aircraft transition between various ATC jurisdictions.

In terms of published arrival and departure procedures, different types are used depending on the phase of a flight. These procedures are published in graphical and text-based formats for use by pilots and ATC. Published procedures define the ground tracks available for use by arriving and departing aircraft, directly influencing the baseline noise exposure patterns experienced by surrounding communities. Procedures include a combination of lateral track definition, altitude constraints, and/or speed guidance for a particular phase of flight to provide for safe, efficient, and predictable aircraft operations.

For departures, predefined procedures are published as obstacle departure procedures (ODPs) or standard instrument departures (SIDs). As implied by their name, ODPs are intended to define safe departure routes from the runway to an altitude above surrounding terrain and obstacles. SIDs are intended to facilitate safe and efficient departure routes from the runway to the enroute environment and may be implemented for operational expedience as well as safety [131]. SIDs may involve conventional navigation, RNAV/RNP waypoint definitions, and/or ATC vectoring. Most jet departures from major airports in the National Airspace System (NAS) follow assigned SIDs, with occasional vector-based departure guidance provided on a case-by-case basis by ATC to address separation issues, avoid weather, or provide operational expedience. Speed is typically restricted to less than 250 knots below 10,000 ft but detailed vertical profile and aircraft speed guidance is often left to pilot and ATC discretion. Speed and altitude constraints can be applied to SIDs on a case-by-case basis for specific waypoints or procedure segments.

For arrivals, two types of procedures impact the lateral track followed by an aircraft. The transition from the enroute airway structure to the terminal environment below 10,000 ft surrounding an airport is defined by standard terminal arrival routes (STARs). These procedures typically define aircraft tracks above the altitude that drives noise complaint behavior. The low-altitude transition routes from initial approach fixes to the runway is defined by instrument approach procedures (IAPs). IAPs use a wide variety of navigation and guidance technologies with varying degrees of precision and flexibility. In terms conventional navigation systems, the ILS is the most

common precision guidance source for IAPs at major airline airports. Non-precision approaches without vertical guidance may be defined using guidance from VOR facilities. Both ILS and VOR procedures require a straight final approach segment geometry due to the limitations of ground-based radio navigation. PBN navigation systems can also be used in IAP design, leveraging either RNAV or RNP guidance technology to enable flexible track geometry independent of ground infrastructure. IAPs affect noise impact on communities because they define flight paths at altitudes where aircraft are clearly visible and audible to underlying communities.

### **7.2.2 Flight-Level Schedule**

The flight-level schedule refers to the specific set of arrivals and departures that use an airport. Airport operators and ATC serve as facilitators to enable smooth and efficient operations while minimizing delays to the extent possible given airline demand. At most airports in the NAS, airlines dictate desired flight schedules and select the aircraft types which operate specific flights. Aircraft fleet mix, time of day effects, and total flight volume all have a direct impact on noise.

## **7.3 Procedure Change Process**

Operational procedure change refers broadly to a change in the manner in which an aircraft is flown. Precise definition of a procedure includes the latitude, longitude, speed, thrust, altitude, and configuration of an aircraft as a function of time throughout a given phase of flight. Depending on the type of analysis, this definition may be limited to the approach, departure, cruise, or other phases of flight. Advanced operational procedures are those that use modern technology and procedures (infrastructure, avionics, and air traffic control) to control speed, thrust, ground track, and other variables in a manner that would not be possible in traditional operations.

Historical flight procedures have been driven primarily by ground-based navigation systems. Limitations of navigation capability constrained the available scope for procedure redesign. However, recent developments in procedure design flexibility have expanded the opportunity for noise mitigation through operational modifications. Advanced flight procedures are a key component of air traffic management modernization efforts in the United States [132] and Europe [133]. Specifically, performance-based navigation (PBN) is intended to play a key role in streamlining

navigation standards and procedures to improve capacity, efficiency, and safety in the future ATM system. PBN enables greater flexibility in terms of lateral and vertical routing, speed control, and procedural design flexibility. The noise impacts of PBN and other advanced operational procedures have been investigated in several specific contexts (for example, [6], [65], [134], [135]), but work remains to model and mitigate noise implications arising from new procedures.

There is potential to use the advanced capabilities of PBN to lessen community noise impact from aviation. These procedures have the possibility to alter the noise footprint near airports relative to current operations due to:

1. Changes in aircraft speed profiles on approach or departure, with a corresponding increase or decrease in aerodynamic noise;
2. Changes in aircraft thrust profiles due to configuration changes, acceleration schedules, or speed targets, with a corresponding increase or decrease in engine noise;
3. Changed aircraft configuration, such as flap settings and landing gear extension, with a corresponding change in aerodynamic noise;
4. Concentration or dispersal of aircraft operations on set RNP tracks or procedural profiles.

### **7.3.1 Visual and Instrument Operations**

Aircraft noise depends on lateral and vertical routing to and from the runway, among other factors. Approach and departure routing depends on the type of operations being conducted at an airport. Most broadly, navigation in the vicinity of airports is performed using visual, instrument, or ATC vector guidance. While all of these procedure types have potential operational modifications with noise reduction potential, the greatest level of control from procedure design comes with instrument approach and departure procedures. Due to variability in flight conditions, traffic levels, pilot and controller technique, and other factors, visual and vector-based procedures do not typically follow precisely-defined ground tracks. This facilitates natural flight track dispersion but introduces a level of randomness in the system with implications for pilot and controller workload.

Visual approaches and departures may be authorized in weather conditions allowing pilots to maintain traffic, terrain, and obstacle avoidance without air traffic control intervention or avionics

guidance. Aircraft assigned to visual approach and departure procedures are not expected to follow precise lateral and vertical paths, leading to increased flight track dispersion and limited control of the resulting noise footprint from a procedure design standpoint. Graphical guidance for preferred visual approach and departure paths may be published for specific airports and runways, although these published visual procedures typically do not provide course guidance and may result in significant variation between the trajectories followed by individual aircraft. Visual approach and departure procedures are not typically subject to detailed flight track design validation because the primary responsibility for safe trajectory selection rests with the pilots.

Instrument approaches and departures enable pilots to follow predefined routes using onboard navigation equipment without ATC intervention or visual acquisition of terrain and obstacles. These procedures are published graphically and textually. Instrument approaches are typically defined from an initial fix or waypoint along a series of initial or intermediate procedure legs to the PFAF. From the PFAF, the aircraft proceeds to the landing runway along the final approach segment. If the runway environment is not visually acquired by the pilots by a predefined altitude or waypoint, a missed approach procedure is also provided to allow safe obstacle and terrain avoidance as the aircraft climbs to a safe altitude.

The final approach segment may or may not include altitude guidance for the pilots. Procedures with only lateral guidance typically have higher minimums than those with vertical guidance. Similar to instrument approach procedures, standard instrument departures are designed to provide safe and efficient routing as well as terrain and obstacle clearance from takeoff to the enroute environment using onboard navigation and guidance. Many different navigation technologies may be used to provide guidance for instrument approach and departure procedures with varying degrees of precision and route flexibility, resulting in variable minimums based on instrument approach type and aircraft performance level. Not all aircraft are able to fly all procedure types due to lack of onboard equipment and/or performance constraints for specific procedures.

Navigation guidance in instrument conditions can also be provided by ATC vectors. ATC vectors may be used to provide traffic, terrain, and obstacle avoidance when an aircraft is not on an instrument approach or departure procedure. For arrivals, vectors are often used in the terminal

environment during the transition from an arrival procedure to a published instrument approach procedure or visual approach. For departures, vectors may be used in lieu of published standard instrument departures to avoid traffic conflicts, expedite traffic flow, or avoid severe weather conditions. In terms of noise reduction, ATC may avoid certain noise-sensitive areas while vectoring an aircraft, but this is a secondary objective to traffic separation and safe routing to ensure terrain and obstacle avoidance.

### **7.3.2 Constraints and Stakeholder Preference in Procedure Design**

Procedure design is a complex problem due to technical and regulatory constraints and varying stakeholder objectives. The procedure design process at an airport or metroplex level involves constraints on procedure design criteria, air traffic control separation requirements, and aircraft flyability/safety constraints. Ultimately, any proposed procedure design must comply with technical constraints, pass through formal FAA design and implementation phases, meet NEPA environmental review and reporting standards, and have sufficient support among the operational community (airlines and ATC) to be used regularly once implemented.

#### **DESIGN CRITERIA**

General procedure design constraints for instrument approach and departure procedures is provided in FAA Order 8620.3B (TERPS) [136]. This document provides detailed obstacle clearance design standards for various types of approach and departure procedures. This is important for PBN procedure design and implementation because the geometry of approach paths, allowed vertical trajectory constraints, and minimum descent heights for various approach types are defined. PBN-specific design criteria are outlined in FAA Order 8260.58A, the United States Standard for PBN Instrument Procedure Design, providing detail on RNAV and RNP leg design constraints necessary for PBN implementation for arrival and departure procedures. Detailed constraints for RNAV and RNP final approach leg geometry were presented in Chapter 4.

#### **AIR TRAFFIC CONTROL CONSTRAINTS AND OBJECTIVES**

The overriding objective of air traffic control is to provide safe and efficient throughput of traffic in the NAS. Other objectives are considered when the baseline conditions of safety and efficiency are

satisfied. For example, noise abatement procedures and fuel efficiency initiatives are considered important objectives but not constraints for regular system operations.

In terms of operational and procedural constraints, air traffic controllers follow an extensive set of procedures prescribed by FAA Order JO 7110.65W [137]. This document outlines in detail the separation standards and standard control procedures for different types of aircraft and operations. While lower separation minima are permitted under certain specific RNAV departure procedures, ATC constraints are primarily defined in terms of pairwise separation between aircraft rather than specific procedure design requirements. There are also important constraints with respect to separation with airspace sector boundaries, with implications for airspace sector design in addition to procedure design. While the standard radar separation minima within 40nm of a radar site is 3nm laterally and 1000 ft. vertically, radar scope resolution, workload, and safety considerations dictate that separation should be provided through procedural design separation rather than active controller intervention whenever practical.

#### **AIRCRAFT FLYABILITY AND SAFETY CONSTRAINTS**

All procedure designs must be flyable using normal operating procedures (bank angles, thrust levels, flap and slat settings, and speed brake usage). Flyability evaluation requires cross-checking proposed procedures against aircraft performance models in worst-case weather conditions as well as application of kinetics modeling to determine required bank angles to comply with turning segments of procedures. Flyability evaluation also includes verification of navigation system performance and procedure interpretation by flight management systems in the cockpit. Encoded procedure segments must perform as expected across the range of aircraft types expected to utilize advanced procedures, including validation of correct waypoint cycling and conformance.

Some procedure concepts change aircraft energy state relative to baseline procedures. For example, steep approaches or delayed deceleration approaches increase the rate at which energy must be dissipated during the final approach phase. Analytical validation and operational testing must confirm that modified profile definitions can be implemented without increasing the risk associated with runway excursions. Another example of safety-related constraints applies to reduced

speed departures for aircraft in a flaps-up configuration. This procedure requires validation that appropriate maneuvering speed margins exist for aircraft using the procedure.

### **OPERATOR OBJECTIVES**

Airline considerations also constrain the procedure design space for several reasons. Avionics equipage levels dictate the types of procedures that specific aircraft can fly. For example, RNP approaches require FMS systems capable of tracking radius-to-fix legs. Additionally, special pilot training requirements apply for certain RNAV and RNP procedures. Installing and maintaining avionics combined with pilot training and currency costs impose a burden on airlines. Without appropriate equipage and pilot training for a significant portion of the fleet mix at a particular airport, advanced operational procedures involving advanced guidance systems such as RNP become impractical due to sequencing and spacing requirements between aircraft using different procedures. For some older fleets of aircraft, vertically-guided RNAV procedures are similarly limited by equipage. Depending on equipage levels in their fleets, some operators prefer advanced PBN procedures to harness efficiency and predictability from avionics and training investments while other operators prefer conventional guidance procedures to allow continued operations with legacy avionics and procedures.

In addition to equipage expense, new procedures add to airline costs through FMS memory constraints. Absolute memory limitations also constrain the total number of new procedures that may be generated and maintained onboard an aircraft at any one time. This constraint reduces the feasibility of concepts that require coding of a significant number of new flight procedures.

In general, operators are incentivized to maintain a safe, reliable, and predictable timetable of flights and operate as cost-efficiently as practical given the operational context. In many cases, these objectives are aligned with the objectives of other stakeholders – for example, reduced fuel consumption has both economic benefit in terms of reduced cost to airlines as well as environmental benefit in terms of reduced emissions. In other cases, stakeholder objectives may be orthogonal. In general, operators and ATC consider issues such as noise reduction in addition to operational imperatives wherever practical to improve stakeholder relationships with airports and communities served by air transportation.

## **7.4 Implementation Process**

### **7.4.1 NEPA Review**

NEPA established three levels of review depending on the nature of the proposed modification and magnitude of expected environmental impact. In all cases, a preferred solution is compared with the baseline (no-action) environmental scenario. Alternative actions are also considered given procedure objectives. The least restrictive level of review is an environmental screening and categorical exclusion (CATEX). For system modifications not qualifying for environmental review exemption under a CATEX, an environmental assessment (EA) is required. The EA can result in either a finding of no significant impact (FONSI) and record of decision (ROD) to proceed with the proposed modification, or a finding of significant environmental impact requiring. For changes found to have significant impact, and Environmental Impact Statement (EIS) is required. The EIS process includes extensive public input and culminates in a record of agreement (EIS/ROD) that often includes environmental commitments (mitigations or other actions) to be executed as part of the project. Figure 90 summarizes the NEPA process and documentation associated with each level of analysis/reporting.



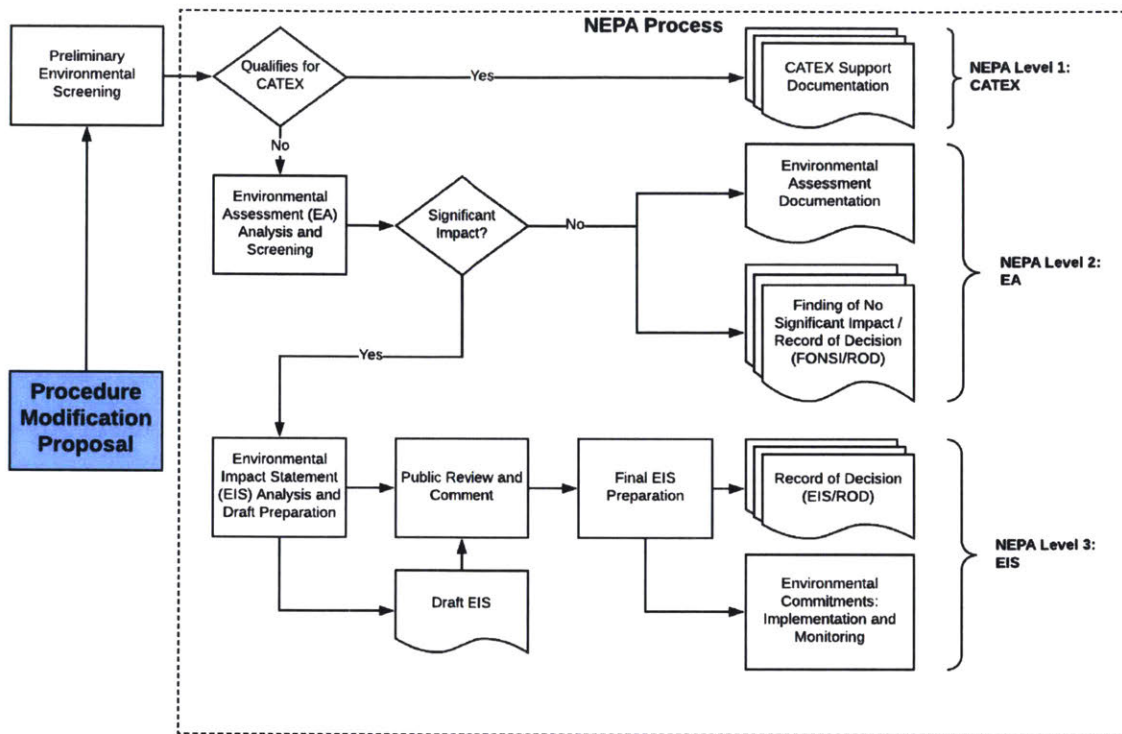


**Figure 90. NEPA environmental review process**

For airport, airspace, and procedure modifications, the EIS process is the most restrictive and costly level of NEPA. Requirements for analysis, documentation, and public input are extensive. Working through the EIS process can slow development projects considerably. The CATEX and EA process are generally less time-intensive and costly than the EIS process. It is desirable to avoid the need for an EIS for procedure development proposals. In order to prevent triggering an EIS, a procedure must be found to have no significant impact under the criteria established in FAA Order 1050.1.

Procedures eligible for CATEX-level review are generally the simplest, although supplemental environmental screening documentation may be prepared to justify the categorical exclusion from EA-level review. Regardless of the required level of NEPA review, procedure modernization and development efforts can be slowed significantly by environmental requirements without appropriate planning and early integration of environmental analysis in the design process [138]. In order to facilitate the implementation of new PBN procedures under NextGen, the FAA

Modernization and Reform Act of 2012 established a new CATEX for RNAV approach and departure procedures not expected to have significant noise impacts on a per-flight basis [139]. Practical guidance for implementation of this CATEX was provided by the FAA in 2016 [140]. Despite the availability of this CATEX for RNAV procedures, community expectations of thorough environmental review in light of increased flight track concentration have dictated that most RNAV procedure implementation processes have been subject to EA-level NEPA screening.

#### **7.4.2 Operational Implementation**

While iterative analysis serves an important role in developing procedure concepts to address noise issues in conjunction with other operational constraints, the ultimate authority for procedure implementation lies with the FAA. Preliminary analysis can provide a detailed noise evaluation, feasibility analysis, and multi-stakeholder benefits evaluation for candidate procedure modifications. However, any proposed change must ultimately proceed through a formal FAA safety and operational review process. This process includes full stakeholder working groups and is intended to ensure compliance with operational and safety constraints.

The formal FAA implementation process for novel PBN approach and departure procedures is defined in Order 7100.41A. This document provides a list of activities, documentation requirements, and responsibilities required for formal procedure evaluation and implementation review. A functional summary of the process is shown in Figure 91.

The formal procedure request that initiates the process can originate from any stakeholder and with any level of supporting analysis via an online request form. The chances of stakeholder buy-in and successful procedure development are significantly improved if the request originates as the result of a collaborative effort with supporting environmental and operational analysis. In this setting, the 7100.41A process serves as a safety check and detailed development process for procedure development rather than a focal component in the preliminary community feedback and negotiation process.

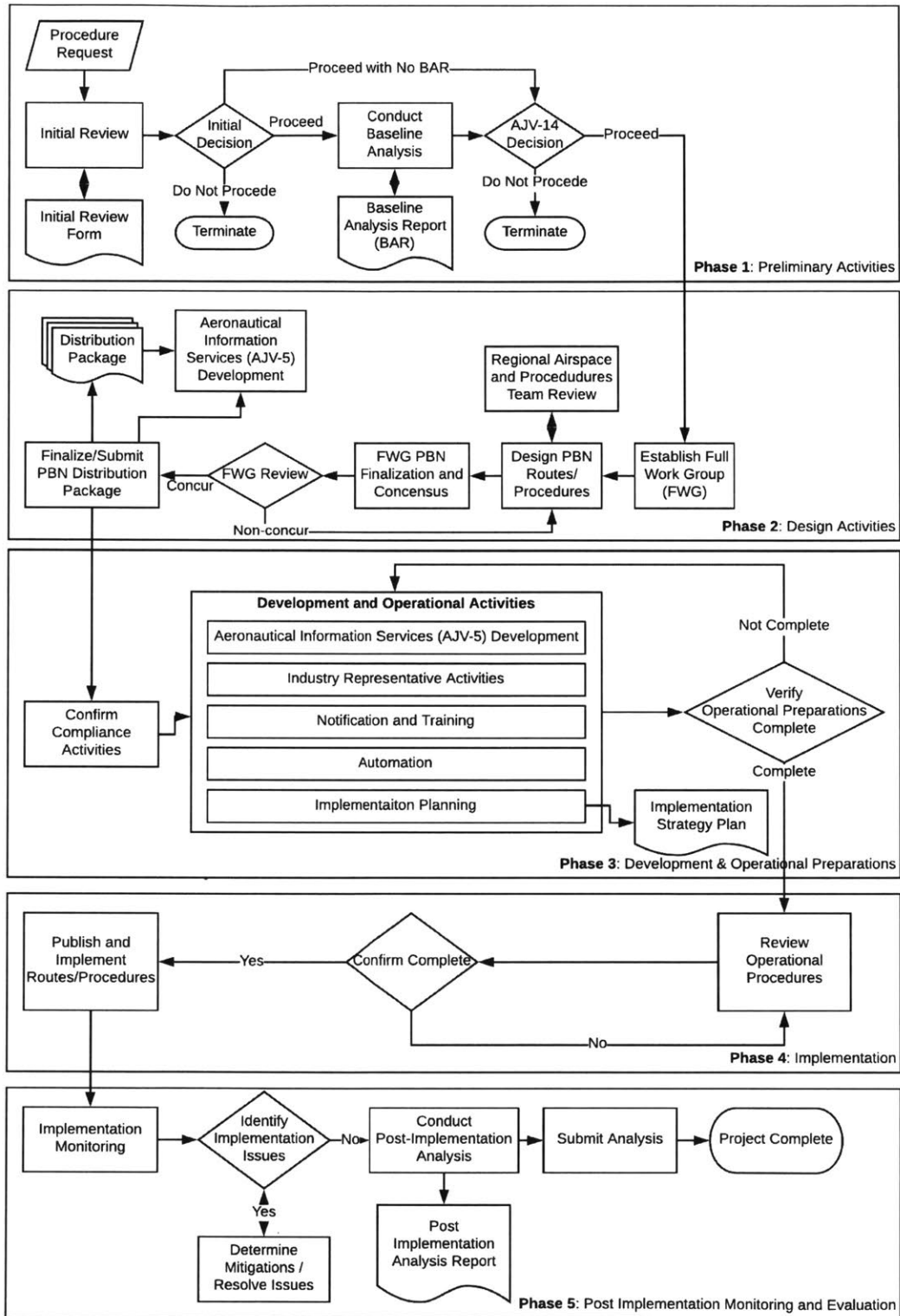


**Figure 91. Summary of FAA JO 7100.41A: PBN Implementation Process**

## 7.5 Case Study at Boston Logan Airport

The design framework introduced in this thesis for noise-motivated procedure design was utilized in a real-world study performed under a memorandum of understanding (MOU) between Massport, operator of BOS, and the FAA. The purpose of this study was to address increased noise concentration issues and complaints that arose following the implementation of RNAV arrival and departure procedures at BOS between 2012 and 2013. As part of this effort, the community and stakeholder engagement strategy described in this thesis were applied in an attempt to increase the transparency and effectiveness of the design process for all parties involved. The noise modeling capabilities for advanced operational procedures described in this thesis enabled identification and analysis of speed-dependent procedures, while industry-standard noise models were used to evaluate RNAV waypoint relocation concepts. Procedure designs were vetted against regulatory criteria and operational consideration through a stakeholder engagement process.

RNAV procedures were implemented at BOS between 2012 and 2013. Candidate approach and departure modifications to address noise concentration concerns were first identified based on an analysis of historical flight track densities over the communities surrounding BOS before and after the implementation of new RNAV procedures coupled with noise complaint records and US Census population data. Potential procedure modifications were considered for each identified arrival and departure runway including: lateral flight track adjustment to avoid noise-sensitive areas, vertical trajectory modifications including speed, thrust or configuration management as well as techniques to reintroduce dispersion into flight trajectories.

This study was an initial investigation to identify potential modifications to approach and departure procedures at BOS with the potential to reduce community noise impact in areas which experience flight track concentration. Potential procedure modifications were separated into two categories:

**Block 1:** The first category of procedures were characterized by clear predicted noise benefits, limited operational/technical barriers and a lack of equity issues. These procedures are best characterized as “win-win” in terms of noise impact, meaning that noise benefits may be realized for certain communities without imposing significant noise burdens on other communities.

**Block 2:** The second category of procedures exhibited greater complexity due to potential operational and technical barriers as well as equity issues. These procedures involve noise redistribution between communities, with the objective of either reducing net population exposure or increasing equity by some metric of choice.

Procedure modification options were evaluated for both Block 1 and Block 2 based on a preliminary evaluation of noise reduction potential, operational/technical feasibility and potential equity issues. Some candidate procedures were rejected for application at BOS due to safety concerns or lack of noise benefits. The noise analysis compared the proposed modification with current procedures on a single-event basis. Noise contours and corresponding population exposures were calculated for  $L_{MAX}$  and SEL metrics. Preliminary development of a set of procedures has been completed, with formal evaluation and implementation processes currently underway between industry stakeholders and the FAA. Continued analysis and community outreach for identification and development of Block 2 procedures are currently underway and are a key part of future work for this research effort.

The technical feasibility analysis included an examination of flight safety, aircraft performance, navigation and FMS limitations, pilot workload, ATC workload, and procedure design criteria. The process of procedure identification and refinement was informed by outreach to impacted stakeholders including community representatives, FAA regional and national offices, ATC managers and specialists, airline technical pilots, and public officials.

As a result of this process the procedures which were identified for Block 1 and their primary noise benefits are listed in Table 22. At a high level, there are two types of modifications proposed among the Block 1 procedure set:

1. Waypoint relocation for PBN arrival and departure procedures and/or development of new PBN arrival and departure procedures (Recommendations 1-D2, 1-D3, and 1-A1)
2. Modification of existing arrival and departure procedures with alternative speed and/or configuration profiles (Recommendation 1-D1)

**Table 22. Block 1 Procedure Recommendations at BOS**

Proc. ID D = Dep. A = Arr.	Procedure	Primary Benefits
1-D1	Restrict target climb speed for jet departures from Runways 33L and 27 to 220 knots or minimum safe airspeed in clean configuration, whichever is higher.	Reduced airframe and total noise during climb below 10,000 ft (beyond immediate airport vicinity)
1-D2	Modify RNAV SID from Runway 15R to move tracks further to the north away from populated areas.	Departure flight paths moved north away from Hull
1-D3	Modify RNAV SID from Runway 22L and 22R to initiate turns sooner after takeoff and move tracks further to the north away from populated areas.	Departure flight paths moved north away from Hull and South Boston
1-D3a	<i>Option A:</i> Climb to intercept course (VI-CF) procedure	
1-D3b	<i>Option B:</i> Climb to altitude, then direct (VA-DF) procedure	
1-D3c	<i>Option C:</i> Heading-based procedure	
1-A1	Implement an overwater RNAV approach procedure with RNP overlay to Runway 33L that follows the ground track of the jetBlue RNAV Visual procedure as closely as possible.	Arrival flight paths moved overwater instead of over the Hull peninsula and points further south
1-A1a	<i>Option A:</i> Published instrument approach procedure	
1-A1b	<i>Option B:</i> Public distribution of RNAV Visual procedure	

Two of the procedures evaluated in the FAA Block 1 study and recommended for detailed review and implementation by the FAA are specific and detailed applications of the operational concepts discussed earlier in this thesis: an overwater PBN arrival concept to runway 33L (Option 1-A1) and a suggested reduced-speed departure profile for runway 33L and runway 27 (Option 1-D1). The specific recommendations made for these procedures at BOS are discussed below and are under operational review by the FAA at the time of writing of this thesis [141].

## 7.5.1 Overwater PBN Approach Procedure for Runway 33L

### SUMMARY

Current approaches to runway 33L overfly the Hull Peninsula from the southeast to the northwest as part of the final approach segment or during vectors to final. This results in noise exposure to underlying communities that are also impacted by departures from runway 22R, 22L, and 15R. There is an opportunity to reduce noise for the communities underlying this final approach course by designing an overwater RNAV procedure with RNP overlay that avoids the Hull Peninsula to the extent possible given procedure design criteria.

### TRACK DENSITY PLOTS

Figure 92 shows jet track concentration for arrivals to Runway 33L before and after implementation of RNAV procedures (2010-2015). Noise concentration along the final approach corridor is evident in both images, spanning several populated land masses to the southeast of the airport. Utilization of the “Light Visual” approach with its overwater dog-leg segment appears to have been more prevalent in 2010 than in 2015.

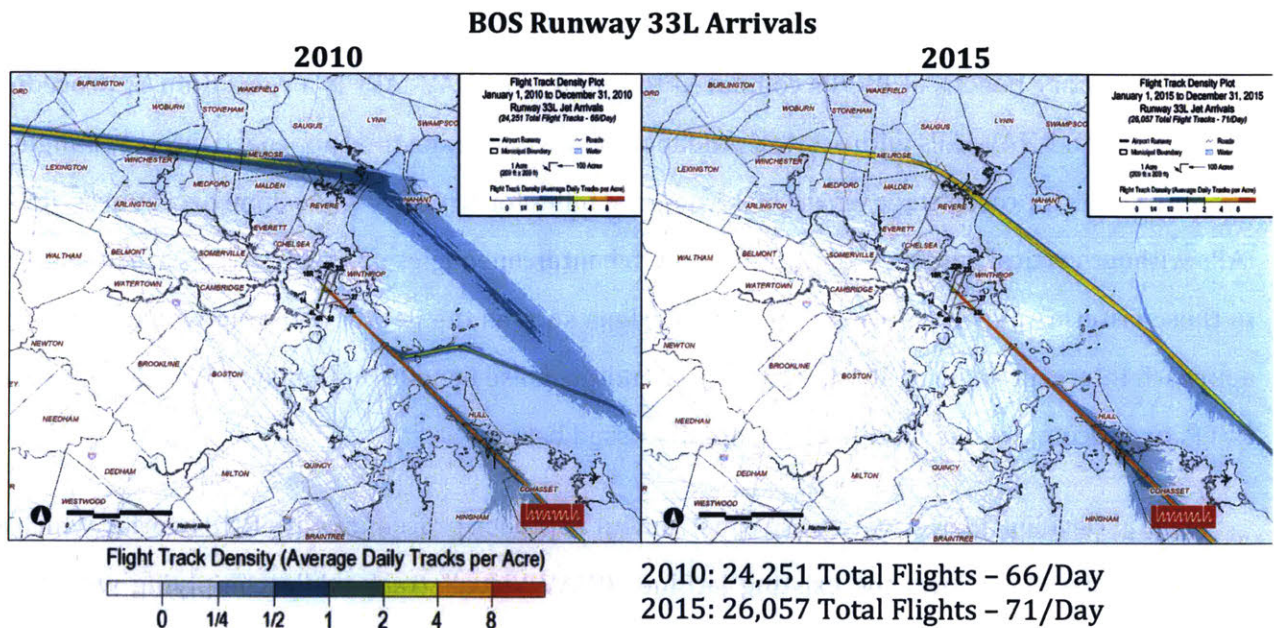


**Figure 92. Comparison between flight track density from BOS Runway 33L jet arrivals between 2010 and 2015 (Source: HMMH via [141])**

## PROCEDURE RECOMMENDATION DETAILS

A visual approach procedure to Runway 33L which moves arrival tracks away from Hull has been available for several years for use in good weather conditions (minimum of 3,000 ft. cloud ceilings and 5 miles of visibility). The procedure, shown in Figure 37(a), includes a dogleg over Boston Harbor with a 55° turn to intercept the final approach path at a point 2.95 nautical miles from the runway threshold. The “Light Visual” procedure was intended for use during low-demand periods, particularly during late night operations. The procedure is operationally challenging as a visual approach due to the lack of lighted features on the water at night.

In an effort to increase utilization of the overwater approach procedure concept, jetBlue Airways developed a company-specific RNAV Visual Flight Procedure (RVFP) approach to Runway 33L that closely mirrored the original Light Visual from the southeast with the addition of an additional feeder route from the northwest. As discussed in Section 4.5, these approaches are not restricted in final turn angle or minimum final leg length because pilots are able to visually monitor and avoid terrain. The jetBlue “RNAV Visual” approach chart is shown in Figure 37(b). The RVFP allows jetBlue pilots and aircraft to fly the visual procedure with improved guidance from the aircraft flight management system, improving safety and helping improve conformance to the desired overwater flight tracks.

The primary benefit of RVFPs compared to published RNAV IAPs is a relaxation of procedure design criteria. RNAV IAPs with vertical guidance have a maximum final approach intercept angle of 15° and a final approach stage length of 3.1 nautical miles for typical 3° glideslope procedures. RNAV IAPs without vertical guidance allow final approach intercept angles up to 30°. RVFPs are not subject to these criteria, allowing noise-minimizing designs such as the jetBlue example which has a final approach intercept angle of 56°. In order to extend the noise benefits of the Light Visual and jetBlue RVFP, two recommended modifications are discussed below:

1-A1a: Develop an overwater RNAV instrument approach procedure with RNP overlay which as closely as possible follows the existing jetBlue “RNAV Visual” track while complying with more stringent IAP design criteria



1-A1b: Develop a public distribution mechanism for RVFP procedures for use by a broader subset of operators at BOS

Figure 93 shows a comparison of the ground track for the jetBlue RVFP (blue track) with an example RNAV instrument approach procedure concept that complies with non-precision (no altitude guidance) approach design criteria (green track). The approach design criteria constraints discussed in Section 4.1 prevented an exact overlay of the jetBlue approach, although the required waypoint changes are not substantial. This ground track is recommended as an example implementation of an RNAV IAP without vertical guidance that can be overlaid with an RNP equivalent for appropriately-equipped aircraft.

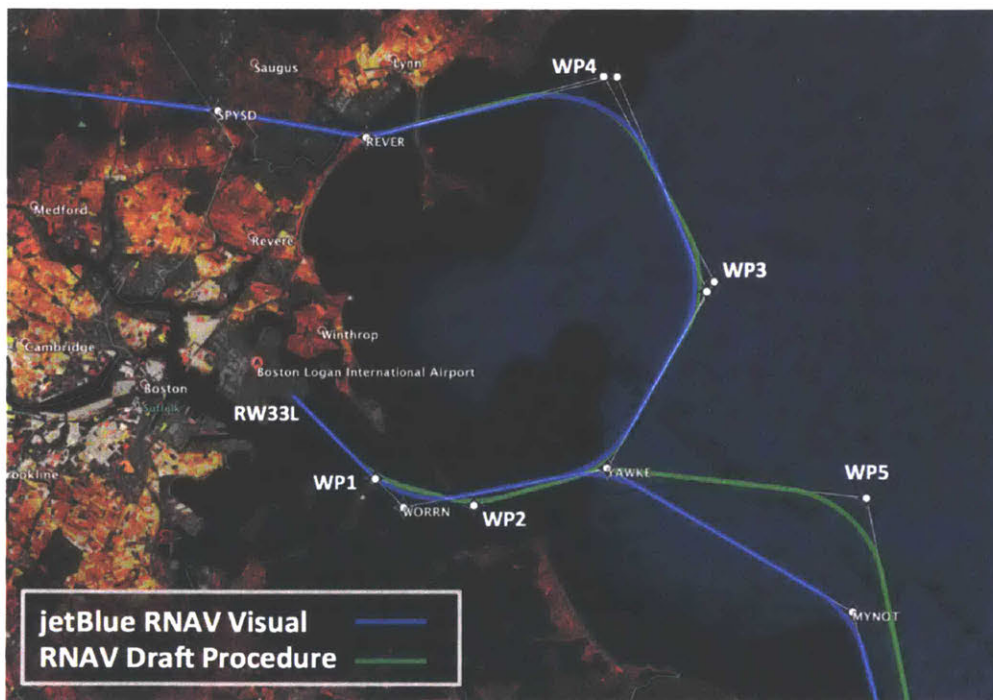


**Figure 93. jetBlue RNAV Visual approach procedure to Runway 33L (blue) compared with an example RNAV draft nonprecision instrument approach procedure**

This recommendation is intended to comply with existing RNAV approach procedure design constraints. Waypoint coordinates are provided in Table 23 for northerly arrivals and Table 24 for southerly arrivals, corresponding to the green tracks shown in Figure 93. All waypoints are designated as flyby rather than flyover.

**Table 23. Waypoint locations and leg type definitions for the northern component of procedure recommendation 1-A1a**

<b>Leg Number</b>	<b>Leg Definition</b>	<b>From</b>	<b>To</b>
1	<i>Direct to Fix (DF)</i>	<b>SPYSD (7,000')</b> 42°26'58.450" N 71°01'37.250" W	<b>REVER (6,600')</b> 42°26'27.480" N 70°57'41.310" W
2	<i>Direct to Fix (DF)</i>	<b>REVER (6,600')</b> 42°26'27.480" N 70°57'41.310" W	<b>WP4 (5,000')</b> 42°27'39.207" N 70°51'27.753" W
3	<i>Direct to Fix (DF)</i>	<b>WP4 (5,000')</b> 42°27'39.207" N 70°51'27.753" W	<b>WP3 (3,500')</b> 42°23'36.905" N 70°48'36.024" W
4	<i>Direct to Fix (DF)</i>	<b>WP3 (3,500')</b> 42°23'36.905" N 70°48'36.024" W	<b>YAWKE (2,200')</b> 42°19'57.400" N 70°51'24.050" W
5	<i>Direct to Fix (DF)</i>	<b>YAWKE (2,200')</b> 42°19'57.400" N 70°51'24.050" W	<b>WP2 (1,400')</b> 42°19'13.850" N 70°54'51.180" W
6	<i>Direct to Fix (DF)</i>	<b>WP2 (1,400')</b> 42°19'13.850" N 70°54'51.180" W	<b>WP1 (800')</b> 42°19'45.338" N 70°57'27.285" W
7	<i>Direct to Fix (DF)</i>	<b>WP1 (800')</b> 42°19'45.338" N 70°57'27.285" W	<b>RW33L (landing)</b> 42°21'16.743" N 70°59'29.710" W

**Table 24. Waypoint locations and leg type definitions for the southern component of procedure recommendation 1-A1a**

<b>Leg Number</b>	<b>Leg Definition</b>	<b>From</b>	<b>To</b>
1	<i>Direct to Fix (DF)</i>	<b>MYNOT</b> 42°17'07.810" N 70°45'01.990" W	<b>WP5 (3,800')</b> 42°19'21.690" N 70°44'39.720" W
2	<i>Direct to Fix (DF)</i>	<b>WP5 (3,800')</b> 42°19'21.690" N 70°44'39.720" W	<b>YAWKE (2,200')</b> 42°19'57.400" N 70°51'24.050" W
3	<i>Direct to Fix (DF)</i>	<b>YAWKE (2,200')</b> 42°19'57.400" N 70°51'24.050" W	<b>WP2 (1,400')</b> 42°19'13.850" N 70°54'51.180" W
4	<i>Direct to Fix (DF)</i>	<b>WP2 (1,400')</b> 42°19'13.850" N 70°54'51.180" W	<b>WP1 (800')</b> 42°19'45.338" N 70°57'27.285" W
5	<i>Direct to Fix (DF)</i>	<b>WP1 (800')</b> 42°19'45.338" N 70°57'27.285" W	<b>RW33L (landing)</b> 42°21'16.743" N 70°59'29.710" W

It is also recommended that an RNP overlay be developed following the RNAV ground track as closely as practical to enable seamless ATC integration between flights using the two different approaches. This would enable RNP-equipped aircraft to fly the procedure with higher precision

including vertical guidance[126]. The overlay would use radius-to-fix turns in lieu of flyby waypoints. The safety and efficiency benefits from the overlay approach would increase as RNP equipage levels increase.

**NOISE MODELING RESULTS AND POPULATION EXPOSURE**

Noise was modeled for the proposed waypoint relocation using the AEDT model described in Section 3.5.1. Analysis was performed for the Boeing 737-800. The baseline procedure was a straight-in ILS to runway 33L at 75% of maximum takeoff weight and a 3° glideslope. The modified procedure used the same weight assumption and glideslope, varying only procedure track. The thrust profile was derived from a force-balance kinematics model.

Noise impacts from procedure recommendations 1-A1a and 1-A1b are nearly identical due to the similarity between the recommended nonprecision RNAV to the jetBlue RVFP. Figure 94 shows single-event L<sub>MAX</sub> contours and population exposure reduction results for a Boeing 737-800 following procedure 1-A1a. All populated landmasses fall outside of the 60 dB L<sub>MAX</sub> contour for the proposed overwater procedure, with Hull being the primary noise reduction beneficiary. No communities experience an increase in noise as a result of the recommended procedure modifications.



L <sub>MAX</sub> Population Exposure	60dB	65dB	70dB
<b>ILS Runway 33L</b>	2,181	154	0
<b>Proc. 1-A1a</b>	0	0	0
<b>Decrease</b>	<b>2,181</b>	<b>154</b>	<b>0</b>

**Figure 94. Noise exposure reduction for the Boeing 737-800 arriving Runway 33L descending via procedure recommendation 1-A1a on 3° descent profile**

## **POTENTIAL BARRIERS TO IMPLEMENTATION**

### *SEQUENCING, MERGING, AND SPACING*

A preliminary implementation of a low-noise overwater approach procedure would likely have lower throughput than a straight-in procedure due to reduced ATC flexibility to sequence, merge, and space arrivals onto final approach. Therefore, the procedure would likely be limited to low-traffic time periods. Utilization would be focused initially on late-night periods when noise relief is most needed. Over time, improved controller experience and decision support tools may allow expanded utilization of this and similar procedures during high-traffic periods.

### *VERTICAL GUIDANCE*

As discussed above, RNAV IAPs with vertical guidance are restricted to final approach intercept angles of 15°. RNAV IAPs without vertical guidance allow final approach intercept angles up to 30°. The 56° final approach intercept angle on the jetBlue RVFP is outside the criteria limits for both types of procedures. In order to follow the ground track of the jetBlue RVFP as closely as possible, it was necessary to design an RNAV approach without vertical guidance. A procedure designed under the criteria for RNAV with vertical guidance would not be sufficiently flexible to avoid overflight of Hull, significantly reducing potential noise benefits. Alternatively, waivers to the procedure design criteria could be considered due to the lack of obstacles on the final approach course and the operational history of the jetBlue RVFP approach.

Some aircraft are not equipped to fly RNAV approaches without vertical guidance. In addition, operators may prefer approaches with vertical guidance for operational consistency. These factors prevent universal adoption of any nonprecision RNAV procedure without vertical guidance. In order to maximize the number of aircraft following the recommended ground track to maximize noise benefits in the vicinity of Hull, an RNP overlay (including vertical guidance) should be designed for use by appropriately equipped aircraft. Operators could elect to use the nonprecision RNAV procedure or the RNP alternative depending on equipage.

## 7.5.2 Reduced-speed departure profile for Runway 33L and Runway 27

### TRACK DENSITY PLOTS

Runway 33L and 27 are the two departure runways at BOS where the climb segment below 10,000 ft occurs primarily over land. Therefore, this procedure recommendation focuses on those runways. Figure 95 shows jet track concentration for departures from Runway 33L before and after implementation of RNAV procedures (2010-2015). Figure 96 shows the same data for Runway 27. In both cases, increased concentration is evident after the implementation of RNAV procedures, especially for communities more than 5 nautical miles away from the airport where tracks were historically dispersed. Reduced speed departures would serve as an initial step to provide noise relief to those underneath the centerline of departure corridors from Runway 33L and Runway 27 by reducing the noise associated with each overflight.

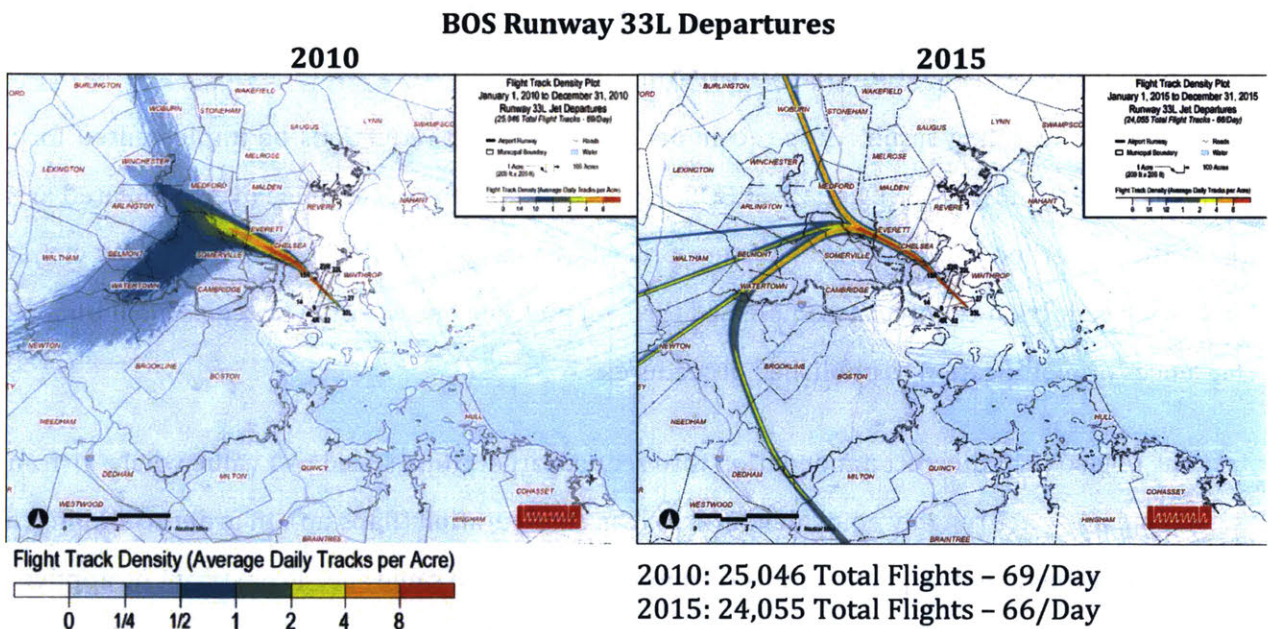


**Figure 95. Comparison between flight track density from BOS Runway 33L jet departures between 2010 and 2015 (Source: HMMH via [141])**

## BOS Runway 27 Departures

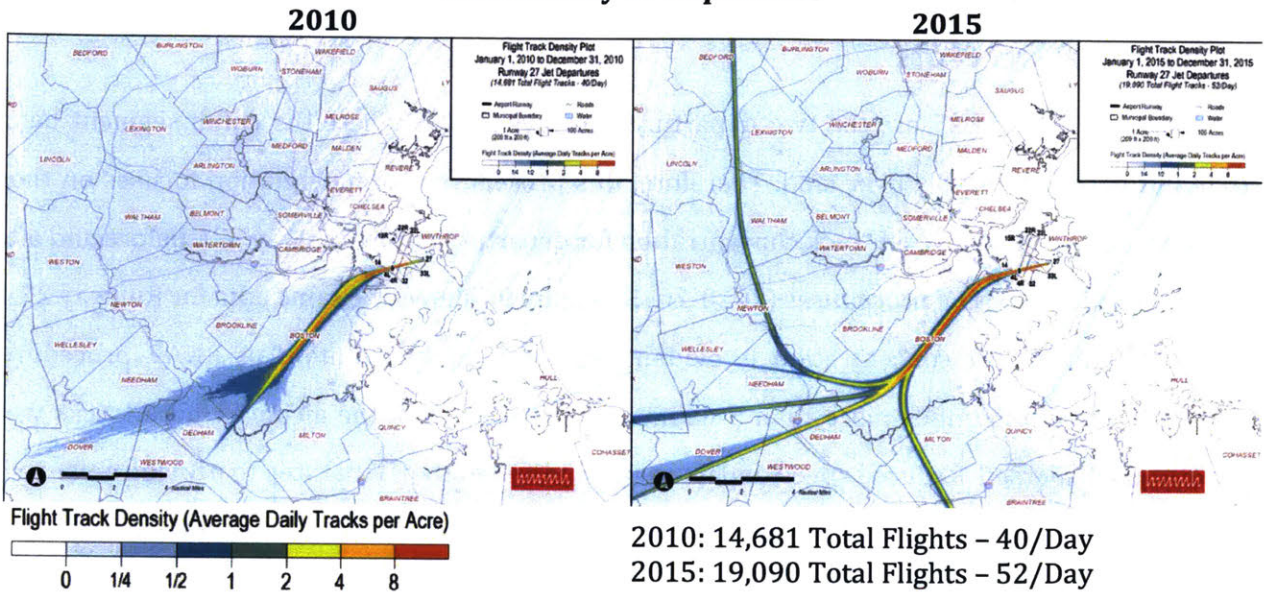


**Figure 96. Comparison between flight track density from BOS Runway 27 jet departures between 2010 and 2015 (Source: HMMH via [141])**

### PROCEDURE RECOMMENDATION DETAILS

Based on modeling results, it is recommended that speed reductions be implemented for jet departures from runways 33L and 27 at BOS. This is expected to reduce noise over populated areas under the centerline of published departure procedures away from the immediate airport vicinity. This speed reduction could be accomplished through multiple operational strategies, including ATC clearances or modification to published procedures.

The objective of this recommendation is to reduce target climb speed to a value where airframe and engine noise are roughly equivalent in the clean configuration (flaps up). In order to simplify air traffic management and sequencing, it is recommended that the same speed constraint be applied to all departing jet traffic. Noise model results indicate that the airframe/engine noise equivalence speed is in the vicinity of 220 knots for most jet aircraft. Therefore, this procedure consists of modifying the standard departure profile with a reduced target climb speed of 220 knots.

Not all aircraft types are capable of operating safely at 220 knots in a clean configuration. There is precedence for safety-based exceptions to speed constraints in the Federal Aviation Regulations under 14 C.F.R. §91.117(d), which state that an aircraft may use the minimum safe airspeed for any particular operation if that speed is greater than the prescribed legal limit. In practice, this would

result in certain aircraft types exceeding the 220 knot limitation. This is driven by multiple factors including aircraft weight and wing design. Analysis of the 2015/2016 fleet mix at BOS indicates that 6.9% of departures would likely need to fly at a minimum safe climb speed higher than 220 knots. The need to fly faster than 220 knots would be determined by airline procedures based on aircraft type, weight, and flight conditions. Traffic spacing would be managed by air traffic controllers using the same techniques currently applied to aircraft operating at different speeds.

In order to observe benefits for outlying communities under the departure flight path, the reduced speed must be maintained until an altitude where noise levels are below an acceptable threshold. Based on noise modeling for the 737-800, 777-300, and E-170, an acceleration altitude of 10,000 ft. captures the noise reduction benefit for both heavy and light aircraft. An acceleration altitude of 6,000 ft. was found to retain the population exposure benefits for light aircraft but significantly reduce benefits for heavy aircraft (which typically generate more source noise and climb at a shallower gradient). Therefore, it is recommended to implement the speed restriction to 10,000 ft. to maximize population exposure benefits from the procedure.

#### **NOISE MODELING RESULTS AND POPULATION EXPOSURE**

Noise was modeled for the proposed reduced speed departure procedures using the NASA ANOPP model described in Section 3.5.2. In order to evaluate population impact for a single representative departure, each of these aircraft was modeled on the “BLZZR Four” RNAV standard instrument departure (SID) from Runways 33L and 27, a typical route used for departures to southwesterly destinations such as Atlanta and Dallas. For a procedure baseline, the analysis uses a standard departure profile with a 250-knot target climb speed and a vertical profile derived from median radar data for that aircraft type and runway. The thrust cutback altitude for the baseline procedure and all modified procedure was also based on this historical data.

For all aircraft types, the contour geometry is unchanged in the immediate vicinity of the airport. Contour contraction occurs approximately five to thirty miles from the departure end of the runway where unrestricted departures would have already accelerated beyond 220 knots. This corresponds to regions of concern for RNAV track concentration.

Figure 97 shows single-event noise contours ( $L_{MAX}$ ) and population exposure results for the 737-800 in a clean configuration with a target climb speed of 220 knots. Figure 98 shows similar results for the 777-300, although the target climb speed was limited to 240 knots due to minimum speed constraints for that aircraft type. Figure 99 shows contours for the E-170 with a target climb speed of 220 knots.

Figure 100 shows contours for 737-800 with a target climb speed of 220 knots from runway 27. According to these modeled results, all three aircraft types show noise reduction due to reduced speed departures. Large population exposure reductions are evident, particularly at the 65 dB level and below. Specific reductions depend on the underlying population density which varies by departure runway and procedure. For both runways, areas of noise reduction occur in locations under the departure procedure centerline corresponding to areas of frequent community noise complaints. No communities experience an increase in noise as a result of reduced speed departures.

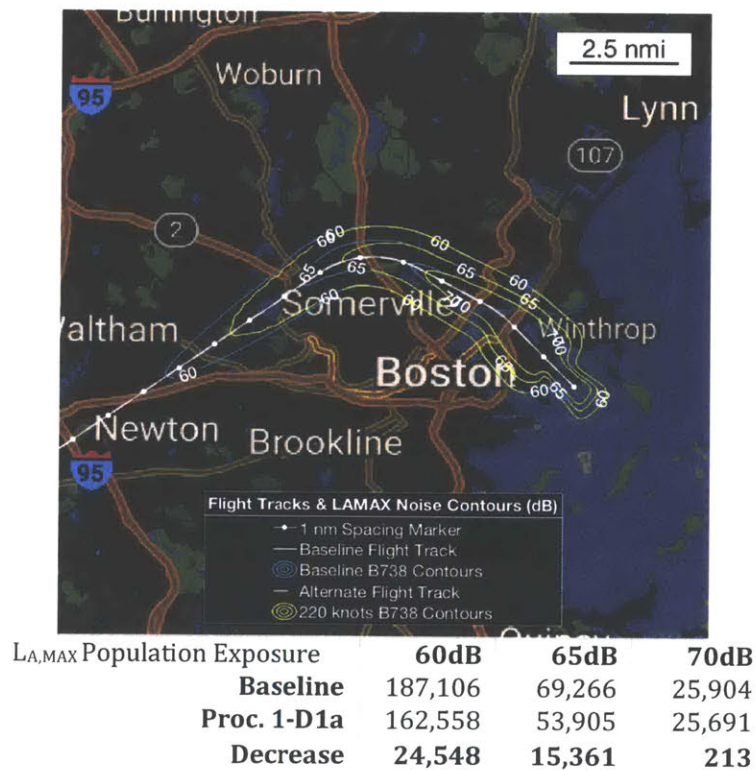


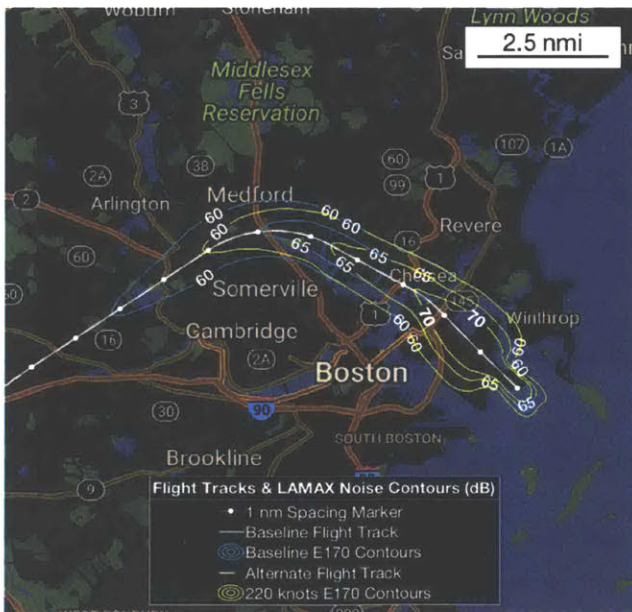
**Figure 97. Noise exposure reduction for the Boeing 737-800 departing runway 33L via the BLZZR4 departure on a standard climb profile compared to a 220-knot reduced speed departure. Noise Model: NASA ANOPP**





L <sub>A,MAX</sub> Population Exposure	60dB	65dB	70dB
<b>Baseline</b>	384,953	197,874	70,839
<b>Proc. 1-D1a</b>	378,425	192,907	69,932
<b>Decrease</b>	<b>6,528</b>	<b>4,967</b>	<b>907</b>

**Figure 98. Noise exposure reduction for the Boeing 777-300 departing runway 33L via the BLZZR4 departure on a standard climb profile compared to a 240-knot reduced speed departure. Noise Model: NASA ANOPP**



L <sub>A,MAX</sub> Population Exposure	60dB	65dB	70dB
<b>Baseline</b>	106,870	30,625	4,495
<b>Proc. 1-D1a</b>	70,310	27,096	4,495
<b>Decrease</b>	<b>36,560</b>	<b>3,529</b>	<b>0</b>

**Figure 99. Noise exposure reduction for the Embraer E-170 departing runway 33L via the BLZZR4 departure on a standard climb profile compared to a 220-knot reduced speed departure. Noise Model: NASA ANOPP**

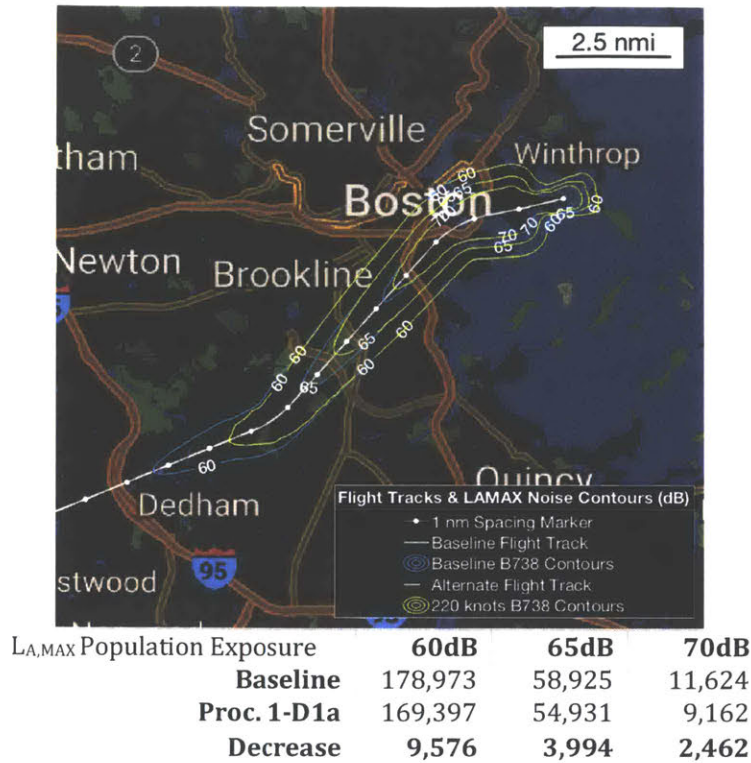


**Figure 100. Noise exposure reduction for the Boeing 737-800 departing runway 27 via the BLZZR4 departure on a standard climb profile compared to a 220-knot reduced speed departure. Noise Model: NASA ANOPP**

**POTENTIAL BARRIERS TO IMPLEMENTATION**

Three potential barriers to entry were identified in consultation with operational stakeholders:

- Fuel burn and flight time increase
- Potential runway throughput reduction
- Limitations on aerodynamic maneuvering margins at 220 knots

Each of these potential barriers to entry was evaluated as part of the study and found not to pose an unmanageable issue. Details of each potential barrier are provided below.

*FUEL BURN AND FLIGHT TIME*

Performance modeling of reduced-speed climbs was conducted using the Eurocontrol BADA-4 model and indicates a slight fuel burn and flight time penalty from the procedure. This is because the aircraft are require to cover the baseline track distance at a slower speed. Naturally, this results in a slight time increase. Fuel burn also increases slightly for each aircraft type examined in this study,

which can be attributed to the increased flight time as well as slightly lower aerodynamic efficiency at reduced speeds. Table 25 shows the fuel burn and time impact for representative reduced-speed departures with an acceleration altitude of 10,000 ft. These relatively small values (under 11 gallons of fuel and 30 seconds of flight time) are not considered significant and are smaller than penalties for other common noise abatement procedures.

**Table 25. Fuel consumption and flight time implications from reduced speed climb procedures**

<b>Aircraft</b>	<b>Climb Speed</b>	<b>Fuel Burn Increase vs. Baseline</b>	<b>Flight Time Increase vs. Baseline</b>
<b>737-800</b>	220 Knots	46 lbs (6.8 gallons)	30 seconds
<b>777-300</b>	240 Knots	71 lbs (10.4 gallons)	12 seconds
<b>E-170</b>	220 Knots	9 lbs (1.3 gallons)	22 seconds

*DEPARTURE SEQUENCING AND RUNWAY THROUGHPUT*

When tower controllers release aircraft for takeoff, they commonly assume that the leading aircraft will accelerate and take this into consideration when determining the departure release time for the trailing aircraft. Airborne aircraft are subject to minimum separation requirements. In general, aircraft must be separated by 3 nautical miles horizontally and/or 1,000 ft. vertically or placed on divergent headings. Detailed separation requirements are specified in FAA Joint Order 7110.65 [142]. For the purpose of departure metering, air traffic controllers must provide a sufficient time interval between takeoff clearances to ensure 3 nautical mile separation between leading and trailing aircraft after the trailing aircraft becomes airborne and throughout the departure procedure. Imposing reduced speed constraints on departing aircraft has the potential to impact the required interval between takeoff clearances.

In order to evaluate potential throughput implications of reduced speed departures, historical radar tracks were analyzed. The analysis data set consisted of 2015 and 2016 departures from Runways 33L and 27 at BOS, for a total of 27,713 operations. Each pair of sequential departures in this set was analyzed on a second-by-second basis using the baseline (as-flown) speed profile as well as a modified speed profile limited to 220 knots or the minimum safe airspeed for the respective aircraft type, whichever was greater. In the reduced speed scenario, the start of takeoff roll time was

maintained at the baseline value. Minimum horizontal separation was determined on a second-by-second basis for both the baseline and modified scenarios.

The historical radar data analysis showed minimal throughput implications for the proposed reduced speed departure procedure. 54 departure pairs that had maintained 3 nautical mile separation in the baseline case would have violated that horizontal spacing after the imposition of reduced speeds if no adjustments to release time occurred. This corresponds to 1 departure out of every 513 that would have required air traffic control action different from what occurred in the 2015-2016 timeframe. The departure release delay required to remove these conflicts was small, with a median delay of 1.1 seconds. Therefore, the potential departure sequencing and runway throughput impact of reduced speed departures is expected to be small and manageable by air traffic controllers without requiring significant changes in standard operating practices.

#### *SLOW-SPEED MANEUVERING*

Some aircraft types cannot operate with adequate maneuvering margins at 220 knots in a clean configuration at high takeoff weights. This is addressed through a provision for minimum safe airspeed in lieu of the 220 knot restriction for aircraft with such constraints. For the majority of the fleet mix at BOS, the 220 knot recommendation is safely flyable in the clean configuration at normal weights. However, airline policy and pilot discretion can guide the use of alternative minimum safe airspeed on a case-by-case basis. This allows sufficient flexibility to pilots and air traffic controllers to implement the noise-driven departure modification without compromising safety.

The recommendation also calls for minimum safe airspeed in the clean configuration rather than with flaps or slats extended. This reduces noise from flap gaps and edges, fatigue on structural components, and potential issues with extended high-lift devices in icing conditions. It also minimizes the fuel burn penalty associated with the recommended procedure. Therefore, concerns regarding flaps-extended climbs have been minimized to the extent possible in this recommendation.

# Chapter 8. Conclusion

## 8.1 Thesis Framework and Analysis Results Summary

This thesis introduced a rapid noise analysis method for evaluating impacts arising from flight procedure modifications. This analysis method is incorporated into a broad system-level sociotechnical framework that incorporates community complaint and organization processes, procedure changes given technical constraints, formal implementation processes, and procedure integration into the set of operational procedures at an airport. The role of the analyst in this framework is to integrate stakeholder priorities, technical constraints, community objectives, and noise analysis results in an iterative solution refinement process prior to forwarding a proposed procedure change for formal FAA review and implementation.

This thesis also discussed prior work in using complaint data to identify noise metrics and thresholds appropriate for capturing noise annoyance effects and supporting the use of  $N_{\text{ABOVE}}$  as a supplemental evaluation metric (60dB daytime  $L_{\text{MAX}}$ , 50dB nighttime threshold). Based on this metric and threshold, flight track dispersion requirements to reduce community noise annoyance were evaluated as a function of runway traffic mix and volume.

The rapid noise analysis method was used to evaluate two specific procedure concepts. The first was a noise benefits analysis for the hypothetical implementation of noise-reduction RNAV and RNP procedures at every runway end in the set of OEP-35 airports. The analysis selected noise-minimal procedures from a set of over 100,000 possible candidate designs for each runway end that are compliant with procedure design criteria. This analysis indicated substantial benefit potential from RNAV procedures (with and without vertical guidance) as well as RNP procedures relative to straight-in baseline comparison cases. Procedures with the largest benefit are at airports located in regions of high population density.

While RNP procedures offer the greatest potential noise benefit due to reduced straight final approach segment length, the majority of noise impact can be achieved through implementation of

RNAV procedures consistent with existing design criteria. Figure 101 shows the unconstrained best-case cumulative person-event impact benefit for PBN guidance technologies at the OEP-35 airports with a notional comparison to RNAV Visual (RVFP) procedures. While RVFP noise results were not calculated explicitly, the procedures are at least as flexible as RNAV approaches without vertical guidance but less flexible than RNP approaches. Therefore, the net noise result is expected to fall between the impact results for those two technology levels. Relative to baseline person-event impact levels assuming straight-in arrivals on all runways, RNAV approaches with vertical guidance have a benefit of 49.1% while RNP procedures provide an even greater potential benefit of 58.2%.

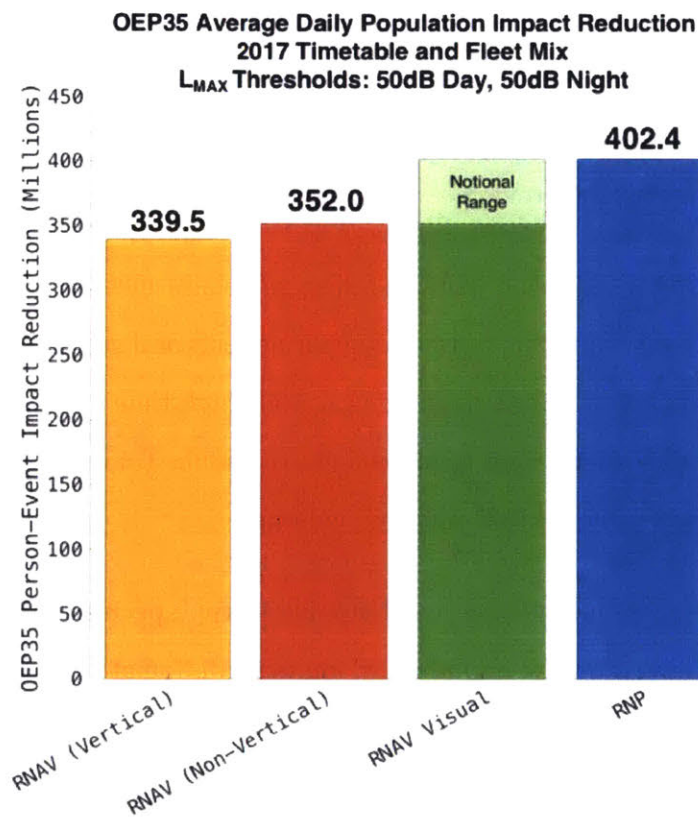


**Figure 101. Unconstrained best-case cumulative person-event impact benefit for PBN guidance technologies at the OEP-35 airports with a notional comparison to RNAV Visual procedures**

The second example procedure analysis was a system-level evaluation of noise reduction potential from the application of reduced speed departures on every RNAV SID procedure published at the OEP-35 airports. This procedure reduces the airframe component of noise for departing aircraft, resulting in a net noise reduction for speed regimes where airframe noise exceeds engine

noise. Results from the ANOPP noise model indicate that airframe noise exceeds engine noise at a transition speed in the vicinity of 220 knots for most modern jet aircraft, suggesting a potential noise benefit from reducing departure speeds to 220 knots (or the minimum safe speed in clean departure configuration). The noise reduction potential is most apparent directly below the departure track centerline at a distance of 5 to 15 NM from the departure end of the runway. Population benefits are greatest for procedures with significant population density underlying that segment of published RNAV SID procedures. This thesis ranked high-benefit procedures for potential implementation of reduced speed departures.

A system-level framework for noise reduction procedure development was also developed that includes an iterative feedback structure between community members, operational stakeholders, and the noise analyst who integrates constraints and objectives from each stakeholder. The objective of this structure is to allow community feedback at an early stage of procedure development for integration into suggested procedure development prior to entering the formal implementation process. This increases the likelihood of community buy-in during the development, implementation, and operational rollout of advanced operational procedures. In order for successful application of this framework, the noise and procedure analyst must integrate the objectives of multiple stakeholders into a coherent objective function and noise metric for the purpose of procedure evaluation and refinement. A preliminary application of this approach was presented for Boston Logan Airport, including recommendation of the RNAV lateral approach redesign concept for Runway 33L and reduced-speed departure concept for Runway 33L and 27 given actual constraints and stakeholder interactions in the context of a contemporary noise-sensitive airport.

## **8.2 Key Outcomes**

The framework and analysis results from this thesis have potential use for determining appropriate next steps in continued development and deployment of advanced operational procedures in the NAS. Development of RNAV and RNP procedures to date have not taken full advantage of the noise reduction potential of PBN track flexibility. As a result, the overriding public perception has been increased overflight concentration rather than beneficial track relocation.

Therefore, a technical and public perception opportunity exists for future rollout of these procedures. The opportunity is runway-specific. In some cases, reduction of the final approach segment length provides the majority of benefit. In other cases, sharper final approach interception angles and tighter maneuvering tolerances from RNAV and RNP guidance provide the benefits mechanism. In either case, this thesis shows that noise reduction potential exists for all runway ends at the OEP-35 airports in the NAS relative to straight-in arrivals by using criteria-compliant RNAV and RNP procedures. In all cases, RNAV provides benefit while RNP provides additional incremental benefit in some cases. Which technology is appropriate for specific runways depends on equipage levels and air traffic control procedures already in place at that airport.

The results from the RNAV and RNP benefits study also demonstrate the sensitivity of noise-reduction procedure design parameters to the chosen objective metric and threshold. Exposure-minimizing ground tracks may differ with a change in aircraft type or  $L_{MAX}$  threshold level. This sensitivity reinforces the nature of procedure design for noise minimization as a “wicked” optimization problem as discussed in Section 2.9. As a result, it is important to include a discussion of procedure objectives and metrics with impacted stakeholders rather than showing optimized procedures based on assumed value structures.

The rapid noise-analysis framework and procedure identification framework in this thesis has potential application as a screening tool for identification of high-value airports for procedure modification in the NAS. The speed of the noise contour generation method also allows for potential interactive noise visualization and design iteration tools for improved communication and negotiation capability between operational and community stakeholders.

### **8.3 Research Recommendations and Future Work**

The first key area for future work is to expand the multi-stakeholder procedure design framework to include additional degrees of freedom for system modification. There are additional mechanisms available for operational noise reduction, each with potential operational, technical, and political issues that must be considered in the development process. Examples include runway use planning, schedule constraints based on noise targets, noise-based fee structures, and infrastructure



development such as new runways. The relative costs, complexity, and environmental benefits of each of these options could be evaluated most effectively with a common analysis framework integrating stakeholder value tradeoffs and negotiation structures.

In addition, the iterative loop connecting the analytical procedure development process with community feedback processes could be formalized and expanded with a robust integration of negotiation theory and game-theoretic convergence on an acceptable solution. The current framework implies that community processes will occur outside of the analytical process to determine equity and acceptability of proposed solutions. This assumption may be inadequate in cases where community objectives are strongly misaligned, potentially resulting in impasse rather than iteration in practical implementation of the framework for contentious system modifications. Formal treatment of equity definition and associated negotiation processes could result in an analysis framework more representative of political realities in procedure design.

In terms of the RNAV and RNP procedure development system-level case study, the results in this thesis do not account for interactions between procedures. Each runway is assumed to operate independently of other arrival and departure procedures. A higher-fidelity airport level benefits analysis could provide refined impact assessment given runway configurations and ATC spacing requirements. In addition, the noise-reduction procedure identification process in this thesis involved precomputing a large set of possible PBN procedure definitions and selecting the minimum impact case. The resulting procedure is not optimal, but the best-case solution of the study's sample set. An optimizer-based solution would be useful to ensure that the best possible solution is identified for each runway end, given criteria constraints and additional limitations with respect to airspace and procedural separation requirements.

While the RNAV and RNP benefits analysis in this thesis focuses on approach procedures, there are also potential benefits from optimal track routing for departure procedures using PBN guidance. Unlike RNAV approach procedure which require a final segment aligned with the landing runway, RNAV SIDs have greater flexibility in terms of leg alignment immediately after takeoff. However, procedures are still subject to criteria constraints in terms of minimum segment lengths and turn

geometry. There is an opportunity for future work to identify noise-optimal routing for departures given RNAV and RNP procedure design criteria for departures.

Communities across the NAS have expressed strong interest in flight track dispersion as an avenue for increasing noise equity and decreasing localized impact due to PBN procedure implementation. Further work is required to quantify the track concentration effects driving this community feedback and evaluate the potential impact of flight track dispersion with RNAV or RNP procedures. It is unclear whether increased track dispersion would alleviate or aggravate community noise annoyance, so the RNAV and RNP procedure evaluation framework introduced in this thesis could be expanded to include explicit integration of dispersion schemes that are compliant with operational constraints. This would provide valuable insight for communities, operational stakeholders, and regulators about the quantitative impact of flight track dispersion.

Further research is recommended for reduced speed departures and other speed/configuration dependent noise mitigation procedures with respect to projected noise benefits as well as operational flyability and safety assessment. The reduced speed departure benefits shown in this thesis are based on modeled results from NASA's ANOPP noise model. While this noise model is based on the best-available calibration data for aerodynamic noise sources, the underlying data was collected in the 1970s with aircraft types and operating speeds not representative of current-generation jet aircraft departures. Further modeling validation work is therefore recommended as future work to increase confidence in projected noise benefits from procedure concepts that primarily impact airframe noise sources. Examples of such procedures include steep approaches, continuous descent approaches, configuration scheduling (gear and flaps) on final approach, delayed deceleration approaches, and thrust/speed scheduling on departure for location-tailored noise reduction. Each of these procedures could be modeled at the system level using ANOPP and the system noise integration approach described in this thesis, although additional model validation through flight testing for extension of source data with modern aircraft types would be useful. Ultimately, each of these procedure concepts will require evaluation under a formal safety management system process.

In terms of clear communication and political utility, effective community engagement is a key challenge in technology development programs. Given the complexity of noise metric selection and impact analysis, community understanding and support for operational changes relies on clear communication of technical constraints as well as potential noise benefits. Continued research and development is necessary to identify opportunities for richer community interaction in the procedure design process while accounting for technical constraints. Examples include simplified user interfaces for procedure design which could allow for rapid evaluation of community-driven ideas as part of the solution refinement process. In addition, continued refinement of visualizations and reporting metrics is required, particularly in a changing noise environment where traditional DNL contours at the 65dB, 70dB, and 75dB levels do not adequately capture community noise concerns. It is currently unclear what visualizations and information communication strategies are required to address new metrics and community frustrations with respect to noise, suggesting a rich area of follow-on research and development.

Finally, it is important to explore trade-offs and valuation strategies between conflicting environmental and economic objectives in the procedure design process. As introduced in Section 5.10, there are widespread tradeoff opportunities between noise, fuel, emissions, time, and operational complexity. In many cases, the balance between conflicting objectives is not clear from the beginning, nor is the effect of emphasizing one objective or stakeholder over another. While multi-objective optimization formulations rely on weighting functions or other assumed valuation structures to find a single “best” solution, an approach to balanced procedure design that incorporates stakeholder input and varied objectives while accounting for the technical constraints of the NAS could serve as a valuable tool for system evolution and improvement.



## Appendix A OEP-35 Airports

The Operational Evaluation Partnership (OEP) 35 airports were originally selected by the FAA as a subset of all commercial airports that represent trends and metrics for the NAS as a whole.<sup>23</sup> All analyses for this thesis were performed for the OEP-35 airports (also shown in Figure 102).

Many recent operational studies use the “Core 30” airports in lieu of the OEP-35 airports. The Core 30 airports are a subset of the OEP-35 (omitting CVG, CLE, PIT, PDX, and STL). Therefore, results in this study can be translated to the Core 30 airports by removing all results referenced to the five non-overlapping airports.

---

<sup>23</sup> [http://aspmhelp.faa.gov/index.php/OEP\\_35](http://aspmhelp.faa.gov/index.php/OEP_35)

**Table 26. Listing of OEP-35 Airports**

ATL - Hartsfield-Jackson Atlanta Intl	DTW - Detroit Metropolitan Wayne County	LGA - New York LaGuardia	PHX - Phoenix Sky Harbor Intl
BOS - Boston Logan Intl	EWR - Newark Liberty Intl	MCO - Orlando Intl	PIT - Pittsburgh Intl
BWI - Baltimore/Washington Intl	FLL - Fort Lauderdale/Hollywood Intl	MDW - Chicago Midway	SAN - San Diego Intl
CLE - Cleveland Hopkins Intl	HNL - Honolulu Intl	MEM - Memphis Intl	SEA - Seattle/Tacoma Intl
CLT - Charlotte Douglas Intl	IAD - Washington Dulles Intl	MIA - Miami Intl	SFO - San Francisco Intl
CVG - Cincinnati/Northern Kentucky Intl	IAH - George Bush Houston Intercontinental	MSP - Minneapolis/St. Paul Intl	SLC - Salt Lake City Intl
DCA - Ronald Reagan Washington National	JFK - New York John F. Kennedy Intl	ORD - Chicago O'Hare Intl	STL - Lambert Saint Louis Intl
DEN - Denver Intl	LAS - Las Vegas McCarran Intl	PDX - Portland Intl	TPA - Tampa Intl
DFW - Dallas/Fort Worth Intl	LAX - Los Angeles Intl	PHL - Philadelphia Intl	

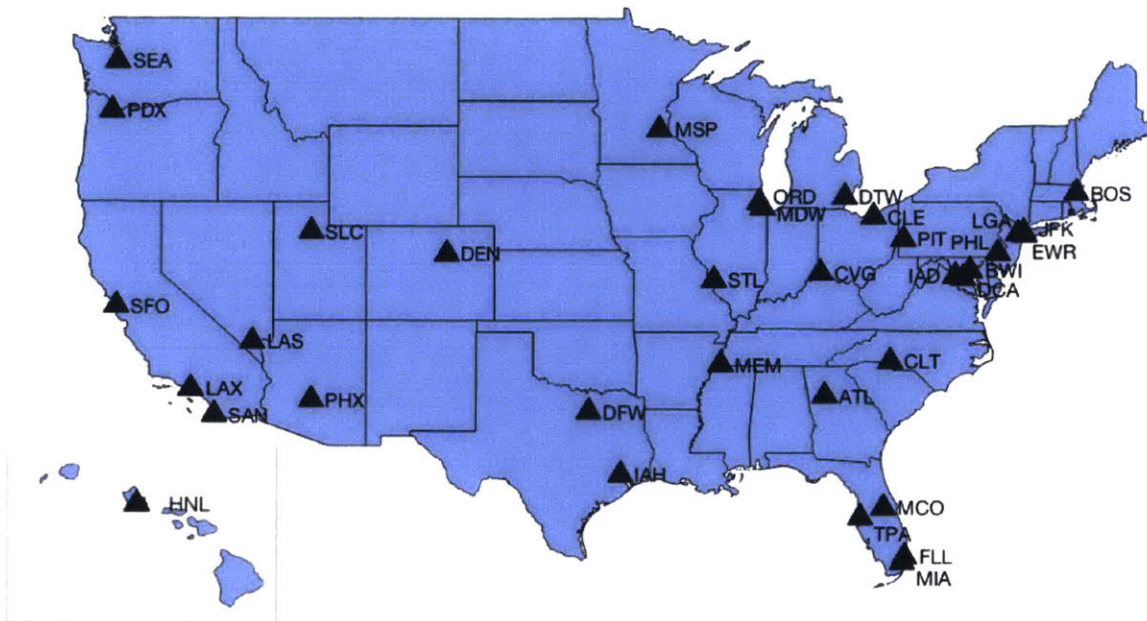


**Figure 102. Map Depiction of OEP-35 Airports**

## Appendix B Full RNAV and RNP Approaches: Population Exposure Results

The following noise exposure results are based on the methodology presented in Section Chapter 1. The exposure values are shown for a Boeing 737-800 flying a radar-median altitude profile based on historical arrivals by that aircraft type at Boston Logan Airport in 2015 and 2016. Population counts are based on 2010 US Census block-level data re-gridded to 0.1 NM x 0.1 NM resolution aligned with the respective runway ends.

Airport	Runway	Boeing 737-800 50 dB L <sub>MAX</sub> Radar Median Altitude Profile				Boeing 737-800 60 dB L <sub>MAX</sub> Radar Median Altitude Profile			
		Straight In	RNAV (Vertical Guidance)	RNAV (No Vert. Guidance)	RNP	Straight In	RNAV (Vertical Guidance)	RNAV (No Vert. Guidance)	RNP
KATL	10	30,371	30,306	30,306	30,209	12,358	11,067	11,067	10,709
	26L	41,828	32,908	32,699	31,996	12,453	8,772	8,772	5,614
	26R	42,115	33,028	33,028	32,961	11,862	8,066	8,066	5,745
	27L	37,377	33,355	32,718	32,028	14,047	10,580	9,851	5,696
	27R	39,153	33,362	32,844	33,677	15,052	12,204	11,611	7,956
	28	37,194	35,346	35,346	37,053	11,637	10,499	10,499	9,560
	8L	36,777	31,465	31,373	30,990	13,214	11,433	11,433	11,468
	8R	32,514	28,655	28,519	28,529	12,329	10,489	10,489	10,292
	9L	26,769	24,879	24,879	24,800	11,908	9,203	8,696	7,567
9R	26,038	24,657	24,629	24,619	11,714	9,441	9,101	7,643	
KBOS	14	248,533	202,198	192,472	176,418	112,909	75,270	71,124	65,084
	15L	231,642	206,444	200,260	143,318	104,915	94,614	88,004	66,770
	15R	230,679	198,681	197,186	160,864	98,846	88,492	81,675	68,031
	22L	168,934	48,741	48,741	40,320	62,240	25,857	23,945	18,993
	22R	163,983	53,160	52,975	45,721	64,440	30,782	28,941	23,159
	27	9,004	9,004	9,004	9,004	2,724	2,724	2,724	2,724
	32	28,247	2,827	2,798	2,798	4,064	0	0	0
	33L	21,739	4,376	3,506	3,108	1,096	0	0	0
	33R	41,730	22,024	22,024	22,024	6,142	4,482	4,482	4,340
	4L	108,794	91,883	70,705	27,092	32,222	25,077	24,211	9,256
4R	89,427	80,843	63,106	21,333	21,688	19,112	19,112	5,341	
9	334,454	265,961	261,226	151,963	148,249	118,495	105,619	52,713	
KBWI	10	47,091	21,978	19,422	17,354	11,598	2,780	2,482	2,739
	15L	70,813	42,609	40,898	38,137	20,714	8,744	7,271	6,408
	15R	38,168	31,872	31,872	32,544	10,727	5,359	4,737	5,614
	28	41,740	27,693	27,220	25,305	21,012	14,208	14,208	9,216
	33L	84,773	49,964	48,280	38,077	34,006	26,238	24,243	16,305
	33R	81,029	61,623	60,947	47,355	34,145	27,088	26,709	20,125

Airport	Runway	Boeing 737-800 50 dB L <sub>MAX</sub> Radar Median Altitude Profile				Boeing 737-800 60 dB L <sub>MAX</sub> Radar Median Altitude Profile			
		Straight In	RNAV (Vertical Guidance)	RNAV (No Vert. Guidance)	RNP	Straight In	RNAV (Vertical Guidance)	RNAV (No Vert. Guidance)	RNP
KCLE	10	71,751	42,003	41,771	37,517	19,134	17,043	17,043	15,513
	24L	126,528	85,333	83,120	54,192	58,862	39,874	38,881	26,156
	24R	114,438	83,162	80,842	48,461	48,831	38,825	38,825	23,953
	28	118,801	83,184	80,181	63,742	31,331	24,210	22,727	20,366
	6L	30,530	22,622	21,277	20,310	11,023	8,886	8,886	7,510
	6R	32,001	21,674	21,257	21,099	10,970	9,047	9,047	7,266
KCLT	18C	29,375	21,080	20,294	16,959	12,305	8,732	7,736	4,931
	18L	28,953	25,795	25,795	22,391	12,503	10,055	9,690	7,827
	18R	26,053	17,424	15,526	15,053	9,372	5,661	4,588	3,352
	23	74,169	40,450	38,270	33,561	20,061	14,973	14,973	12,663
	36C	27,307	24,588	24,588	16,538	6,275	5,332	5,204	5,082
	36L	31,670	25,600	22,999	15,931	10,589	6,002	6,002	4,615
	36R	30,220	26,531	24,945	22,570	12,055	7,628	7,628	3,817
	5	14,517	8,551	8,317	6,987	2,504	1,031	1,031	1,078
KCVG	18C	31,129	17,123	14,974	10,439	10,858	6,576	5,352	4,382
	18L	45,660	21,337	19,981	12,432	14,668	8,183	7,011	2,999
	18R	27,147	19,633	16,789	11,996	10,951	8,865	7,424	5,163
	27	53,875	34,278	33,908	33,832	19,270	12,490	11,343	8,803
	36C	35,816	25,513	24,452	22,039	18,387	12,739	12,585	10,243
	36L	35,085	26,724	25,359	19,941	15,354	13,046	12,584	7,513
	36R	38,178	28,844	27,839	26,920	16,094	12,352	11,063	7,578
	9	9,454	6,486	6,486	6,518	1,247	1,141	1,141	993
KDCA	1	59,750	51,759	51,759	52,960	13,898	10,056	10,056	7,286
	15	119,403	105,749	105,749	106,713	40,317	36,694	36,694	34,565
	19	313,754	196,734	176,613	121,774	88,703	68,955	64,419	37,962
	22	228,017	171,085	164,231	158,647	73,499	46,761	46,761	45,543
	33	84,188	82,564	81,900	66,076	39,577	36,324	36,174	18,940
	4	143,057	94,464	91,073	77,083	74,836	48,135	44,844	36,069
KDEN	16L	1,225	898	898	255	248	213	213	95
	16R	1,906	1,026	878	214	373	197	197	101
	17L	3,983	479	441	140	617	91	81	0
	17R	2,169	456	394	104	310	72	46	0
	25	264	92	87	87	42	3	1	0
	26	301	182	165	73	101	35	31	18
	34L	13,154	43	43	46	723	4	4	0
	34R	9,090	38	38	37	222	2	1	0
	35L	2,102	72	51	80	174	3	2	1
	35R	493	53	53	87	6	2	2	1
	7	74,228	5,536	5,536	2,707	1,976	1	1	1
8	55,275	1,304	1,210	15	5,930	0	0	0	
KDFW	13L	15,964	10,493	10,051	6,404	5,083	2,285	1,423	687
	13R	32,113	24,366	24,366	26,294	10,016	6,914	6,914	6,903
	17C	72,526	12,164	9,237	5,743	17,871	2,118	1,464	949
	17L	65,538	11,804	9,506	5,643	18,053	1,663	885	118
	17R	72,441	10,944	8,240	5,933	18,580	2,194	1,176	997
	18L	69,015	10,140	8,922	8,398	14,464	2,070	1,548	1,142
	18R	66,276	11,125	10,075	9,836	15,620	2,580	2,105	1,256
	31L	117,439	40,410	34,632	19,006	26,018	5,102	2,808	794



Airport	Runway	Boeing 737-800 50 dB L <sub>MAX</sub> Radar Median Altitude Profile				Boeing 737-800 60 dB L <sub>MAX</sub> Radar Median Altitude Profile			
		Straight In	RNAV (Vertical Guidance)	RNAV (No Vert. Guidance)	RNP	Straight In	RNAV (Vertical Guidance)	RNAV (No Vert. Guidance)	RNP
	31R	120,643	58,006	54,372	33,099	25,520	14,348	13,027	8,285
	35C	87,888	28,537	28,537	36,290	14,387	5,156	4,789	3,461
	35L	73,298	23,496	23,496	32,193	14,251	2,385	2,317	1,428
	35R	121,807	55,317	55,317	60,393	35,717	26,133	26,114	18,374
	36L	99,997	41,338	40,291	37,068	11,033	5,102	3,606	2,324
	36R	90,971	32,400	32,400	32,811	6,500	2,923	1,904	1,354
KDTW	21L	158,700	67,320	67,210	35,259	27,319	17,203	16,795	11,514
	21R	159,653	66,978	66,978	41,710	28,578	18,436	18,436	15,576
	22L	151,881	69,851	69,681	44,516	29,057	18,523	18,523	15,738
	22R	145,605	75,349	75,349	27,744	29,449	18,121	18,121	6,591
	27L	65,048	43,797	43,797	32,150	30,130	16,898	14,458	13,811
	27R	65,388	40,214	40,214	25,685	27,692	13,499	9,574	6,481
	3L	6,541	5,807	5,807	5,355	1,522	594	592	608
	3R	8,445	7,605	7,605	6,953	1,835	1,307	1,167	1,103
	4L	7,951	6,916	6,844	6,901	2,541	2,315	2,315	2,053
	4R	6,286	5,612	5,543	5,586	2,439	1,970	1,968	1,039
	9L	44,816	15,701	13,260	10,287	9,566	5,448	5,448	3,207
	9R	35,339	11,479	10,253	8,584	9,256	4,311	3,840	2,610
KEWR	11	184,410	161,444	161,144	149,139	79,419	64,675	60,462	56,327
	22L	164,488	106,902	104,762	115,571	25,461	25,256	25,228	22,365
	22R	191,927	119,735	115,622	122,961	32,563	31,337	31,299	28,255
	29	853,007	106,617	105,305	94,021	87,766	32,812	28,943	16,775
	4L	159,866	105,696	105,696	111,364	45,306	34,771	34,617	29,884
	4R	150,787	93,970	93,970	102,970	39,412	29,135	29,135	24,756
KFLL	10L	73,043	68,488	67,617	69,393	19,151	16,170	16,170	11,966
	10R	81,308	71,357	71,357	72,979	30,134	23,382	22,770	22,390
	28L	6,033	6,033	6,033	6,031	1,311	1,311	1,311	1,311
	28R	3,131	3,131	3,131	3,131	182	182	182	177
KIAD	12	2,037	1,738	1,738	1,756	355	336	336	302
	19C	19,164	12,768	11,060	9,462	6,684	3,006	2,725	2,627
	19L	28,228	23,613	23,529	18,216	6,389	4,318	4,273	3,090
	19R	43,269	29,743	23,850	13,959	21,045	12,354	8,634	4,367
	1C	88,815	9,491	7,458	7,912	17,829	2,938	2,938	2,248
	1L	76,644	10,648	10,648	11,506	7,897	3,180	3,180	2,401
	1R	99,043	45,097	39,707	19,186	30,116	19,338	16,879	3,379
	30	126,306	45,869	45,869	41,562	19,296	15,583	15,583	15,435
KIAH	15L	66,188	33,179	32,529	23,764	18,649	12,674	11,301	8,556
	15R	67,611	32,654	32,654	25,181	18,110	12,320	11,199	9,810
	26L	55,250	26,983	26,916	14,050	17,634	6,587	6,094	3,603
	26R	54,677	37,813	37,301	23,499	20,738	13,587	13,554	12,054
	27	48,888	28,876	26,032	16,974	17,343	5,999	5,999	6,295
	33L	82,742	25,643	23,613	18,515	18,220	4,516	3,767	3,288
	33R	80,463	26,776	24,942	18,658	18,874	7,585	5,705	4,407
	8L	99,717	70,174	66,932	43,137	28,772	25,471	24,693	10,900
	8R	102,526	70,443	65,355	44,856	20,795	16,665	16,665	10,678
	9	105,138	65,999	56,169	23,657	27,368	13,074	9,679	3,903

Airport	Runway	Boeing 737-800 50 dB L <sub>MAX</sub> Radar Median Altitude Profile				Boeing 737-800 60 dB L <sub>MAX</sub> Radar Median Altitude Profile			
		Straight In	RNAV (Vertical Guidance)	RNAV (No Vert. Guidance)	RNP	Straight In	RNAV (Vertical Guidance)	RNAV (No Vert. Guidance)	RNP
KJFK	13L	895,514	633,293	590,842	160,159	232,171	171,110	165,053	62,745
	13R	1,126,222	688,605	589,886	128,085	310,250	164,998	164,998	36,602
	22L	259,806	236,893	232,257	165,468	111,173	98,796	98,596	83,435
	22R	274,030	250,051	244,611	160,376	107,137	94,948	91,677	76,456
	31L	81,487	56,903	56,326	49,315	34,145	23,056	22,308	19,413
	31R	82,594	60,483	58,801	51,495	34,473	20,674	20,674	17,557
	4L	44,858	41,123	40,266	35,624	25,276	24,493	23,341	13,249
	4R	50,615	48,358	46,831	38,852	28,949	27,586	26,345	19,659
KLAS	19L	201,570	163,560	156,523	125,042	87,767	67,755	66,426	49,490
	19R	194,392	157,694	156,376	122,060	92,313	64,697	63,554	47,292
	1L	29,556	26,739	26,572	26,472	12,970	7,770	6,302	6,892
	1R	29,897	27,387	27,139	27,293	13,473	7,702	7,577	6,489
	26L	63,922	55,768	55,768	56,326	28,056	20,579	20,579	21,037
	26R	65,380	56,636	56,636	57,532	28,724	19,654	19,654	20,118
	8L	40,448	34,897	34,897	34,098	12,531	7,083	7,083	6,928
	8R	38,082	35,146	35,146	35,345	11,126	6,910	6,910	7,217
KLAX	24L	503,362	244,812	244,651	190,450	128,037	82,958	82,660	70,742
	24R	500,693	251,243	249,587	192,379	130,022	85,132	83,435	72,208
	25L	515,405	254,780	245,346	222,456	151,792	98,734	94,210	82,490
	25R	522,404	256,619	248,668	222,790	151,028	100,193	96,348	84,851
	6L	19,356	19,356	19,356	19,355	8,388	8,388	8,388	8,388
	6R	16,451	16,451	16,451	16,451	4,123	4,123	4,123	4,123
	7L	12,266	12,266	12,266	12,266	4,326	4,326	4,326	4,326
	7R	15,271	15,271	15,271	15,271	6,965	6,965	6,965	6,965
KLG A	13	664,190	476,398	476,398	478,062	232,372	191,001	191,001	183,769
	22	297,617	178,589	168,055	124,787	79,129	56,351	54,078	36,891
	31	531,549	382,790	373,165	282,194	202,103	172,277	171,063	159,623
	4	1,270,806	766,918	745,381	644,153	353,298	290,602	279,205	265,813
KMCO	17L	111,381	55,272	49,272	26,536	34,141	23,248	21,712	13,749
	17R	127,108	53,555	49,165	24,308	30,450	24,129	23,498	10,448
	18L	131,997	86,616	78,931	51,727	31,155	28,840	28,060	15,589
	18R	118,943	85,582	78,196	50,386	34,410	29,704	26,722	15,839
	35L	29,167	6,094	5,837	1,960	2,616	1,756	1,237	117
	35R	24,555	5,810	4,514	2,978	2,562	1,155	798	182
	36L	28,835	10,404	9,093	3,643	8,202	2,509	2,145	363
	36R	25,547	9,114	8,539	3,127	5,006	1,889	1,798	137
KMDW	13C	192,055	141,608	141,608	98,027	62,917	46,997	46,997	31,336
	13L	199,339	147,615	147,615	103,863	67,272	50,293	50,293	31,140
	13R	192,512	143,055	143,055	96,349	61,492	48,364	48,364	30,998
	22L	325,785	214,278	206,890	205,897	130,040	85,191	85,191	81,836
	22R	334,321	216,585	206,431	203,903	131,847	82,136	82,136	78,749
	31C	248,107	203,502	201,660	184,805	92,518	75,526	75,526	73,830
	31L	245,939	200,210	198,892	179,499	91,509	76,527	76,322	73,273
	31R	256,169	212,775	208,719	192,837	98,262	79,506	79,506	77,308
	4L	116,268	98,436	96,741	88,296	42,572	40,427	35,542	23,827
4R	117,628	100,244	96,073	86,371	39,805	37,879	34,553	21,263	

Airport	Runway	Boeing 737-800 50 dB L <sub>MAX</sub> Radar Median Altitude Profile				Boeing 737-800 60 dB L <sub>MAX</sub> Radar Median Altitude Profile			
		Straight In	RNAV (Vertical Guidance)	RNAV (No Vert. Guidance)	RNP	Straight In	RNAV (Vertical Guidance)	RNAV (No Vert. Guidance)	RNP
KMEM	18C	80,451	65,432	63,787	39,326	29,657	23,588	23,588	13,474
	18L	79,615	66,523	62,754	35,551	28,003	23,087	22,828	10,500
	18R	90,502	59,953	56,454	32,569	28,613	22,493	22,493	11,838
	27	99,751	67,018	56,010	31,867	39,587	32,024	26,523	13,572
	36C	33,633	25,039	25,039	22,612	9,293	8,435	8,144	5,365
	36L	39,685	29,407	29,360	29,791	15,564	14,046	14,046	10,784
	36R	31,869	24,414	24,414	21,604	9,833	8,796	8,564	5,703
9	22,640	18,184	17,523	16,991	11,495	7,601	6,780	5,845	
KMIA	12	41,224	29,678	22,960	13,028	19,608	9,468	8,036	6,747
	26L	126,651	108,748	108,748	110,194	60,010	52,282	52,282	51,713
	26R	127,080	111,746	111,746	112,937	60,203	54,699	53,317	50,986
	27	181,934	147,516	147,176	140,691	73,538	59,814	59,814	60,329
	30	155,214	136,095	134,786	125,208	79,052	70,446	68,406	64,974
	8L	24,315	21,560	21,560	20,032	8,891	8,255	7,513	5,176
	8R	17,583	16,615	16,615	17,519	5,032	4,272	3,940	1,924
9	77,108	62,561	57,268	50,599	36,040	23,119	21,929	14,212	
KMSP	12L	132,997	112,817	111,901	103,860	46,900	37,330	37,330	36,005
	12R	129,946	105,491	104,410	96,107	49,092	34,596	34,164	33,844
	17	214,166	155,486	150,870	107,493	73,443	61,478	54,263	39,148
	22	166,438	106,064	96,908	50,418	62,239	39,708	36,965	18,938
	30L	20,231	9,836	9,390	8,968	4,454	3,328	2,429	1,862
	30R	20,709	10,060	10,060	10,308	3,926	1,740	1,735	1,957
	35	79,837	41,745	41,745	30,719	20,637	11,601	9,983	3,802
4	72,655	57,589	54,709	52,063	29,260	24,498	24,433	19,246	
KORD	10C	88,683	71,629	68,614	59,594	28,057	26,761	26,761	19,879
	10L	85,300	69,118	66,132	55,881	27,181	22,773	22,341	17,018
	10R	93,433	76,732	73,149	64,129	34,110	29,483	29,483	19,834
	15	91,801	47,565	44,185	44,167	23,907	5,241	5,241	4,866
	22L	113,927	109,551	109,551	99,616	38,567	33,589	33,261	18,596
	22R	109,080	103,411	99,475	88,263	49,894	41,147	40,265	22,341
	27L	300,660	126,814	122,832	113,079	66,189	42,535	39,968	34,989
	27R	249,407	111,513	109,236	104,189	51,388	38,132	38,132	34,610
	28C	358,306	148,004	144,052	128,868	106,520	51,310	49,587	32,026
	28L	377,791	150,886	149,213	105,920	85,206	46,860	44,923	25,473
	28R	346,608	153,229	143,512	131,240	116,932	60,642	56,271	49,584
	33	335,519	119,334	116,837	99,540	51,221	29,883	29,595	25,801
	4L	116,980	92,047	89,558	73,010	29,507	17,870	17,870	18,098
	4R	124,019	86,663	86,663	78,392	33,713	18,448	16,839	14,629
9L	120,727	51,038	51,038	46,465	30,755	13,774	12,388	8,488	
9R	86,931	46,456	43,676	38,323	12,034	7,322	7,322	6,632	
KPDX	10L	20,075	13,677	11,504	8,006	4,939	2,897	2,492	2,293
	10R	10,136	8,878	8,527	5,734	4,688	4,150	4,125	3,029
	21	57,353	54,558	54,558	41,594	27,872	25,549	24,765	21,250
	28L	87,591	22,327	19,490	11,328	25,423	7,402	5,380	1,090
	28R	59,633	12,140	9,915	4,596	14,807	994	837	289
3	175,140	72,236	66,466	63,437	58,118	32,965	32,965	31,941	

Airport	Runway	Boeing 737-800 50 dB L <sub>MAX</sub> Radar Median Altitude Profile				Boeing 737-800 60 dB L <sub>MAX</sub> Radar Median Altitude Profile			
		Straight In	RNAV (Vertical Guidance)	RNAV (No Vert. Guidance)	RNP	Straight In	RNAV (Vertical Guidance)	RNAV (No Vert. Guidance)	RNP
KPHL	17	216,591	162,226	151,286	132,437	95,087	71,586	68,209	60,788
	26	104,080	52,353	47,670	31,700	28,608	10,377	3,167	7,347
	27L	101,202	38,295	38,029	23,954	16,872	1,597	1,597	803
	27R	104,975	43,110	40,722	30,936	24,412	1,236	1,236	3,463
	35	29,609	14,722	12,680	9,335	8,700	3,693	3,118	1,386
	8	96,737	8,270	7,295	6,138	20,623	4,110	3,583	441
	9L	91,007	8,779	6,786	5,837	23,643	3,719	3,718	3,200
9R	83,845	13,228	9,264	5,685	24,873	2,275	2,119	2,084	

# Appendix C Reduced Speed Departures: Population Exposure Results

This appendix present population exposure reduction results for introducing reduced speed departures on the 200 highest-impact published SIDs. Results are separated by airport, SID, and runway designation. Additional segregation by transition waypoint is included in the table when the choice of transition impacts noise exposure results. When all transitions for the same SID and runway have the same noise impacts for reduced speed departures, the procedure is included in the table only once. By this method, there are 1,590 different departure procedures where noise results were calculated in this analysis. The 200 shown below are those with the largest product between average daily jet departure rate from the runway in question and the total population reduction for the Boeing 737-800 at the 60dB L<sub>MAX</sub> threshold level.

Rank	Airport	Rwy	Avg Jet Deps/Hr (2017)	SID	Transition	B738 250 Kt Dep	B738 220 Kt Dep	B738 Noise Pop. Δ	B773 Noise Pop. Δ	E170 Noise Pop. Δ
1	KLGA	13	13.7	GLDMN5	-	537,856	438,472	99,384	21,405	115,379
2	KLGA	13	13.7	NTHNS4	-	423,092	403,860	19,232	1,560	74,437
3	KEWR	22R	18.0	PORTT4	ELIOT	56,949	43,061	13,888	3,495	2,200
4	KEWR	22R	18.0	PORTT4	BIGGY	56,534	43,119	13,415	6,597	2,063
5	KEWR	22R	18.0	PORTT4	LANNA	56,534	43,119	13,415	6,597	2,063
6	KEWR	22R	18.0	PORTT4	PARKE	56,534	43,119	13,415	6,597	2,063
7	KIAH	15R	15.6	BNDT05	All	45,019	29,966	15,053	4,147	10,226
8	KDFW	17R	18.4	HRPER3	HULZE	27,226	15,076	12,150	3,078	4,093
9	KDFW	17R	18.4	HUDAD2	-	27,226	15,076	12,150	3,033	4,093
10	KPHX	25R	18.7	LALUZ5	All	45,277	33,422	11,855	7,282	5,462
11	KPHX	25R	18.7	SNOBL5	All	45,277	33,422	11,855	7,282	5,462
12	KPHX	25R	18.7	YOTES5	All	45,277	33,422	11,855	7,282	5,462
13	KPHX	25R	18.7	MAYSA5	All	45,023	33,422	11,601	3,085	5,439
14	KIAH	15L	15.1	BNDT05	All	42,261	28,332	13,929	4,902	9,702
15	KPHX	7L	13.2	IZZZ06	All	46,024	31,304	14,720	4,337	9,791
16	KPHX	7L	13.2	JUDTH6	MOHAK	46,024	31,304	14,720	4,418	9,791
17	KDFW	17R	18.4	ARDIA6	All	20,874	11,778	9,096	1,815	4,728
18	KDFW	17R	18.4	DARTZ7	All	20,874	11,778	9,096	1,815	4,728
19	KDFW	17R	18.4	JASPA5	WINDU	20,874	11,778	9,096	1,815	4,728
20	KDFW	17R	18.4	NELYN5	All	20,874	11,778	9,096	1,815	4,728
21	KDFW	17R	18.4	FORCK2	-	20,873	11,778	9,095	94	4,728
22	KDFW	17R	18.4	MRSSH2	All	20,873	11,778	9,095	70	4,728
23	KPHX	7L	13.2	KATMN5	PHASE	60,984	48,521	12,463	582	14,229
24	KDFW	18L	17.8	AKUNA7	MLC	29,879	21,098	8,781	2,137	4,941
25	KDFW	18L	17.8	BLECO8	All	29,879	21,098	8,781	2,137	4,941
26	KDFW	18L	17.8	GRABE8	All	29,879	21,098	8,781	2,137	4,941
27	KDFW	18L	17.8	HRPER3	HULZE	29,879	21,098	8,781	3,365	4,941
28	KDFW	18L	17.8	HUDAD2	-	29,879	21,098	8,781	3,157	4,941
29	KDFW	18L	17.8	LOWGN8	All	29,879	21,098	8,781	2,137	4,941
30	KDFW	18L	17.8	FORCK2	-	18,028	9,292	8,736	-282	2,878

Rank	Airport	Rwy	Avg Jet Deps/Hr (2017)	SID	Transition	B738 250 Kt Dep	B738 220 Kt Dep	B738 Noise Pop. Δ	B773 Noise Pop. Δ	E170 Noise Pop. Δ
31	KDFW	18L	17.8	MRSSH2	All	18,028	9,292	8,736	-280	2,878
32	KPHX	25R	18.7	WETAL1	-	21,124	12,985	8,139	20	2,005
33	KBOS	33L	6.3	PATSS5	-	188,708	165,594	23,114	3,486	35,742
34	KBOS	33L	6.3	BRUWN5	-	188,172	165,594	22,578	6,807	35,742
35	KBOS	33L	6.3	CELTk5	-	188,172	165,594	22,578	6,807	35,742
36	KBOS	33L	6.3	SSOX5	-	188,172	165,594	22,578	6,807	35,742
37	KPHX	7L	13.2	BNYRD5	TUS	71,530	61,234	10,296	2,490	14,360
38	KPHX	25R	18.7	ZIDOG1	-	35,647	28,512	7,135	8,403	8,442
39	KPHX	7L	13.2	FTHLS5	All	28,116	18,001	10,115	2,994	1,022
40	KJFK	13R	7.6	DEEZZ4	All	62,131	44,536	17,595	7,865	7,828
41	KIAH	15L	15.1	PITZZ4	All	37,302	28,677	8,625	2,309	13,332
42	KSEA	16L	10.7	BANGR9	All	84,675	72,649	12,026	-83	15,058
43	KSEA	16L	10.7	HAROB6	All	84,675	72,649	12,026	-214	15,058
44	KIAH	15R	15.6	PITZZ4	CRGER	38,673	30,662	8,011	1,783	13,451
45	KIAH	15R	15.6	PITZZ4	MNURE	38,660	30,662	7,998	1,923	13,451
46	KIAH	15R	15.6	PITZZ4	SAT	38,660	30,662	7,998	1,923	13,451
47	KIAH	15R	15.6	PITZZ4	WAILN	38,660	30,662	7,998	678	13,451
48	KBOS	33L	6.3	BLZZR4	-	175,979	157,555	18,424	-442	36,005
49	KPHX	7L	13.2	MAYSA5	All	39,202	30,873	8,329	2,704	9,145
50	KPHX	7L	13.2	SNOBL5	All	39,202	30,873	8,329	2,803	9,145
51	KPHX	7L	13.2	YOTES5	All	39,202	30,873	8,329	2,692	9,145
52	KBWI	28	7.9	TERPZ6	JERES	36,934	26,538	10,396	330	11,328
53	KBWI	28	7.9	TERPZ6	MCRAY	36,934	26,538	10,396	330	11,328
54	KATL	8R	12.6	PADGT2	All	25,866	19,518	6,348	4,003	5,615
55	KATL	8R	12.6	PENCL2	All	25,866	19,518	6,348	4,003	5,615
56	KATL	8R	12.6	SMKEY2	BOBBD	25,866	19,518	6,348	4,003	5,615
57	KATL	8R	12.6	VARNM2	All	25,866	19,518	6,348	4,003	5,615
58	KBWI	28	7.9	TERPZ6	FLASK	36,721	26,569	10,152	615	11,323
59	KBWI	28	7.9	TERPZ6	GSO	36,721	26,569	10,152	615	11,323
60	KBWI	28	7.9	TERPZ6	LYH	36,721	26,569	10,152	615	11,323
61	KBWI	28	7.9	TERPZ6	MAULS	36,721	26,569	10,152	615	11,323
62	KBWI	28	7.9	TERPZ6	OTTTO	36,721	26,569	10,152	625	11,323
63	KBWI	28	7.9	TERPZ6	RAMAY	36,721	26,569	10,152	625	11,323
64	KBWI	28	7.9	TERPZ6	SBV	36,721	26,569	10,152	615	11,323
65	KATL	8R	12.6	GAIRY2	IRQ	25,827	19,529	6,298	3,478	5,615
66	KATL	8R	12.6	JACCC2	KELLN	25,827	19,529	6,298	3,478	5,615
67	KATL	8R	12.6	PHIIL2	GRD	25,827	19,529	6,298	3,478	5,615
68	KATL	8R	12.6	PLMMR2	SPA	25,827	19,529	6,298	3,478	5,615
69	KSEA	16C	6.7	BANGR9	All	82,780	71,074	11,706	116	14,337
70	KSEA	16C	6.7	HAROB6	All	82,780	71,074	11,706	7	14,337
71	KMIA	8R	12.0	PADUS2	-	97,094	90,687	6,407	-6	5,576
72	KMIA	8R	12.0	VAIY2	-	97,094	90,687	6,407	-6	5,576
73	KATL	8R	12.6	CUTTn2	HANKO	20,877	14,842	6,035	5,584	3,576
74	KATL	8R	12.6	KAJIN2	STNGA	20,877	14,842	6,035	5,584	3,576
75	KATL	8R	12.6	NASSA2	All	20,877	14,842	6,035	5,584	3,576
76	KATL	8R	12.6	POUNC2	All	20,877	14,842	6,035	5,584	3,576
77	KATL	8R	12.6	BANNG2	LUCKK	27,605	21,675	5,930	396	2,891
78	KATL	8R	12.6	HAALO2	SARGE	27,605	21,675	5,930	400	2,891
79	KATL	8R	12.6	SMLTZ2	WALET	27,605	21,675	5,930	398	2,891
80	KATL	8R	12.6	VRSTY2	MCN	27,605	21,675	5,930	398	2,891
81	KMIA	8R	12.0	HITAG2	All	92,810	86,664	6,146	-410	6,652
82	KBOS	33L	6.3	REVSS4	-	165,104	153,610	11,494	-986	33,328
83	KATL	9L	12.6	BANNG2	LUCKK	22,352	16,733	5,619	188	2,942
84	KATL	9L	12.6	CUTTn2	HANKO	22,352	16,733	5,619	127	2,942
85	KATL	9L	12.6	HAALO2	SARGE	22,352	16,733	5,619	191	2,942

Rank	Airport	Rwy	Avg Jet Deps/Hr (2017)	SID	Transition	B738 250 Kt Dep	B738 220 Kt Dep	B738 Noise Pop. Δ	B773 Noise Pop. Δ	E170 Noise Pop. Δ
86	KATL	9L	12.6	KAJIN2	STNGA	22,352	16,733	5,619	127	2,942
87	KATL	9L	12.6	NASSA2	All	22,352	16,733	5,619	127	2,942
88	KATL	9L	12.6	POUNC2	All	22,352	16,733	5,619	127	2,942
89	KATL	9L	12.6	SMLTZ2	WALET	22,352	16,733	5,619	188	2,942
90	KATL	9L	12.6	VRSTY2	MCN	22,352	16,733	5,619	188	2,942
91	KDFW	35L	5.4	TRYTN3	LOOSE	26,004	13,375	12,629	266	6,395
92	KDFW	35L	5.4	ZACHH3	BSKAT	26,004	13,375	12,629	262	6,395
93	KDFW	35L	5.4	AKUNA7	MLC	25,970	13,375	12,595	-181	6,395
94	KDFW	35L	5.4	BLECO8	All	25,970	13,376	12,594	770	6,395
95	KDFW	35L	5.4	GRABE8	All	25,970	13,376	12,594	613	6,395
96	KDFW	35L	5.4	LOWGN8	All	25,970	13,376	12,594	1,021	6,395
97	KATL	27R	22.1	GAIRY2	IRQ	17,422	14,365	3,057	567	2,609
98	KATL	27R	22.1	JACCC2	KELLN	17,422	14,365	3,057	567	2,609
99	KATL	27R	22.1	PHIL2	GRD	17,422	14,365	3,057	567	2,609
100	KATL	27R	22.1	PLMMR2	SPA	17,422	14,365	3,057	567	2,609
101	KATL	8R	12.6	WIGLE2	All	24,282	19,161	5,121	300	5,847
102	KDFW	36R	5.0	TRYTN3	LOOSE	25,559	12,735	12,824	224	5,710
103	KDFW	36R	5.0	ZACHH3	BSKAT	25,559	12,735	12,824	224	5,710
104	KMIA	8L	9.2	PADUS2	-	95,788	88,926	6,862	-127	6,362
105	KMIA	8L	9.2	VAILY2	-	95,788	88,926	6,862	-127	6,362
106	KPHX	25R	18.7	KEENS1	All	16,420	13,135	3,285	806	1,993
107	KDCA	1	15.8	BOOCK3	COLIN	80,030	76,322	3,708	8,128	5,708
108	KDCA	1	15.8	DOCTR4	AGARD	80,030	76,322	3,708	8,817	5,708
109	KDCA	1	15.8	DOCTR4	DQO	80,030	76,322	3,708	8,817	5,708
110	KDCA	1	15.8	SOOKI4	SWANN	80,030	76,322	3,708	10,444	5,708
111	KMIA	8R	12.0	HEDLY2	-	94,082	89,230	4,852	8,066	7,881
112	KMIA	8R	12.0	WINCO2	-	94,082	89,230	4,852	8,066	7,881
113	KDFW	18L	17.8	ALIAN2	-	14,782	11,508	3,274	4,867	3,870
114	KDFW	18L	17.8	KATZZ2	BRHMA	14,782	11,508	3,274	4,923	3,870
115	KDFW	18L	17.8	WSTEX2	All	14,782	11,508	3,274	4,867	3,870
116	KDFW	18L	17.8	ARDIA6	All	14,771	11,508	3,263	4,355	3,870
117	KDFW	18L	17.8	DARTZ7	All	14,771	11,508	3,263	4,355	3,870
118	KDFW	18L	17.8	JASPA5	WINDU	14,771	11,508	3,263	4,344	3,870
119	KDFW	18L	17.8	NELYN5	All	14,771	11,508	3,263	5,733	3,870
120	KMIA	8L	9.2	HITAG2	All	93,880	87,716	6,164	-89	5,979
121	KJFK	4L	2.9	DEEZZ4	All	147,943	128,630	19,313	7,650	26,553
122	KCLT	18L	9.4	KRITR4	All	18,916	13,127	5,789	3,412	858
123	KBOS	33L	6.3	HYLND5	-	130,683	122,152	8,531	2,451	8,667
124	KDEN	25	10.6	CONN4	-	5,088	1	5,087	8,469	-1
125	KDEN	25	10.6	EPKEE4	All	5,054	1	5,053	1,218	0
126	KBOS	33L	6.3	LBSTA6	-	130,505	122,152	8,353	383	8,667
127	KLAS	26R	3.0	STAAV8	All	40,174	22,695	17,479	11,109	8,558
128	KJFK	31L	18.2	SKORR3	RNGRR	30,571	27,699	2,872	-838	3,641
129	KCLT	18L	9.4	WEAZL3	CLAWD	18,666	13,198	5,468	118	878
130	KDFW	35L	5.4	HRPER3	HULZE	19,049	9,804	9,245	184	5,117
131	KDFW	35L	5.4	HUDAD2	-	19,049	9,804	9,245	184	5,117
132	KDCA	19	7.9	HORTO3	All	58,223	52,182	6,041	5,685	11,315
133	KDCA	19	7.9	REBLL4	OTTTO	58,223	52,182	6,041	5,206	11,315
134	KDCA	19	7.9	WYNGS4	RAMAY	58,223	52,182	6,041	4,453	11,315
135	KDFW	36R	5.0	LOWGN8	All	21,964	12,401	9,563	4,768	5,507
136	KSLC	16R	2.8	WEVIC6	All	50,735	34,027	16,708	4,420	17,599
137	KDFW	36R	5.0	AKUNA7	MLC	21,914	12,401	9,513	1,925	5,507
138	KDFW	36R	5.0	BLECO8	All	21,914	12,401	9,513	1,961	5,507
139	KDFW	36R	5.0	GRABE8	All	21,914	12,401	9,513	1,861	5,507
140	KATL	27R	22.1	BANNG2	LUCKK	17,064	14,941	2,123	-57	3,425

Rank	Airport	Rwy	Avg Jet Deps/Hr (2017)	SID	Transition	B738 250 Kt Dep	B738 220 Kt Dep	B738 Noise Pop. Δ	B773 Noise Pop. Δ	E170 Noise Pop. Δ
141	KATL	27R	22.1	HAALO2	SARGE	17,064	14,941	2,123	-57	3,425
142	KATL	27R	22.1	SMLTZ2	WALET	17,064	14,941	2,123	-57	3,425
143	KATL	27R	22.1	VRSTY2	MCN	17,064	14,941	2,123	-57	3,425
144	KATL	26L	22.2	CUTTN2	HANKO	22,209	20,103	2,106	1,789	2,488
145	KATL	26L	22.2	KAJIN2	STNGA	22,209	20,103	2,106	1,804	2,488
146	KATL	26L	22.2	NASSA2	All	22,209	20,103	2,106	1,789	2,488
147	KATL	26L	22.2	POUNC2	All	22,209	20,103	2,106	1,811	2,488
148	KATL	27R	22.1	CUTTN2	HANKO	17,053	14,941	2,112	3	3,425
149	KATL	27R	22.1	KAJIN2	STNGA	17,053	14,941	2,112	-7	3,425
150	KATL	27R	22.1	NASSA2	All	17,053	14,941	2,112	-7	3,425
151	KATL	27R	22.1	POUNC2	All	17,053	14,941	2,112	-13	3,425
152	KLGA	13	13.7	TNNIS6	-	272,485	269,102	3,383	-766	8,575
153	KCLT	18L	9.4	JOJJO3	All	18,122	13,198	4,924	396	878
154	KMIA	27	3.2	DEEEP2	All	86,652	72,543	14,109	5,249	10,275
155	KMIA	8L	9.2	HEDLY2	-	96,010	91,109	4,901	8,103	5,537
156	KMIA	8L	9.2	WINCO2	-	96,010	91,109	4,901	8,103	5,537
157	KDCA	19	7.9	CLTCH2	All	57,885	52,182	5,703	2,032	11,315
158	KDCA	19	7.9	JDUBB2	All	57,885	52,182	5,703	2,038	11,315
159	KDCA	19	7.9	SCRAM4	LYH	57,885	52,182	5,703	2,118	11,315
160	KBOS	27	3.4	WYLYY3	-	184,996	171,929	13,067	2,087	29,141
161	KDEN	25	10.6	EXTAN4	-	4,178	1	4,177	370	0
162	KDFW	36R	5.0	HRPER3	HULZE	21,324	12,401	8,923	180	5,507
163	KDFW	36R	5.0	HUDAD2	-	21,324	12,401	8,923	177	5,507
164	KDFW	35L	5.4	ARDIA6	All	28,055	19,910	8,145	9,850	9,864
165	KDFW	35L	5.4	DARTZ7	All	28,055	19,910	8,145	9,850	9,864
166	KDFW	35L	5.4	FORCK2	-	28,055	19,910	8,145	9,247	9,864
167	KDFW	35L	5.4	JASPA5	WINDU	28,055	19,910	8,145	9,850	9,864
168	KDFW	35L	5.4	MRSSH2	All	28,055	19,910	8,145	10,527	9,864
169	KDFW	35L	5.4	NELYN5	All	28,055	19,910	8,145	9,850	9,864
170	KCLT	18C	9.4	JOJJO3	All	15,301	10,689	4,612	377	1,958
171	KPHX	25R	18.7	IZZZO6	All	30,595	28,320	2,275	6,665	7,806
172	KCLT	18C	9.4	WEAZL3	CLAWD	15,197	10,689	4,508	267	1,958
173	KLAS	1R	3.1	SHEAD1	All	118,144	104,588	13,556	-413	23,264
174	KSTL	12L	3.0	BGOOD4	VIH	72,871	59,158	13,713	2,660	15,117
175	KSTL	12L	3.0	BRAKK4	HLV	72,871	59,158	13,713	1,615	15,117
176	KSTL	12L	3.0	JAHNY4	MAP	72,871	59,158	13,713	3,059	15,117
177	KSTL	12L	3.0	WHRLI5	MCM	72,871	59,158	13,713	1,615	15,117
178	KSFO	1R	13.9	SSTIK3	All	47,762	44,787	2,975	652	19,445
179	KCLT	36R	11.0	KWEEN3	All	22,597	18,842	3,755	6,269	3,200
180	KCLT	36R	11.0	BEAVY4	All	22,568	18,842	3,726	3,028	3,200
181	KCLT	36R	11.0	ICONS3	NOOKS	22,568	18,842	3,726	3,674	3,200
182	KCLT	18C	9.4	BOBZY3	All	15,039	10,689	4,350	314	1,958
183	KCVG	27	4.0	ROCKT8	All	22,843	12,706	10,137	6,214	3,439
184	KPHX	25R	18.7	BNYRD5	TUS	37,285	35,148	2,137	-252	9,800
185	KPHX	25R	18.7	FTHLS5	All	37,285	35,148	2,137	-254	9,800
186	KPHX	25R	18.7	JUDTH6	MOHAK	37,285	35,148	2,137	-221	9,800
187	KPHX	25R	18.7	KATMN5	PHASE	37,285	35,148	2,137	-251	9,800
188	KSLC	16L	2.9	WEVIC6	All	47,987	34,121	13,866	3,953	15,841
189	KLAS	1R	3.1	BOACH8	All	117,742	104,726	13,016	-347	23,395
190	KBOS	27	3.4	HYLND5	-	187,811	176,074	11,737	5,767	32,780
191	KBOS	27	3.4	LBSTA6	-	187,811	176,074	11,737	5,848	32,780
192	KBOS	27	3.4	REVSS4	-	187,808	176,074	11,734	3,699	32,780
193	KATL	27R	22.1	ZELAN4	All	16,821	15,033	1,788	2,190	3,093
194	KSTL	12L	3.0	BERYY4	LIT	72,693	59,668	13,025	2,581	15,128
195	KSTL	12L	3.0	CHUUC4	All	72,693	59,668	13,025	2,719	15,128



Rank	Airport	Rwy	Avg Jet Deps/Hr (2017)	SID	Transition	B738 250 Kt Dep	B738 220 Kt Dep	B738 Noise Pop. Δ	B773 Noise Pop. Δ	E170 Noise Pop. Δ
196	KCLT	36R	11.0	LILLS1	-	22,440	18,842	3,598	2,898	3,200
197	KCLT	36R	11.0	KILNS3	AUDII	22,411	18,843	3,568	2,708	3,200
198	KCLT	36R	11.0	BARMY3	All	22,379	18,842	3,537	4,714	3,200
199	KMSP	17	5.8	SLAYR4	TEYOU	26,526	19,948	6,578	1,095	1,330
200	KATL	27R	22.1	PADGT2	All	14,695	12,964	1,731	3,157	1,746



## References

- [1] ICAO (International Civil Aviation Organization), "On Board a Sustainable Future: ICAO Environmental Report 2016," 2016.
- [2] M. Brink *et al.*, "Annoyance responses to stable and changing aircraft noise exposure," *J. Acoust. Soc. Am.*, vol. 124, no. 3432, 2008.
- [3] Federal Aviation Administration, "Performance Based Navigation: PBN NAS Navigation Strategy 2016," 2016.
- [4] G. C. Oates, *Aerothermodynamics of Aircraft Engine Components*. American Institute of Aeronautics & Astronautics, 1985.
- [5] C. K. W. Tam, "Jet Noise: Since 1952," *Theor. Comput. Fluid Dyn.*, vol. 10, no. 1–4, pp. 393–405, 1998.
- [6] W. Dobrzynski, "Almost 40 Years of Airframe Noise Research: What Did We Achieve?," *J. Aircr.*, vol. 47, no. 2, pp. 353–367, 2010.
- [7] M. R. Fink, "Airframe Noise Prediction Method," 1977.
- [8] M. Pott-Pollenske, W. Dobrzynski, H. Buchholz, B. Gehlhar, and F. Walle, "Validation of a semiempirical airframe noise prediction method through dedicated A319 flyover noise measurements," *8th AIAA/CEAS Aeroacoustics Conf. Exhib.*, no. June, pp. 1–11, 2002.
- [9] O. Zaporozhets, V. Tokarev, and K. Attenborough, *Aircraft noise: assessment, prediction and control*. New York: Spon Press, 2011.
- [10] R. H. Randall, *An Introduction to Acoustics*. New York: Dover Publications, 2005.
- [11] K. Attenborough, "Sound Propagation in the Atmosphere - Springer Handbook of Acoustics," T. D. Rossing, Ed. New York, NY: Springer New York, 2007, pp. 113–147.
- [12] C. M. Harris, "Absorption of Sound in Air Versus Humidity and Temperature," *J. Acoust. Soc. Am.*, vol. 40, no. 1, pp. 148–159, 1966.
- [13] M. Basner *et al.*, "Aviation Noise Impacts: State of the Science.," *Noise Health*, vol. 19, no. 87, pp. 41–50, 2017.
- [14] R. Guski, U. Felscher-Suhr, and R. Schuemer, "The Concept of Noise Annoyance: How International Experts See It," *J. Sound Vib.*, vol. 223, pp. 513–527, 1999.
- [15] J. E. Green, "Civil aviation and the environmental challenge," *Aeronaut. J.*, vol. 107, no. 1072, pp. 281–300, 2003.
- [16] K. D. Kryter, "Scaling Human Reactions to the Sound from Aircraft," *J. Acoust. Soc. Am.*, vol. 31, no. 11, pp. 1415–1429, 1959.
- [17] K. D. Kryter, "The Meaning and Measurement of Perceived Noise Level," *Noise Control*, vol. 6, no. 5, pp. 12–27, 1960.
- [18] S. R. More, "Aircraft Noise Characteristics and Metrics," Purdue University, 2011.
- [19] T. J. Schultz, "Synthesis of Social Surveys on Noise Annoyance," *J. Acoust. Soc. Am.*, vol. 64,

- no. 2, pp. 377–405, Aug. 1978.
- [20] H. M. E. Miedema and C. G. M. Oudshoorn, “Annoyance from transportation noise,” *Environ. Health Perspect.*, vol. 109, no. 4, pp. 409–416, 2001.
- [21] S. Fidell, “The Schultz curve 25 years later: A research perspective,” *J. Acoust. Soc. Am.*, vol. 114, no. 6, pp. 3007–3015, 2003.
- [22] L. S. Finegold, C. S. Harris, and H. E. Von Gierke, “Community Annoyance and Sleep Disturbance: Updated Criteria for Assessing the Impacts of General Transportation Noise on People,” vol. 42, no. 1, pp. 25–30, 1994.
- [23] W. Babisch *et al.*, “Annoyance due to aircraft noise has increased over the years—Results of the HYENA study,” *Environ. Int.*, vol. 35, pp. 1169–1176, 2009.
- [24] P. Brooker, “Do people react more strongly to aircraft noise today than in the past?,” 2008.
- [25] Federal Aviation Administration, *Code of Federal Regulations (CFR) Title 14, Part 36: Noise Standards: Aircraft Type and Airworthiness Certification.* .
- [26] J. Hileman, “FAA Perspectives on Challenges Posed by Aircraft Noise.” Federal Aviation Administration, 2017.
- [27] R. J. Astley, “Can technology deliver acceptable levels of aircraft noise?,” *Inter-noise 2014*, no. 3, pp. 1–12, 2014.
- [28] C. Frömming *et al.*, “Climate cost functions as a basis for climate optimized flight trajectories,” in *Tenth USA/Europe Air Traffic Management Research and Development Seminar (ATM2013) Airport*, 2013.
- [29] R. F. S. Job, “Community response to noise: A review of factors influencing the relationship between noise exposure and reaction,” *J. Acoust. Soc. Am.*, vol. 83, no. 3, p. 991, 1988.
- [30] R. Guski, “Personal and social variables as co-determinants of noise annoyance,” *Noise Heal.*, vol. 1, no. 3, pp. 45–56, 1999.
- [31] A. Muzet, “Environmental noise, sleep and health,” *Sleep Med. Rev.*, vol. 11, no. 2, pp. 135–142, 2007.
- [32] M. Basner, A. Samel, and U. Isermann, “Aircraft noise effects on sleep: Application of the results of a large polysomnographic field study,” *J. Acoust. Soc. Am.*, vol. 119, no. 5, pp. 2772–2784, 2006.
- [33] World Health Organization, “Night noise guidelines for Europe,” 2009.
- [34] S. Hygge, G. W. Evans, and M. Bullinger, “A prospective study of some effects of aircraft noise on cognitive performance in schoolchildren,” *Psychol. Sci.*, vol. 13, no. 5, pp. 469–474, 2002.
- [35] C. Clark *et al.*, “Exposure-effect relations between aircraft and road traffic noise exposure at school and reading comprehension: The RANCH project,” *Am. J. Epidemiol.*, vol. 163, no. 1, pp. 27–37, 2006.
- [36] World Health Organization, “Guidelines for community noise.” World Health Organization Europe, 2000.
- [37] W. Andrew, L. Junenette, I. Jonathan, S. Melly, and F. Dominici, “Residential exposure to aircraft noise and hospital admissions for cardiovascular diseases: Multi-airport retrospective study,” *BMJ*, vol. 347, no. 7928, pp. 1–11, 2013.
- [38] L. Anna *et al.*, “Aircraft noise and cardiovascular disease near Heathrow airport in London: Small area study,” *BMJ*, vol. 347, no. 7928, pp. 9–12, 2013.

- [39] W. Babisch and I. Kamp, "Exposure-response relationship of the association between aircraft noise and the risk of hypertension," *Noise Heal.*, vol. 11, no. 44, p. 161, 2009.
- [40] S. Floud *et al.*, "Medication use in relation to noise from aircraft and road traffic in six European countries: Results of the HYENA study," *Occup. Environ. Med.*, vol. 68, no. 7, pp. 518–524, 2011.
- [41] M. Lijesen, W. Van Der Straaten, J. Dekkers, R. Van Elk, and J. Blokdijk, "How much noise reduction at airports?"
- [42] J. K. Brueckner and R. Girvin, "Airport noise regulation, airline service quality, and social welfare."
- [43] V. Been, "What's fairness got to do with it? Environmental justice and the siting of locally undesirable land uses," *Cornell Law Rev.*, vol. 78, 1992.
- [44] D. J. Forkenbrock and L. A. Schweitzer, "Environmental Justice in Transportation Planning," *J. Am. Plan. Assoc.*, vol. 65, no. 1, pp. 96–112, 1999.
- [45] R. R. Sobotta, H. E. Campbell, and B. J. Owens, "Aviation noise and environmental justice: The barrio barrier," *J. Reg. Sci.*, vol. 47, no. 1, pp. 125–154, 2007.
- [46] Y. Schipper, P. Nijkamp, and P. Rietveld, "Why do aircraft noise value estimates differ? A meta-analysis," *J. Air Transp. Manag.*, vol. 4, no. 2, pp. 117–124, 1998.
- [47] D. Uyeno, S. W. Hamilton, A. J. G. Biggs, B. D. Uyeno, and J. G. Biggs, "Density of Residential Land Use and the Impact of Airport Noise," vol. 27, no. 1, pp. 3–18, 2010.
- [48] H. E. Campbell, "The politics of requesting: Strategic behavior and public utility regulation," *J. Policy Anal. Manag.*, vol. 15, no. 3, pp. 395–423, 1996.
- [49] P. Morrell and C. H. Y. Lu, "Aircraft noise social cost and charge mechanisms - a case study of Amsterdam Airport Schiphol," *Transp. Res. Part D Transp. Environ.*, vol. 5, no. 4, pp. 305–320, 2000.
- [50] D. P. Mcmillen, "Airport expansions and property values: the case of Chicago O'Hare Airport," *J. Urban Econ.*, vol. 55, pp. 627–640, 2004.
- [51] P. Habuda O 'byrne, J. P. Nelson, and J. J. Seneca, "Housing Values, Census Estimates, Disequilibrium, and the Environmental Cost of Airport Noise: A Case Study of Atlanta'," *J. Environ. Econ. Manage.*, vol. 12, pp. 169–178, 1985.
- [52] S. A. Morrison, C. Winston, and T. Watson, "Fundamental Flaws of Social Regulation: The Case of Airplane Noise," *J. Law Econ.*, vol. 42, no. 2, pp. 723–744, 1999.
- [53] Federal Aviation Administration, "FAA Order 1050.1F Desk Reference," no. July. 2015.
- [54] International Civil Aviation Organization (ICAO), "Guidance On The Balanced Approach To Aircraft Noise Management: 2nd Edition," 2007.
- [55] R. Girvin, "Aircraft noise-abatement and mitigation strategies," *J. Air Transp. Manag.*, vol. 15, no. 1, pp. 14–22, 2009.
- [56] F. Netjasov, "Contemporary measures for noise reduction in airport surroundings," *Appl. Acoust.*, vol. 73, no. 10, pp. 1076–1085, 2012.
- [57] GAO, "Aviation and the Environment - Airport Operations and Future Growth Present Environmental Challenges," no. August, 2000.
- [58] D. Casalino, F. Diozzi, R. Sannino, and A. Paonessa, "Aircraft noise reduction technologies: A bibliographic review," *Aerosp. Sci. Technol.*, vol. 12, pp. 1–17, 2008.

- [59] Y. Guo, "Aircraft Flap Side Edge Noise Modeling and Prediction," *AIAA/CEAS Aeroacoustics Conf.*, no. 17, pp. 1–25, 2011.
- [60] R. W. Stoker, Y. Guo, C. Streett, and N. Burnside, "Airframe noise source locations of a 777 aircraft in flight and comparisons with past model scale tests," *9th AIAA/CEAS Aeroacoustics Conf. Exhib.*, no. May, pp. 1–10, 2003.
- [61] W. Dobrzynski, R. Ewert, M. Pott-Pollenske, M. Herr, and J. Delfs, "Research at DLR towards airframe noise prediction and reduction," *Aerosp. Sci. Technol.*, vol. 12, no. 1, pp. 80–90, 2008.
- [62] J.-P. B. Clarke *et al.*, "Continuous Descent Approach: Design and Flight Test for Louisville International Airport," *J. Aircr.*, vol. 41, no. 5, pp. 1054–1066, Sep. 2004.
- [63] G. Gershzohn, J. Wat, J. P. Dwyer, K. Elmer, J.-P. Clarke, and N. tan Ho, "Advanced Noise abatement procedures An experimental study of flight operational acceptability," in *AIAA's Aircraft Technology, Integration, and Operations (ATIO)*, 2002, no. October, pp. 1–10.
- [64] J.-P. Clarke, "The role of advanced air traffic management in reducing the impact of aircraft noise and enabling aviation growth," *J. Air Transp. Manag.*, vol. 9, pp. 161–165, 2003.
- [65] B. Kim *et al.*, "ACRP Report 86 - Environmental Optimization of Aircraft Departures: Fuel Burn, Emissions, and Noise," 2013.
- [66] J. T. Betts, "Survey of Numerical Methods for Trajectory Optimization," *J. Guid. Control. Dyn.*, vol. 21, no. 2, pp. 193–207, 1998.
- [67] H. G. Visser, "Generic and site-specific criteria in the optimization of noise abatement trajectories," *Transp. Res. Part D*, vol. 10, pp. 405–419, 2005.
- [68] B. Capozzi, S. Augustine, T. R. Thompson, and M. Aviation, "Dynamic Noise Avoidance Routing Through Terminal Airspace," no. August, pp. 1–15, 2003.
- [69] X. Prats, V. Puig, J. Quevedo, and F. Nejari, "Multi-objective optimisation for aircraft departure trajectories minimising noise annoyance," *Transp. Res. Part C Emerg. Technol.*, vol. 18, no. 6, pp. 975–989, 2010.
- [70] L. J. J. Erkelens, "Research into new noise abatement procedures for the 21st century," in *Aviation*, 2000, no. August, pp. 1–10.
- [71] A. Filippone, "Comprehensive analysis of transport aircraft flight performance," *Prog. Aerosp. Sci.*, vol. 44, pp. 192–236, 2008.
- [72] S. Hably and H. G. Visser, "Advanced Noise Abatement Departure Procedures: Custom Optimized Departure Profiles," in *AIAA Guidance, Navigation and Control Conference and Exhibit*, 2008, no. AIAA 2008-7405, pp. 1–11.
- [73] H. G. Visser and R. A. A. Wijnen, "Optimisation of noise abatement arrival trajectories," *Aeronaut. J.*, vol. 107, no. 1076, pp. 607–615, 2003.
- [74] J. L. Thomas and R. J. Hansman, "Modeling Performance and Noise of Advanced Operational Procedures for Current and Future Aircraft," 2017.
- [75] T. Reynolds, M. Sandberg, J. Thomas, and R. J. Hansman, "Delayed Deceleration Approach Noise Assessment," in *16th AIAA Aviation Technology, Integration, and Operations Conference*, 2016.
- [76] G. G. Fleming, "Aviation Environmental Design Tool (AEDT) Technical Manual, Version 2c," 2016.
- [77] Federal Aviation Administration, "FAA Order 1050.1E, CHG 1 - Environmental Impacts:

- Policies and Procedures,” 2006.
- [78] C. L. Burley and J. W. Rawls, “Aircraft Noise Prediction Program (ANOPP) Theoretical Manual,” 2014.
  - [79] A. Filippone, “Aircraft noise prediction,” *Prog. Aerosp. Sci.*, vol. 68, pp. 27–63, 2014.
  - [80] T. G. Reynolds, Y. Rodriguez, M. Mcpartland, and M. Sandberg, “Assessment of Delayed Deceleration Approach Opportunities at US Airports,” in *15th AIAA Aviation Technology, Integration, and Operations Conference AIAA*, 2015.
  - [81] F. Farassat and J. H. Casper, “Towards an Airframe Noise Prediction Methodology: Survey of Current Approaches,” *44th AIAA Aerosp. Sci. Meet. Exhib.*, no. January, p. AIAA 2006-210, 2006.
  - [82] SAE Aerospace, “SAE-AIR-1845A: Procedure for the Calculation of Airplane Noise in the Vicinity of Airports.” 2012.
  - [83] D. Mavris and C. Perullo, “ASCENT Project 43: Noise Power Distance Re-Evaluation,” in *Spring 2017 ASCENT COE Advisory Board Meeting*, 2017.
  - [84] I. Jopson, D. Rhodes, and P. Havelock, “Aircraft Noise Model Validation - How Accurate Do We Need To Be?”
  - [85] C. L. Moulton, “Air Force Procedure for Predicting Aircraft Noise around Airbases: Noise Exposure Model (Noisemap) User’s Manual,” *Security*, 1990.
  - [86] L. Bertsch, S. Guérin, G. Looye, and M. Pott-Pollenske, “The Parametric Aircraft Noise Analysis Module - status overview and recent applications,” *17th AIAA/CEAS Aeroacoustics Conf. (32nd AIAA Aeroacoustics Conf.)*, no. June, pp. 1–24, 2011.
  - [87] J. R. Stone, E. A. Krejsa, and B. J. Clark, “Philosophy and Evolution of a Semi-Empirical Model for Jet Noise Prediction,” *& Proc. 저널. 프로시딩즈 기술보고서*, no. January, pp. 1–10, 2004.
  - [88] V. N. Vatsa, M. R. Khorrami, and D. P. Lockard, “Aeroacoustic Simulations of a Nose Landing Gear with FUN3D: A Grid Refinement Study,” *23rd AIAA/CEAS Aeroacoustics Conf.*, no. June, pp. 1–27, 2017.
  - [89] E. R. Boeker *et al.*, “Integrated Noise Model (INM) Version 7.0 Technical Manual,” 2008.
  - [90] J. B. Ollerhead, “The CAA Aircraft Noise Contour Model: ANCON Version 1.” UK Civil Aviation Authority, 1992.
  - [91] S. Pietrzko and R. Bütikofer, “FLULA - Swiss Aircraft Noise Prediction Program,” in *2002 Annual Conference of the Australian Acoustical Society*, 2002, no. November, pp. 92–99.
  - [92] L. Bertsch and U. Isermann, “Noise prediction toolbox used by the DLR aircraft noise working group,” *42nd Int. Congr. Expo. Noise Control Eng. 2013 Noise Control Qual. Life, INTER-NOISE 2013*, vol. 1, no. May, pp. 833–841, 2013.
  - [93] R. L. S. Pierre and D. J. Maguire, “The Impact of A-weighting Sound Pressure Level Measurements during the Evaluation of Noise Exposure,” in *Noise-Con*, 2004.
  - [94] J. Parmanen, “A-weighted sound pressure level as a loudness/annoyance indicator for environmental sounds - Could it be improved?,” *Appl. Acoust.*, vol. 68, no. 1, pp. 58–70, 2007.
  - [95] D. Southgate, “Expanding Ways to Describe and Assess Aircraft Noise,” pp. 1–87, 2000.
  - [96] S. J. Hebly and H. G. Visser, “Advanced noise abatement departure procedures: Custom-optimised departure profiles,” *Aeronaut. J.*, vol. 119, no. 1215, pp. 647–661, 2015.

- [97] Federal Aviation Administration, "The FAR Part 150 Airport Noise Compatibility Planning Program: An Overview."
- [98] P. of Portland, "Portland International Airport: Noise Compatibility Study," 2006.
- [99] M. Brenner, "Comparison of Methods for Evaluating Impacts of Aviation Noise on Communities," no. May, 2017.
- [100] A. Yu, "Methods for Analyzing Noise Impacts of Dispersed Flight Tracks." 2018.
- [101] R. Buchanan, "Wicked Problems in Design Thinking," *Source Des. Issues*, vol. 8, no. 2, pp. 5–21, 1992.
- [102] H. W. J. Rittel and M. M. Webber, "Dilemmas in a general theory of planning," *Policy Sci.*, vol. 4, no. 2, pp. 155–169, 1973.
- [103] M. W. Kreuter, C. De Rosa, E. H. Howze, and G. T. Baldwin, "Understanding Wicked Problems: A Key to Advancing Environmental Health Promotion," *Heal. Educ Behav*, vol. 31, 2004.
- [104] E. M. van Bueren, "Dealing with Wicked Problems in Networks: Analyzing an Environmental Debate from a Network Perspective," *J. Public Adm. Res. Theory*, vol. 13, no. 2, pp. 193–212, 2003.
- [105] E. D. G. Fraser, A. J. Dougill, W. E. Mabee, M. Reed, and P. McAlpine, "Bottom up and top down: Analysis of participatory processes for sustainability indicator identification as a pathway to community empowerment and sustainable environmental management," *J. Environ. Manage.*, vol. 78, no. 2, pp. 114–127, 2006.
- [106] R. Gregory, T. McDaniels, and D. Fields, "Decision aiding, not dispute resolution: Creating insights through structured environmental decisions," *J. Policy Anal. Manag.*, vol. 20, no. 3, pp. 415–432, 2001.
- [107] S. van den Hove, "Between consensus and compromise: acknowledging the negotiation dimension in participatory approaches," *Land use policy*, vol. 23, no. 1, pp. 10–17, Jan. 2006.
- [108] M. G. O'Neill and R. J. Hansman, "An Approach to Analyze Tradeoffs for Aerospace System Design and Operation," Massachusetts Institute of Technology, 2012.
- [109] H. Cho, M. Azzam, R. J. Hansman, and L. L. Jensen, "Noise Analysis and Negotiation Tool for Terminal RNP Procedure Design," in *2013 Aviation Technology, Integration, and Operations Conference*, 2013, pp. 1–12.
- [110] H. M. Regan, M. Colyvan, and L. Markovchick-Nicholls, "A formal model for consensus and negotiation in environmental management," *J. Environ. Manage.*, vol. 80, no. 2, pp. 167–176, Jul. 2006.
- [111] T. L. Saaty, "Decision making with the analytic hierarchy process," *Int. J. Serv. Sci.*, vol. 1, no. 1, pp. 83–98, 2008.
- [112] S. A. Hajkovicz, "Supporting multi-stakeholder environmental decisions," *J. Environ. Manage.*, vol. 88, no. 4, pp. 607–614, Sep. 2008.
- [113] J. O'Hara, G. Stump, M. Yukish, E. Harris, G. Hanowski, and A. Carty, "Advanced Visualization Techniques for Trade Space Exploration," *48th AIAA/ASME/ASCE/AHS/ASC Struct. Struct. Dyn. Mater. Conf.*, no. April, pp. 1–6, 2007.
- [114] A. Sahai, F. Wefers, S. Pick, E. Stumpf, M. Vorländer, and T. Kuhlen, "Interactive simulation of aircraft noise in aural and visual virtual environments," *Appl. Acoust.*, vol. 101, pp. 24–38, 2016.



- [115] E. Condon, B. Golden, and E. Wasil, "Visualizing group decisions in the analytic hierarchy process," *Comput. Oper. Res.*, vol. 30, no. 10, pp. 1435–1445, 2003.
- [116] A. Mozdzanowska and R. J. Hansman, "System transition: dynamics of change in the US air transportation system," 2008.
- [117] R. K. Mitchell, B. R. Agle, and D. J. Wood, "Toward a Theory of Stakeholder Identification and Salience: Defining the Principle of Who and What Really Counts," *Source Acad. Manag. Rev.*, vol. 22, no. 4, pp. 853–886, 1997.
- [118] D. L. Allen, A. Haraldsdottir, R. W. Lawler, K. Pirotte, and R. W. Schwab, "The Economic Evaluation of CNS/ATM Transition."
- [119] C. L. Scovel, "FAA's Progress and Challenges in Advancing the Next Generation Air Transportation System," 2013.
- [120] L. L. Jensen, J. Thomas, C. Brooks, M. Brenner, and R. J. Hansman, "Development of Rapid Fleet-Wide Environmental Assessment Capability," *AIAA Aviat. Forum*, pp. 1–14, 2017.
- [121] Eurocontrol, "User Manual for the Base of Aircraft Data (BADA) Family 4," 2014.
- [122] M. Drela, "TASOPT 2.00 Transport Aircraft System OPTimization Technical Description," 2010.
- [123] Eurocontrol, "User Manual for the Base of Aircraft Data (BADA) Family 4." 2016.
- [124] J. Thomas, L. L. Jensen, C. Brooks, M. Brenner, S. Salgueiro, and R. J. Hansman, "Investigation of aircraft approach and departure velocity profiles on community noise," in *23rd AIAA/CEAS Aeroacoustics Conference, 2017*, 2017.
- [125] Federal Aviation Administration, "FAA Order 8260.3D: United States Standard for Terminal Instrument Procedures (TERPS)." 2018.
- [126] Federal Aviation Administration, "FAA Order 8260.58A: United States Standard for Performance Based Navigation (PBN) Instrument Procedure Design," no. 2. 2016.
- [127] Federal Aviation Administration, "FAA Order 8260.55: Special Area Navigation Visual Flight Procedures."
- [128] D. Southgate, N. Fisher, and D. Perera, "The Person-Events Index – A Simple but Invaluable Aircraft Noise Assessment Tool," in *Inter-Noise 2001*, 2001, pp. 1181–1186.
- [129] J. Thomas, L. L. Jensen, C. Brooks, and M. Brenner, "Investigation of Aircraft Approach and Departure Velocity Profiles on Community Noise," *AIAA Aviat. Forum*, pp. 1–12, 2017.
- [130] A. H. Midkiff, R. J. Hansman, and T. G. Reynolds, "Air Carrier Flight Operations," 2004.
- [131] Federal Aviation Administration, "FAA Order 8260.46F: Departure Procedure (DP) Program," 2015.
- [132] Federal Aviation Administration, "PBN NAS Navigation Strategy Report 2016," 2016.
- [133] Eurocontrol, "European ATM Master Plan: The Roadmap for Delivering High Performing Aviation for Europe," 2015.
- [134] M. E. Eagan, R. Hanrahan, and R. Miller, "Implementing performance based navigation procedures at US airports: improving community noise exposure," in *InterNoise 2013*, 2013.
- [135] A. Filippone and A. Harwood, "Flyover Noise Measurements and Predictions of Commercial Airplanes," *J. Aircr.*, vol. 53, no. 2, pp. 396–405, 2016.
- [136] Federal Aviation Administration, "FAA Order 8260.3C: United States Standard for Terminal

- Instrument Procedures (TERPS)," 2016.
- [137] Federal Aviation Administration, "Order JO 7110.65W: Air Traffic Control," 2015.
- [138] T. Cuddy, "Guidance Memorandum on Preparing Focused, Concise and Timely Environmental Assessments." Federal Aviation Administration, 2011.
- [139] J. Marks, "Guidance for Implementation of the Categorical Exclusion in Section 213(c)(1) of the FAA Modernization and Reform Act of 2012." Federal Aviation Administration, 2012.
- [140] J. Marks, "Guidance for Implementation of the Categorical Exclusion in Section 213(c)(2) of the FAA Modernization and Reform Act of 2012." Federal Aviation Administration, 2016.
- [141] R. J. Hansman, L. Jensen, J. Thomas, G. O'Neill, and A. Yu, "Block 1 Procedure Recommendations for Logan Airport Community Noise Reduction," 2017.
- [142] Federal Aviation Administration, "FAA Order JO 7110.65X: Air Traffic Control," 2017.